The Neocortex in Alzheimer's Disease

A study of the distribution of senile plaques, neurofibrillary tangles and congophilic amyloid angiopathy.

C.A.J. Broere

THE NEOCORTEX IN ALZHEIMER'S DISEASE

A study of the distribution of Senile Plaques, Neurofibrillary Tangles and Congophilic Amyloid Angiopathy

This investigation was generously sponsored by the JANIVO Foundation, Breda, The Netherlands.
The research was conducted in the Research Laboratory for Morphological Neurology, Institute of Neurology, Nijmegen.

THE NEOCORTEX IN ALZHEIMER'S DISEASE

A study of the distribution of Senile Plaques, Neurofibrillary Tangles and Congophilic Amyloid Angiopathy

Een wetenschappelijke proeve op het gebied van de geneeskunde en tandheelkunde, in het bijzonder de geneeskunde

PROEFSCHRIFT

ter verkrijging van de graad van doctor
aan de Katholieke Universiteit te Nijmegen,
volgens het besluit van het college van decanen
in het openbaar te verdedigen op
vrijdag 23 februari des namiddags te 13.00 uur precies

door

Cornelis Anne Jan Broere
geboren op 10 maart 1959
te Sliedrecht

Promotores: Prof. Dr. R. Nieuwenhuys
Prof Dr. B.P M. Schulte

Co-Promotor: Dr. A. Keyser

CIP-GEGEVENS KONINKLIJKE BIBLIOTHEEK, DEN HAAG

Broere, C A J

The neocortex in Alzheimer's disease a study of the distribution of senile plaques, neurofibrillary tangles and congophilic amyloid angiopathy/C A J Broere – [S l s n] - III
Proefschrift Nijmegen – Met lit opg
ISBN 90 - 9003295 - 9
SISO 605 93 UDC 616 89(043 3)
Trefw ziekte van Alzheimer

Deze CIP-gegevens alleen afdrukken in de proefschriftedition

Aan mijn ouders

'Ottilie, ik smeek je, wees stil. O wees stil Waarom spreek je zo. Jaren is het zo kalm geweest Zie Ottilie, wij zijn te oud Wij zijn zo oud mogen worden. Wij zijn al gestraft. O, laten wij er niet meer over spreken, nooit meer over spreken. Laten wij kalm, kalm afwachten, en de dingen, die na ons komen, dulden, want wij kunnen er niets aan doen.'

Louis Couperus, Van oude mensen, de dingen die voorbijgaan, 1904

Dementia is a clinical condition occurring in various neurological disorders of different pathogenetic background like Creutzfeld-Jacob Disease (CJD), Parkinson's Disease (PD), Down's Syndrome (DS), Pick's Disease, Alzheimer's Disease (AD) and traumatic or vascular encephalopathy.
In general, clinical manifestations of memory impairment and of cognitive dysfunction may be similar in beginning AD and normal senescence. These disturbances of cognitive function manifest themselves not only as a loss of intellectual functions, but also as disturbances of thought, of adaptation to new circumstances, of abstract thinking and of problem solving abilities. Furthermore, the patient suffers from disturbances of judgement. Disturbances of attention and concentration are among the first symptoms of the dementia syndrome.
The anatomical substrates in the brain, responsible for dementia in both the process of normal aging and of AD, may be similar: in the brain from both conditions, senile plaques and fibrillary degeneration of neuronal cytoplasm are present. Neuropathological changes differ in quantity, but not in quality. Therefore, an intriguing question is whether AD is an acceleration of the aging process, provoked by unknown factors or a separate nosological entity. This problem remains unsolved, despite intensive multidisciplinary research.
The occurrence of similar neuropathological changes in the brains of those patients with diseases like Down's Syndrome (DS), Parkinson's Disease (PD) or Amyotrophic Lateral Sclerosis (ALS) that show clinical dementia, suggests a relationship between these neuropathological changes and the corresponding clinical picture of dementia. In addition to SP and NFT, cell loss in the cortex and in subcortical areas like the nucleus Basalis Magnocellularis (NbM) (Meynert), Locus Coeruleus (LC) or Substantia Nigra (SN) have been reported [1, 2, 3].
Neuronal cell loss and the resulting disconnection of the cerebral cortex from the subcortical nuclei may be related to the dementia syndrome. Recently published observations do show cell loss in several of these subcortical nuclei and insufficiency of the corresponding neurotransmitter function, especially so in cholinergic nuclei. Characteristic neuropathological changes in demented patients and dysfunction of several neurotransmitter systems can only partly explain the pathogenesis of AD. Thus, current research in AD takes into consideration neuropathological phenomena, biochemical aspects of the disease, genetic determinants and environmental and epidemiological factors.
The investigations into the cause and treatment of AD are beset with many pitfalls. First it has to be clarified whether AD is a nosological entity or a syndrome. Arguments that speak in favor of a heterogeneity within the group of AD patients come from the areas

of genetics and of classical neuropathology.
In this introductory chapter, the anatomy of the cerebral cortex is reviewed to some extent as knowledge of normal anatomy is a first step to appreciate the possible consequences of the lesions found in AD for its function. Next, the morphological data from the literature concerning AD, are reviewed. Also a survey is given of current theories on neurofibrillary tangle and senile plaque formation and distribution. This chapter concludes with the formulation of the aim of the present study.

The telencephalon or 'endbrain' consists of two hemispheres. The surface of these hemispheres is formed largely by the cerebral cortex, where olfactory and other sensory information modalities are integrated. During evolution, visual, auditory and other projections which are relayed in the thalamus attain different cortical areas. Each hemisphere thus is enlarged by additional neocortex. In the hemisphere's medial wall, the hippocampal formation maintains its position as a voluminous archicortical structure.
The outer rim of the hemispheres forms a vast cortical surface. The neocortex of the human brain has been subdivided on the basis of regional variations in the architectonic arrangement of neurons and myelin. The schemes of neocortical subdivision presented in the literature, may be divided into two groups: they either are based on unique local properties of the individual regions or on the presence of patterns formed by regions sharing common characteristics.
The first scheme of subdivision was used in the descriptions of the neocortex by Exner in 1881 [4], Brodmann in 1909, Vogt and Vogt in 1920, Von Economo in 1927 [5] and Bailey & Von Bonin in 1951 [6]. Exner proposed 367 different cortical areas whereas Brodmann limited the number of subdivisions to 48. The subdivision by Brodmann was widely accepted. and so was the subdivision by Von Ecomono.
The subdivision by Brodmann is used in this study. When the word 'area' is used to denote this subdivision, it is spelled with a capital.
The second way of subdividing was used by investigators, including such theoreticians of brain function, as Broca in 1878, Abbie in 1942, Filimonoff in 1947, Yakovlev and Sanides in 1970.
In practical neuroanatomy, the subdivision of Brodmann still is widely used as a map for first orientation.

I.2.1. Macroscopic anatomy

On cross section, the cerebral cortex shows a complex pattern of folds of the outer rim of the telencephalon. The grooves, resulting from the folding of the cortical plate are referred to as sulci. These sulci delineate the so called gyri of the cerebral cortex. This folding of the neocortex allows for storage of a far larger surface of cortex than the inside surface of the neurocranium. This pattern of folding of the neocortex can be considered a solution to the problem of storing the large plate of cortex tissue in a limited space.

Because of a differential local increase of cortical volume, some macroscopical landmarks in cortical topography emerge early during development, like for instance the sulcus principalis, the sulcus centralis (Rolandi) and the fissura lateralis. This increase in volume leads initially to the development of entire lobi of the cortex, e.g. the frontal lobe. This results in the formation of the large fissurae. Later in development, parts of the lobi will increase in volume differentially. In this way the sulci are emerging. Apparently, in the process of localized volume increase, various solutions of the volume-storage problem (i.e. how to store an increasing volume within the limited space of the developing neurocranium) exist and result in the variation observed in the pattern of sulci and gyri [7]. Only the early formed sulci, such as the sulcus circularis insulae and the sulcus cinguli, display a fairly constant pattern. As a consequence, in the subdividing the cortex, the sulcus cinguli and the sulcus limitans insulae can be used in order to delineate the neocortical parts which are bordered by these sulci.
In studying the thickness of the cortex or of its individual layers, the folding of the cortex has always to be taken into account. Because of the curvature, the outer layers of the cortical surface of a gyrus are stretched and the inner layers thickened. Exactly the opposite is the case at the depth of a sulcus [8]. This complex cortical geometry makes it extremely difficult to derive exact figures concerning overall thickness of the whole neocortex or its subdivisions. In general, it will not suffice to take just the average of for example measurements of cortical thickness in one section only: in case of the cortex the curvature is three-dimensional: not only are the measurements in one section influenced by the foldings in the sectioning plane, but also by the curvature of the cortex perpendicular to this plane. It may be concluded therefore, that histometrical results are influenced by the three-dimensional architecture of the neocortex.
In summary, the complex geometrical structure called the human neocortex necessitates the use of methods for estimation of volume, of surface and of thickness that are independent of the geometry of the structure itself.

I.2.1.1. Cortical Volume

"The accurate measurement of the surface or volume of the cortex is surprisingly difficult [9]". One of the first measurements of the cortical surface was made in 1895 [10]. The figure produced was 2354 square centimeters, denoting the surface of a male human brain weighing 1360 grams. With a mean cortical thickness of 2.5 mm, a cortical volume of 290 cc results. Other values are found in table I.
The determination of cortical volume is important: every other

measurement is influenced by it. In nearly every study on neuron numbers, a neuronal concentration is given. This concentration is defined as a number per unit of volume. When changes in this value are considered to be a reflection of the changes in absolute number, a severe mistake can be made because changes in concentration are also due to changes in volume. When accurate information about the volume change of a structure is lacking, no useful interpretation of change in neuronal concentration can be made. This is not only true for the hemispheres as a whole, but especially so when parts of these are considered. In order to determine the volume of a structure, one should be able to identify all the borders of this structure in a confident manner.
In the neocortex this cannot be done per area or per lamina, making thereby the determination of the neuron loss in AD, quite futile.

I.2.1.2. Cortical surface

In Table I, the values available from the literature for the total surface of the neocortex are given. For the area striata, the neocortical surface area is available from the work of Filimonoff [11]. In this study, the surface of the area striata was determined in nine brains. After correction for shrinkage, the smallest value was 2650mm**2 and the largest 3452mm**2. The mean value was 3036 mm**2 and the coefficient of variation about 8 percent.

I.2.1.3. Cortical thickness

In man, the thickest part of the cortex is along the precentral gyrus and the thinnest part is found in the visual Area 17. In general, only the mean values of the thickness of the cortex in different regions of the brain are available. The values for cortical thickness as given in the literature, are presented in Table II. In this table it can be seen, that the values for mean cortical thickness range from 1400 - 2500 micron for Area 17 of the occipital lobe, to 2650 - 2800 micron in the motox cortex (Area 4).

I.2.2. The description of the microscopical structure of the neocortex.

I.2.2.1. Historical introduction.

On February 2, 1776, an Italian medical student found within the cerebral cortex of the human brain a white line, most obvious in the occipital lobe. This " line of Gennari" is a remarkable landmark of the primary visual cortex, the "area striata" [12, 13]. This discovery was the first occasion on which one part of the cerebral cortex was singled out. Thus, the first observation in myeloarchitectonics was made [1]. After this discovery by Gennari, which later was confirmed independently by Vicq d'Azyr in 1786 and Soemmering in 1788, the next major advance in the more detailed description of the cerebral cortex was made by Baillarger [21],who for the first time, observed a six layered pattern that showed regional differences. When viewed with transmitted light, he observed the layers to alternate between opaque and transparent and numbered them from within outward, his layer VI corresponding to the molecular layer. His opaque layers II and IV corresponded respectively to what now are referred to as the inner and the outer stripes of Baillarger, tangential bands of myelinated fibers that occur in layers Vb and IV of the modern nomenclature. Another significant contribution to the study of the neocortex was made by Flechsig [14], who introduced the concept of association areas, by studying the development of myelination of the cerebral cortex and the underlying white matter, eventually recognizing 45 different fields. Those fields displaying stainable myelin at birth were called premature fields and the surrounding fields, which myelinated next were referred to as the marginal zones. The last myelinating fields Flechsig designed as "association areas". These were supposed to have their major connectivity to the sensory cortical areas, rather than to subcortical formations and were perceived as the substrate for more specifical human "psychic function".

With the distinction by Meynert of two types of cortex, a cortex with a white surface (weisse Rinde) and a cortex with a grey surface (graue Rinde), neocortical architectonics were born [15]. The first important contribution to cytoarchitectonics was made by

---

[1] Later, this line proved to be the landmark of the only cortical area or cytoarchitectonic field which macroscopically can readily be identified. This area was later categorized as the (primary) visual field and denoted as area 17 in the cytoarchitectonical study of Brodmann.

Berlin in 1858 [16], who introduced cell staining tas a method to study the cerebral cortex. With the use of the carmine stain he recognized six layers and numbered them, like Baillarger [17], from within outward and coined the terms pyramidal, spindle and granule cell. Additional important contributions were made by Betz, who described gigantic pyramidal cells in the area directly anterior to the sulcus centralis and who divided the cortex in granular and dysgranular parts [18]. Later Betz described the calcarine cortex, stating that he considered it a sensory center [19]. In 1881 Betz described among other parts of the human neocortex, the cortex of the transverse temporal gyrus (primary auditory cortex) in some detail, stating that this part of the cortex resembled that of the postcentral convolution (primary somesthetic cortex) [20]. A detailed account of the cytoarchitecture of the human motor cortex was given by Lewis and Clarke in 1878 [21]. In their paper, a drawing of the motor cortex was given, in which six layers were numbered, starting with number 1 under the pial surface. After the studies of Hammarberg [22], who provided the first atlas illustrating regional variation in the cerebral cortex, and of Schlapp [23], who provided the first complete cytoarchitectonic atlas of the cynomolgus monkey, and Bolton [24], who introduced the use of human disease states to define cytoarchitectonic areas, the first cytoarchitectonic (and myeloarchitectonic) map of the human brain was produced by Campbell [25]. The Nissl staining technique was introduced in 1894 [26]. Using this staining technique, Brodmann performed his studies on the comparative cytoarchitectonics of the neocortex . In his studies, Brodmann used a microtome [27], that could only accommodate a bloc size of 70 x 80 mm. He therefore was limited in his human studies to blocking the brains, generally cutting the blocks in serial sections that were orientated perpendicular to the gyri. Using this technique Brodmann performed his studies which culminated in his widely known mapping of the human brain [28], which is also used for orientation in our study.

Later, a parcellation of the neocortex was developed, based not so much on architectonical characteristics of the neocortex, but more on the connections with other cortical areas. This subdivision is particulary useful in describing the sensory systems of different modality and the flow of information through these systems. This nomenclature is used in section I.2.3. , describing the cortico-cortical connections. A recent review is given by Pandya et al. [29].

I.2.2.2. Cytoarchitectonics

The study of regional peculiarities of the structure of the cerebral cortex as revealed by differences in shape, size and density of neuronal perikarya in sections stained according to the Nissl technique is called cytoarchitectonics. The criteria used here are of varying value, although some of them are of major importance and could form a basis for subdividing the cerebral cortex into main territories (e.g. the identification of the koniocortex of the area striata using the subdivision of the fourth cortical lamina). Neocortical features, such as the presence of larger densities in the cortical layers II and IV that distinguish granular from agranular cortical regions, or the presence of specific types of neurons (e.g. the Betz neurons characteristic for Area 4) are of specific significance for subdivisions of the cerebral cortex. Neocortical features may serve to subdivide the main territories into regions, subregions, areas and subareas, according to a certain hierarchical order and depending on their relative importance. Finally, a number of less important features may allow subdivision of the cortex literally AD INFINITUM. As a matter of fact, no part of the cortex, however small it may be, exhibits absolute similarity to the neighboring part [30]. Accordingly, practically all subdivisions, solely based on cytoarchitectonics are arbitrary. Therefore, no sharp borders can be determined in the large majority of the neocortical areas, if neocortical subdivisions are made on cytoarchitectonical criteria alone.
Thus, it is not possible to determine the volume of each of these cortical areas separately, let alone of their cortical laminae. As the cortical volume is of vital importance in order to ascertain the neuron number and as no technique exists to determine these, no such determination of neuron number is feasible.

I.2.2.2.1. Cortical lamination

In 1919, C. and O. Vogt defined Architectonics in a more operational way as the doctrine, studying local differences of the structure of the total neocortex observed at low magnification as clearly distinguishable differences in arrangement, number and gross shape of elements visible in specifically stained sections [31]. The particular method used is denoted by a prefix. Thus, cytoarchitectonics refers to the study of the arrangement of perikarya which have been stained after Nissl. Other forms of architectonics include myeloarchitectonics, pigmentoarchitectonics and angioarchitectonics.

From the start of cytoarchitectonics, the actual number of the

layers, constituting the neocortex, varied from 5 to 9 between the different investigators [32] up to Brodmann's layering scheme. According to Brodmann, the following six layers can be recognized throughout most of the neocortex:

L I :Lamina zonalis
L II :Lamina granularis externa
L III:Lamina pyramidalis
L IV :Lamina granularis interna
L V :Lamina ganglionaris
L VI :Lamina multiformis

Lamina I is the layer immediately beneath the pia mater and contains only very few neuronal cell bodies. Here, only a few non-pyramidal neurons are found with wide horizontally spreading dendrites and axons- hence the alternative name of molecular layer. The external granular layer consists of small tightly packed neurons of mainly the pyramidal type. This layer is strongly demarcated from the first layer, but the boundary with Layer III is more gradual, especially so in the frontal lobe, where the pyramidal cells of layer II are relatively large, so that they mostly form a gradient to the bordering medium sized pyramidal cells of Layer III. Mostly, this last layer is not as densely packed as Layer II and the pyramidal cells are larger. Moreover practically no non-pyramidal cells are observed. The size of the pyramidal cells in this layer is increasing with cortical depth (i.e., with increasing distance to the pial surface). The lamina III pyramidal neurons exhibit in sections stained after the Golgi method, the typical pattern of the pervading cell type of the cerebral cortex, with its apical shaft and apical bouquet in Lamina I and basal skirt reaching partly into Lamina IV. The axons descend into the white matter [33]. The lower border with layer IV, the internal granular layer, is encountered when a sudden increase in density of non-pyramidal neurons is observed. The cellular density of this layer can be nearly as large as Layer II, especially so in the primary sensory regions. Layer IV is referred to as the internal granular layer and consists mainly of large pyramidal cells at low cellular densities. The border with layer V is reached when a more or less sharp increase of the density of non-pyramidal neurons is observed. Also the density of smaller pyramidal cells increases in this layer. Because of the mixed character of the neuronal population, the layer VI is known as the polymorph layer.

This general scheme of laminar cortical organization as seen in Nissl stained cross sections of the neocortex can show considerable regional variation in different neocortical regions. Homotypical areas differ only in details of the layering pattern described above, whereas heterotypical areas reveal considerable variations of the normal layering or specialization of certain laminae. For instance, the heterotypical area striata (Area 17 according to

Brodmann's map) shows a remarkably broad fourth layer, filled with small nerve cells distinguishing this hypergranular cortex or koniocortex from the homotypical cortex. An agranular cortex can be observed in the prefrontal cortex and in the cortex of the temporal pole: here small granulate cells have nearly disappeared, rendering it very difficult to decide the location of layer IV. Dysgranular and intermedio-granular cortical fields, with a rather thin granular layer mediate between agranular areas on the one hand and eugranular ones on the other [34]. Often a further subdivision of certain laminae in some cortical fields can be given. In this study no attempt is made in this direction.

The cerebral cortex also is laminated in terms of the endings of afferent axons, as well as in terms of some of its intrinsic axonal systems. The layers can be discerned both in myelin-stained preparations and in reduced silver preparations [35]. In these preparations, a condensation of fibers can be noticed in the deeper zone of the first cortical layer, especially so in some sensory areas, e.g. the somatic parakoniocortex (Brodmann Area 1 and 2) and the auditory region [36]: this has become known as the stria of Kaes-Bechterew. The lower border of this stria coincides with a steep increase of neural density, marking the upper border of Layer II. In most areas, the easily recognizable horizontal plexus of fibers is called the outer layer of Baillarger and coincides with the inner granular layer IV. A less clearly visible plexus of fibers is located deep in layer V: the inner layer of Baillarger. The intensity of staining of these fiber plexus in the different cortical areas can be illustrated by the area striata, where an intensely staining outer layer of Baillarger is referred to as the line of Gennari.

In the present study a modification of the Bielschowsky silver staining according to Yamamoto is used [37], to visualize Senile Plaques. In this material, the cells and the neuropil are stained yellow-brown. Often, the fiber architectonics can be discerned. In our material, fibers running parallel with the pial surface could be identified in the layers II and IV in most cortical areas. These fibers were used as an additional marker for the inner and outer granular layers.
The neocortex can be subdivided according to two organizational principles: on the one hand according to the subdivision of the cerebral cortex as derived from comparative neurology [38] and on the other on the basis of cortical cytoarchitectonics [39, 40]. The term ISOCORTEX is an abbreviation for isogenetic or homogenetic cortex. The latter was introduced by Brodmann in 1909 in order to indicate the mature convexity cortex of higher mammals, indicating that ontogenetically it passes through a six-layered stage. Allocortex means allogenetic cortex, indicating a principally different development. The determination of these differences in various parts of the neocortex, and of the resultant boundaries

in one field. According to his opinion, the connections of a cortical field remain the most reliable basis in order to decide to call that part of the cortex a neocortical field.
In practical analysis, every identification of a cytoarchitectonic field using Nissl stained material alone is more or less disputable.

Although there exists a large variety in the cyto- and myeloarchitecture in the neocortex, attempts have been made to draw 'wiring' diagrams of the intercortical circuits, thought to be basic for cortical functioning in general, culminating in the concept of modular organization of the neurons.

I.2.2.2.2. Columnar arrangements

Superimposed on the tangentially orientated layer pattern of the cortex is a radial arrangement of the cortical neurons, extending from the surface of the cortex down across all layers.
The first to mention such an arrangement was Lorente de No in 1938 [42], using Golgi stained cortical material of various rodents. The first physiological evidence of a vertical organization in the neocortex was presented by Mountcastle in 1957 for the cat [43], and later for the monkey [44]. Using a microelectrode, he demonstrated that in a somatosensory region, all neurons, situated along a radial penetration, were activated by sensory stimulation in the same modality, e.g., light touch on the skin of a finger or joint movement of the same finger. However, when a microelectrode was moved parallel to the cortical surface, the modularity of the neurons changed regularly.
Mountcastle referred to a cluster of functionally related neurons as a column. The term has since been used to refer to a number of similar relationships in auditory and visual cortical areas, as well as in motor and association cortices. Vertical units, or columns, are defined in three general ways: by the input characteristics of the neurons (what stimuli are effective in activating the neurons); by the output characteristics and by the pattern of connectivity with other parts of the central nervous system. In the 1972 Ferrier lecture [45], Hubel & Wiesel presented evidence of a functional vertical organization in the primary visual cortex. They described cells with common physiological properties to be grouped together in vertically organized systems of columns. Within such a column, information from preferentially one of the two eyes is processed: the ocular dominance column. Using four independent anatomical methods it has been shown that these columns have the form of vertically disposed alternating left-eye and right-eye slabs, which in horizontal section form alternative stripes of about 400 micron thick, with occasional bifurcations and blind endings. This type of columnar arrangement is defined by the pattern of axonal input to a region of cortex.

A similar arrangement also exists in the motor and premotor cortex, but here the boundaries of the columns have been demonstrated by observing the response after electrical peripheral stimulation, using microelectrodes. Microstimulation throughout the depth of the cerebral cortex here produces contractions of the same muscles, with the lowest stimulus threshold in layer V, the layer where the corticospinal fibers originate [46]. In the association cortex, columnar organization related to the sensory stimuli that activate the neurons has been described in the prestriate and temporal visual areas [47].

Not only physiological evidence exists for a 'columnar' arrangement of functional neurons, but also anatomical: Proof that predominantly vertical connectivity can be demonstrated is already found in the work of Lorente de No in 1922 [48]. More direct evidence for the concept of a 'cortical module' as developed by Szentagothai [49], only came after the becoming available of information about specific inhibitory elements and after the traditional view of neurons working strictly in chains was abandoned. The concept of a columnar cortical module was reinforced after the demonstration of column-wise ending of corticocortical projection fibers: after injection of a radioactive tracer in the frontal lobe ([3H]leucine and [3H]proline; dorsal bank of the principal sulcus in a 4-day old rhesus monkey), well defined columns, 200 - 500 micron wide, with different degrees of radiolabeling could be observed in the ipsilateral retrosplenial cortex. "Spatial periodicity in the pattern of transported label in such regions as the prefrontal association cortex, the retrosplenial limbic cortex and the motor cortex indicates that columnation in the intracortical distribution of afferent fibers is not unique to sensory specific cortex, but is instead a general feature of neocortical organization [50]". More anatomical support for the concept of a columnar organization came from studies, demonstrating a columnar aggregation of cortical cells projecting to the thalamus [51]. These type of studies gave rise to the idea, that the immense plate of the neocortex is subdivided into a mosaic of quasi-discrete spaced units, the cortical columns. The whole human neocortex would contain about 3 million of such modules [52]. Comparison of the column width of corticocortical projections between the squirrel monkey and the rhesus monkey, showed surprisingly similar dimensions. The fourfold increase in neocortical volume of the rhesus versus the squirrel monkey suggests that the phylogenetic expansion of the neocortex in cortical surface area is accompanied by an increase in number of afferent fibre columns [53], echoing an earlier finding that, despite the marked difference in the cortical thickness in different species (mouse, rat, monkey (Maccaca mulatta) and man), the total number of neurons below a standard cortical surface is fairly constant [54]. The increase in number of cortical columns with the level of phylogenetic development may reflect the increasing computational and information processing capacity of

the cerebral cortex in the course of evolution.

I.2.3. Intracortical connections

Although there exists a large variation in the cyto- and myeloarchitecture in the neocortex, attempts have been made to draw 'wiring' diagrams of the intracortical circuits, thought to be basic for cortical functioning in general, culminating in the concept of modular organization of the neurons.

The presence of well organized interlaminar and intralaminar connections in the cortex have been demonstrated by Golgi studies as well as by a number of degeneration- and axoplasmatic transport studies. Pronounced vertical, interlaminar and intralaminar projections from superficial to deep layers (particularly from layers II and III to layer V) have been known for some time. Quite extensive lateral, intralaminal connections, mainly in layers III and V also were demonstrated. Axoplasmatic transport methods have revealed that intra-areal connections are patchy, i.e., commonly in the form of multiple column-like foci with intervening unconnected regions [55]. From work on the visual cortex of the cat, the following pattern of intra-cortical connectivity could be obtained [56]:

-1 non-pyramidal cells of L IV have predominant axonal ramifications ascending into layers L II and L III.
-2 pyramidal cells with their somata deep in L III have axons projecting to other areas and give rise to a substantial number of collaterals in both layers L III and L V.
-3 The pyramidal cells of the layers L II and L III issue numerous ascending collaterals into layers II and I.
-4 The pyramidal neurons of layer V all project outside the cortex, but most of these neurons have substantial collaterals to L VI and also to L III.
-5 the axons of the modified pyramidal neurons of L VI are provided with collaterals, that ascend and terminate densely in L IV.

I.2.4. Corticocortical connections

Cortico-cortical connections interconnect different cortical areas and are known as association and commissural fibers. Commissural fibers [57] interconnect areas in two hemispheres, by crossing the Corpus Callosum, the caudal part of the anterior commissure and the hippocampal commissure. The association systems are subdivided in long and short fibers. The short fibers interconnect neighboring areas or remain inside the grey matter. The long association fibers constitute the connection systems between different, non-neighboring parts of the cortex or between cortical areas. In the brain corticocortical connections adhere to some general principles of organization [58]:

-1: there are fibers, connecting the primary sensory areas with the unimodal parasensory association areas.
-2: The unimodal association areas are connected with the multimodal sensory areas.The long association fibers connect the modality-specific parasensory association cortex and the multimodal areas with the premotor and the prefrontal cortex. Between the prefrontal, the premotor and the motor cortex the connections are made by the short association fibers.
-3: The connections from the parasensory and multi-association cortices and the prefrontal cortex to the limbic structures pass through the cingulate gyrus, the hippocampal gyrus and the insula. The pathways from the paralimbic association cortex of the cingulate gyrus and the caudal parahippocampal gyrus to the hippocampal formation pass through the perirhinal and entorhinal cortices. The insula projects on the olfactory limbic areas.
-4: As a rule, the majority of the commissural fibers are reciprocal.
-5: Connections from the primary sensory areas to their neighboring association areas usually originate from the supragranular layers and terminate in and around layer IV. This projection is known as the forward projection of information whereas the reverse projection (backward projection of information) is directed from the infragranular layers to the molecular layer (L I).
-6: Homotopical commissural fibers connect the same areas in both hemispheres, whereas heterotopical commissural fibers connect one cortical area with other cortical areas in the contralateral hemisphere.
-7: The commissural and association fibers terminate and originate in a columnar fashion. These "columns" are typically 200-1000 micron wide.
-8: The interruption of the commissural or a s s o c i a t i v e

connections between uni-modal, multi-modal and paralimbic association fibers may lead to the so called 'disconnection syndromes' [59].

These somewhat general remarks on the associative and commissural fibers can be applied to one specific sensory modality, e.g. the visual system or the auditory system.
The architectonics and the intrinsic connections of the cortical systems were recently reviewed by Yeterian and Pandya [60].
The important point is that from the primary sensory areas, which receive their information input largely from nuclei of the thalamus, e.g. the corpus geniculatum mediale for the auditory information system, the information is transfered to other cortical regions, the association areas.
This information is received in the primary sensory area by neurons of L IV, but as is stated in the paragraph on the columnar organization of the cortex, also a thalamocortical projection exists which projects somewhat more diffusely among all cortical layers.

I.2.4.1. Corticocortical connection schemes

To review cortico-cortical connection schemes, a parcellation of the neocortex is used, based on the connections of one cortical area with other cortical areas. This subdivision is particulary useful in describing the sensory systems of different modality and the flow of information through these systems.
A recent review is given by Pandya et al. [61].

a) Corticocortical connections of the auditory system

The primary auditory area (AI), receiving its input from the corpus geniculatum mediale consists of Area 41 and Area 42, located in the supratemporal plane of the temporal lobe in the rhesus monkey and in Heschl's gyrus in the human. The information is transported to the secondary auditory region (AII) and next to the more laterally situated auditory association area (AA1). These areas are thought to be situated whithin three strips or 'belts' laying between the sulcus limitans insulae and the Sulcus Temporalis Superior and covering the superior temporal gyrus to the temporal pole. These belts are referred to as the 'root', containing the AI, the 'core', with the AII and the 'belt' with the auditory association area AA1. In each of these belts at least four centers of integration are situated. The information is projected forward from one center to another within one belt but also between the three belts themselves. The connections between these centers are of a reciprocal nature. Following the forward projection leads the information to arrive in the proiscortex of Area 38, from which it

is projected on Area 28, the entorhinal cortex [62].

b) Corticocortical connections of the visual system

As in the auditory system, within the visual system there are sequential patterns of connectivity that show systematic laminar origins and terminations. Thus there is a stepwise series of forward connections relating Areas 17, 18, 19, 20, 21 and the temporal cortex, Area 38. These forward projections have their origin primarily in L III, with terminations in and around L IV of the rostral adjacent regions. There are reciprocal connections which originate from neurons in L V and L VI and terminate in L I of the caudally adjacent regions. As described above for the auditory system, in addition to a sequential forward set of connections, there exists a set of reciprocal connections within the parahippocampal gyrus, progressing to the visual areas of the occipital lobe.

c) The somatosensory system.

The cortical sensory system is located within the parietal lobe. The primary somatosensory area of the postcentral gyrus is composed of Brodmann's area 3-1-2, and has major thalamic connections with the ventroposterior nuclei [e.g. 63].
The somatosensory association areas are located more caudally, the regions Area 5 and Area 7.

d) long corticocortical connections [64] involving:

Cortical auditory areas
The belt zone of the auditory association region is divided into three major sections on the basis of the differential long corticocortical connections: AA1, AA2, AA3, from caudal to frontal, i.e. the first-, second-, and third-order association areas.
AA1 projects to the dorsal periarcuate cortex (Areas 8 and 9), AA2 to the prearcuate region (Areas 46 , 9 and 10), and,
AA3 projects to the Areas 12, 13, 25 and 32.
Each cortical auditory area has distinctive paralimbic projections. AA1 sends fibers to the caudal portion of the gyrus cinguli , Area 23, and the medial part of Area 7 (the supplementary sensory area (SSA). AA2 projects to areas of the gyrus parahippocampalis and AA3 sends fibers to the perirhinal Area 35.

Cortical visual areas
The visual association areas are analogous to the auditory areas divided in primary (VA1 = Area 19), secondary (VA2 - TE2 and TE3, visual areas in the lower temporal lobe,) and tertiary (VA3 - temporal pole (= Area 38) + TE1) associations areas.

VA1 projects to the arcuate region (Area 8),
VA2 to the prearcuate region (Area 46), and,
VA3 to the ventrolateral and orbital frontal (e.g. Area 11) regions. As with the auditory association areas, the visual association cortices also project to the lobus frontalis, to the superior temporal sulcus, and to paralimbic (parahippocampal and perirhinal) regions.
VA1 projects to Area 8 (lobus frontalis), to the superior temporal sulcus (OAa) and to the caudal area of the gyrus parahippocampalis (Area TF and TL)
VA2 projects to the ventral part of Area 46 in the frontal lobe, to the superior temporal sulcus (caudal part of region TEa) and to the rostral part of the gyrus parahippocampalis.
VA3 sends its fibers to Area 11 in the frontal lobe, to the superior temporal sulcus (STS) (especially to the rostral part of region TEa and the proiscortex of the temporal pole) and to the caudal part of the gyrus parahippocampalis (TF,TL).

Cortical Somatosensory areas
The somatosensory areas in the superior parietal lobe (SPL) and the inferior parietal lobe (IPL) contain the three somatosensory association areas , SA1, SA2 and SA3. The SA1 sends its fibers originating from the SPL to Areas 4, 6 and the supplementary motor area (MII). SA1 of the IPL projects to the ventral part of Area 6 and the frontal opercular region. From the SPL, SA2 sends its projections to the rostral part of Area 6 and to MII. SA3 of the SPL projects to the most rostral part of Area 6 and to the dorsal part of Area 8. SA3 of the IPL projects to Area 46.
The association areas of the parietal lobe also project to the superior temporal sulcus, and to the paralimbic regions [65].

I.2.5. Diffuse corticopetal projections

In AD, changes in the content of the neocortex of various neurotransmitters has been found. These neurotransmitters are mainly transported along corticopetal projection systems. Examples are the cholinergig fibers originating the cholinergic nucleus of the basal forebrain, the adrenergic fibers from the locus coeruleus. The cortical organization of these projection systems are briefly reviewed in the following sections of this chapter.

I.2.5.1. Acetylcholine (ACh) projections to the neocortex.

Markers for the projection of Cholinergic fibers to the neocortex are the immunoreactivity for the ACh synthesizing enzyme, Choline Acetyltranferase (ChAT) and the activity of the degrading enzyme Acetylcholine esterase (AChE).
Ninety-six percent of the nucleus basalis neurons that project to the neocortex contain ChAT. These projections from the cholinergic component of the nucleus basalis (Ch4) are topographically organized so that each cortical area receives most of its cholinergic input from a different Ch4 sector [66].
In primates, regional variations in cortical cholinergic innervation are apparent, with the hippocampus, amygdala and piriform regions showing the highest levels of cortical AChE-fibers. The paralimbic regions such as the insula, caudal orbito-frontal cortex, the temporal pole, and the parahippocampal gyrus receive more cholinergic innervation than the adjacent association cortical areas [67, 68, 69]. The same AChE-distributions have been demonstrated in the human except for the paralimbic region of the cingulate cortex, that contains high levels of cholinergic markers in the human but not in the monkey [70].
In one of the more detailed studies [71], devoted to the primate brain, Mesulam reported on the neocortical distribution of AChE distribution in Maccaca Mulatta. In this study it was described that there are marked regional variations in the laminar distribution and intensity of acetylcholinesterase containing fibers in cortex. These fibers were particularly prominent in the five major paralimbic regions of the brain: the insula, the caudal orbito-frontal cortex, the temporal pole, the cingulate gyrus and the parahippocampal region. Within these five areas, the part of cortex which is adjacent to allocortex contains most acetylcholinesterase and there is a gradual decline towards the granular isocortex. The primary sensori-motor areas have different distinctive laminar patterns of enzyme distribution. For example, primary visual, auditory and somesthetic konio-cortices are characterized by a salient band in layer IV. On the other hand, motor and premotor areas are characterized by a concentration of radially arranged Ach-esterase positive fibers within the deeper layers of cortex. High order sensory association areas throughout the cortical mantle consistently contain the least amount of acetylcholinesterase-positive fibers. It is conceivable that these patterns reflect regional variations in the distribution of cortical cholinergic innervation. In a recent study on the distribution of different neurotransmitter systems in the human cerebral cortex, Javoy-Agid [72] demonstrated ChAT activity to be distributed throughout the entire cerebral cortex. The cholinergic marker was most dense in the temporal and post- and paracentral areas, and on the orbito-frontal surface, and least dense in the occipital lobe. These results are in keeping with those reported

previously [e.g. 73].
Laminar variations of cortical cholinergic innervation exists among different regions within and across species, but no conclusive remarks can yet be made on this issue [74]. For instance, in the rat cerebral cortex 13 different laminar patterns of ChAT staining can be found [Lysakowski et al, 1989].
In human controls, the ChAT-activity is highest at the level of layers II and IV of the temporal and frontal cortex, whereas in Alzheimer's disease the topographical laminar distribution of ChAT-activity seems completely lost [75, 76]. No data on the laminar distribution of ChAT-activity in the parietal and occipital human cortex are available.
Single reports are available, demonstrating in rat the existence of a reciprocal, descending projections from the neocortex to the basal forebrain [77]. This observation finds its reflection in the primate brain in the study of Mesulam and Mufson [78]: they reported that the basal forebrain cholinergic neurons of the monkey appear to receive input from only a limited number of cortical areas.
Concerning the question of the amount of neocortical surface innervated by one cholinergic neuron in the Ch4 area of the nucleus basalis the only information available, is based on rat material. Because the basic organization of the neocortex is strictly conserved in the mammalian series for as far the columnar organization is concerned, these non-primate data are remembered here. In two of these studies, the diameter of this area was reported to be small: about 1.5 mm [79,80]. In another study by McKinney, this area is reported to be somewhat larger [81].Because in Alzheimer's Disease a large change in cortical surface is demonstrated in this study, an interesting question could be the possible relationship between volume changes in the neocortex and neuropathological changes in the nucleus basalis.

I.2.5.2. Monoaminergic projections to the primate cortex.

The distribution of the catecholamines (CA) dopamine (DA) and Noradrenaline (NA) is largely based on inferences from observations made in animal models, generally rodents [82, 83, 84], and more recently in human primates. However, major differences in the intracortical distribution of the CA innervation, particularly the dopamine innervation, have been demonstrated between these two species. According to the theory of Morrison et al. [85] the greater differentiation of primate cortex in comparison to the rodent is parallelled by a specialization of the LC innervation. Thus, inferences from the rodent to the human brain as far as noradrenergic innervation is concerned, seem less warranted. Therefore, only information on primate brain is considered in this paragraph.

I.2.5.2.1. Noradrenergic neocortical fiber distribution

Until now, no intrinsic noradrenergic neuronal cell bodies are found within the neocortex. Most, if not all of the NA innervation of the cerebral cortex originates in the nucleus locus coeruleus, an elongated brain stem nucleus in the floor of the fourth ventricle. The NA containing neurons of the locus coeruleus project diffusely to the cortex in the monkey [86].
In a recent study on monkey brain, Lewis et al. [87] investigated the distribution of dopamine -beta- hydroxylase (DBH) immunoreactive fibers in the prefrontal regions Area 9, Area 11, Area 12, Area 13, Area 24, Area 25 and Area 46. The density of DBH-immunoreactive fibers exhibited substantial heterogeneity, both across and within cytoarchitectonic regions of the cortex of the Cynomolgus monkey. The density in Area 8 was the highest, followed by Areas 9 and 24. The Areas 11, 12, 13 and 25 were of intermediate density, and proportions of Areas 10 and 46 had the lowest density of immunoreactive fibers. In their analysis of the laminar distribution pattern of these fibers in the cortex, it was noticed that this distribution was very similar across cytoarchitectonic areas of the frontal cortex in the Cynomolgus monkey. L I contained a low density of labeled fibers, the deep portion of L III had a slightly greater density of labeled fibers than did L II and the superficial part of L III. The density in labeled fibers increased substantially in layer V. This density decreased in layer VI. In this study, two species were analyzed: the cynomolgus monkey (Maccaca Fasciolaris) and the squirrel monkey (Saimiri sciureus). Species comparison showed similar topographic patterns in the distribution of DBH-immunoreactive fibers. The laminar distributions of labeled fibers were very similar in both species, although minor differences existed.
This may be important to realise when comparing fiber distribution of the projections of the locus coeruleus with the laminar distribution of SP, NFT and CAA in the AD patient.
However, due to the recent study of Gaspar et al. [88] the regional and laminar distribution patterns of the catecholamineric fibers in the human cortex are known. They studied DBH-immunoreactivity in 13 cytoarchitectonic areas (Areas 4, 6, 9, 3, 5, 40, 17, 18, 23, 24, 29, insula and hippocampus). The noradrenergic innervation displayed a characteristic density gradient in the neocortex (the highest in the primary sensory-motor areas, decreasing rostrally and caudally) that contrasted with the more uniform density in the limbic cortices (Areas 24, 23, 29, insula): The prevailing pattern of the DBH-IR was characterized by a peak around the principal sulcus in the primary motor (Area 4) and primary sensory area (Area 3), where the density of fibers was maximal, with decreasing gradients rostrally and caudally. A moderate to low immunoreactivity was found in the secondary motor area (Area 6) and

throughout the limbic associated cortices (Areas 23, 24, 29, insula, hippocampus). The lowest DBH-IR fiber density was found in the prefrontal cortex (Area 6), the visual Areas 17 and 18 and the gyrus supramarginalis.
With respect to the laminar density and organization, the DBH-IR fibers tended to be rather uniformly distributed throughout L I-L VI, with a slight preponderance in L III and L V, and relatively lower number of fibers in L I. There were subtle differences in the extent of DBH-IR innervation in L IV: it was dense in the parietal Areas 3-1-2; moderate in Areas 9 and 23; and only partial in the primary visual cortex (upper part of L IV only). Another prominent feature was the presence of long horizontal fibers usually found in the superficial (subpial) part of L I, in layers L V- L VI, and to a lesser extent in L III. Vertical fibers were more frequent in L II and L III; some ascended from the infragranular to the supragranular layers or reached the pial surface, where they occasionally bent to follow an horizontal direction.
Important to note is the decline of density of the fibers with the age of the subject investigated and the fact that the DBH-immuno-staining varied significantly in the amount of fibers stained.

I.2.5.2.2. Dopaminergic innervation of the cerebral cortex.

Cortical DA projections are much more widespread in nonhuman primates than in rodents [89]. The dopaminergic innervation of the primate cortex is particularly striking in motor areas [90], but also involves the remainder of the cortical mantle [91, 92].
In a study on the distribution of various neurotransmitters in human neocortex [93], substantial amounts of DA were detected. The DA levels varied considerably: DA concentrations were highest in the temporal and the prefrontal cortex, and decreased along the fronto-occipital axis. The concentrations found were 3.6(1.1) in the prefrontal areas, 6.7(1.3) in the frontal areas, 17.6(2.5) in the temporal and 4.2(1.3) ng per gram cortex tissue (SEM), demonstrating clearly the heavy DA innervation of the temporal cortex.
In the study of Gaspar et al. [94], the regional and laminar distribution of immunoreactivity for tyrosine hydroxylase (TH-IR), the rate-limiting biosynthetic enzyme for DA, was investigated in the human brain. In this study, the maximal numbers of TH-IR fibers were found in the agranular (Areas 4, 6, 24) and dysgranular (insula) cortical areas lacking a distinct L IV. The primary motor cortex (Area 4) and the anterior cingulate cortex exhibited the most dense innervation. In all these agranular areas, the TH-IR fibers was present in all layers, but most prominent in L I and L V-VI and occasionally formed small, local accumulations in L II - III. The density of TH-IR innervation was consistently lower in the granular cortical areas: Area 9, postcentral, posterior cingulate, supramarginal gyri and occipital cortex (lowest

density). Within these cortical areas, changes in density of the TH-IR network appeared to follow the boundaries between cytoarchitectonic areas. In all these granular cortices, there was a clear cut bilaminar pattern of distribution: TH-IR fibers showed a marked predilection for L I and L V -VI and were far less numerous in the intermediate layers L II, L III and L IV.
In conclusion, the relative complexity of the DA innervation of the human neocortex reflects the increased cortical differentiation and specialization as expressed in the considerable expansion of the DA terminal fields, in comparison with the rodent brain and in the predominance of DA innervation in the motor and anterior cingulate areas.

I.2.6. Cortical neuron number

Several quantitative studies have shown that cell density may vary in different laminae and in different areas of the neocortex in the same brain and between different species [95, 96, 97]. This complicates the way, in which the total nerve cell number of the cerebral cortex can be estimated. The same problems, apply to the determination of the total cell number in part of the cortical structure.

Only absolute neuron numbers, not neuron concentrations, are of interest to answer to the question of neuron loss in the cerebral cortex in AD, because change in volume has no effect on these data, in contrast with neural densities.

Estimation of neocortical neuron number necessitates a reliable determination of cortical volume. In the literature, one on the most reliabe estimation of total neuron number in the cortex is given by Haug, because his study an effort was made to correct for concomiitant change in volume [98].

The early estimates of the total neuron number are presented in Table III.

I.3. NEUROPATHOLOGICAL FINDINGS IN ALZHEIMER'S DISEASE

I.3.1. Macroscopical changes of the cerebral cortex in AD

The most conspicuous neuropathological change in the brain of a patient, suffering from AD is a global cerebral or more precisely cortical atrophy. Mostly, this atrophy is described by assessing shrinkage of the gyri and widening of the sulci. This atrophy is noticed particularly within the frontal and temporal lobes though sometimes it extends into the parietal and occipital regions. A more general distribution of neocortical atrophy is frequently seen in younger patients (<65 years), though only few older (>80 years) patients show such a general pattern of atrophy. In the group of older patients, the atrophy is more confined to the temporal lobe [99, 100, 101].

I.3.2. Microscopical changes and their distribution

I.3.2.1. Neuron loss in the cerebral cortex in aging and AD

The extent of neuronal cell loss in the cerebral cortex in AD is controversial [102]. Hodge described in 1894 [103] cell loss during normal aging. Early systematic studies of specific areas of cortex showed no significant loss of neurons in dementia compared to controls [104] though later studies showed loss of large neurons in the cortex [105]. Whereas Terry [106] recorded a 40% reduction in neurons larger than 9.5 micron in diameter in the frontal cortex and a 46 % decrement in the temporal region, Mountjoy [107] found deficits to an average of 23 % in the frontal and 31 % in the superior temporal gyrus. Hubbard and Anderson [108] also found neuronal loss in AD and they recorded the volume of neurons larger than 12 micron diameter of the cortex to be reduced by 26 % for the frontal and 33% for the temporal gyrus. The small neurons were found unchanged in this study [109]. This is in contrast to the study of Braak et al.[110], in which the small, non-pyramidal neurons are preferentially reduced in number in AD.

One of the main difficulties is that, until now, no reliable figures concerning absolute cell number in the neocortex are available. Studies reporting cell loss in the neocortex or in particular cortical fields are generally based on a decrease of cell densities.

I.3.2.2. Neurofibrillary changes

Ultrastructural examination showed the neurofibrillary tangle to consist of mutually twisted structures known as Paired Helical Filaments (PHF). These PHF are not specific for Alzheimer's Disease but also do occur in Down's Syndrome (DS) and other diseases and even in normal aging, be it to a much slighter degree. Immunologic techniques demonstrated cross reactivity between PHF and components of the normal cytoskeleton: neurofilaments and the so-called microtubule-associated proteins (MAP's). Map-Tau (a collection of proteins enhancing microtubular formation) probably is the most important component of the PHF and has been shown to be phosphorylated in an abnormal fashion. These Tau-antibodies are also known as Alz-50. Because of the topographical distribution of neurons containing NFT, it has been suggested that staining for Alz-50 may mark an early point in cellular pathology, before the occurrence of irreversible and degenerative changes. Recently it has been demonstrated that the accumulation of abnormally phosphorylated Tau precedes NFT-formation. Alz-50 immunoreactivity appeared to be present in NFT, that reacted positively with

antibodies directed against ubiquitine: ubiquitine-binding on PHF might point to an unusual degree of resistance of these proteins against intracellular breakdown. The Alz-50 antigen (also indicated as the A68 protein), Tau and ubiquitin occur both in Pick-bodies - the neuropathological characteristic of Pick's Disease- and in Lewy-bodies -the neuropathological hallmark for diagnosing Parkinson's Disease. They are considered a general neuronal reaction to the presence of abnormal intracellular structures. These alterations of the cytoskeleton may impair intraneuronal transport of proteins and organelles and therefore the overall functioning of the nerve cell.

I.3.2.3. Senile Plaques (SP)

Morphological (light and electron microscopy) studies of SP have revealed that the SP consist of three elements: dystrophic and degenerating nerve cell processes, reactive non-neuronal cells (microglia, phagocytes), and amyloid. It is the particular arrangement of two of the three components in a particular senile plaque that determines its type. The first type is made up of darkly stained rods and dots in Bodian-stained material, and wisps of amyloid between normal and abnormal neuronal and astrocytic processes (as seen in Congo Red staining in fluorescence microscopy). This type of plaque is called a "primitive plaque". Plaques with a central core of amyloid surrounded by degenerating and dystrophic neurites are called "typical" or "classical" plaques. Plaques made up almost exclusively of amyloid material are called "amyloid plaques" or "burned out plaques" [111].
Recently, attention was drawn to a type of SP which differed significantly from the three types described above and which is characterized by slight densification of the neuropil but without the obviously altered neurites and without amyloid deposition at the light microscopic level [112]. This plaque is denoted as "plaques A". It is unknown whether the various types of plaques represent the same structure in different stages of development or are structures in their own right.

I.3.2.4. Congophilic angiopathy

Amyloid angiopathy, an important alteration encountered in AD was described as the "plaque-like angiopathy" by Scholz in 1932 [113]. The other form of cerebrovascular amyloidosis was described by Pantelakis in 1954 as " congophilic angiopathy" (CA) [114]. The two forms differ essentially as to the type and location of the vessel involved. In congophilic angiopathy, leptomeningeal vessels are mainly affected and the amyloid is confined to the vessel wall (especially the media); in plaque-like angiopathy intrinsic cortical vessels are involved and the deposits infiltrate adjacent

nervous tissue [115].
Because the presence of amyloid has been demonstrated in both the vessel wall (congophilic angiopathy) and the senile plaque and because the green birefringence under polarized light after alkaline Congo Red staining [116] has been demonstrated both in SP and CA, a possible relationship between amyloid, SP and CA was suggested by several authors: Schwartz believed the amyloid of SP to originate by seepage through cortical blood vessels [117], which was later substantiated by the findings of Powers and Skeen [118]; these authors demonstrated evidence of multiple plasma proteins in the amyloid core of senile plaques, indicating a probable origin from pathological changes of vascular permeability. It appeared possible to demonstrate the presence of gammaglobulin and albumin in the amyloid of plaques in a minority of cases of dementia, suggestive for an indiscriminate macromolecular leakage [119]. This suggestion was made earlier by Morel in 1952, who postulated an increased permeability in capillaries showing vascular amyloid [120]. Other investigators, however, such as Divry were unable to show any correlation between vascular amyloid and the development of senile dementia [121]. Isolation of microvessels from AD patients made a characterization of the amyloid material feasable [122]. This appeared to consist of a protein of 4200 dalton with a unique aminoacid composition and sequence. Antibodies to a synthetically derived peptide encompassing the first 10 aminoacids of this sequence were shown to label not only these parenchymal microvessels affected by congophilic angiopathy but also the amyloid core of senile plaques [123]. The amyloid found in congophilic angiopathy is very similar to the amyloid core isolated from NFT [124]. The similarity of these various types of amyloid, found in AD led to the hypothesis of " multiple cerebral amyloidosis" [125], which postulates the presence of a circulating amyloid precursor passing from the blood through injured cerebral microvascular endothelium, resulting in vessel wall amyloid deposition (in the form we detect as congophilic angiopathy), and amyloid deposition within the neuropil in the core of many senile plaques. The same theory proposes that the identical amyloid precursor is toxic to neurons and causes the formation of intra-cytoplasmic neurofibrillary tangles (NFT) [126].
Ultrastructural analysis of amyloid fibrils by Miyakawa et al. [127] showed amyloid masses, seen around the blood vessels by light microscopy, to consist of numerous amyloid fibrils spreading as a radial structure from the walls of the blood vessels to the brain parenchyma. Amyloid fibrils forming the core of senile plaques existed around the blood vessels. Using immunogold labeling, Ikeda et al. [128], showed that a monoclonal antibody to a synthetic peptide, consisting of residues 8 to 17 of the amyloid beta protein, labeled the amyloid fibrils in cerebral blood vessel wall and SP.

I.3.2.5. Granulovacuolar degeneration (GVD)

In his classical description of neuro-pathological changes in Alzheimer's Disease, published in 1911, Simchowicz gave the first description of Granulovacuolar Degeneration (GVD), to which his name is connected [129]. This pathological feature, which was originally observed in Ammon's horn of the hippocampus in senile dementia, was described as follows:

"It concerns the localization of large, round or oval granules in the pyramidal cells. Every granule is situated in a vacuole. Sometimes only 2-3 granules are visible in the cell, but often the entire cell body is completely filled by these granules and also in the protoplasmatic protrusions, most often in the tampered protrusions are these vacuoles with the containing granules observed."

Of interest is, that in this original publication, Simchowicz mentions the absence of granular degeneration from the neocortex. Furthermore, a relationship was suggested between the GVD and the neurofibrillary tangle (NFT). In some hippocampal pyramidal cells, this degenerative change was noticed to coexist in neurons with the neurofibrillary change of the Alzheimer type.
The limitation of GVD to the hippocampus has been reported repeatedly by modern investigators such as Ball and Low [130, 131]. According to them, the affected cells present one or more (up to 20) clear, rounded vacuoles measuring 3-5 micron in diameter, each containing a single hematoxylin-eosinophilic, argentophilic granule, 0.5-1.5 micron in width. A high degree of negative correlation was found between the density of neurones/mm^3 of hippocampal cortex and both the number of neurones with neurofibrillary degeneration and the number of neurons with granulovacuolar degeneration in the hippocampus. Therefore, the functional significance of the latter changes is probably greater than previously assumed, given the diminished number of surviving neurones in which these alterations appear [132]. Furthermore, because of the relationship between the frequency of GVD and neuron loss (Ball & Lo, 1977), the occurrence of the GVD could be linked with the degeneration of these cells, which are known to be involved in memory processes.
GVD was reported to be present in other structures of the brain such as the nucleus basalis of Meynert [133], but not in the neocortex.
Immunohistochemistry showed the granules to possess a tubulin-like immunoreactivity suggesting that GVD, like the Senile Plaque (SP) and the NFT, may involve an abnormality of the cytoskeletal structure of the neurons [134]. A monoclonal antibody, raised against extracts from Alzheimer brain, that recognizes a phosphorylated epitope in high molecular weight neurofilament proteins and tau proteins, also immunostains GVD. This finding

suggests that GVD contains phosphorylated proteins, possibly due to autophagy of phosphorylated perikaryal proteins that are increased in Alzheimer's disease [135].

I.3.2.6. Hirano bodies

Eosinophilic, ovoid or spheroidal structures which frequently appear hyaline, though sometimes distinctly striated are called Hirano bodies. Hirano bodies are frequently seen in the hippocampus being present there in most old people and especially so in AD patients [136]. In our study of the neocortex, Hirano bodies were never observed, therefore these structures are not further discussed here.

I.3.3. Neurochemical changes

I.3.3.1. Changes in neurotransmitters in the cerebral cortex in Alzheimer's disease.

In AD, changes in the density of fibers containing different neurotransmitters are mentioned inthe literature. In this section changes in two neurotransmitters are briefly reviewed.

Monoaminergic changes.
Monoaminergic changes have been reported in AD: early studies using fluorometric assays revealed reduced concentrations of norepinephrine in the neocortex and hippocampus [137].These observations were later confirmed [138,139].The Dopaminergic, serotonergic and noradrenergic afferents to the cerebral cortex originate, respectively from the ventral tegmental area, the dorsal and medial raphe nuclei, and the locus coeruleus [140]. It has been known for a long time that these cell groups contain NFT in AD [141, 142]. Recent studies have emphazised this distribution and its close correlation with pathological degrees of cortical degeneration [143, 144, 145].

Acetylcholinergic changes.
In 1979 and the following years it had become apparent that the major source of cortical ACh was the nucleus basalis Magnocellularis (Meynert) and its associated cell groups [146,147]. Three years earlier a substantial depletion of biochemical markers of cholinergic innervation of the cerebral cortex was demonstrated in AD [148,149]. Histochemical studies of the cholinergic fiber projections to the cerebral cortex in AD suggest these fibers to contribute to SP formation in the cerebral cortex [150,151].

I.4.1. The distribution of Senile Plaques.

I.4.1.1. The regional distribution of Senile Plaques as reported in the literature.

Senile plaques were originally referred to as miliary plaques (Redlich [152]). They were first described by Blocq and Marinesco [153]. In the early studies, a preferential localization of SP in the superficial layers of the cerebral cortex was noticed, particularly so in the banks [154] and the depths of the sulci [155,156].(These findings, however must be taken cautiously: the geometrical properties of the cortex, as explained in the section on cortical geometry, prompts this type of results.) The two reports last referred to, also demonstrated a preferential localization in the layers III and V. Regional differences in SP distribution were demonstrated by Mandybur [157]. Plaques were also demonstrated to occur in small numbers in the subcortical white matter [158]. No right-left [159] and no male-female [160] differences were observed.

As an age related change, the Senile Plaque was first described by Simchowicz [161]. The first occurrence of SP in the fifth decade of life [162] and the subsequent increase in number with normal aging [163] were reported.

In a study of the hippocampus and all four lobes of brains, a predilection for the parahippocampal and occipito-temporal gyrus, with less frequent involvement of the frontal and insular cortex were reported [163].Tomlinson et al. [157], who also compared the four lobes of the brain, noted in this respect the presence of SP in the occipital lobe. He observed that, in general, when more than two SP per high power field were present in this location, all four lobes of the brain are involved.

In demented individuals, the full extent of the distribution of the senile plaque is seen, with patients with AD showing a higher density of SP in any single cortical area as well as an even more increased frequency throughout the areas of predilection [165].

In an early quantitative study of the hippocampus and of the frontal lobe, no significant difference in the density of SP in SDAT was noticed when compared to controls [164]. This result was confirmed later by Tomlinson et al. [157]. However, other authors demonstrated a significantly increased number of SP in SDAT in these regions [165].

Of all cortical regions, the senile plaque is reported most frequently in the temporal lobe, with the highest concentrations in the association cortices of the middle and inferior temporal gyri [166]. In the same study, Goodman described the SP distribution in 9 cortical areas in AD and found the three lowest SP counts in the primary motor (Area 4), primary sensory (Area 2-

1-3) and the primary visual area (Area 17). In the frontal lobe (Areas 10 and 44) a higher SP count was found than in Area 4, with Broca's area showing the highest average plaque count.
In the study of Jamada et al. [161], SP densities were measured in six cortical areas: Area 9 (26.3), Area 4 (15.5), Area 38 (29.2), Area 7 (13.4) Area 19 (25.0) and Area 24 (27.1). The concentration of SP per square millimeter is put between brackets. There was considerable variability in the relative involvement of the various areas, but in general the prefrontal and cingulate fields had the highest SP counts, the association areas being next highest, and the primary motor cortex lowest.
In four AD cases, similar quantitative measurements of density of SP in the Areas 9, 24, 41-42, 17, were obtained in a more recent study [167].
In a qualitative study of a much larger sample of cortical areas, Brun et al. [168], graded the severity of cell loss, SP, NFT, gliosis and spongiosis on a four point scale. In this study a similar variation of severity and distribution of the degenerative features was noticed from case to case. The results of this study were in general agreement with the study of Jamada et al. [161].
A consistant finding was a severe involvement of the medial temporal lobe cortex, followed by the higher order polymodal association cortices of the temporal lobe, and a severe involvement of the higher-order polymodal association areas of the cingulate gyrus and the parietal and frontal lobes. In some cases, there were moderate to severe changes found in the unimodal association areas, but in all cases examined, the areas, which demonstrated the fewest changes were always the primary sensory and motor cortices.

I.4.1.2. Laminar distribution pattern of Senile Plaques

Although the earliest studies on the distribution of SP suggested a laminar distribution pattern, only recently quantitative data became available in the studies of Rogers et al. [168] and Duyckaerts et al. [169].
Rogers reported significant differences ($p<0.0001$) in the concentrations of SP among the various laminae, with the layers II,III and IV having the highest concentrations [X(gem)(SEM)=60.8(7.6), 51.4(6.1) and 59.5(13.4) plaques/mm**2, respectively], and the layers I and VI having the lowest concentrations [31.3(5.3) and 21.8(3.7) plaques/mm**2, respectively].
In the study of Duyckaerts, the Areas 4, 40, 18 and 22 were investigated.
A remarkably small variation was found in these two studies in the laminar distribution of SP. The largest concentrations of SP were found in layers II-III, and to a lesser extent layers V-VI. By contrast, much lower SP densities were observed in layers I and IV.

A study limited to the visual and auditory cortices [170], demonstrated the distribution patterns in specific areas and laminae. The total number of SP were similar in the three visual areas studied [Area 17, Area 18 and Area 19, number of SP: 17.9(2.2); 18.2(1.9) and 21.3(0.9)/500 micron wide strip of cortex, respectively]. In this study, Thioflavin S staining was used. Thus, it was possible to distinguish between SP with and without a dense, brightly fluorescent core. In the various visual cortical areas the ratio between these two types of plaques was found to vary. In Area 17, 79% of the SP were of the core type, whereas the vast majority of the SP in Areas 18 and 20 were of the non-core type (72% and 76%, respectively).

From this review of the literature, it became clear that no single study on the global distribution of senile plaques over both cerebral hemispheres has been published up to now.

I.4.2. The distribution of Neurofibrillary Tangles.

I.4.2.1. Regional distribution of neurofibrillary tangles.

A striking feature of NFT in aging and dementia is its predilection for certain cell groups and its rarity or absence in others. In cerebral structures, nearly all authors from the earliest studies onwards (e.g. Simchowicz, [162]) emphasize the involvement of the hippocampus and the adjacent entorhinal cortex. In this region, the areas of predilection are CA1 (Sommer's Sector), the subiculum, and the entorhinal cortex [171], or especilally the lateral part of the entorhinal cortex [172].
The NFT distribution shows no male-female or left-right predilection [161,173]. The overall number of NFT increases with age, with the greatest density in Sommer's sector, the subiculum and the entorhinal cortex. As an age-related change, the NFT is either rare or absent in the neocortex [143 156,161,172]. In a series of 617 brains only five brains with NFT were found in this location [161].
According to Goodman [167], the Areas 37 and 38 have an even greater density of NFT than the hippocampus. The lowest densities of NFT were in the primary and motor cortices [160,167,174] Morel [cited in 175] studying a single case of Alzheimer's Disease, noticed that the primary visual area, Area 17, and the adjacent Area 18,showed a lower density of the NFT than the higher-order association Area 19. Mutrux [175] noticed a similar gradient from the primary auditory cortex to its association areas.
One of the older studies on NFT distributions noted lower densities of NFT in Area 4(6) , Area 3-1-2(19) and Area 17(10) (the number in brackets is the percentage of neurons with tangles) [167]. In the study of Jamada et al. [160] the following results were obtained:Area 4:1.1; Area 7:2.7; Area 19:1.9; Area 9:5.0 and Area 38:3.4 tangles per square millimeter. From these two studies it was concluded that NFT formation was especially found in the higher order association areas and relatively absent from the primary sensory and motor areas.
In a more recent study, the regional distribution of NFT in the visual and auditory cortices was analyzed [171]. The primary visual area, Area 17, showed 0.9(1.0), Area 18: 19.7(3.6) and Area 20: 35.5(8.8) NFT pro 250 micron wide cortical strip (SEM). The same tendency of increase of occurrence of NFT was found in the auditory regions. In the primary auditory cortex, Area 41, a very low number of NFT was demonstrated (1.6(0.5)), whereas Area 22 (auditory association cortex) had a more than 10-fold increase in NFT number (18.9(5.4)). These differences were present in each of the five cases investigated in this study.
The most recent study on laminar distribution of SP was performed by Rafalowska et al. [175]. Only sparsely statistically documented

results are given. No significant differences between the cortical laminae in the number of SP was demonstrated.
From the literature, the existence of a non-random distribution of NFT over the different neocortical areas is very probable. However, the data of these studies are all limited to a small part of the neocortex. No studies exist, in which data concerning NFT distribution in a large number of cortical areas are available from the same brain.

I.4.2.2. Laminar distribution of Neurofibrillary Tangles.

On the laminar distribution of NFT in the neocortex in Alzheimer's Disease only limited data are available. The first modern quantitative study was performed by Pearson et al. [176].In this study the distribution of NFT in a number of areas was investigated in six Alzheimer cases. The areas of neocortex from which blocks and sections were taken in most brains included Brodmann's Areas 9, 46, 6, 4, 39, 7, 20, 21, 38, 17 and 18, although in the article describing the studies however, only quantitative data were given for the visual Areas 17, 18 and 21. The authors reported the largest number of NFT in the supra- and infragranular layers L III and L V, with the layer L IV virtually unaffected in between. In most areas, L V was more affected than L III, but in the occipital Area 18 the reverse was found. Most NFT were noticed to be localized in pyramidal cells. Furthermore the NFT in L II, L III and L V tended to cluster vertically into a pattern reminiscent of columnar organization.
Another report on laminar distribution of NFT was published by Lewis et al. [171]. In this Thioflavine S study, the distribution of Thioflavine S positive tangles was determined in the visual and auditory cortices. The distribution pattern of NFT was a distinct one. The NFT were predominantly found in L III and L V, although there were striking regional differences in the proportion of NFT in L III and L V. Layer III contained 79 % of the total number of NFT in layers III and V in Area 18, 41 % in Area 20 and only 27 % in Area 22.

I.4.3. The distribution of Congophilic Amyloid Angiopathy. (CAA).

One of the few studies in this field was published by Vinters [177]. In this study, 10 histologic sections were sampled from similar cortical regions in each of 84 brains from patients aged 60 to 97 years. The sections were stained by the Congo-Red method and examined under polarized light for the presence of cortical (parenchymal) cerebral amyloid angiopathy. Some degree of CAA was found in 36% of the cases of over 60 years old. CAA is a focal, patchy, often asymmetric process that is most likely to involve the parieto-occipital cortex and to spare the hippocampi, even with severe involvement elsewhere. In another study, Tomonaga [178] found the frequency of CAA to be 8% in the 60-69 decade, 23 % in the 70-79 decade, 37 % in the 80-89 decade, and 58 % in patients older than 90 years. Mandybur [179] found CAA in 13 out of 15 patients with AD. Qualitatively, the temporal and occipital cortex appeared involved most, whereas Ammon's horn was spared by the vascular pathologic change. This high incidence of CAA in AD has been confirmed in other studies [180, 181, 182]. In summary, although CAA is found in 90 % of AD cases [183] no comprehensive study concerning areal and laminar distribution is available.

I.5. THEORIES ON SENILE PLAQUE AND NEUROFIBRILLARY TANGLE DISTRIBUTION IN ALZHEIMER'S DISEASE.

I.5.1. Theories on spreading of the disease along neuroanatomical pathways.

Several theories propose that the disease spreads along neuroanatomical pathways as a result of orthograde and/or retrograde degenerative mechanisms. For instance, in the theory of Appel [184] loss of the cholinergic neurons in the basal forebrain results from a lack of a neurotrophic factor in the cortex and hippocampus. Rogers and Morrison [185] found the cortical laminae containing the highest densities of senile plaques to coincide with laminar regions containing corticocortical axon terminals. They proposed that AD is a cortical disease and spreads from cortical region to cortical region via cortico-cortical pathways. Pearson speculated in 1985 that the disease might begin in the olfactory cortical regions and spread subsequently via retrograde and orthograde degenerative mechanisms to involve both cortical and subcortical regions [186]. In 1987, German et al. [187] proposed that cortical regions, which contain high densities of neuropathology (the association areas and temporal lobe structures), are the primary target of AD, and diffuse cortical projection neurons which innervate these regions are secondarily affected via retrograde axonal transport of some AD-related pathogen. They also speculated, that the disease may spread as a result of failure of normal transport of a trophic agent.
In order to verify the existence of a scheme of projection, along which such an agent, be it biological or chemical, may be transported or may be failing to be transported (i.e. a growth factor, like NGF) it is interesting to see if NFT degeneration is present in all diffuse corticopetal projecting systems, like the basal cholinergic forebrain nuclei or the locus coeruleus and, secondly, to investigate whether the distribution of senile plaques parallels the cortical laminar distribution of corticocortical and diffuse cortical projecting systems.
Pearson [188] recently elaborated on this theory: In his view, these Senile Plaques are formed at the endings of the degenerating projection systems, which are characterized by the formation of NFT in the neurons of the projecting subcortical nuclei. In the neocortical areas with direct connections with structures of the medial temporal lobe, such as the amygdala, entorhinal cortex and hippocampus, an intermediate degree of pathological involvement is observed. In the areas, without such connections far less pathology is seen. Therefore, he suggested the olfactory pathway to be the site of initial involvement in the disease. The disease would then spread in the olfactory system from the nucleus olfactorius anterior to the amygdaloid nuclei [189] and to the uncus. Next, the

disease process is supposed to spread to involve the hippocampal formation and the association areas of the neocortex in the parietotemporal and frontal lobes through the cortico-cortical pathways described earlier.
Important for this theory is that:
* the NFT are found in the pyramidal neurons,
* all cortical efferent fibers are derived from pyramidal cells,
* the NFT are arranged in cortical columnar clusters.
* The distribution of SP and NFT as a parameter of cortical involvement, should be arranged in such a fashion, that the higher order integration centers of information are the most affected, because these areas have the most strong projections to the affected areas in the temporal lobe.
From the corticocortical connections a scheme may be derived of forward projection e.g. for
1) somatosensory information:
SI - SII - 5 - 7 - 39/40 - 21 - 20 - Entorhinal cortex
2) visual information:
17 - 18 - 19 - TE3 - TE2 - TE1 - 38 - Entorhinal cortex
3) cingulate information system:
24 - 23 - TH/FF - Entorhinal cortex
According to this theory SP are considered to coincide with the endings of the projection fibers of neurons which are degenerated due to tangle formation in their perikaryon. The pathologic agent, however, is also present in the fiber endings of these neurons, and may be able to transmit itself to the postsynaptic neurons. In the process of degeneration, the projecting fibers cause local changes in the neuropil in the cortex. These local changes induce the formation of a SP. Because of this, the SP not only show a gradient of density distribution over the different Brodmann areas, showing the areas with the heaviest projections on the temporal regions, like the Gyrus parahippocampalis and the entorhinal cortex, being the most affected, but also a laminar distribution pattern resembling the laminar distribution patterns of these fiber endings in the normal brain.
In conclusion, according to the transneuronal spread theory of a pathologic agent, the distribution pattern of SP (and NFT) should reflect the pathways of spreading of the disease.
Because the cortico-cortical projection systems are known to be reciprocal, the forward projection schemes, within one modality should correlate with a corresponding ranking order of senile plaque densities within those areas.

I.6. AIM OF THE STUDY

In this study the involvement of the neocortex in Alzheimer's disease, in comparison with age and sex-matched controls is investigated. The aim of our study is:

* to demonstrate the degree of involvement of various neocortical areas in the disease process by analyzing a large number of cortical areas.
* to investigate the overall involvement of the neocortex in the disease process; therefore, a method to measure volume and surfaces change of the neocortex in AD was developped.
* to map the distribution of SP in individual cases in the different areas selected, in order to evaluate individual patterns of SP distribution.
* to evaluate the distribution of the SP as seen in a sensitive silver staining per area and per lamina using a sufficiently large sample of cortex material in order to make statistical analysis possible.
* to quantify the distribution of SP, NFT and CAA in a sensitive fluorescent method per cortical area and per lamina
* to analyze a possible relationship between SP, NFT and CAA distribution patterns on the one hand, and the neurotransmitter distribution patterns known from the literature on the other hand.
* to discuss the results in terms of the global hodology of the neocortex and to study the role of neocortical involvement in the pathogenesis of Alzheimer's Disease.

TABLE I.Values for the total cortical surface and volume

Author	Surface(cm**2)	Volume(cm**3)
Donaldson [14]	2352	290
Henneberg [190]	2188	274
Jeager [191]	-	289
Tramer [192]	2290	286
Shariff [193]	-	15.2*

* Only one hemisphere

TABLE II Values for cortical thickness (micron)

Author	Cortical region	Thickness
Van Alphen (1945) [194]	motor cortex	1900-2000
	visual cortex	1400-2500
Sholl [195]	motor cortex	2650-2800

TABLE III. The total number of neurons in the cortex

Author	Estimation
Donaldson [14]	1.2 * 10**9
Thompsom (1899) [196]	9.3 * 10**9
Von Economo (1925) [197]	1.4 * 10**10
Shariff (1953) [198]	6.9 * 10**9
Haug [100]	13.9 * 10**9 (range:10-20)

1.Rogers J, SD Styren. Neuroanatomy of Aging and Dementia. In: H Rothstein (ed.) Review of biological research in aging (1987) 3:223-253.

2.Mann DMA, PO Yeates, B Marcyniuk. Correlation between senile plaque and neurofibrillary tangle counts in the cerebral cortex and neuronal counts in cortex and subcortical structure in Alzheimer's disease. Neurosc Lett (1985) 56:51-55.

3.Tabaton M, P Schenone, P Romagnoli, GL Mancardi. A quantitative and ultrastructural study of substantia nigra and nucleus centralis superior in Alzheimer's disease. Acta Neuropathol (1985) 68:218-223.

4.Exner S. Untersuchungen Ueber die Lokalisation der Functionen in der Grosshirnrinde des Menschen. Wien, W Braunmueller, (1881).

5.Von Economo C. Zellaufbau der Grosshirnrinde des Menschen. Berlin, J Springer (1927).

6.Bailey P and G von Bonin. The Isocortex of man. Urbana, UIP (1951).

7.Kahle W, Die Entwicklung des menschlichen Grosshirnhemisphaere. Springer-Verlag, Berlin-Heidelberg (1969).

8.Bok ST. Der Einfluss der in den Furchen und Windungen auftretenden Kruemmungen der Grosshirnrinde auf die Rindenarchitectur. Z ges Neurol Psychiat (1929) 121:682-750.

9.Sholl DA, The organization of the Cerebral Cortex,London (1956).

10.Donaldson HH. The growth of the Brain. Chicago (1895).

11. Filimonoff IN. Ueber die Variabilitaet der Grosshirnrindestruktur. J Psychol Neurol (1932) 44:1-96.

12.Smith E. The morphology of the occipital region of the Cerebral Hemisphere in Man and the Apes. Anat Anz (904) 24.

13.Lorente de No R. Cerebral Cortex: Architecture, Intracortical Connections, Motor projections. In: Physiology of the nervous system, New York (1938).

14.Flechsig P. Anatomie des Menschlichen Gehirns und Rueckenmarks auf myelogenetischer Grundlage. Thieme, Leipzig (1920).

15.Meynert R. The brain of mammals. In: Manual of Histology, Vol. 2,(SA Stricker ed.) pp 650-766, Wood, New York (1872).

16.Berlin R. Beitrag zur Strukturlehre der Grosshirnwindungen. (1858). cited in: Schlapp M. Der Zellenaufbau der Grosshirnrinde des Affen Macacus Cynomolgus, Arch Psychiatr Nervenkr (1898) 30:583.

17.Baillarger JGF. Recherches sur la structure de la cuoche des circonvolutions du cerveau. Mem Acad R Med (1840) 8:149.

18.Betz W. Anatomischer Nachweiss zweier Hirncentra. Centralbl Med Wiss (1874):578.

19.Betz W. Anatomischer Nachweiss zweier Gehirncentra. Centralbl Med Wiss (1874) :595.

20.Betz W. Ueber die feinere Struktur der Gehirnrinde des Menschen. Centralbl Med Wiss (1881):193; (1881):209 and (1881):231.

21.Lewis WB, Clarke H. The Cortical Lamination of the Motor Area of the Brain. Proc Roy Soc (London), (1878) 27:38-49.

22.Hammerberg H. Studien ueber Klinik und Pathologie der Idiotie, nebst Untersuchungen ueber die normale Anatomie der Hirnrinde. Druk der akademischen Buchdruckerei, Upsala (1895).

23.Schlapp M. Der Zellenbau des Grosshirnrinde des Affen Maccacus Cynomolgus. Arch Psychiatr Nervenkr (1898) 30:583.

24.Bolton JS. The exact localization of the visual area of the human cerebral cortex. Philos Trans Roy Soc (London) Ser B (1900) 193:165.

25.Campbell AW. Histological Studies on the Localization of Cerebral Function. CUP, London (1905).

26.Nissl F. Ueber die sogenannten Granula der Nervenzellen. Neurol Centralbl (1894) 13:781.

27.Brodmann K. Zwei neue Apparate zur Paraffinserientechnik. J Psychol Neurol (1903) 2:206.

28.Brodmann K. Beitaege zur histologischen Lokalisation der Grosshirnrinde. VI. Mitteilung, Die Cortexgeliederung des Menschen. J Psychol Neurol (1908) 10:231-246.

29.Pandya DN, EH Yeterian. Architecture and connections of cortical association areas. In: Cerebral Cortex, Vol. 4: Association and Auditory Cortices. A Peters, EG Jones (Eds.), New York (1985):3-61.

30.Filimonoff IN. A rational subdivision of the cerebral cortex. Arch Neurol Psychiat (1947) 58:296-311.

31. Vogt C, O Vogt. Algemeine Ergebnisse unserer Hirnforshung. J Psychol Neurol (1919) 25:279-461.

32.Brodmann K. Vergleichende Lokalisationslehre der Grosshirnrinde in ihren Prinzipien dargestellt auf Grund des Zellenaufbaus. J A Barth, Leipzig, (1909).

33.Sanides F. Representation in the Cerebral Cortex and its areal lamination patterns. In: The structure and function of nervous tissue. GH Bourne (ed), Vol V, New York, Academic Press (1972).

34.Sanides F. Die Architectonik des Menschlichen Stirngehirns. In: M Mueller, H Spatz and P Vogel (eds) Monographien aus dem Gesamtgebiete der Neurologie und Psychiatrie, vol. 98. Berlin, Springer, (1962).

35.Jones EG. Cerebral Cortex. In: Encyclopedia of Neuroscience. G. Adelman (ed), Basel, Birkhaeuser, (1987).

36.Hopf A. Die myeloarchitectonik des Isocortex temporalis beim Menschen. J Hirnforsch (1954) 1:208-279.

37.Yamamoto T and A Hirano. A comparative study of modified Bielchowski, Bodian and Thioflavin S stains on Alzheimer's Neurofibrillary tangles. Neuropathol Appl Neurobiol (1986) 12:3-9.

38.Kappers A, CNG Huber, EC Crosby. The comparative Anatomy of the Nervous System of Vertebrates, Including Man. New York, MacMillan, (1936).

39.Filiminoff IN. A rational subdivision of the cerebral cortex. Arch Neurol Psychiatr (1947) 58:296-311.

40.Stephan H. Vergleigend-anatomische Untersuchunen am Uncus bei Insektivoren und Primaten. In: The rhinencephalon and related structures. Prog Brain Res (1963) 3:111-121.

41.Jones EG. Brodmann's Areas. In: Encyclopedia of Neuroscience. G. Adelman (ed), Birkhaeser, Basel, (1987).

42.Lorente de No R. The cerebral cortex: architecture, intracortical connections and motor projections. In: Physiology of the Nervous System, Fulton JF (ed) pp 291-339 OUP London, (1938).

43.Mountcastle VB. Modularity and topographic properties of single neurons of cat's somatic sensory cortex. J Neurophysiol (1957) 20:408-434.

44.Powell TPS, VB Mouncastle. Some aspects of the functional organization of the cortex of the postcentral gyrus of the monkey: a correlation of findings obtained in a single unit analysis with cytoarchitecture. Bull Johns Hopkins Hosp (1959) 105:133-162.

45.Hubel DH, TN Wiesel. Functional architecture of macaque monkey visual cortex. Ferrier Lecture, delivered 2 March 1972. Proc R Soc Lond B (1977) 198:1-59.

46.Asanuma H. Recent development in the study of the columnar arrangement of neurons within the motor cortex. Physiol Rev (1957) 55:143-156.

47.Lynch JC. Columnar organization of the cerebral cortex (cortical columns) In:Neuroscience year. Supplement 1 to the Encyclopedia of Neuroscience, G Adelman (ed) Basel, Brikhaeuser, (1989).

48.Lorente de No R. La cortezza cerebral del ration. Trab Lab Invest biol Univ Madrid (1922) 20:41-78.

49.Szentagothai J. The 'Module-concept' in the cerebral cortex architecture. Brain Res (1975) 95:475-496.

50.Goldman PS, WJH Nauta. Columnar distribution of cortico-cortical fibers in the frontal association, limbic and motor cortex of the developing rhesus monkey. Brain Res (1977) 122:393-414.

51.Arikuni T, M Sakai, K Kubota. Columnar aggregation of prefrontal and anterior cingulate cortical cells projecting to the thalamic mediodorsal nucleus in the monkey. J Comp Neurol (1983) 220:116-125.

52.Eccles JC. The modular operation of the cerebral neocortex considered as the material basis of mental events. Commentary. Neuroscience (1981) 6:1839-1856.

53.Bugbee NM, PS Goldman-Rakic. Columnar organization of corticocortical projections in Squirrel and Rhesus monkeys: Similarity of column With in species differing in cortical volume. J Comp Neurol (1983) 220:355-364.

54.Rockel AJ, RW Hiorns, TPS Powell. The basic uniformity in structure of the neocortex. Brain (1980) 103: 221-244.

55.Jones EG. Connectivity of the primate sensory-motor cortex. In: Cerebral Cortex, vol 5. EG Jones and A Peters (eds), pp 113-184, Plenum, New York (1986).

56.Martin KAC. Neuronal circuits in the cat visual cortex, In: Cerebral Cortex, vol 2, EG Jones and A Peters (eds), pp 241-284. New York, Plenum (1984).

57.Cusick CG, JH Kaas. Interhemispheric connections of cortical sensory and motor representations in primates. In:Lepore F, M Ptito, HH Jasper (Eds.) Two hemispheres - one brain. Functions of the corpus callosum. New York (1986):83-102.

58.Markowitsch HJ (ed). Information Processing by the brain. Views and Hypotheses from a Physiological-Cognitive Perspective. Toronto (Canada) (1988).

59.Mesulam MM. The functional anatomy and the hemispheric specialization for directed attention. The role of the parietal lobe and its connectivity. TINS (1983) 6:384-387.

60.Yeterian EH, DN Pandya. Architectonic features of the primate brain: Implications for Information processing and behavior. In: see ref. nr.57.

61.Pandya DN, EH Yeterian. Architecture and connections of cortical association areas. In: Cerebral Cortex, Vol. 4: Association and Auditory Cortices. A Peters, EG Jones (Eds.), New York (1985):3-61.

62.Galaburda AM, DN Pandya. The instrinsic architectonic and connectional organization of the superior temporal region of the rhesus monkey. J Comp Neurol (1983) 221:169-184.

63.Pons TP, JH Kaas. Connections of area 2 of somatosensory cortex with the anterior pulvinar and subdivisions of the ventroposterior complex in macaque monkeys. J Comp Neurol (1985) 240:16-36.

64.Pandya DN, EH Yeterian. Architecture and connections of cortical association areas. In: Cerebral Cortex Vol 4:Association and Auditory Cortices. A Peters, EG Jones (eds.) New York (1985).

65.Seltzer B, DN Pandya. Further observations on parietotemporal connections in the rhesus monkey. Exp Brain Res (1984) 55:301-312.

66.Mesulam MM, Mufson EJ, Wainer BH. Three-dimensional representation and cortical projection topography of the nucleus basalis (Ch4) in the macaque: concurrent demonstration of choline acetyltransferase and retrograde transport with a stabilized tetramethylbenzidine method for horseradish peroxidase. Brain Res (1986) 367:301-308.

67.Lehmann J, Struble RG, Antuono PG, Coyle JT, Cork LC and Price DL. Regional heterogeneity of choline acetyltransferase activity in primate neocortex. Brain Res (1984) 322:361-364.

68.Mesulam M-M, Rosen A and Mufson EJ. Regional variations in cortical cholinergic innervation: chemoarchitectonics of acetylcholinesterase-containing fibers in the macaque brain. Brain Res (1984) 311:245-258.

69.Mesulam M-M, Volicer L, Marquis JK, Mufson EJ, Green RC. Systematic regional difference in the cholinergic innervation of the primate cerebral cortex: distribution of enzyme activities and some behavioral implications. Ann Neurol (1986) 19:144-151.

70.Mesulam M-M and Geula C. Nucleus basalis (Ch4) and cortical Cholinergic innervation in the human brain: observations based on the distribution of acetylcholinesterase and choline acetyltransferase. J Comp Neurol (1988) 275:216-240.

71.Mesulam MM, Rosen AD, Mufson EJ. Regional variations in cortical cholinergic innervation: chemoarchitectonics of acetylcholinesterase-containing fibers in the macaque brain. Brain Res [B5L] (1984) 311:245-258.

72.Javoy-Agid F, B Scatton, M Ruberg, R L'Heureux, P Cervera, R Raisman, J-M Maloteaux, H Beck, Y Agid. Distribution of monoaminergic, cholinergic and GABA-ergic markers in the human cerebral cortex. Neuroscience (1989) 29:251-259.

73.Davies P, AH Verth. Regional distribution of muscarinic acetylcholine receptor in normal and Alzheimer type of dementia. brains. Brain Res (1978) 138:385-392.

74.Lysakowski A, Wainer BH, Bruce G, Hersh LB. An atlas of the regional and laminar distribution of choline acetyltransferase immunoreactivity in rat cerebral cortex. Neuroscience (1989) 28:291-336.

75.Perry EK, Atack JR, Perry RH, Hardy JH, Dodd PR, Edwardson JA, Blessed G, Tomlinson BE, Fairbairn AF. Intralaminar neurochemical distributions in human midtemporal cortex: comparison between Alzheimer's disease and the normal. J Neurochem (1984) 42:1402-1410.

76.Sorbi S, Piacentini S and Amaducci L. Intralaminar distribution of neurotransmitter-related enzymes in cerebral cortex of Alzheimer's disease. Gerontology (1987) 33:197-202.

77.Saper CB. Organization of cerebral cortical afferent systems in the rat. I. Magnocellular basal nucleus. J Comp Neurol (1984) 222: 313-342.

78.Mesulam MM, EJ Mufson. Neural inputs into the nucleus basalis of the substantia innominata (Ch 4) in the rhesus monkey to neocortex. Brain Res (1984) 107:253-274.

79.Price JL, R Stern. Individual cells in the nucleus basalis-diagonal band complex have restricted axonal projection patterns to the cerebral cortex. Brain Res (1983) 269:352-356.

80.Saper CB. Organization of cerebral cortical afferent systems in the rat. I. Magnocellular basal nucleus. J Comp Neurol (1984) 222:131-342.

81.McKinney M, JT Coyle, JC Hedreen. Topological analysis of the innervation of the rat neocortex and hippocampus by the basal forebrain cholinergic system. J Comp Neurol (1983) 217:103-121.

82.Levitt P, RY Moore. Noradrenaline neuron innervation of the neocortex in the rat. Brain Res (1978) 139:219-231.

83.Bjoerklund A, O Lindvall. Dopamine containing systems in the CNS. In: A Bjoerklund, T Hoekfelt (eds):Handbook of Chemical Neuroanatomy, Vol 2. Classical neurotransmitters in the CNS, Part 1. Amsterdam (1984):55-122.

84.Lindvall O, A Bjoerklund. General organization of cortical monoamine systems. In: Monoamine Innervation of the Cerebral Cortex. L Descarries, T Reader, H Jasper (eds.) New York (1984) :9-40.

85.Morrison JH, SL Foote, D O'Connor, FE Bloom. Laminar, tangential and regional organization of the noradreneregic innervation of monkey cerebral cortex: Dopamine-beta-hydroxylase immunohistochemistry. Brain Res Bull (1982) 9:309-319.

86.Porrino LJ, PS Goldman-Rakic. Brainstem innervation of the prefrontal and anterior cingulate cortex in the rhesus monkey revealed by retrograde transport of HRP. J Comp Neurol (1982) 205:63-76.

87.Lewis DA, Morrison JH. Noradrenergic innervation of the prefrontal cortex: a dopamine-beta-hydroxylase immunohistochemical study. J Comp Neurol (1989) 282:317-330.

88.Gaspar P, B Berger, A Febret, A Vigny, JP Henry. Catecholamine innervation of the human cerebral cortex as revealed by comparative immunohistochemistry of tyrosine hydroxylase and dopamine -beta hydroxylase. J Comp Neurol (1989) 279:249-271.

89.Philipson OT, IC Kilpatric, MW Jones. Dopaminergic innervation of the primary visual cortex in the rat and some correlations with human cortex. Brain Res Bull (1986) 18:621-633.

90.Berger B, S Trottier, P Gaspar, C Verney, C Alvarez. Major dopamine innervation of the cortical motor areas in the Cynomolgus monkey. A radiographic study with comparative assessment of serotonergic afferents. Neurosci Lett (1986) 72:121-127.

91.Lewis DA, MJ Campbell, SL Foote, M Goldstein, JH Morrison. The distribution of tyrosine hydroxylase immunoreactive fibers in the primate neocortex is widespread but regionally specific. J Neurosci (1987) 7:279-290.

92.Berger B, S Trottier, C Verney, P Gaspar, C Alvarez. Regional and laminar distribution of the dopamine and serotonin innervation in macaque cerebral cortex. A radiographic study. J Comp Neurol (1988) 273:99-119.

93.Javoy-Agid F, B Scatton, M Ruberg, R L'Heureux, P Cervera, R Raisman, J-M Maloteaux, H Beck, Y Agid. Distribution of

monoaminergic, cholinergic and gaba-ergic markers in the human cerebral cortex. Neurosc (1989) 29:251-259.

94.Gaspar P, B Berger, A Febvret, A Vigny, JP Henry. Catecholamine innervation of the human cerebral cortex as revealed by comparative immunohistochemistry of tyrosine hydroxylase and dopamine -beta-hydroxylase. J Comp Neurol (1989) 279:249-271.

95.Tower DB, Structural and functional organization of mammalian cerebral cortex: the correlation of neurone density with brain size. J Camp Neurol, 101:19-52 (1954).

96.Brody H, Organization of the cerebral cortex. III. A study of aging in the human cerebral cortex. J Comp Neurol (1955) 102:511-556.

97.Cragg BG, The density of synapses and neurons in the motor and visual areas of the cerebral cortex. J Anat (1967) 101:639-654.

98. Haug H. Brain sizes, surfaces, and neuronal sizes of the cortex cerebri: A stereological investigation of man and his variability and a comparison with some mammals (Primates, Whales, Marsupials, Insectivores, and one Elephant). Am J Anat (1987) 180:126-142.

99.Tomlinson BE, Blessed G, Roth M, Observations on the brains of demented old people. J Neurol Sci (1970) 11:207-242.

100.Hubbard BM, Anderson JM, A quantitative study of cerebral atrophy in old age and senile dementia. J Neurol Sci (1981) 50:135-145.

101.Mann DMA, The neuropathology of Alzheimer's Disease: A review with pathogenetic, etiological and therapeutic complications. Mech Ageing Dev (1985) 33:213-255.

102.Coleman PD, Flood DG, Neuron numbers and dendritic extent in normal aging and Alzheimer's Disease. Neurobiol Aging (1987) 8:521-545.

103.Hodge CF, Changes in ganglion cells from birth to senile death. Observations on man and honey bee. J Physiol (Lond) (1894) 17:129-134.

104.Tomlinson BE, Henderson G, Some quantitative cerebral findings in normal and demented old people. Neurobiol Aging (1976) 3:183-204.

105.Terry RD, Fitzgerald C, Peck A, Miller J, Farmer P, Cortical cell counts in senile dementia. J Neuropathol Exp Neurol (1977) 36:633.

106.Terry RD, Peck A, DeTeresa R, Schechter R, Horoupian DS, Some morphometric aspects of the brain in senile dementia of the Alzheimer Type. Ann Neurol (1981) 10:184-192.

107.Mountjoy CQ, Roth M, Evans NJR, Evans MH, Cortical neuron counts in normal elderly controls and demented patients. Neurobiol Aging (1983) 4:1-11.

108.Hubbard BM, JM Anderson. A quantitative study of cerebral atrophy in old age and senile dementia. J Neurol Sci (1981) 50:135-145.

109.Hubbard BM, Anderson JM, Age-related variations in the neuron content of the cerebral cortex in senile dementia of Alzheimer Type. Neuropathol Appl Neurobiol (1985) 11:369-382.

110.Braak H, Braak E, Ratio of pyramidal cells versus non-pyramidal cells in the human frontal isocortex and changes in ratio with ageing and Alzheimer's Disease. Prog Brain Res (1986) 70:185-212.

111.Wisniewski HM, Neuritic (Senile) and Amyloid PLaques, In: Alzheimer's Disease, Reisberg, B (ed), London, 57-61 (1983).

112.Probst A, Brunnschweiler H, Lautenschlager C, Ulrich J. A special type of senile plaque, possibly an initial stage. Acta Neuropathol. (Berl) (1987) 74:133-141.

113.Scholz W. Studien zur Pathologie der Hirngefasse: II. Die drusige Entartung der Hirnarterien und Kapillaren. Z Gesamte Neurol Psychiat (1938) 162:694-715.

114.Pantelakis S. Un type particulier d'angiopathie senile du systeme nerveaux central: Un angiopathie congophile. Topographie et frequence. Monatsschr Psychiat Neurol (1954) 198:219-256.

115.Mandybur TI. The incidence of cerebral amyloid angiopathy in Alzheimer's Disease. Neurology (1975) 25:120-126.

116.Eanes ED, Glenner GD. X-ray diffraction studies on amyloid filaments. J Histochem Cytochem (1968) 16:673-677.

117.Schwartz P. Amyloidosis- Cause and Manifestation of Old Age. Thomas, Springfield, IL (1970).

118.Powers JM, Skeen JT. An immunoperoxidase study of neuritic plaques. J Neuropath exp Neurol (1980) 39:385.

119.Torack RM, Lynch RG. Cytochemistry of brain amyloid in adult dementia. Acta neuropath (Berl) (1981) 53:189-196.

120.Morel F, Wildi E. General and cellular pathochemistry of senile and presenile alterations of the brain. Proceedings of the First

International Congress on Neuropathology, Vol. 2, Rome. Turin, Rosenberg and Seller, p 347 (1952).

121.Divry P. De l'amyloidose vasculaire cerebral et memingee (meningopathie amyloide) dans la demence senile, J belge Neurol Psychiat (1941/1942):41/42:141-158.

122.Glenner GG, Wong CW. Alzheimer's Disease: initial report of the purification and characterization of a novel cerebrovascular amyloid protein. Biochem Biophys Res Comm (1984) 120:885-890.

123.Masters CL, Simms G, Weinman NA. Amyloid plaque core protein in Alzheimer's Disease and Down's Syndrome. Proc Natl Acad Sci (USA) (1985) 82:4245-4249.

124.Masters CL, Multhaup G, Simms G. Neuronal origin of a cerebral amyloid: neurofibrillary tangles of Alzheimer's Disease contain the same protein as the amyloid of plaque cores and blood vessels. EMBO J (1985) 4:2757-2763.

125.Glenner GG. Alzheimer's Disease. The commonest form of amyloidosis. Arch Pathol Lab Med (1983) 107:281-282.

126.Vinters HV, Pardridge WM. The Blood-Brain Barrier in Alzheimer's Disease. Can J Neurol Sci (1986) 13:446-448.

127.Miyakawa T, Katsuragi S, Watanabe K, Shimoji A, Ikeuchi Y. Ultrastructural Studies of Amyloid Fibrils and Senile Plaques in Human Brain, Acta Neuropath (1986) 70:202-208.

128.Ikeda S-I, Wong CW, Allsop D, Landon M, Kidd M, Glenner GG. Immunogold labeling of Cerebrovascular and Neuritic Plaque Amyloid Fibrils in Alzheimer's Disease with an Anti-beta Protein Monoclonal Antibody. Lab Invest (1987) 57:446-449.

129.Simchowicz T. Histologische Studien ueber die senile Demenz. In: Histologische und Histopathologische Arbeiten ueber die Gorsshirnrinde mit besonderer beruecksichtigung der pathologischen Anatomie der Geisteskrankheiten. (edited by F Nissl & A Alzheimer), pp. 267-444, Jena (1911).

130.Tomlinson BE, D Kitchener. Granulovacuolar degeneration of the hippocampal cells. J Neurol Sci (1972) 7:331-356.

131.Ball JM, Lo P. Granulovacuolar degeneration in the ageing brain and in dementia. J Neuropathol Exp Neurol (1977) 36:474-87.

132.Ball MJ. Neuronal loss, neurofibrillary tangles and granulovacuolar degeneration in the hippocampus with ageing and dementia. A quantitative study. Acta Neuropathol (Berl) (1977) 37(2):111-118.

133.Jacobs RW, N Farivar, LL Butcher. Plaque-like lesions in the basal forebrain in Alzheimer's disease. Neurosci Lett (1985) 56:347-351.

134.Price DL, RJ Altschuler, RG Struble, MF Casanova, LC Cork, DB Murphy. Sequestration of tubulin in neurons in Alzheimer's Disease. Brain Res (1986) 385:305-310.

135.Dickson DW, H Ksiezak-Reding, P. Davies, SH Yen. A monoclonal antibody that recognizes phosphorylated epitope in Alzheimer neurofibrillary tangles, neurofilaments and tau proteins immunostains granulovacuolar degeneration. Acta Neuropathol (Berl) (1987) 73:254-258.

136.Mann DMA, PO Yates, B Marcyniuk. Some morphometric observations on the cerebral cortex and hippocampus in presenile Alzheimer's disease, senile dementia of Alzheimer type and Down's syndrome in middle age. J Neurol Sci (1985) 69:139-159.

137.Adolfsson R, CG Gottfries, BE Roos, B Winblad. Changes in the brain catecholamines in patients with dementia of Alzheimer type. Br J Psych (1979) 135:216-223.

138.Cross AJ, TJ Crow, JA Johnson, MH Joseph, EK Perry, RH Perry, G Blessed, BE Tomlinson. Monoamine metabolism in senile dementia of the Alzheimer type. J Neurol Sci (1983) 60:383-392.

139.Arai H, K Kosaka, T Iizuka. Changes of biogenic amines and their metabolism in postmortem brain from patients with Alzheimer-type of dementia. J Neurochem (1984) 43:388-393.

140.Saper CB, BH Warner, DC German. Axonal and transneuronal transport in the transmission of neurological disease: POtential role in system degenerations, including Alzheimer's disease. Neuroscience (1987) 23:389-398.

141.Ishii T. Distribution of Alzheimer's disease neurofibrillary changes in the brain stem and hippocampus. Acta Neuropathol (1966) 6:181-187.

142.Hirano A, HM Zimmerman. Alzheimer neurofibrillary changes. A topologic study. Arch Neurol (1962) 7:227-242.

143.Mann DMA, PO Yates, B Marcyniuk. Correlation between senile plaque and neurofibrillary tangle counts in cerebral cortex and neuronal counts in cortex and subcortical structures in Alzheimer's disease. Neurosc Lett (1985) 56:51-55.

144.Mann DMA, PO Yates, B Marcyniuk. A comparison of nerve cell loss in cortical and subcortical structures in Alzheimer's disease. J Neurol Neurosurg Psychiatry (1986) 49:310-312.

145.Marcyniuk B, DMA Mann, PO Yates. Loss of nerve cells from the locus coeruleus in Alzheimer's disease is topologically arranged. Neurosci Lett (1986) 64:247-252.

146.Johnston MV, M McKinney, JT Coyle. Evidence for a cholinergic projection to neocortex from neurons in the basal forebrain. Prc Natl Acad Sci (USA) (1979) 76:5392-5396.

147.Lehmann J, JI Nagy, S Atmadja, HC Fibiger. The nucleus basalis magnocellularis: The origin of a cholinergic projection to the neocortex of the rat. (1980) 5:1161-1174.

148.Bowen DM, CB Smith, P White, AN Davison. Neurotransmitter-related enzynmes and indices of hypoxia in senile dementia and other abiotrophies. Brain (1976) 99:459-496.

149.Davies P, AJF Maloney. Selective loss of central cholinergic neurons in Alzheimer's disease. Lancet (1976) 2:1403.

150.Struble RG, LC Cork, PJ Whitehouse, DL Price. Cholinergic innervation in neuritic plaques. Science (1982) 216:413-415.

151.Tago H, PL McGeer, EG McGeer, BR Sastry. Acetylcholinesterase histochemistry in the cerebral cortex of Alzheimer's disease. Soc Neurosci Abstr (1986) 12:1245.

152.Redlich E. Ueber Miliare Skerose der Hirnrinde bei seniler Atrophie. Jahrbucher Psychiat Neurol (1898) 17:208-216.

153.Blocq P, G Marinesco. Sur les Lesions et la pathogenie de l'epilepsie dite essentielle. Semaine Med.(1892) 12:445-446.

154.Fuller SC. A study of miliary plaques found in the brain of the aged. Amer J Insanity (1911) 68:147-219.

155.Tomlinson BE, Blessed G, Roth M. Observations on the brains of non-demented old people. J Neurol Sci (1968) 7:331-356.

156.Tomlinson BE, G Blessed, M Roth. Observations of the brains of demented old people. J Neurol Sci (1970) 11:205-242.

157.Mandybur T. The incidence of cerebral amyloid angiopathy in Alzheimer's Disease. Neurology (1975) 25:120-126.

158.Fuller SC. A study of miliary plaques found in the brain of the aged. Amer J Insanity (1911) 68:147-219.

159.Jamada M, P Mehraein. Verteilungsmuster der Senilen Veranderungen im Gehirn. Die Beteiligung des limbischen Systems bei Morbus Alzheimer. Arch Psychiat Neurol (1968) 211:308-324.

160.Matsuyama H, S Nakamura. Senile changes in the brain in the Japanese: Incidence of Alzheimer's Neurofibrillary change and Senile Plaque. In: Alzheimer's Disease: Senile dementia and related disorders. Vol. 7. Aging. R Katzman, RD Terry and KL Blick (Eds.) New York (1978): 287-297.

161.Simchowicz T. Histologische Studien ueber die senile Demenz. In; Histologische und histopathologische Arbeiten ueber die Grosshirnrinde mit besonderer Beruecksichtigung der pathologischen Anatomie der Geisteskrankheiten. F Nissl and A Alzheimer (Eds.) Jena (1911).

162.Jordan SW. Central Nervous System. Human Pathol (1971) 2:561.

163.Dayan AD. Quantitative histopathological studies on the aged human brain I. Senile plaques and neurofibrillary tangles in "normal" patients. Acta Neuropath (1970) 16:85-94.

164.Dayan AD. Quantitative histological studies on the aged human brain II. Senile plaques and neurofibrillary tangles in senile dementia. Acta Neuropathol (1970) 16:95-102.

165.Roth M, BE Tomlinson, G Blessed. Correlation between scores for dementia and counts of "senile plaques" in cerebral grey matter of elderly subjects. Nature (1966) 209:109-110.

166.Goodman L. Alzheimer's Disease: A clinicopathologic analysis of 23 cases with a theory on pathogenesis. J Nerv Ment Dis (1953) 118:97-130.

167.Rogers J, JH Morrison. Quantitative morphology and regional and laminar distributions of Senile Plaques in Alzheimer's Disease. J Neurosci (1985)10:2801-2808.

168.Brun A, E Englund. Regional pattern of degeneration in Alzheimer's Disease: neuronal loss and histopathological grading. Histopathol (1981) 5:549-564.

169.Duyckaerts C, J-J Hauw, F Bastenaire, F Piette, C Poulain, V Rainsard,F Javoy-Agid, P Berthaux. Laminar distriburion of neocortical plaques in senile dementia of the Alzheimer type. Acta Neuropath. (1986) 70:249-256.

170.Lewis DA, MJ Campbell, RD Terry JH Morrison. Laminar and regional distributions of Neurofibrillary Tangles and Neuritic plaques in Alzheimer's Disease: A quantitative study of visual and auditory cortices. J Neurosci (1987) 7:1799-1808.

171.Kemper T. Senile dementia: A focal disease in the temporal lobe. In: Senile dementia: A biochemical Approach. K Nandy (Ed.) New York (1978).

172.McLardy T. Memory function in hippocampal gyri but not in hippocampi. Intern J Neurosci (1970) 1:(113-118.

173.Ball MJ. Neuronal loss, neurofibrillary tangles and granulovacuolar degeneration in the hippocampus with ageing and dementia. Acta Neuropath (1977)37:111-118.

174.Mutrux S. Diagnostic differentiel histologique de la maladie d'Alzheimer et de la demence senile: Pathophobie de la zone de projection corticale. Mschf Psych Neurol (1947)113:100-107.

175.Rafalowska J, M Bracikowska, GY Wen, HM Wisniewski. Laminar distribution of neuritic plaques in normal aging, Alzheimer's disease and Down's syndrome. Acta Neuropath (1988) 77:21-25.

176.Pearson RCA, MM Esiri, RW Hiorns, GK Wilcox and TPS Powell. Anatomical distribution of the pathological changes in the neocortex in Alzheimer's Disease. Proc Natl Acad Sci (USA) (1985) 82:4531-4534.

177.Vinters HV, JJ Gilbert. Cerebral Amyloid Angiopathy: Incidence and Complications in the Aging Brain. II. The Distribution of Amyloid Vascular Changes. Stroke (1983) 14:924-928

178.Tomonaga M. Cerebral amyloid angiopathy in the elderly. J Am Geriatr Soc (1981) 29:151-157.

179.Mandybur TI. The incidence of cerebral amyloid angiopathy in Alzheimer's disease. Neurology (1975) 25:120-126.

180.Mountjoy CQ, BE Tomlinson, PH Gibson. Amyloid and senile plaques and cerebral blood vessels - a semi quantitative investigation of a possible relationship. J Neurol Sci (1982) 57:89-103.

181.Glenner GG, JH Henry, S Fujihara. Congophilic angiopathy in the pathogenesis of Alzheimer's degeneration. Ann Pathol (1981) 1:120-129.

182.Vanley CT, MJ Aguilar, RJ Kleinhenz, MD Lagios. Cerebral amyloid angiopathy. Hum Pathol (1981) 12:609-616.

183.Castano EM, B Frangione. Biology of Disease. Human amyloidosis, Alzheimer Disease and Related disorders. Lab Invest (1988) 58:122-132.

184.Appel SH. A unifying hypothesis for the cause of amyotrophic lateral sclerosis, Parkinsonism, and Alzheimer disease. Ann Neurol (1981) 10:499-505.

185.Rogers J, JH Morrison. Quantitative morphology and regional and laminar distributions of senile plaques in Alzheimer's disease. J Neurosc (1985) 5:2801-2808.

186.Pearson RCA, MM Esiri, RW Hiorns, GK Wilcox and TPS Powell. Anatomical distribution of the pathological changes in the neocortex in Alzheimer's Disease. Proc Natl Acad Sci (USA) (1985) 82:4531-4534.

187.German DC, CL White, DR Sparkman. Alzheimer's disease: Neurofibrillary tangles in nuclei that project to the cerebral cortex. Neurosc (1987) 21:305-312.

188.Pearson RCA. The evolution of Alzheimer neuropathological changes. At the conference: Aging of the brain and Dementia:Ten Years Later. Florence May 31-June 3, 1989.

189.Herzog AG,TL Kemper. Amygdaloid changes in aging and dementia. Arch Neurol (1980) 37:625-629.

190.Henneberg R, Messung der Oberflaechenausdehnung der Grosshirnrinde. J Psychol Neurol, Lpz. 17:144-158 (1910).

191.Jeager R, Inhaltberechnungen der Rinden und Marksubstanz des Grosshirns durch planimertrische Messungen. Arch Psychiat (1914) 54:261-272.

192.Tramer M, Ueber Messung und Entwicklung der Hirnrindenoberflaeche des menschlichen Grosshirns. Arb hirnanat Int Zuerich (1916) 10:5-57.

193.Shariff GA, Cell counts in the primate cerebral cortex. J Comp Neurol (1953) 98:381-400.

194.Alphen GWHM van, Kernmetingen in de Neocortex van de mens. Leiden (1945).

195.Sholl DA, The measurable parameters of the cerebral cortex and their significance in its organi. Folia psychiat neerl (Supplement) (1956).

196.Thompson H, The total number of functional nerve cells in the cerebral cortex of man. J Comp Neurol (1954) 101:19-52.

197.Economo E, Koskinas GN, Die cytoarchitectonik der Hirnrinde des erwachsenen Menschen, Berlin, (1925).

198.Shariff GA, Cell counts in the primate visual cortex. J Comp Neurol (1953) 98:381-400.

II.1. INTRODUCTION

In this study on the cortical distribution of SP, NFT and CAA the brains of five Alzheimer patients were studied and compared with three age- and sex-matched controls.
During this study, brains were fixed, sectioned, stained and analyzed employing various methods, in order to answer specific questions. In this chapter a general outline of these techniques and their mutual limitations is discussed. In the next chapter, describing the results of this study, specific details will be given concerning the technique used, if relevant to the results presented.

II.2. SHORT DESCRIPTION OF CASE HISTORY AND NEUROPATHOLOGY

II.2.0. Cases used in the distribution study of SP, NFT and CAA.

For the study on distribution of SP, NFT and CAA five AD brains were available. In table I the case numbers, diagnosis, age and sex are given.
The brain 88271 was chosen as a control case for brain 88177 and 89033. For the brain 87068, no sex matched control was available in our series.

TABLE I: BRAINS AVAILABLE FOR QUANTITATIVE ANALYSIS

Case Number:	NP Diagnosis:	Age:	Sex:	Weight:	Volume:
87068	AD	65	F	865	na
87395	AD	69	M	1100	1071
88177	AD	76	F	970	942
89033	AD	77	F	855	840
88243	AD	77	M	962	948
88268	Control	65	M	1570	1557
88271	Control	75	F	1250	1200
88269	Control	80	M	1475	1450

NP dignosis: Neuropathological diagnosis
AD: Alzheimer's Disease
M : Male
F : Female
na: not available

II.2.1. Case 87068.

This patient, suffering from Alzheimer's Disease was born in 1921 as the second child in a family of eight children. She attended a primary school after which she worked in a textile factory and later in a restaurant.
In 1980 she presented in a neurological clinic for the first time, because of memory-impairment. During this first examination, a moderate desorientation and more severe memory disturbances were noticed. Additional neurological examination showed no particularities.
Using computer tomography, a diffuse cortical atrophy was demonstrated, especially in the temporal regions. No enlargement of the ventricular system was seen, thus excluding a normal pressure hydrocephalus. On psychological examination, an I.Q. was found of 61 (verbal I.Q. of 71; performance I.Q. of 54). These results made a clinical diagnosis of a presenile dementia likely. From August 1981 onwards, the patient was treated for essential hypertension.
From January until March 1984, the patient was admitted to a Psychiatric ward for evaluation. During this period she made a psychiatrically disturbed impression and suffered from thought disturbances of a hallucinatory nature, and from anxiety. Psychological examination demonstrated a severe agnosia and apraxia, with relatively intact language functions. During this period, the patient suffered from a T.I.A. of the right hemisphere, with a concommitant epileptic seizure. After this period she was admitted to a nursery home for the elderly. In May 1986, she died of the consequences of an urosepsis.

Clinical Diagnosis: Alzheimer's Disease.

Neuropathological Description:

In all layers of the neocortex after routine staining (HE, Kluver-Barrera and Nissl) the following changes are noticed:
* a uniform diffuse loss of neurons, especially advanced in the pyramidal layers L III and L V.
* various changes, characteristic of neuronal damage:
  -the neurons seem shrunken
  -Nissl granulation is not clear
  -the nuclei are often pushed to the border of the cells
  -the cells are filled with some storage material

These changes correspond to changes in the silver stainings (Bodian and Gallyas). The silverstainings show dispersed senile plaques. NFT are seen in the same slices. SP and the NFT are noticed in the frontal lobe, not only in the prefrontal area (Area 6), but also in the fronto-orbital region (Area 11), in the temporal lobe (Area 20) and in the Insula of Reill. Even in the occipital lobe (Area 17) SP and NFT were observed in material stained after the Gallyas silver method.

In the white matter, the vessels are surrounded by enlarged perivascular spaces. Only few vessels show arteriosclerotic changes. Lafora bodies are found sporadically and only in small numbers.

Neuropathological Diagnosis: Alzheimer's Disease.

II.2.2. Case 87395.

At the age of 69, this male patient died at 24-10-1987, after a stay of 4 years and 5 months in a nursery home for the elderly. The patient was admitted under the clinical diagnosis of senile dementia of the Alzheimer Type (SDAT). From the history of the patient's premorbid life appeared that he was the eldest out of ten children. After primary school, he worked as a house painter and later in a house decoration shop. In the evening hours he followed courses for commercial design.
From 1973, at the age of 55, he was found unfit for this job, because of medical reasons. Two years later, a gradual decline of cognitive functioning was noticed. This was concluded from increasing forgetfulness, vagabunding, disorientation and self-neglect. In the second half of 1983, the patient had an accident with his bicycle and was admitted to a general hospital, where the clinical diagnosis SDAT was made.
In addition, a form of chronic aspecific respiratory distress syndrome, signs of ataxia, increased muscle tone, orthostatic hypotension and regularly occurring generalized tonic-clonic epileptic seizures were noted.
At admission to a nursery home, hardly any psychiatric and neuropsychologic examination was possible because of his failure to understand the test instructions. It was concluded that the patient suffered from serious cognitive disturbances, resulting in memory disturbances, apraxia, aphasia and intellectual deterioration. During the time of the patient's stay at the nursery home, the main clinical problem consisted of repeatedly occurring generalized epileptic seizures, notwithstanding anti-epileptic medication. A CT-scan showed an enlarged ventricle system, broadening of the sulci, especially so in the basal area and broadening of the cisternae, with no left-right differences. No signs of irregularities in density were seen.

Clinical Diagnosis: Alzheimer's Disease

Neuropathologic description:
No macroscopical description is available in this case. On cortical sections, stained after Congo-Red, numerous SP and NFT are visible. Congophilic angiopathy is present in practically every field of vision.

Neuropathologic diagnosis: Alzheimer's Disease.

II.2.3. Case 88177

This female patient was admitted to a nursery home at 3-10-1985 at the age of 74. After attending secondary school (MULO) and a commercial trading-school, she became a bartender.
The first signs of the disease were noticed at 62 years of age. During an HTG investigation performed in 1985, carotid artery insufficiency was found present on both sides. From 1983 through 1985, she consumed large quantities of alcoholic beverages, as a reaction to the death of her husband.
At admission to the nursery home (3-10-1985), the patient suffered from anxiety. The diagnosis made by a psychiatrist was a reactive depression combined with a dementia syndrome. The depressive state was treated by amytriptiline, to which the patient responded well. During the next 2 years and 7 months, the patient suffered from atrial flutter, which was treated by digoxin and Norduretic. Mid May 1987, she was troubled by periods of angina pectoris. During the last two months of her life, understanding and expression in language, both oral and in writing, all memory functions, together with the ability to concentrate, were severely disturbed.
Eventually, the patient died at 25-5-1988.

Neuropathologic description:
On macroscopical inspection, signs of a generalized atrophy were noticed, with accentuation in the frontal lobes. The ventricles were much enlarged. Microscopical investigation revealed a large number of cerebral NFT and SP. Also congophilic angiopathy was noticed.

Neuropathological diagnosis: Alzheimer's Disease.

II.2.4. Case 89033

This female patient, married to a farmer and a mother of five children, was born at 27-1-1913. After the death of her husband, she menaged the farm on her own. In 1980, a slight forgetfulness was noticed. In 1984, she got disorientated in place, person and time. She also developed an expressive aphasia and was unable to recognize her children and her second husband any more. During the first half of 1985, the patient was no longer capable to perform ADL functions on her own: in June 1985, the patient was admitted to a nursery home for the elderly.
At the intake in the nursery home, the patient seemed to suffer also of cognitive dysfunctions: she was incapable to name objects and didn't recall the name of her children. During conversations, the patient pretended to know the activities of the family, but in reality, she referred to activities of about twenty years ago. During the three years of her stay in the nursery home, she gradually lost the ability to speak, but hearing and vision remained fairy intact. ADL functions and the ability to recognize members of the family were severely disturbed from the day of admission. Gradually, she got bedridden and eventually died at the

age of 76 years, at 6 -2-1989.

At general section, which was performed 20 hours after the patient died the following abnormalities were found:
- an atrophia of the internal organs i.e. a weight loss of approximately 65 % of the heart, liver and spleen.
- signs of an acute absceding pyelonephritis and
- an infiltrate in the left lung, suspect of a bronchopneumonia.
Immediate cause of death:bronchopneumonia.

Clinical Diagnosis: Senile Dementia of the Alzheimer Type (SDAT)

Neuropathologic Diagnosis: Alzheimer's Disease.

II.2.5. Case 88243.

This male patient was born 11-7-1911. After attending primary school, he became a carpenter and started a carpenter shop on his own. At the age of 64, he noticed a decline of memory, causing him to abandon his business. Except for an acute abdominal illness of unknown origin, the last two years before admission to a nursery home (June 1982) were free from disease. Since 1982, a gradual decline in the patient's condition was reflected by increasingly aggressive behavior, especially during the night. At first, orientation in time and later in both place and person got disturbed. During the last two years of his life, he suffered from severe mixed aphasia, and was unable to orient himself, to concentrate and to act intentionally. Two of his sisters suffered from the same disease.
The patient died at 4-9-1988.

Clinical Diagnosis: Senile Dementia of the Alzheimer Type (SDAT) with a familiarly predisposition.

Neuropathological Description:
No macroscopical neuropathological description is available.
On microscopical investigation of sections of frontal, temporal and hippocampal origin, large numbers of SP and NFT (>20 pro field; 250x) were seen in the Bodian and Yamamoto silver impregnations. Amyloid deposits, as shown in Congo-Red fluorescence were also present in numerous vessels of various caliber, both in the tissue and the meninges. SP and NFT were dispersed in the pyramidal cell layer of the hippocampus, prominently so in the CA 1 area. In the HE staining, vascular arteriosclerotic changes (advanced thickening of the vessel wall and multiplication of the adventitial layer) were obvious. Most of the vessels were empty and patent. No signs of focal necrosis were seen.

Neuropathological Diagnosis: Alzheimer's Disease (AD), with amyloidosis and moderate arteriosclerosis.

II.2.6. Case 88268

No clinical history is available.

Neuropathologic description:
No signs of atrophy nor signs of arteriosclerosis of the cerebral vessels were present on macroscopical examination.
Routine histological sections from the temporal, frontal and hippocampus revealed no structural changes. In silver staining (Bodian, Yamamoto) no SP nor NFT were seen.

Neuropathologic diagnosis: No neuropathological signs of neurological disease.

II.2.7. Case 88271

Female, aged 75 years.

No clinical history available.

Neuropathological description:
On macroscopic examination, no signs of cerebral atrophy were noticed. At the brain's base, advanced arteriosclerotic changes (Third Degree) could be seen. On frontal sections, the ventricles were slightly enlarged. In the basal ganglia, small, dispersed lacunae of vascular origin were seen.
In routine HE staining of the frontal, temporal and hippocampal regions, the structure of the brain was well preserved. The vessels showed moderate arteriosclerotic changes. The neurons were well preserved. No signs of gliosis were present. In silver stainings (Bodian, Yamamoto) no SP and NFT could be observed. Only in the hippocampal structure, single plaques and a few tangles were present (0-1 / 3 fields of vision; 250 x). In Congo-Red, no SP nor NFT could be demonstrated.

Neuropathological diagnosis: No signs of neurological disease, except for moderate arteriosclerotic changes.

II.2.8. Case 88269.

No clinical description available.

Neuropathological description:
On macroscopical examination, no signs of atrophy or arteriosclerosis were present. In HE stained sections of the frontal, temporal and hippocampal regions, the morphological picture of the cortical architecture, neurons and glial cells was normal. No morphological changes in the blood vessels could be noticed. Silver stainings (after Bodian or after Yamamoto) revealed no SP nor NFT. Congo-Red stained sections in fluorescent microscopy, failed to show any signs of aging or cerebral amyloidosis.

Neuropathological Diagnosis: Normal structure of the brain.

II.3. THE BRODMANN AREAS SELECTED FOR THE STUDY

The parts of the cortex examined in this study are chosen from all cortical lobes. All different types of neocortical architecture were sampled.
The cortical samples are taken from both hemispheres in a symmetrical fashion, in order to cover the whole surface of the neocortex (sample numbers in fig. II.1 in brackets):

1. regio Frontalis:

   Area 10: area frontopolaris,
   Area 11: area prefrontalis (2),
   Area 8: area frontalis intermedia (1),

2. regio Temporalis:

   Area 20: area temporalis inferior (8),
   Area 21: area temporalis media (7),
   Area 22: area temporalis superior (6),
   Area 42: area temporalis transversa (6),
   Area 37: area occipito-temporalis lateralis (12),
   Area 37: area occipito-temporalis medialis (12),
   Area 38: area temporopolaris

3. regio Insularis (5)

4. regio Parietalis

   Area 7: area parietalis superior (10)

5. regio Occipitalis

   Area 17: area striata (13),
   Area 18: area occipitalis (13),

6. regio Cingularis

   Area 23: area cingularis posterior ventralis (11),
   Area 24: area cingularis anterior ventralis (9),

7. regio Postcentralis

Area 2: area postcentralis caudalis (4),

8. regio Praecentralis

Area 4: area gigantopyramidalis (3).

These areas may also be classified as primary motor areas (e.g. Area 4), primary sensory areas (e.g. Area 17, Area 2), secondary sensory areas (e.g. Area 18) and multi-modal association areas (e.g. Area 7).
In this study, the anatomical distribution of the pathological changes in the neocortex in Alzheimer's Disease is investigated.

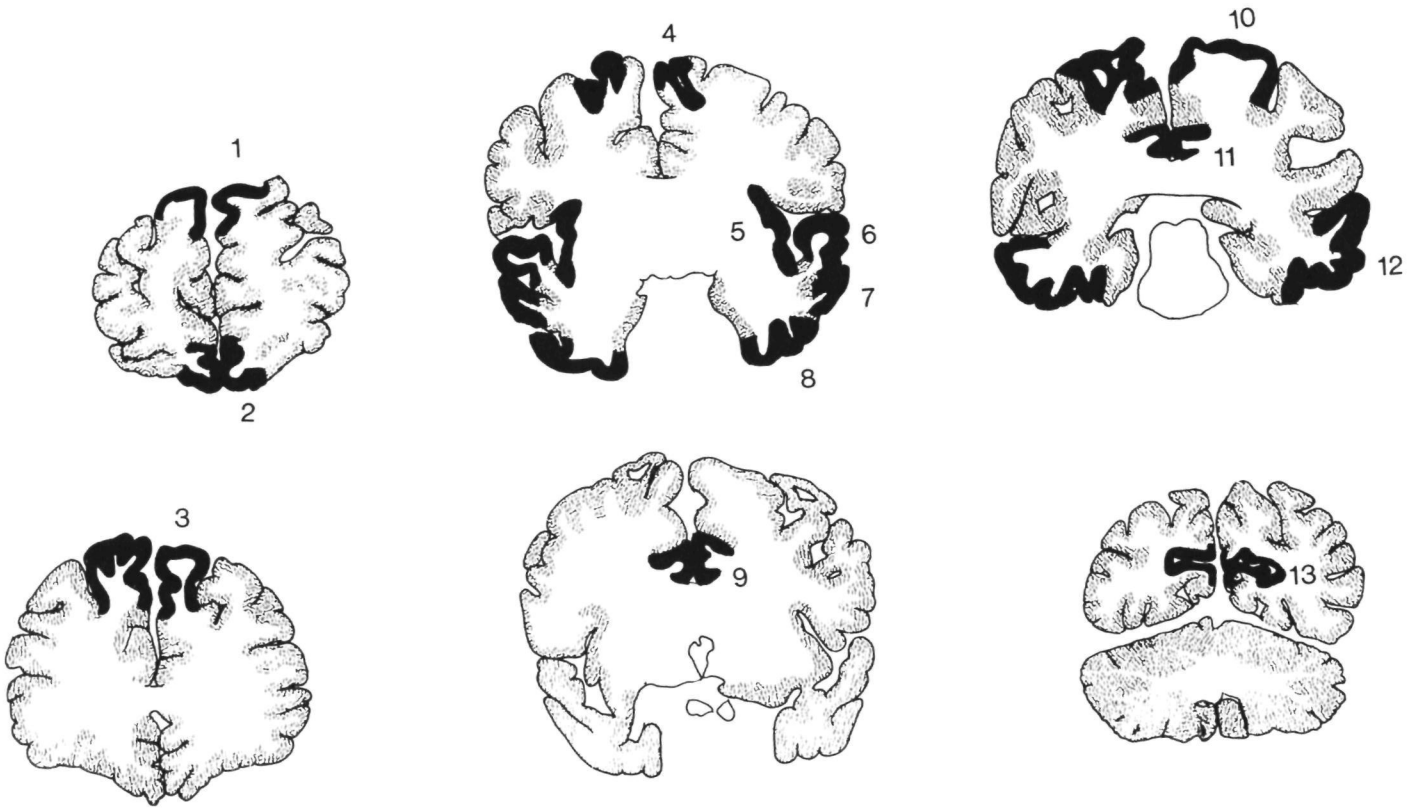
1
2
3
4
5
6
7
8
9
10
11
12
13

II.4. TISSUE PROCESSING

II.4.1. General outline.

In this study, the tissue is embedded in paraffin after a 5 month period of fixation in buffered Formaldehyde. After this fixation period, the process of shrinkage due to fixation has come to a stand still [1].
Next, the brain is sectioned in three or two blocks, in order to sample non-neocortical structures, such as the hippocampus, the Nucleus Basalis Magnocellularis (Meynert) (nBM) and the brain stem. The remainders of these blocks were put on a flat horizontal surface and the height (h) of the blocks perpendicular to this plane was measured (3x).
In order to estimate total cortical volume and surface, the blocks were put in polystyrene boxes, embedded in agar-agar, and sectioned. The total number of sections made from the polystyrene box was counted (n). Taking the quotient of h and n results in a accurate estimation of the mean slice thickness. On the average, this thickness was in the order of 1.5 - 2 mm. These thin coronal slices were necessary to estimate the total surface and volume of the human neocortex, as described in the last paragraph of the next section concerning the determination of macroscopic change in volume and surface in AD, where this procedure is described in more detail.

All our microscopic quantitative data are sampled on 10 micron thick sections, which are mounted and stained according to various methods (TABLE II).

TABLE II: STAINING USED

STAINING:	SECTION THICKNESS:	AIM:
NISSL	10 micron	Identification of cortical area
CONGO-RED	10 micron	Determination distribution of NFT, SP and CAA
YAMAMOTO	10 micron	Plotting and calculation of the SP distribution
HAEMATOXILIN-EOSIN	10 micron	Demonstrating GVD.

NFT : Neurofibrillary Tangles
SP : Senile Plaques
CAA : Cogophilic Amyloid Angiopathy
GVD : Granulo-vacuolar degeneration.

II.4.2. Mounting and staining procedures.

Sections were mounted on object-glasses coated with 0.5% gelatin and cleaned with NaOH (pH 13) and rinsed in 96% EtOH prior to this coating. Those sections prepared for the modified Bielchowski after Yamamoto [2] were mounted on object glasses coated with chrome-alum/gelatin [3]:
Chrome-alum/gelatin solution is prepared by weighing 0.5 g Gelatin and 50 mg chrome-alum for every 100 ml distilled water (dH2O) and warming this solution until boiling. Next, the solution is filtered and cooled to 20 degrees Celsius. The slides are dipped in the solution and air-dried for at least two hours at 80 degrees Celsius.

The classical staining after NISSL and the HAEMATOXILIN-EOSIN method are aptly described in histotechnical reference manuals [eg in 4], to which we refer for description of these methods.

II.4.2.1. The Congo-Red method.

The Congo-Red method used in this study was described by Puchtler, Sweat and Levine in 1962 [5]. The Congo-Red method used in combination with fluorescence to demonstrate amyloid, was described in 1965 [6].

In this study, a Congo-Red staining method in combination with fluorescence (CR-F) is employed to demonstrate SP, NFT and CAA. The choice of CR-F was made after comparison of other methods available, such as the Thioflavine-S [7] and the Gallyas modification of the Bielchowsky silver method [8]:
a comparison of the number of NFT visible under different staining conditions of sister-sections from entorhinal cortical material resulted in the conclusion that the sister-sections stained after CR-F showed NFT and SP most convincingly.

The Congo-Red sections were examined using illumination with a Mercury-lamp (HBO 50) using the filters BP 546/12 with filter 1 mm BG 38 and a LP 590 ocular filter.
The staining method used is known as the "alkaline Congo red method" after Puchtler and briefly described as follows:
The sections have to be
1. dewaxed and rehydrated
2. stained with Mayer's acid hem-alum for 10 min.
3. rinsed 3x in distilled water
4. transferred to an alkalic NaCl solution (Stock solution: 80% ethyl alcohol saturated with NaCl; Working solution: Add 0.5 ml 1% aqueous NaOH to 50 ml of the stock solution and filter. Use this solution within 15 minutes.
5. stained with Congo red solution. Stock Solution Congo-Red: 80 % ethyl ethanol saturated with Congo-Red and NaCl. Working solution: Add 0.5 ml 1 % aqueous NaOH to 50 ml of the stock

solution, filter and use within 15 minutes.
6. dehydrated rapidly in three changes of absolute alcohol.
7. treated 2x with xylene, and finally:
8. mounted.

Because we are particularly interested in amyloid distribution in the cases studied, it was decided to use the Congo-Red fluorescence method, which was recommended for this purpose by Puchtler et al. The silver stain according to Bielschowsky, in the Yamamoto modification is far from ideal for the demonstration of amyloid, and other stainings, such as the Thioflavine staining colors the amyloid only faintly.
When the sections were investigated under the fluorescence microscope, the bright red of the amyloid stood out clearly against the dark background. The Congo-red stain was found advantageous for fluorescence microscopic studies of amyloid because it permitted direct comparison of the familiar staining pattern as seen in transmission light microscopy, with the fluorescent microscopic picture. The twin lamp unit in combination with a brightfield condensor allowed instantaneous changeover from normal to fluorescence microscopy and vice versa. This arrangement thus facilitated the study of topographical relationships of the amyloid with the laminar arrangement of the structural elements of the neocortex. The high contrast between bright red amyloid and grayish autofluorescence of other tissue structures aided in the detection of traces of amyloid which were not clearly visible in the normal microscopy. The selectiveness of the alkaline Congo-red stain as used in this study, was already described by Puchtler et al. These properties, namely the comparison of the inspection of the field of vision with fluorescent microscopy and the possibility to inspect in normal microscopy exactly the same field of vision in order to pinpoint exactly the localization of this particular field in terms of the laminar pattern of the area investigated, made this method superior to all others available.
Unfortunately, no comparison of this method with material immunochemically stained material by a monoclonal Ab against the A4-protein was available.
In cortical strips of 400 micron width, the total number of NFT and SP were analyzed on three locations in the entorhinal cortex. This was done on approximately the same location in sister sections. The total number of NFT and SP in a 20 micron thick section is given in table III:

TABLE III:
A COMPARISON BETWEEN THE NUMBER OF SP AND NFT IN SECTIONS STAINED AFTER CONGO-RED AND THIOFLAVINE-S STAININGS UNDER FLUORESCENT MICROSCOPY

Method:	NFT	SP
Congo-Red	103.0 (6.2)	16.3 (3.8)
Thioflavin-S	85.3 (5.5)	13.8 (4.6)

The numbers are given as the mean of the three values, representing the total number in each strip of tissue investigated. The number in brackets is the SEM.
According to statistical analysis (Tukey's test), no statistical difference was found between the yield of these two staining methods.

From this comparison of these two fluorescent methods, it seems feasible to compare the results of this study with those studies, using the Thioflavin staining e.g. Lewis et al. [9].

Photograph 1.

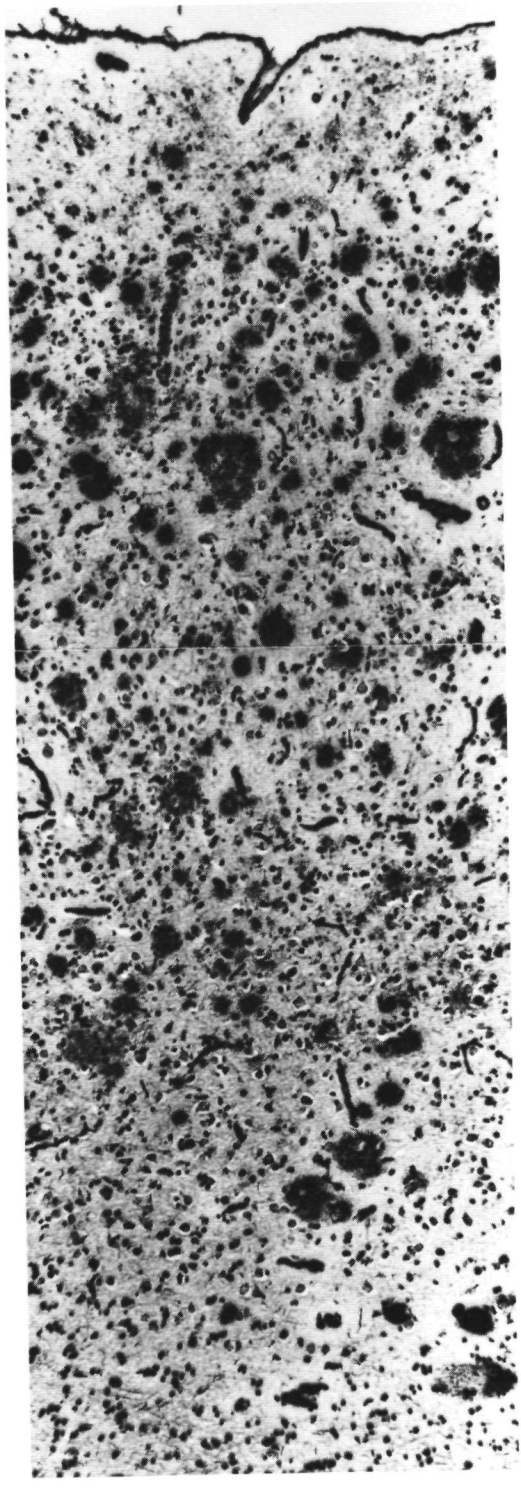

photograph 1.
Cross section through the neocortex (Temporal cortex, Area 20), stained after the Yamamoto-staining method. Manification 80x. This image is comparable with the projected images, on which the SP distribution maps represented in the figs. Ia-VIId are based.

II.4.2.2. The Yamamoto method.

The silver method after Yamamoto (Ya) [2] was a modification of the Gros-Schultze's modification of the Bielschowsky method.
This Yamamoto stain was used in this study, because it results in optimal contrast between SP and the remainder of the neuropil.This contrast made SP mapping possible in comparatively large parts of cortical sections (vide infra).

The Yamamoto staining method is described as follows:
Sections have to be
1. dewaxed and rehydrated
2. placed in silver nitrate solution (20%) for 20 minutes
3. held in distilled water
4. put in the dark in the silver solution for 15 minutes, after adding drop by drop of evaporated ammonia, under vigorously stirring, until the precipitate turns clear. Then two more drops of the ammonia solution are added.
5. immersed in distilled water to which 3 drops of the evaporated ammonia are added.
6. immersed again in the silver/ammonia solution to which 3 drops of developer are added. The slides remain in this solution, until the fibers of the white matter are turned black (after approx. 3-5 minutes).
7. washed in distilled water.
8. put in hypo for 5 minutes
9. washed in distilled water, and,
10. dehydrated, cleared and mounted.

The Yamamoto-staining, is a modified Bielschowsky stain [10]. It was originally derived from the Gros-Schultze modification of the Bielschowsky method. Bielschowsky's method and this modification were originally developed as stains for the visualization of normal components of neurons [11]. Using this staining, a high contrast between SP and surrounding neuropil was obtained, which made our method of analysis a feasible one. The method not only stains SP with high specificity, but also the arterial elastica, axons and NFT. Other structures were discernable by a slight, golden background staining. The contrast between the SP and the yellowish stained structures may be modulated by the influence of the developer used during the procedure (1).
It is important to realize, that the Yamamoto-staining possibly has a somewhat lower affinity for eosinophilic material, as stated in the Yamamoto paper. In our material, however, SP with a central core were visualized with a dense dark core. Also neuropathologically changed vessel walls, which appeared Congo-Red positive under fluorescence, stained dark. Therefore, it may be expected, that this staining also stains (part) of those SP that contain only congophilic material (the so called 'burned out' plaque).
It is interesting to note, that the Bielschowsky method, using

20 % of silvernitrate, demonstrated as many cortical plaques as an immunostaining with a primary mouse IgG mAb (4G8, IgG2h) to the beta-amyloid peptide in a comparative study of four different stainings by Wisniewski et al. [12]. In the same cortical area of five AD patients the Bielschowsky method demonstrated 35.8(3.5) SP and the immunostaining 33.2(3.0) SP per square millimeter. There was no significant difference between these two mean values at 99 % level of the two-sided Student's t-test. In this same study, the non-specificity of the Bielschowsky method was stressed. This method also stains NFT and blood vessels.
In summary, although the Yamamoto staining is not specific for SP, these structures are easily identified when a Yamamoto-stained cortical cross section is projected at a magnification of 80x. Therefore the distribution pattern of the SP as observed in our analysis, conforms to the distribution pattern of SP as demonstrated by immunocytochemical methods.

II.5. PLOTTING OF SENILE PLAQUES IN SECTIONS STAINED AFTER YAMAMOTO

After staining of the sections according to the Yamamoto method reviewed above, the quality of the sections is evaluated.

The quality of the section is determined by:

1. the absence of folding of the neocortex, which may arise easily during the staining procedure. It is important to use the Chrome-alum/gelatine coating of the object glasses when working with these stains, in order to promote adherence of the cortex. Partial loosening of the cortex during the staining procedure results in a highly folded cortex, which renders the sections useless for further analysis.

2. proper staining of the "background", ie the non-degenerated neurons should stain faintly yellow, and some of the nerve fibers brownish-yellow. This "background staining" is necessary to obtain a proper contrast between the neuropil and unaffected neurons on the one hand and the SP on the other.

If the sections meet those quality criteria, they are projected on white paper at a magnification of 80 x. This results in a strip of neocortex, comparable with photograph I. As demonstrated in this picture, the SP are clearly distinguishable from all other structures, and no confusion is likely to arise with vessels, neurons or artefacts. Furthermore, not only SP can be distinguished, but also the various types of neurons and the density and direction of the fiber-network can be noticed. Using these, an estimate of the location of the border between the subsequent cortical layers is given. Plotting the pial surface, the estimated borders of the cortical layers (according to the scheme of Brodmann) and the SP in one figure, a strip of about 2500 micron wide (a "macrostrip") is obtained.
In order to arrive at a representation of the SP distribution in a large number of cortical area's, the original SP registrations are reduced in size and put together in maps. These maps show the real, and not a schematic drawing of the distribution of SP in the brains of the AD patients described earlier.

Furthermore, in order to answer several questions concerning the numerical distribution of SP in AD/SDAT, a method was developed to analyze these SP registrations: According to this method, the SP registration was divided into 10 small strips. The SP number in each strip pro cortical lamina was determined. As a counting rule, the SP transected by the upper border of the strip were counted, but those transected by the lower border excluded (fig. II.2.). Next, the surface of the particular cross-section of this very same lamina was determined using pointcounting methods. Taking the

quotient between the obtained number of SP and the number of points counted, a local mean SP concentration can be determined. This last figure (#SP/strip/point/lamina) can be expressed as the number of SP pro standard counting volume. In this way, the concentration of the SP in the different laminae can be studied. This figure is independent of the thickness of the individual layer. Because of the large sample size (>2500 micron wide strip of cortex), and the subdivision of this sample in ten smaller ones, the statistical correlation between SP concentration in various cortical layers can be calculated.
It is also possible, to pool data from various brains and various cortical areas, and to answer the question, whether there exists a distinct laminar distribution pattern in SP distribution or not.

II.6. CALCULATION OF THE DISTRIBUTION OF SENILE PLAQUES, NEUROFIBRILLARY TANGLES AND CONGOPHILIC ANGIOPATHY USING THE CONGORED STAINING

After staining according to the Congo-Red method, the sections of the cortex are illuminated with a Mercury-lamp (HBO 50) using the filters BP 546/12 with filter 1 mm BG 38 and looked at, using ocular filter LP 590.
In order to distinguish thin tangles and tangle-like threads, a standard magnification of 400x is used. Calculation of the distribution pattern of SP, NFT and CAA, required a square ocular grid to delineate a field of vision of 250x250 square micron. Within this square field, all calculations were made.

In analyzing the distribution of NFT, SP and CAA the following identification criteria for Congo-Red positive structures were used:

NFT:
- display the typical flame shaped structure (picture II), or
- display a thread-like structure of at least 50 micron length.

SP:
- display a core of Congo-Red positive material with a cross section larger than 25 micron.
- display a round collection of Congo-Red positive fibers, together with other Congo-Red material

CAA:
- display an intense staining of Congo Red material accumulating in a vessel wall, in comparison with the faint coloration of normally slightly Congo-Red positive vessel structures.

The following sampling procedure was used to collect the data:
1. a location in the section was chosen with the least possible distortion as due to the geometry of the cortex.
2. one side of the ocular quadrant was aligned to the pial surface of the cortex, by repositioning the section.
3. the structures of interest (SP,NFT,CAA) were scored and
4. the illumination was shifted from fluorescent to normal transmitted illumination and the field of vision distributed over the cortical laminar pattern.
5. the section was shifted in order to position the upper border of the next field of vision with the lower border of the former.
6. repeating 3 trough 4, until the white matter was reached, resulted in a registration with cortical depth of the structures of interest in a strip of cortex, 250 micron wide.

7. the field of vision was aligned again to the pial surface and the bordering strip of 250 wide was analyzed according to point 2 through 5.

This procedure was performed thrice on the same cortical area, resulting in a cortical strip of 750 micron wide.

Ad 3. The scoring of the structures of interest in a field of vision was performed using an exclusion principle, in order to avoid double counting of structures: the structures, being intersected by the lower border of the square field of vision formed by the ocular grid were counted, but those intersected by the upper border were not counted. The same principle was applied to the right and left border of the field of vision: only structures intersected by the left border were counted and not those intersected by the right border, in order to avoid double counting the same structures in neighboring strips.

In order to calculate the distribution of NFT, SP and CAA over the various cortical laminae, all fields analysed with the Congo-Red Fluorescence method were viewed in normal transmission light microscopy.
The ocular grid has outer dimensions of 250 x 250 square micron measured on the section, using a standard 40 x objective and 10 x wide field oculars. This square grid itself was subdivided in 10 strips vertical and 10 strips horizontal. In transmitted light, the location of the border of the cortical laminae could be determined. Using the subdivision of the grid all structures above the strip containing the border were counted for the upper layer in the field of vision. The remainder of the field of vision was considered to belong to the lower cortical layer. The number of strips, 250 micron wide, covering one cortical layer was also registered. Using this sampling scheme, the number of items counted could be related to the surface of the cortical layer under investigation.

The prevalence of CAA was expressed in the 'CAA-score'. This score was constructed in order to evaluate the distribution of the CAA. Scoring the same material three times resulted in a reliable figure. Each time, three visual fields of 250*250 square micron on a section of 10 micron thickness was evaluated. The scores for each single layer were calculated, correcting for the differences in thickness of the individual layers.

CAA-score 1: a single lesion on a microvessel suffering from congophilic angiopathy
CAA-score 2: a moderate prevalence of congophilic degenerated microvessel walls
CAA-score 3: an abundant quantity of congophilic angiopathy

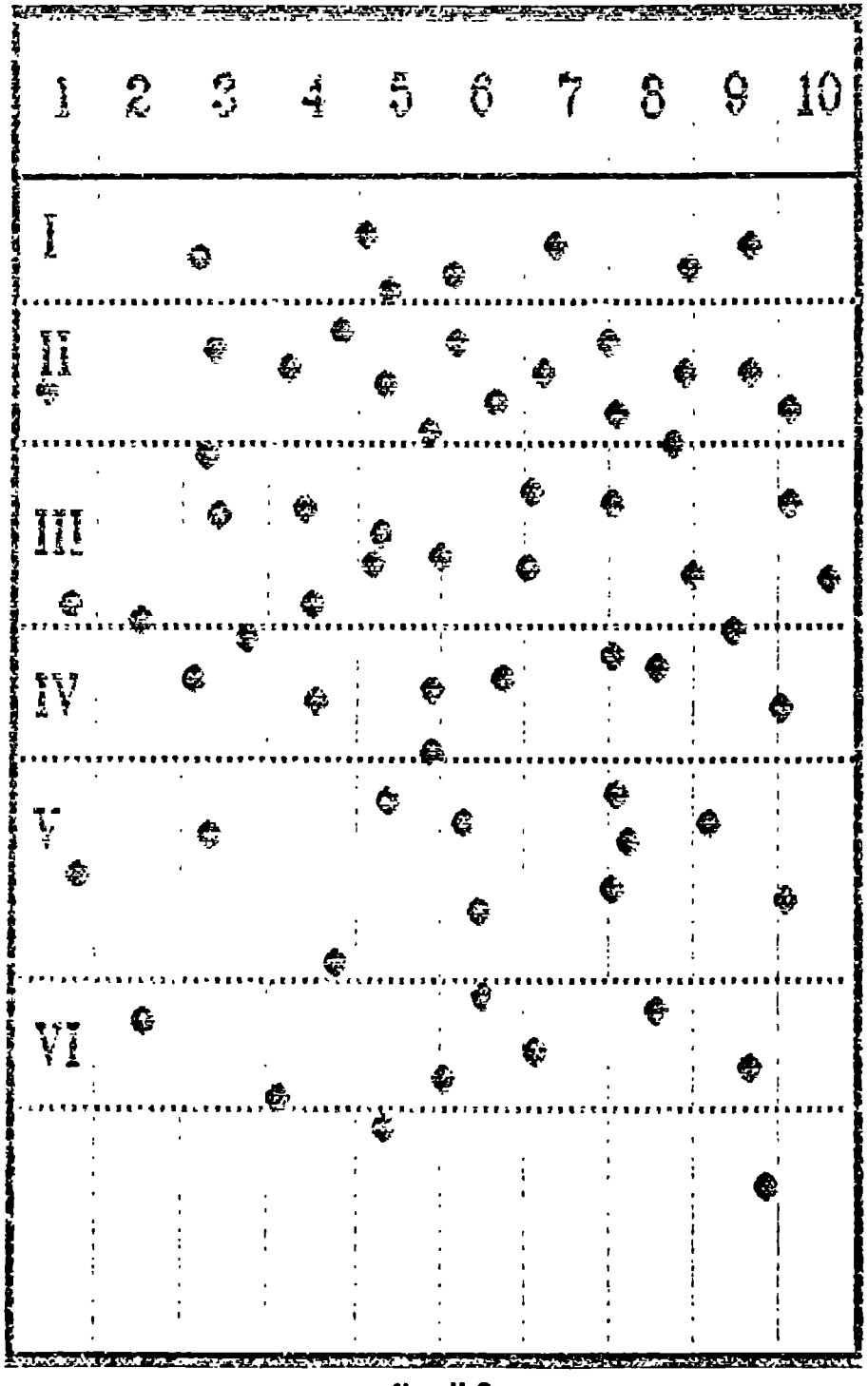

fig. II.2.

1.Haug H, S Kuhl, E Mecke, N-L Sass and K Wasner. The significance of Morphometric Procedures in the investigation of Age Changes in Cytoarchitectonic Structures of Human Brain. J Hirnf (1984) 25(4):353-374.

2.Yamamoto Y, A Hirano. A Comparative study of modified Bielchowski, Bodian and Thioflavin S stains on Alzheimer's Neurofibrillary Tangles. Neuropath Appl Neurobiol (1986) 12:3-9.

3.Uhl GR. In Situ Hybridization in Brain. New York, Plenum Press (1986) pp265-6.

4.Carson F. Nerve Tissue. In: Theory and practice of Histotechnology, 2nd Ed. eds. D C Sheenan, B Hrapchak, Mosby, St. Louis, USA (1980).

5.Puchtler H, F Sweat, M Levine. On the binding of Congo-Red by amyloid. J Histochem Cytochem (1962) 10:355-364.

6.Puchtler H, F Sweat. Congo Red as a stain for fluorescence microscopy of Amyloid (Letter). J Histochem Cytochem (1965) 13:693-694.

7.Kelenyi GK. Thioflavine S fluorescent and Congo-Red anisotropic staining in the histologic demonstration of amyloid. Acta Neuropathol (1967) 7:336-348.

8.Gallyas F. Metal-catalyzed oxidation renders silver intensification selective. J Hystochem Cytochem (1986) 12:1667-1672.

9.Lewis DA, MJ Campbell, RD Terry JH Morrison. Laminar and regional distributions of Neurofibrillary Tangles and Neuritic plaques in Alzheimer's Disease: A quantitative study of visual and auditory cortices. J Neurosci (1987) 7:1799-1808.

10.Yamamoto Y, A Hirano. A comparative study of modified Bielschowsky, Bodian and Thioflavin S stains on Alzheimer's Neurofibrillary tangles. Neuropath Appl Neurobiol (1986) 12:3-9.

11.Bielschowsky M. Die Silberimpraegnation der Neurofibrillen. Einige Bemerkungen zu der von mir angegebenen Methode und von mir gelieferten Bildern. J Psychol Neurol (1904) 3:169-189.

12.Wisniewski HW, GY Wen KS Kim. Comparison of four staining methods on the detection of neuritic plaques. Acta Neuropathol (1989) 78:22-27.

III.1. MACROSCOPIC NEOCORTICAL ATROPHY IN ALZHEIMER'S DISEASE IS DUE TO SELECTIVE LOSS OF NEOCORTICAL SURFACE.
An unbiased macroscopic estimation of neocortical atrophy in Alzheimer's Disease.
(submitted to Neurobiology of Aging).

MACROSCOPIC NEOCORTICAL ATROPHY IN ALZHEIMER'S DISEASE IS DUE TO SELECTIVE LOSS OF NEOCORTICAL SURFACE.

An unbiased macroscopic estimation of neocortical atrophy in Alzheimer's disease

C.A.J. Broere, O.J.M. Vogels, A. Keyser

Institute of Neurology,

University of Nijmegen,

PO Box 9101,

6500 HB Nijmegen,

The Netherlands

Correspondence to

C.A.J. Broere, MD, Institute of Neurology, PO Box 9101,

6500 HB Nijmegen, The Netherlands.

RUNNING TITLE: NEOCORTICAL ATROPHY IN ALZHEIMER'S DISEASE

ABSTRACT
BROERE,C.A.J., O.J.M. VOGELS AND A. KEYSER, Macroscopic neocortical atrophy in Alzheimer's disease is due to selective loss of neocortical surface. NEUROBIOL AGING. Analysis of the neocortex, using unbiased stereolgical methods showed in patients a volume loss of 41 % as compared to sex and age-matched controls ($p = 0.0008$, MW-test). This suggests a preferential atrophy of the neocortex. Moreover, analysis showed a loss of 38 % in neocortical surface ($p = 0.017$ MW-test), and no significant loss of neocortical thickness. Thus, global neocortical atrophy, defined as macroscopic loss of volume, can be explained in terms of surface loss and not as a decrease in cortical thickness. At the regional neocortical level, the Insular neocortex demonstrates a volume loss of 46 % ($p = 0.0019$, MW-test) whereas the neocortex volume of the Gyrus Cinguli decreases with 30 % ($p = 0.0157$ MW-test). This difference proved to be significant ($p = 0.05$, Student t-test). This implies regional differences in macroscopic neocortical atrophy.

KEYWORDS:
Stereology, Alzheimer's Disease, Neocortex, Cerebral Atrophy, Human

INTRODUCTION

Macroscopic atrophy of the cerebrum in Senile Dementia of the Alzheimer Type (SDAT) and in Alzheimer's disease (AD) is a well known neuropathological finding.

Parameters employed to express cerebral atrophy are total brain weight and total brain volume. According to older data, total brain weight in healthy individuals is reduced by less than 30 gram for both sexes, until 60 years of age [2]. In the next decade, loss of brain weight accelerates slightly, and after 70 years of age a stronger decline reduces the total brain weight with approximately 100 to 200 gram, as compared to the normal brain weight of 1320-1390 gram for man and of 1204-1250 gram for females in the third decade of life [3]. These data are not corrected for the secular trend of body length [8]. An increase of 10 cm in body length corresponds statistically with an increase of 55 gram of brain weight. A significant mean brain weight loss has been demonstrated after the age of 55, for both sexes [16].

Total brain volume is also reduced with aging: at the age of 55, approximately 92 % of the inner skull volume is occupied by the brain volume. In the 8th and the 9th decade, the brain volume is reduced to 83 and 81 % of the inner skull volume respectively [5].

Brain weight and total brain volume reduction are considered as parameters for atrophy. Alzheimer [1] presented his first case as a neocortical disease. Because of the involvement of the neocortex, a more selective measure for the atrophy of the neocortex should be considered. The amount of change in cortical volume is a likely candidate for this measure.

The degree of the macroscopic neocortical atrophy, however, is not the same in all different cortical areas: after dissection and weighing of particular subdivisions of the cortex, specific parts of the parietal and temporal lobe showed significantly more severe weight loss than other cortical regions, indicating a differential atrophy [18].

The number of quantitative studies devoted to atrophy of the neocortex is limited. This is mainly due to the complexity of neocortical geometry [2]. This geometry influences variations of local volume and also of local cortical thickness. Often, shape assumptions are made in order to simplify these geometrical problems. The neocortex is a 3-dimensionally highly folded structure. Sections from the neocortex have to be considered as a 2-dimensional representation and therefore cannot give the 3-dimensional information necessary to make valid measurements of cortical thickness or local variations in volume. Furthermore, accounting for estimations of these local variations in neocortical volume is important, because they result in a local change of the neuronal density, cell densities being the quotient of the absolute cell number in a particular structure and the volume of that structure. In order to quantify the absolute cell number of the neocortex in a particular region in AD and subsequently probable cell loss in the cerebral cortex in that particular region, the (changes in) volume of these regions have to be determined first.

This loss of volume of the neocortex can be explained either by a decrease of cortical thickness, by a decrease in cortical

length (defined as the length of a hypothetical rectangle replacing the cortex on cross section [6]) or by a combination of these two possibilities. In order to resolve this question, an unbiased method was used to calculate the volume, surface and thickness of the neocortex.

MATERIALS AND METHODS

The patients and controls included male (n=20) and controls (n=17) and female AD patients (n=14) and controls (n=9). The postmortem delay ranged from 4 to 48 hours, but no statistical difference existed between these four groups.
The mean age of the female control group was 71 years (Standard Error of the mean, SEM: 2.92, range: 27) and was not significantly different from the female AD group: 79.8 years (SEM: 2.12; Range:29). In the male groups no statistical difference in age was found either (AD group: 78.9; SEM: 1.84; Range: 33 and control group: 72.44; SEM: 3.0; Range: 51 years).

The neuropathological diagnosis was performed on paraffin embedded sections stained for Nissl, Bodian, Yamamoto-Bielschowsky, fluorescence Congo Red [13,14] and Thioflavine S, using neuropathological criteria, based on the presence and distribution of NFT and SP [10].

In all these subjects, total brain weight and total brain volume were measured after 4 weeks fixation in buffered formaldehyde according to standard procedures. Total volume was determined by measuring the amount of water displacement after complete submersion.

Four AD brains and four age and sex matched control brains were employed for further analysis (Table 1). Of these brains both hemispheres were studied.

The brains were put in a polystyrene box and embedded in Agar-Agar 5 %. This box was sectioned in 1.5 mm thick slices, using a mechanical sectioning device. The distance from the first to the last slice was measured and divided by the total number (n) of slices, resulting in an accurate estimation of the mean slice thickness, t(mean). Using a standard photocopier, photocopies (scale 1:1) of all brain slices were made. From the total amount of approximately 90 brain slices (range:80-100), each fifth slide (fraction F=1/5) was systematically selected for further analysis: the first slide was randomly selected from the first 5 slices. Consequently, the mean thickness of our measuring slide,

$$T(\text{mean}) = t(\text{mean}) * 1/F, \quad (1)$$

or in our cases 1.5*1/0.2=7.5 mm.

The procedure of volume determination used is an application of Cavalieri's principle [4,11,17]. Cavalieri's principle provides an unbiased volume estimator and can be applied to any structure without any assumptions upon shape or geometry. For determination of the volume of the neocortex a grid of evenly spaced points on a transparent plastic sheet was constructed, the test system. The distance between two neighboring points (d) is chosen to optimize the efficiency of the counting procedure. The test grid is applied to the photocopies of the selected slices, and the grid points, hitting the neocortex, Pi, are counted. The actual volume, V, is given by the expression:

$$V(\text{neocortex}) = T(\text{mean}) * d^2 * (\text{Total sum Pi}), \quad (2)$$

where d^2 is the total area of the test system divided by the total number of counting-points in this test system.

For the calculation of the surface of the cortex, a transparent sheet with line segments is used. The number of intersections, Ii, of the line-segments with the outer surface of the neocortex is counted and the neocortical surface is determined, using the equations:

$$Sv = (p/l) * (\text{Sum Ii})/(\text{Sum Pi}), \quad (3)$$
$$S = Sv * V \quad (4)$$

where p/l is the number of counting points pro unit length of the line segment, Sv is the Volume weighted surface, (Sum Ii) the total sum of intersections of the line-segments with the pial surface and (Sum Pi) the total number of points of the grid hitting the neocortical rim on the cross section.

To ascertain absence of bias due to a possible preferential orientation of the pial surface, each time the transparent is applied to the photocopy, the orientation of the measuring grid is randomized [9].

The mean cortical thickness is obtained by dividing the cortical volume (V) by the cortical surface (S). This result is also free of bias and therefore independent of the cortical geometry.

The systematic sampling procedure enables us to estimate the coefficient of error (CE) for the individual measurements, according to the procedure described by Gundersen [7].

Using the same method, described above for the global neocortex, the volume and surface of the neocortex of the Insula and Gyrus Cinguli was determined. The only difference was that every section through the structure was analyzed, so F = 1.0 in expression (1).

The insular cortex was defined as the cortex delineated by the Sulcus Circularis Insulae. As its anterior border, the line was taken where the cortex of the temporal lobe is separated from the insular cortex by the fissura lateralis. The borders of the Cingulum were defined to be the Sulcus Cinguli, which was easily recognized in all our material, and anteriorly and posteriorly by the Rostrum and Splenium Corporis Callosi respectively. In AD, the length of the Corpus Callosum is not changed [18], resulting in fixed borders for the Cingulum.

RESULTS

The determination of mean total brain weight and volume demonstrates a weight loss of 16.6 % (Mann Whitney test (MW test): $p = 0.0006$) in females and of 13.0 % (MW test: $p = 0.016$) in males in AD, compared to sex matched controls. The loss in volume revealed similar figures: 16.2 % (MW test: $p = 0.0028$) and 14.1 % (MW test: $p = 0.0271$), respectively. The differences between females and males were not significant (Table 3). Regression analysis revealed a negative correlation between age and total brain weight in the two control groups (Pearson's r: -0.457 (females); -0.375 (males)). In the AD groups, however, no such correlation could be demonstrated (Pearson's r: -0.079 (females); -0.0805 (males)). In the male control group, a decrease of 5.17 gram pro annum (Standard error: 3.19) was found and in the female group a decrease of 5.98 gram pro annum (Standard error: 4.4). These results were not corrected for the secular trend of increasing body length.

Determination of the individual values for the total cortical volume, surface and thickness (Table 2), results in a mean neocortical volume of 239.875 cm^3 (SEM: 9.100) for the controls and 140.750 cm^3 (SEM: 6.800) for the AD group, a difference of approximately 100.000 cm^3 or 41% (MW test: $p = 0.0008$) (Table 4). Unbiased measurements of surface resulted in mean surface values of 93.125 mm^2 in the control cases and 56750 mm^2 in the Alzheimer group (MW test: $p = 0.0117$). This means a decrease of approximately 36000 mm^2 or 39 % in the AD group (Table 4).

Applying the same technique, an unbiased estimate of the volume, surface and cortical thickness of the insular and the cingular cortex was obtained (Table 5).

The mean cortical volume of the Insula was 7.037 mm^3 in control brains and 3.822 mm^3 in AD. This difference of 46 % is highly significant (MW test: $p = 0.0019$). The mean cortical surface of the Insula was 2.725 mm^2 in control brains, and 1.650 mm^2 in AD, a difference of 40 % (MW test: $p = 0.0019$). Combining these results, an unbiased estimate of the cortical thickness of the Insula could be obtained of 2.582 mm for controls and 2.316 mm in AD, a difference of 10% (MW test: $p = 0.01$) (Table 5).

In the Gyrus Cinguli, a mean cortical volume of 5.687 mm^3 and of 3.950 mm^3 was found for controls and AD respectively. The difference of 30% proved to be significant (MW test $p = 0.0157$). No difference in neocortical surface of the Gyrus Cinguli could be found. The cortical thickness for the cortex of the Gyrus Cinguli was 3.92 mm in the control brains and 2.67 mm for the AD brains. This difference of 30 % is significant (MW test: $p = 0.05$). The data are summarized in Table 5.

DISCUSSION

From the data on the changes in total brain weight and brain volume, a trend for a somewhat more pronounced atrophy in the male patient group than in the female patient group can be identified. However, this difference is not significant. In the two control groups, a negative correlation between brain weight and age is noticed. The majority of the cases was older than 70 years (>80%), and was therefore subjected to a more severe physiological volume change [3]. Because the age of the majority of the control cases is within an interval of 15 years (from 75-90 years), secular trends may not be important. Interestingly, in our AD group an age - total brain weight correlation could not be demonstrated, probably because cerebral atrophy is an important feature itself of the disease process. Because, the age of onset is not the same for every patient, we correlated total brain weight loss with the duration of the disease. As the criterium of the duration of the disease, the period of professional care in a nursery home for the elderly was taken. Regression analysis demonstrated a weak positive correlation between the duration of the disease and the total brain weight (Pearson's r=0.16). The most strongly atrophied brains, defined as having a total brain weight less than 1000 gram in this study, are from patients, who had an average nursing home time of 64 months. Apparently, a possible subtype, which evolves very slowly clinically, results in a major brain atrophy.

The difference of the total brain atrophy of 16 % weight loss or 13 % volume loss, contrasts with the 41 % volume loss in the neocortex. This can be explained as a result of the selective strong involvement of the neocortex in the pathology in AD, and a relatively spaering of the white matter. According to our results, the global neocortical atrophy must be explained by a similar loss of cortical surface. This general result is in agreement with the model study after the change in cortical length in the Lobus Temporalis [7]. However, analysis of the Insula and the Gyrus Cinguli demonstrated the possibility of a preferential macroscopic atrophy in some cortical regions. This is in accordance with the finding of a preferential weight loss in certain neocortical regions [12]. Furthermore, our results do indicate, that not in every cortical region the same explanation is applicable. In the Insula about 25% of the atrophy is to be explained by loss of cortical thickness and as far as the Gyrus Cinguli is concerned, no loss of neocortical surface could explain the atrophy demonstrated in this study.

The global absence of significant reduction of cortical thickness also agrees with another study [16], which demonstrated that the thickness of the coronal section of the midfrontal and superior temporal cortex showed not to be statistically different in normal subjects and in AD patients. Our results prove, that the cortical atrophy in AD is due to loss of neocortical surface, since our method is independent of the complex cortical geometry. If affected elements were distributed in a laminar fashion, atrophy would mainly be localized in some cortical layers,and a prominent loss of cortical thickness should result. If on the other hand, the affected elements were arranged in a columnar fashion, a loss of

cortical surface should result.

The possibility of columnar atrophy is supported by our findings of global cortical atrophy, without decrease of neocortical thickness, but regional differences in macroscopic atrophy still leaves open the possibility of both laminar and columnar atrophy in some cortical regions, such as the Gyrus Cinguli.

We would like to thank mr. C. Cornelissen (Department of Anatomy and Embryology) for excellent technical assistance. Neuropathological diagnosis was carefully performed by Dr. K. Renkawek. Brain material was kindly provided by Dr. P. van Kalmthout and Dr. T. Vereecken, and was partially obtained from the Brain Bank of the Netherlands Institute for Brain Research (Dr. R. Ravid). This study was supported by a grant from the JANIVO-foundation.

TABLE 1: BRAIN MATERIAL FOR NEOCORTICAL ANALYSIS

case	dia-gnosis	sex	age (y)	brain weight (gram)	brain volume (cm^3)	fixation time (months)	death cause	post-mortem delay (h)
1	AD	F	76	855	840	0.5	uremia	3
2	AD	M	77	985	948	1	pneumonia	<1
3	SDAT	M	90	1160	1100	6	sepsis	<12
4	SDAT	F	93	842	819	7	pneumonia	<12
5	Control	F	75	1250	1200	6	mamma CA	36
6	Control	M	65	1570	1557	2	pneumonia	36
7	Control	M	80	1450	1475	7	cardiac arr.	48
8	Control	F	58	1235	1190	4	cardiac arr.	36

TABLE 1: List of data of the detailed analyzed material, with neuropathological diagnosis, sex, age, brain weight, brain volume fixation time, cause of death, post-mortem delay.
Abbreviations:
AD: Alzheimer's Disease; SDAT: Senile Dementia of Alzheimer Type;
F: Female; M: Male; y = years; h = hours; cm^3 = cubic centimeter;
CA: carcinoma; arr.:arrest.

TABLE 2: TOTAL NEOCORTICAL VOLUME, SURFACE AND THICKNESS

Case	Left Hemisphere					Right Hemisphere				
	Volume (cm^3)	CE	Surface (cm^2)	CE	T (mm)	Volume (cm^3)	CE	Surface (cm^2)	CE	T (mm)
1	121	0.033	450	0.038	2.68	108	0.035	510	0.038	2.1
2	137	0.014	730	0.025	1.88	136	0.031	730	0.035	1.8
3	146	0.011	490	0.018	2.98	164	0.016	550	0.016	2.9
4	157	0.018	590	0.031	2.66	157	0.014	490	0.024	3.2
5	224	0.015	900	0.019	2.49	238	0.019	940	0.034	2.5
6	277	0.025	980	0.036	2.83	295	0.02	1070	0.031	2.7
7	231	0.02	790	0.034	2.92	239	0.019	740	0.025	3.2
8	239	0.013	1040	0.02	2.30	226	0.015	990	0.024	2.2

TABLE 2: Results of the total neocortical volume, surface and thickness
Abbreviations: T: Thickness; CE: Coefficient of Error.

TABLE 3 : MACROSCOPIC BRAIN CHANGES IN ALZHEIMER'S DISEASE
Total Weight and Volume changes

	MALES			FEMALES		
	Controls (n=17)	AD (n=20)	% Change	Controls (n= 9)	AD (n=14)	% Change
WEIGHT:	1334 (41.6)	1113 (32.8)	- 16.6*	1188 (38.3)	1034 (38.3)	- 13.0**
VOLUME:	1305 (46.0)	1093 (38.0)	- 16.2***	1176 (48.0)	1010 (41.6)	- 14.1****
AGE :	72.4 (3.0)	78.1 (1.8)	+ 7.2#	71.0 (2.9)	79.8 (2.2)	+ 11.0##

Table 3: Mean values of Total Brain Weight, Total Brain Volume and Age are given.
(....) = SEM : Standard Error of Mean.
Statistical analysis: non-parametric Mann-Whitney U test:
*:p=0.0006; **:p=0.0157; ***: p=0.0028
****: p=0.0272
#:p=0.17 (ns); ## :p=0.15 (ns)
Units: Weight: gram; Volume: cubic centimeter; Age: years

TABLE 4: MACROSCOPIC CHANGES IN THE NEOCORTEX IN ALZHEIMER'S DISEASE

	CONTROLS	ALZHEIMER'S DISEASE	% CHANGE
TOTAL VOLUME :	239875 (8200)	140750 (6800)	- 41 %*
TOTAL SURFACE :	93125 (4100)	56750 (3800)	- 39 %**
AVERAGE THICKNESS:	2.55 (0.18)	2.66 (0.11)	+4.5 %#

TABLE 4: Macroscopic changes in AD in the total neocortex.
(...) = SEM.
Units: Volume: mm^3; Surface: mm^2; Thickness: mm.
*:p = 0.0008; ** p = 0.017; # :p = 0.48 (not significant)
Used test: Mann- Whitney U test.

TABLE 5: LOCAL DIFFERENTIAL MACROSCOPIC CHANGES IN THE NEOCORTEX

Cortical Structure:	INSULA			GYRUS CINGULI		
	Control	AD	Change	Control	AD	Change
MEAN VOLUME :	7039 (358)	3822 (278)	- 46 %*	5687 (460)	3950 (227)	- 30 %**
MEAN SURFACE :	2725 (140)	1650 (71)	- 40 %*	1450 (148)	1475 (86)	0 %
MEAN THICKNESS :	2.58 (0.02)	2.32 (0.16)	- 10 %#	3.92 (0.25)	2.68 (0.23)	- 31 %***

TABLE 5:Local differential macroscopic changes in the neocortex in AD
Units: Volume: mm^3 ; Surface: mm^2 ; Thickness: mm.
*:p = 0 .0019;**:p = 0.0157;***:p = 0.027;#:p = 0.16 (ns).

1.Alzheimer, A. Ueber eigenartige Krankheitsfaelle des spaeteren Alters. Z Ges Neurol Psychiat 4:356-385, 1911.

2.Blinkov, S.A. and I.I. Glezer. Das Zentralnervensystem in Zahlen und Tabellen. VEB G. Fisher, Jena, 1968.

3.Bok, S.T. Histonomy of the cerebral cortex. Elsevier, Amsterdam, 1959.

4.Buerger, M. Altern und Krankheit als Problem der biomorphose. G. Thieme, Leipzig, 1960.

5.Cruz-Orive, L.-M. Estimating volumes from systematic hyperplane sections. J Appl Prob 2:518-530, 1985.

6.Davis P.J.M. and E.A. Whight. A new method for measuring the cranial cavity volume and its application to the assessment of cerebral atrophy at autopsy. Neuropathol Appl Neurobiol 3:341-358, 1985.

7.Duyckaerts C., J.J. Hauw, F. Piette, V. Rainsard, V. Poulain, P. Berthaux, R. Escourolle. Cortical atrophy in senile dementia of the Alzheimer type is mainly due to a decrease in cortical length. Acta Neuropathol (Berl) 66:72-74, 1986.

8.Gundersen, H.J.G. and E.B. Jensen. The efficiency of systematic sampeling in stereology and its prediction. J Microsc 17:229-263, 1987.

9.Haug, H. Macroscopic and microscopic morphometry of the human brain and cortex. A survey in the light of new results. In: Brain Pathology. G. Pilleri and F. Tagliavini (Eds.). Vol. 1, 1984, pp. 123-149.

10.Haug, H. Brain sizes, surfaces, and neuronal sizes of the cortex cerebri: A stereological investigation of man and his variability and a comparison with some mammals (Primates, Whales, Marsupials, Insectivores, and one Elephant). Am J Anat 180:126-142, 1987.

11.Khachaturian, Z.S. Diagnosis of Alzheimer's Disease. Arch Neurol 42:1097-1105, 1985.

12.Mattfeldt, T. Volume estimation of biological objects by systematic sections. J Math Biol 25:685-695, 1987.

13.Najlerahim, A.and D.M. Bowen. Regional weight loss of the cerebral cortex and some subcortical nuclei in senile dementia of the Alzheimer type. Acta Neuropathol 75:509-512, 1988.

14.Puchtler H., F. Sweat and M. Levine. On the binding of Congored by amyloid. J Histochem Cytochem 10:355-364, 1962.

15.Puchtler H. and F. Sweat. Congored as a stain for fluorescence microscopy of amyloid. J Histochem Cytochem 13:693-694, 1985.

16.Terry R.D., A. Peck, R. DeTeresa, R. Schechter and D.S. Horuopian. Some morphometric aspects of the brain in senile dementia of the Alzheimer type. Ann Neurol 10:184-192, 1981.

17.Terry, R., R. DeTeresa and L.A. Hansen. Neocortical cell counts in normal human adult aging. Ann Neurol 21:530-539, 1987.

18.Uylings, H.B.M., C.G. van Eden and M.A. Hofman. Morphometry of size/volume variables and comparison of their bivariate relations in the nervous system under different conditions. J Neurosci Meth 18:19-37, 1986.

19.Weis, S., H. Hinsberger and K. Jellinger. Veraenderungen des Corpus callosum in der pathologischen Alterung. 33. Jahrestagg. Dtsch. Ges. Neuropath. Neuroanat. 1988.

III.2. THE DISTRIBUTION OF NEUROFIBRILLARY TANGLES, SENILE PLAQUES AND CONGOPHILIC ANGIOPATHY.

III.2.1. Introduction

In this study, the distribution of Neurofibrillary Tangles (NFT), Senile Plaques (SP) and Congophilic Amyloid angiopathy (CAA) is investigated. The distribution of SP is studied using two methods: the Congo-Red fluorescence (CR-F) method and the Bielschowsky method in a modification after Yamamoto.
In Congo-Red, the distribution of NFT, SP and the Congophilic Angiopathy (CAA) is analyzed because the amyloid component of these structures is stained intensely, whereas the modified Bielschowsky (Yamamoto) has more affinity for neuritic fibre components. Because of this difference in affinity, the intensity and the morphology of the plaques is observed to be different in these stains: the silver stain preferentially stains nerve fibers, whereas CR-F visualizes more the amyloid component. This may result in a different staining pattern [1] and hence in a different SP distribution pattern.

The large contrast between SP and the background in the Yamamoto-staining allowed mapping the SP distribution using the projection method described in the previous chapter.

III.2.2. Distribution of Senile Plaques in Yamamoto-stained sections.

Employing the method of analysis described in the previous chapter, the distribution of SP was studied in a large number of cortical areas in 5 AD patients and 3 matched controls. An atlas of the distribution of SP of each brain investigated was produced (Fig a-z). In these figures, the results of the plotting procedure are on display. A drawing of a cerebral hemisphere, in medial or lateral view, is given, with the borders of the cortical areas as copied from Brodmann's classical monograph [2]. A cortical area is connected by a line-segment with a diagram of plotted SP in a Yamamoto-stained cross section, taken from that particular area. On these plottings, the probable border between the various cortical laminae is represented by a dotted line. In these maps, each plotted Area has its own place in the setup of the map, making comparison between the various brains easy.

III.3. THE YAMAMOTO STUDY OF THE DISTRIBUTION OF SENILE PLAQUES

III.3.1. A short description of the Yamamoto cortex maps of the individual cases.

THE ALZHEIMER CASES:

III.3.1.1. Case 87068 (fig. III.1a-d).

In this case 30 cortical areas were available for examination. SP were present in every area studied. Inspection of the map learns that the concentration of SP is more or less the same in corresponding cortical areas within both hemispheres. SP are noticed in the cortical areas 20, 21 and 22, of the temporal lobe, and in the occipital cortex, noticeably so in Area 17. In Area 37, especially in the part on the lateral aspect of the hemisphere, a concentration above average of SP is noticed. This latter area is considered to be an area of integration of visual information. Area 7, a center of multi-modal information integration seems relatively spared in this case.

III.3.1.2. Case 87395 (fig. III.2a-d).

In this case, 37 cortical areas are plotted. From the plottings, a heavy involvement of the structures of the temporal lobe can be deduced, Area 20 being the most involved followed by Area 21 and Area 22. The plottings of the SP in corresponding cortical areas do show considerable variation: in the left hemisphere, Area 8 and the insular region display more SP's than their counterparts in the right hemisphere. For other areas, no such conspicuous asymmetry can be noticed. The areas which are least affected, are Area 17 and 7.

III.3.1.3. Case 88177 (fig. III.3a-d).

Case 88177 demonstrates SP to be present in every cortical area examined, but, like case 87068, a relative "immunity" of plaque formation in Area 7. The cortical areas of the temporal region seem to be affected most, but also the cingulate cortex and insular cortex are heavily involved. As in case 87068, the lateral part of the Area 37 is more involved than the medial part. There is a slight involvement of the primary sensory areas 4 and 17.

III.3.1.4. Case 89033 (fig.III.4a-d).

Case 89033 shows a strong involvement of the frontal region: both hemispheres display large numbers of SP's in the Areas 11 and 10. The cingulate cortex of Area 24 and Area 23 is strongly affected by plaque formation. According to this plotting, the cingulate regions display more SP's than the temporal regions Area 20, Area 21 and Area 22, which are traditionally thought to be most severely involved in the process. The primary visual cortical region, Area

17 shows as many SP's as Area 7, a multi-modular integration area.

III.3.1.5. Case 88243 (fig.III.5a-d).
When the plottings of SP in this brain are reviewed, the first item to be noticed, is the lack of SP in Area 7. The number here is the lowest of all neocortical areas studied in this brain. In the primary sensory areas, such as Area 17 and Area 2 SP also are relatively rare. In the planum temporale or the primary acoustic area more SP are seen. However, the most abundant areas are located in the temporal and frontal lobe.

THE CONTROL CASES:

III.3.1.6. Case 88268.
In reviewing the Yamamoto stained sections from case 88268 no SP were observed. Therefore no mapping of the SP was performed.

III.3.1.7. Case 88271 (fig.III.6a-d).
The plotting of the SP in the Yamamoto-staining in the sections available in this case shows an absence of SP's in the cingulate gyrus (Area 23 and 24), in the primary sensory areas (Area 2 and 17) and a paucity of SP's in the lateral areas of the temporal lobe (Area 37lat, Area 22, Area 21 and Area 20). In the latter region, single plaques are noticed in the left hemisphere, but not in the right one. The plaques are most abundant in the medial part of Area 37 of both hemispheres.

III.3.1.8. Case 88269 (fig.III.7a-d).
In this control brain few SP are noticed. A curious finding is their relative abundance in Area 10 of the right hemisphere. This region outnumbers all other regions in SP. Repeating of the plotting resulted in more or less the same result. As in the previous case, the number of SP in the cingulate gyrus is very low. A moderate number of SP in the temporal lobe, especially so in the right hemisphere is observed.

III.3.2. The interpretation of the Yamamoto-maps of Senile Plaques.

Analyzing the figures of the five cases of AD, one should consider the following types of differences between the cases studied, namely differences

a) in distribution pattern of SP over the various layers,
b) in overall concentration of SP over the whole cortical cross section,
c) in distribution of the overall concentration over the areas analysed,
d) between the left and right hemispheres, and,
e) between the individual cases.

ad a) differences in distribution pattern of SP over the various layers:
For the analysis of the individual plottings of each cortical area the following possibilities are to be considered:

-1: does a laminar distribution exist ?

In studying the Yamamoto maps of SP, two patterns can be distinguished: sometimes SP seem to be fairly homogeneously distributed (eg. case 89033, Area 4), whereas a clear preference for SP formation in certain cortical lamina is noticed in other cortical areas (eg. case 89033, Area 22, L III).

-2: is the distribution within one lamina homogenous ?

Studying the intralaminar distribution sometimes leads to the conclusion that a gradient of increasing or decreasing SP density exists within a cortical layer. Often, a zone of largest SP density is identified. The SP density, gradually then decreases with increasing distance from this layer.
A SP density maximum is also often formed at the border between two layers (eg. case 89033, Area 21, the border between L II and L III). The density of SP then decreases gradually with increasing distance from this border.

From analysis of each single areal SP plotting it is concluded that the intralaminar SP distribution looks sometimes homogeneous and sometimes not.

ad b) differences in overall concentration of SP over the whole cortical cross section:
When the plotting maps of the individual areas are inspected, an impression of the mean density of the SP in a cortical area is obtained. According to those interpretations, the cortical areas may be arranged according to the overall density of senile plaques. However, no constant distribution pattern over the various cortical areas exists. The fact, that by averaging of numerical data, some significant differences are demonstrated, points to the importance of considering the individual SP distribution pattern, although some general basic scheme of plaque distribution exists. Taking into account other areas confirms the existence of an individual plaque distribution pattern. To evaluate differences in mean cortical plaque distribution between different cortex areas, these areas can be put in an order reflecting the difference in SP concentration.
A different sequence of cortical areas in different brains does not preclude however the existence of a preferential pattern, obtained

by averaging homologous cortical areas of different brains (cf. point e.).

To illustrate this type of evaluation of mean cortical SP distribution over a whole cross-section, the cortical areas of the left hemisphere (lateral aspect) of case 89033, are arranged in a decreasing order:
A37L - A38 - A8 - INSULA - A4 - A20 - A21 - A22.

Doing the same for case 87395 demonstrates that a large distributional variation exists between individual cases:
INSULA - A8 - A20 - A21 - A22 - A37l - A4 - A2.

ad c) differences in distribution of the overall concentration over the areas analysed:
When the four maps of one brain of the SP plotting from the Yamamoto-stained material are considered together, and are compared with the set of another case, the cases can be arranged in a ranking order with decreasing global SP concentration:
89033 - 87395 - 88177 - 88243 - 87068.
This order of global SP concentration reflects the difference between the brains investigated in the total number of SP in the neocortex.

ad d) differences between the left and right hemispheres:
For a comparision between the distribution of SP in the right and left hemisphere, the items a) through c) should be considered on a hemisphere basis. The concentration of SP in a particular layer in one hemisphere can be compared with the corresponding layer of the other hemisphere (cf. a)), or the mean density in a particular Area can be compared with the same Area in the contralateral hemisphere (cf.b)), or the involvement of all Areas in one cortical map together can be put next to the map of the other hemisphere.
Using this scheme of analysis, the difference in distribution of SP between the left and right hemisphere is evaluated.
To illustrate this methodologic analysis the following observations from the Yamamoto-maps are made:
When considering the lateral aspects of the left and right hemispheres of case 88243, and using the three above discussed comparison-items, the following observations are made:

d(-a)):for both left and right hemispheres of case 88243, the same distribution observations (as described at point a)) are made for A 21: the concentration of SP in L III is the largest of all six layers in this Area. The SP are homogenously distributed in this layer.
The SP density of SP in Area 37L, in the left and right hemisphere of the same case is the largest in L III, the distribution in this L III itself is not homogeneous, the density of SP being higher in the upper region of this layer.

d(-b)):the arrangement of Areas according to their SP density (conform item b)) can be given for eg. the lateral aspect of the right hemisphere of case 89033:
A4 - A37L - INSULA - A8 - A20 - A21 - A22 - A42 - A2.
and for case 87395:
A20 - A21 - A22 - INSULA - A8 - A42 - A4 - A37L - A2.
Comparison of these two sequences stress the important individuality of the SP distribution.

d-c):When the figures presenting the plotting data are considered

as a whole, the maps of the lateral aspect of the right hemisphere of every brain studied, can be put in order of decreased Mean SP concentration:
87395 - 89033 - 88177 - 88243 - 87068.

From these three types (d-a,d-b,d-c) of analysing the SP Yamamoto - figures, it may be concluded, that differences in SP concentration exist between the two hemispheres considered as a whole, but also between the two Areas with the same Brodmann number within the same brain. Within one single area, a difference in SP distribution can be noticed between the different laminae, and, even within one lamina, the distribution need not to be homogenous.

e) differences between the individual cases:
When the cases as a whole are compared, a ranking order of the cases in severity of plaque formation can be made. A ranking order of brains after SP concentration calls for comparison with the clinical data concerning those cases, in order to establish a relationship between the neuropathological and the clinical data.

III.4. QUANTIFICATION OF YAMAMOTO-STAINED SENILE PLAQUES.

Quantification of SP, enables one to detect cortical areas, in which a prominent number of SP is found. Quantitative data on SP distribution were pooled to investigate the possibility of a clustering of SP in a particular cortical area. Within each area, the pattern of SP distribution over the various cortical laminae is studied. By pooling the data of the individual layers from the various cortical areas studied, a general distribution of SP over the cortical layers results.

III.4.1. General distribution of Senile Plaques (SP), as observed in Yamamoto stained sections.

The plottings of the SP's, as depicted and described in the previous paragraph demonstrates an inter-individual difference between the various cases. In order to make some general remarks about the SP distribution, the data derived from the same cortical layer and the same cortical area are averaged. In this process, the data derived from both left and right hemispheres are pooled. These data are represented in figure III.8.

This figure demonstrates the number of SP pro unit area in the different cortical areas. This unit area is chosen to conform to a square of vision using an magnification of 400x, as used in the Congo-Red study.

At the abscissa of the figure, the cortical area is indicated by its number in the cytoarchitectonical cortical map of Brodmann.

In the figure, every bar is of the same width. The height of the bar corresponds to the average number of SP in a field of vision. Taken together, the surface of the six bars represent the mean concentration of senile plaques in a particular cortical field. Considered in this way, the figure rase the impression that there are two different types of cortical areas as far as SP distribution is concerned: the areas of the center of the figure, between Area 20 and Area 38 together with Area 8 and the Insula of Reil and areas on the other hand areas like the Areas 17, 18, 2, 4, 42 and 7. In the first type a relative abundance of SP, in the second a relative paucity of SP is observed.
In addition, it can be observed that in most areas the highest concentration of senile plaques is found in L III.
In order to detect statistical differences between the number of SP in the various layers within one cortical area, the pooled data are compared, using the two tailed Student's T-test. The pooled data are given in the next table (Table 1), with the standard error

(SE) in combination with a table giving the t-value for every combination possible.

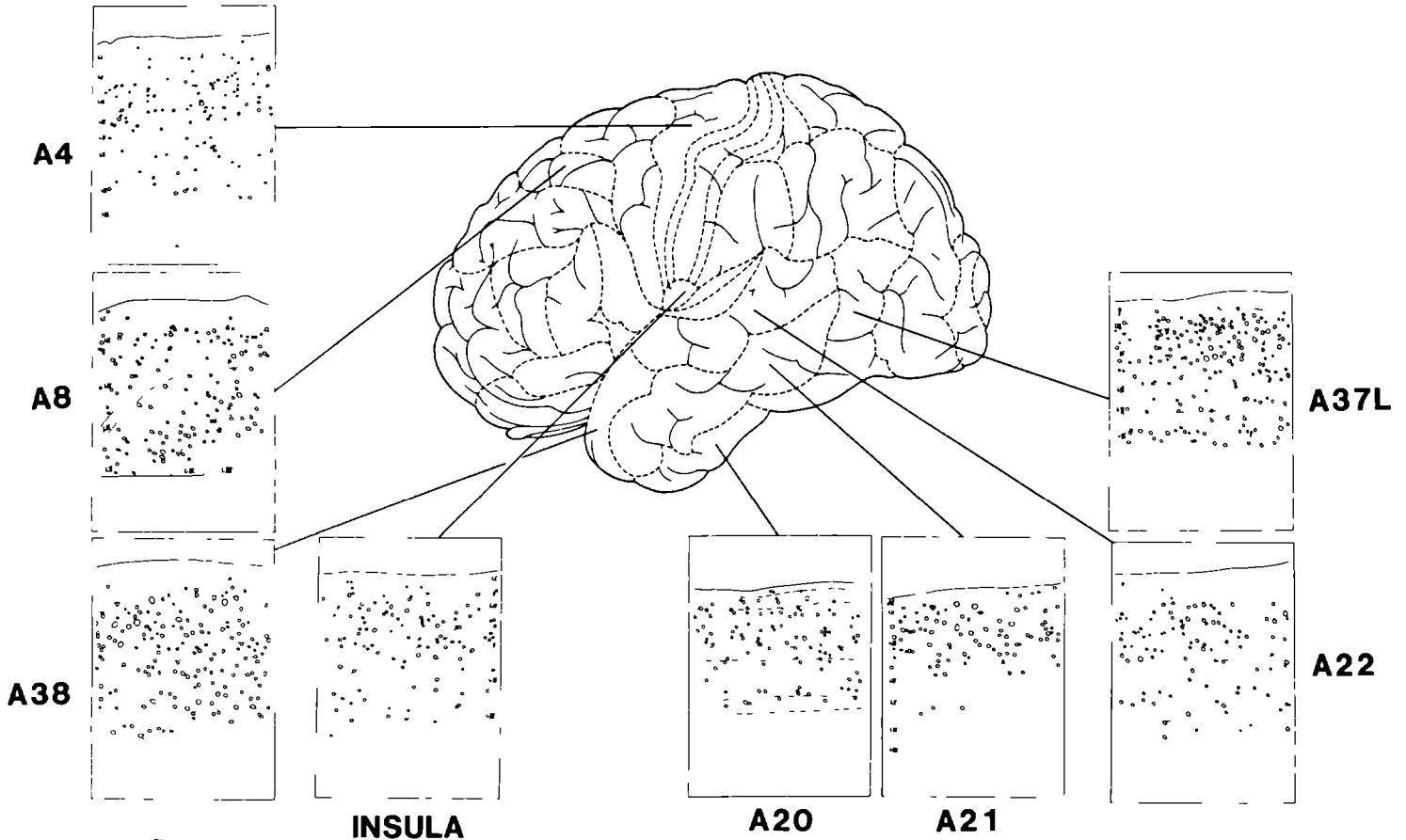

fig. III.1a

CASE 87068

LEFT HEMISPHERE

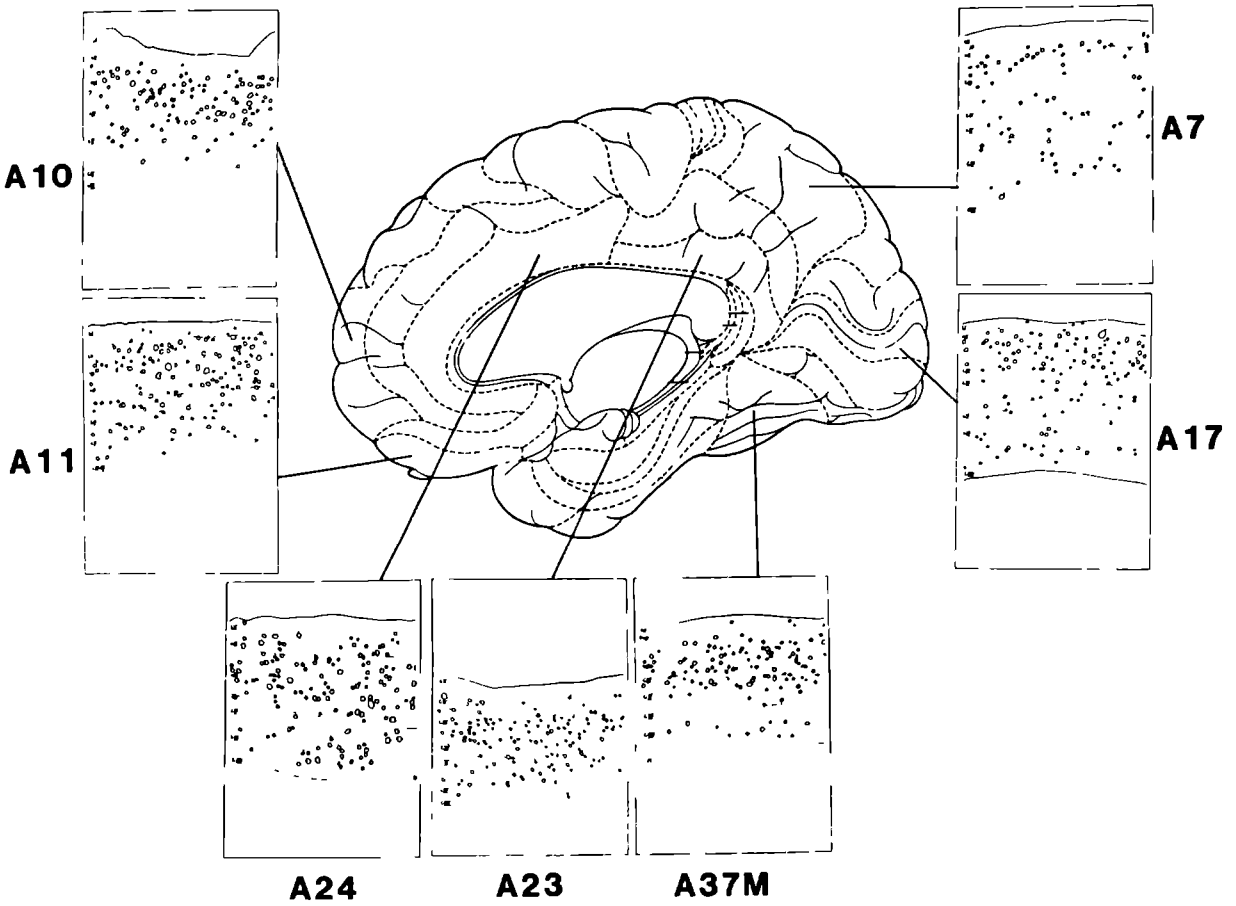

fig.III.1b

CASE 87068

RIGHT HEMISPHERE

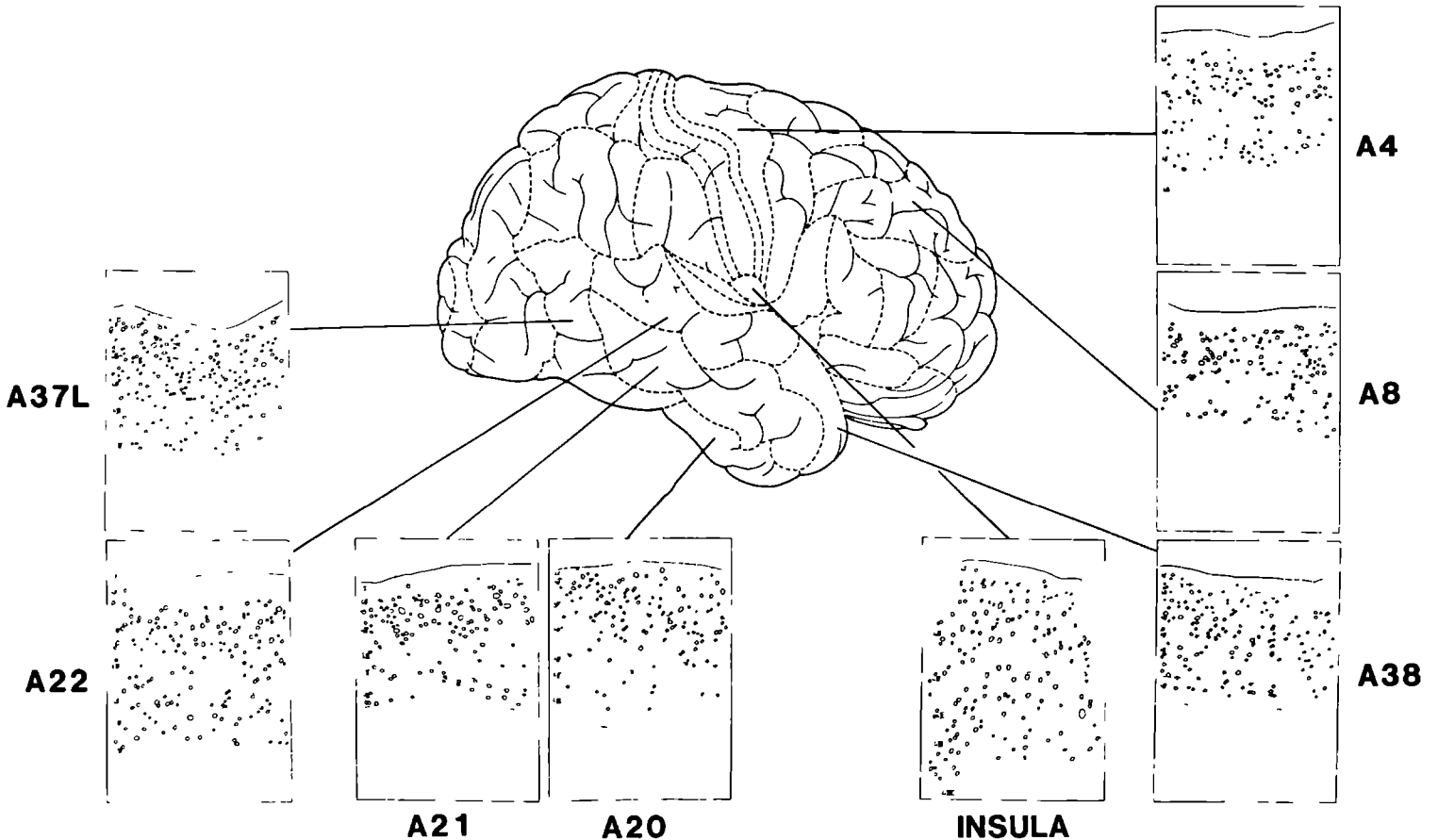

fig III.1c

CASE 87068

RIGHT HEMISPHERE

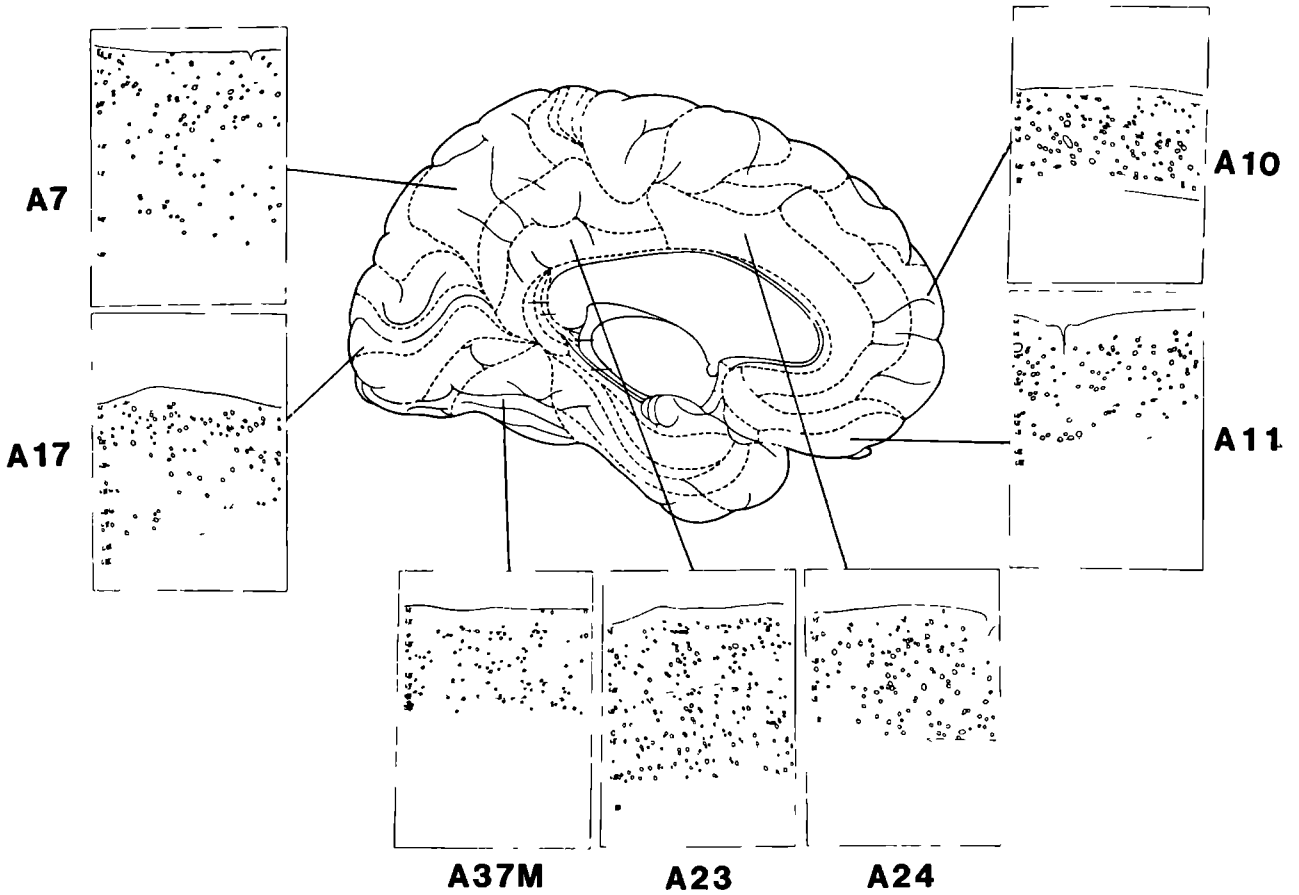

fig. III.1d

CASE 87068

LEFT HEMISPHERE

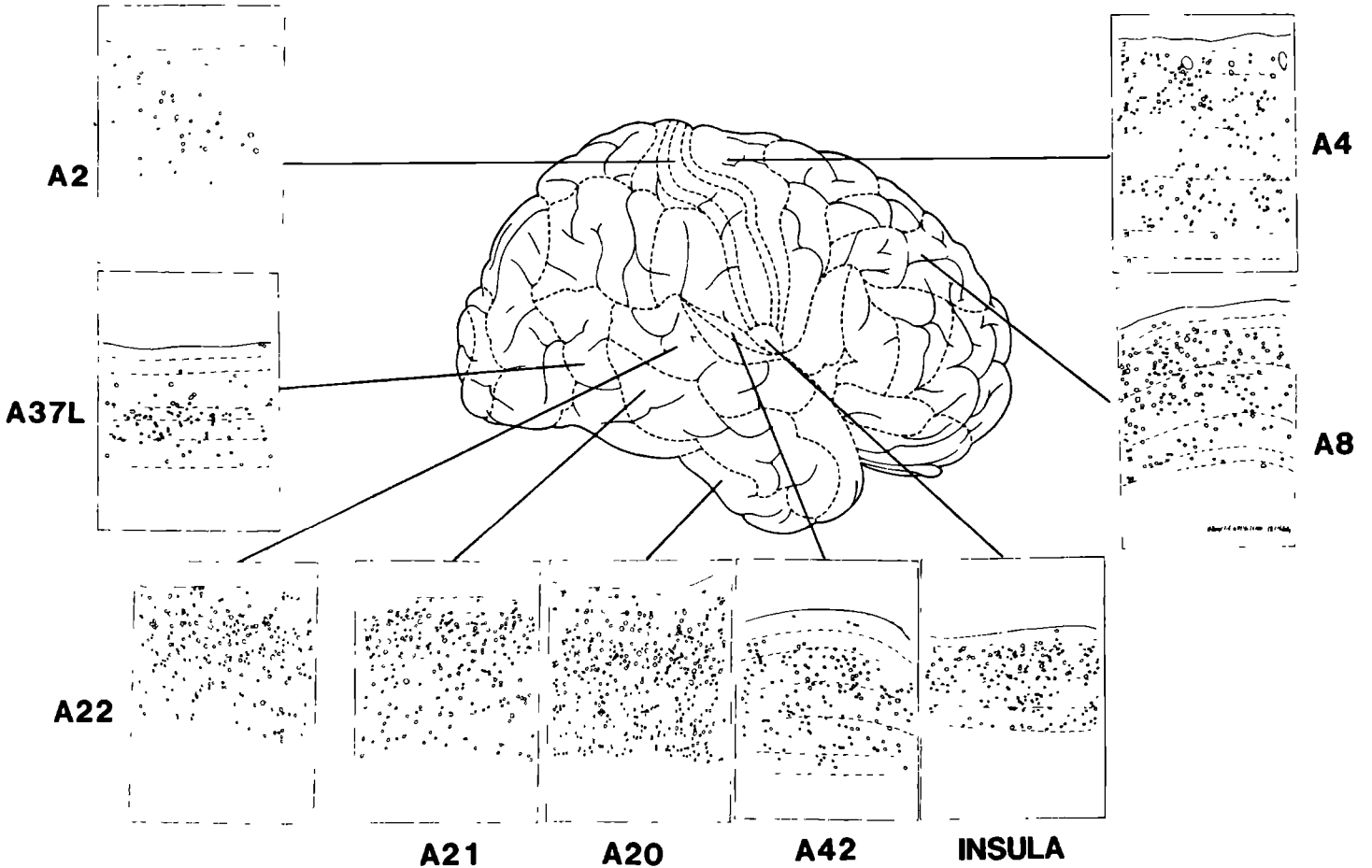

fig. III.2a

CASE 87395

RIGHT HEMISPHERE

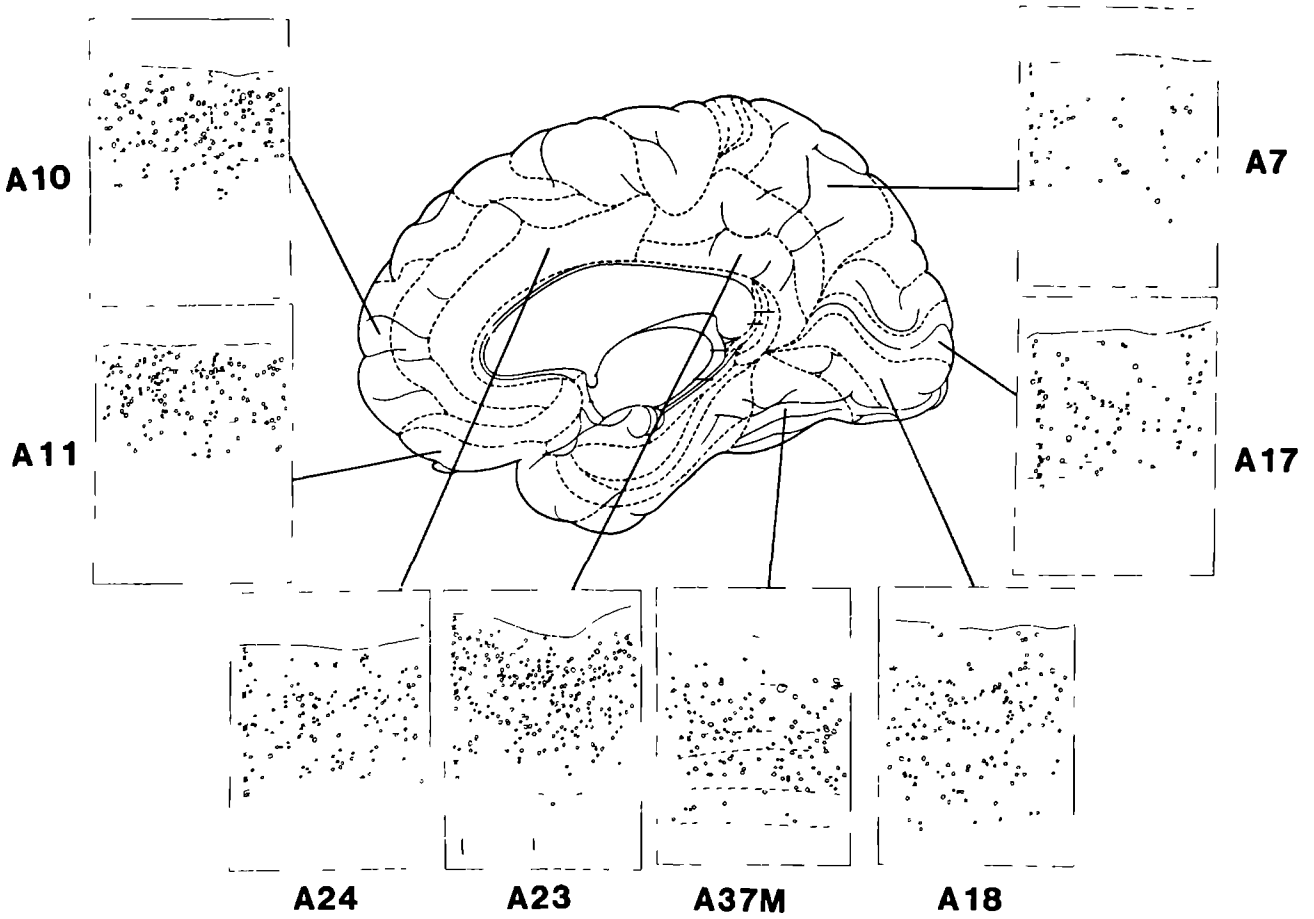

fig. III.2b

CASE 87395

RIGHT HEMISPHERE

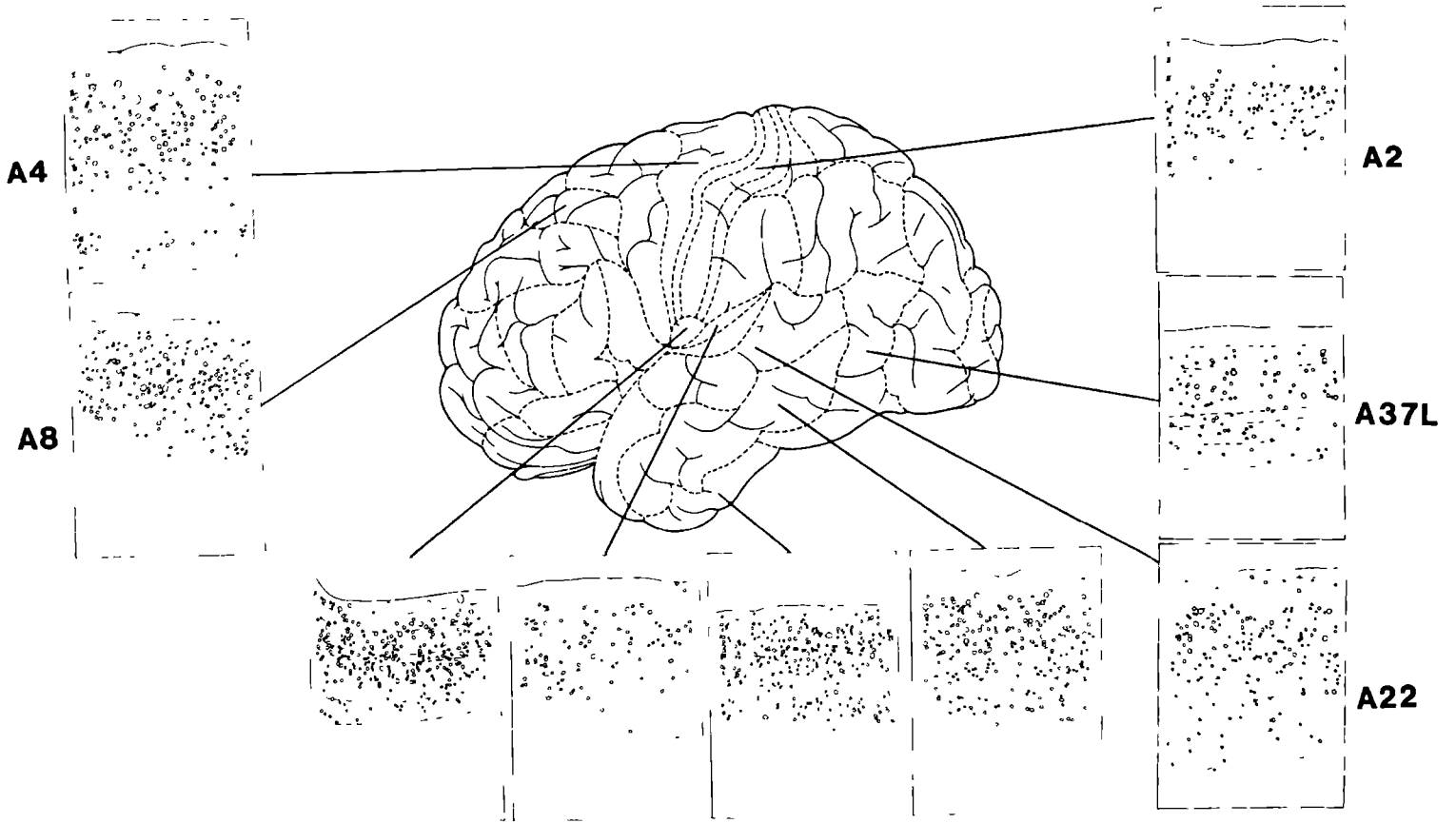

fig. III.2c

CASE 87395

LEFT HEMISPHERE

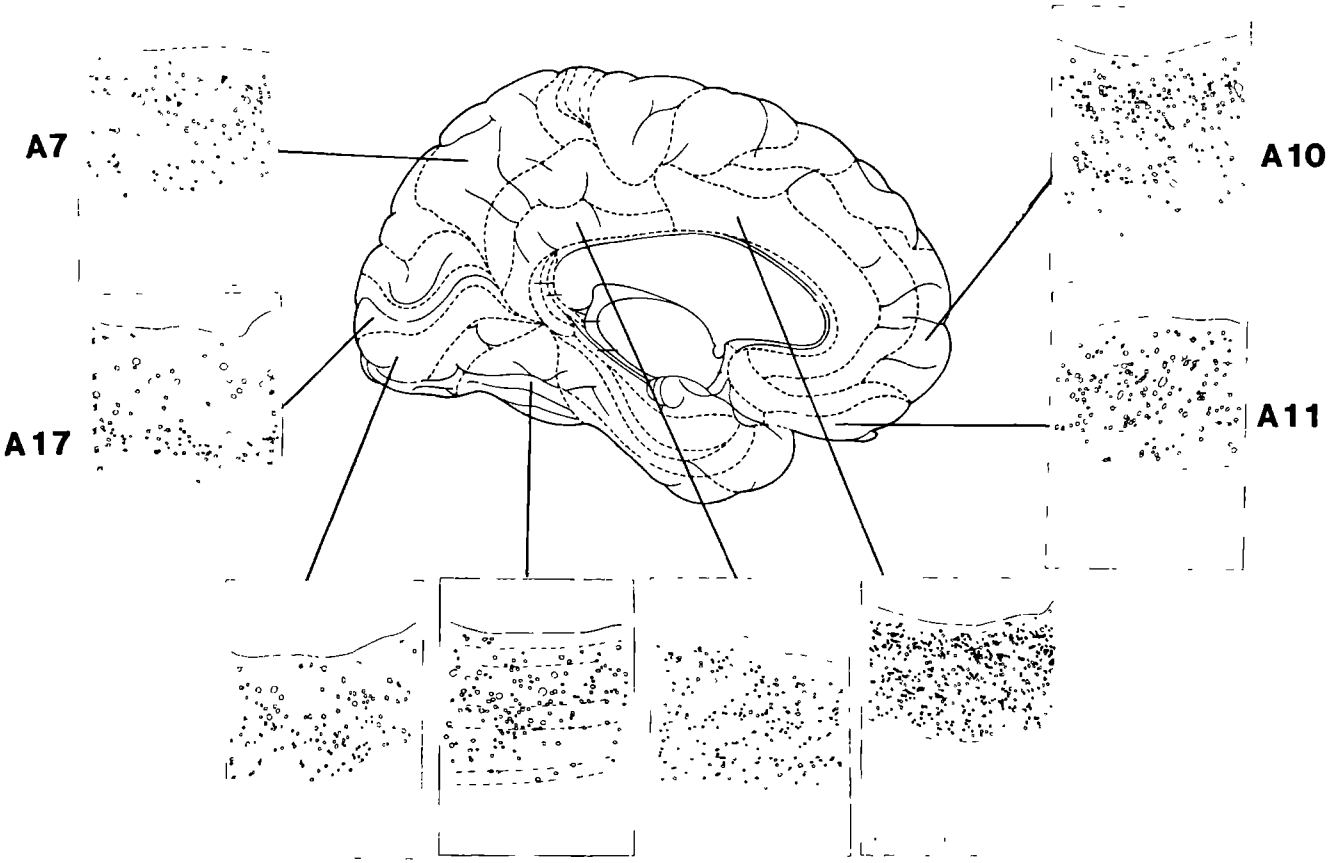

fig. III.2d

CASE 87395

LEFT HEMISPHERE

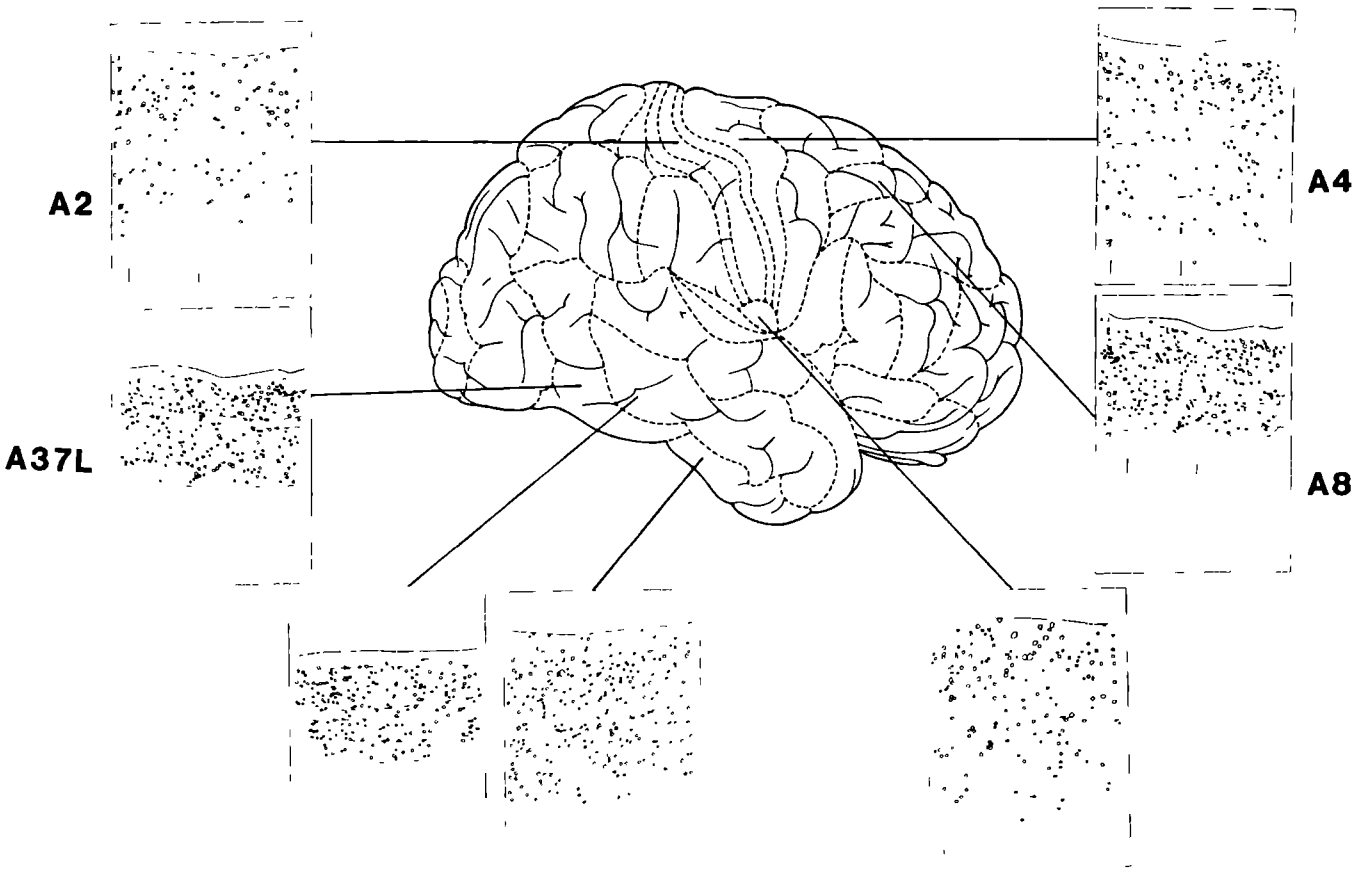

fig. III.3a

CASE 88177

RIGHT HEMISPHERE

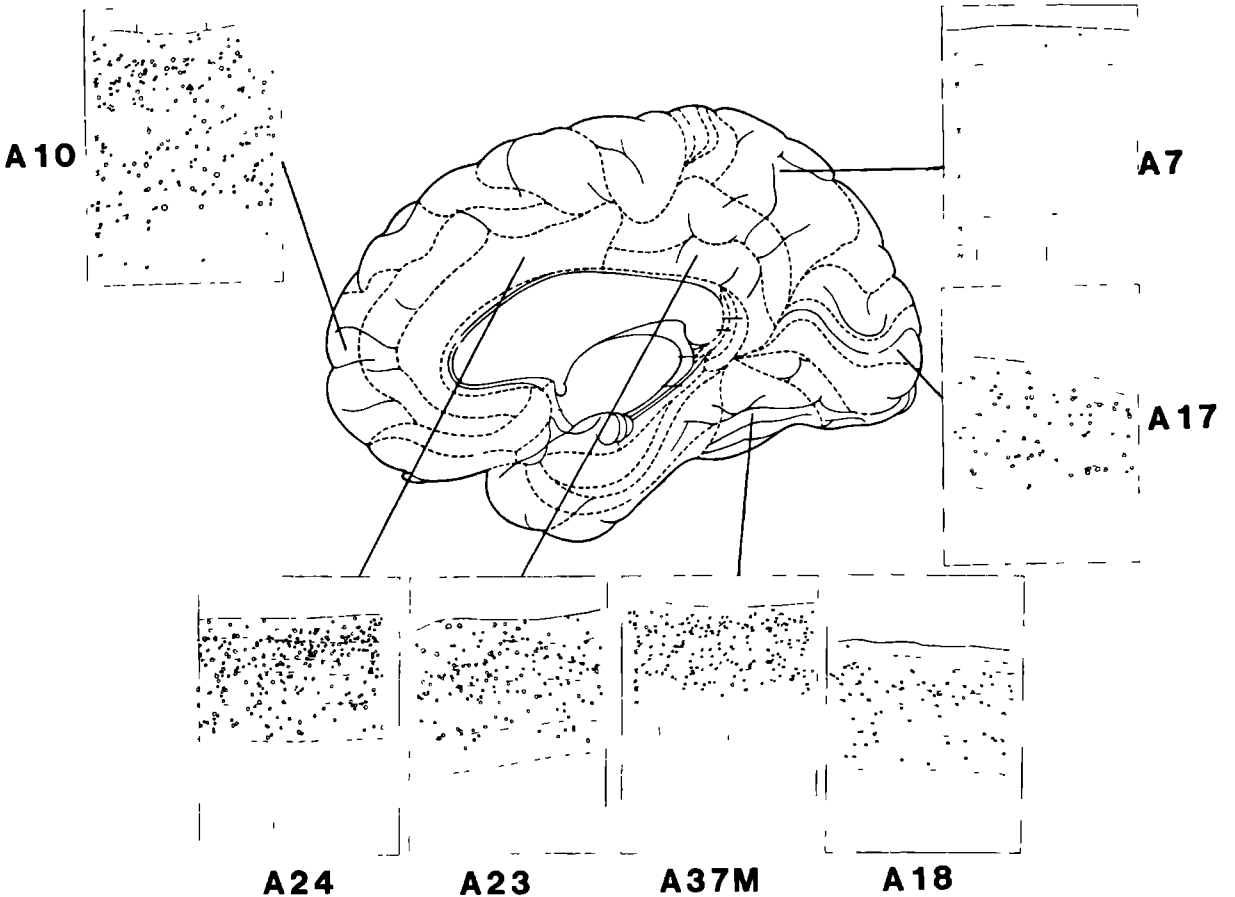

fig. III.3b

CASE 88177

RIGHT HEMISPHERE

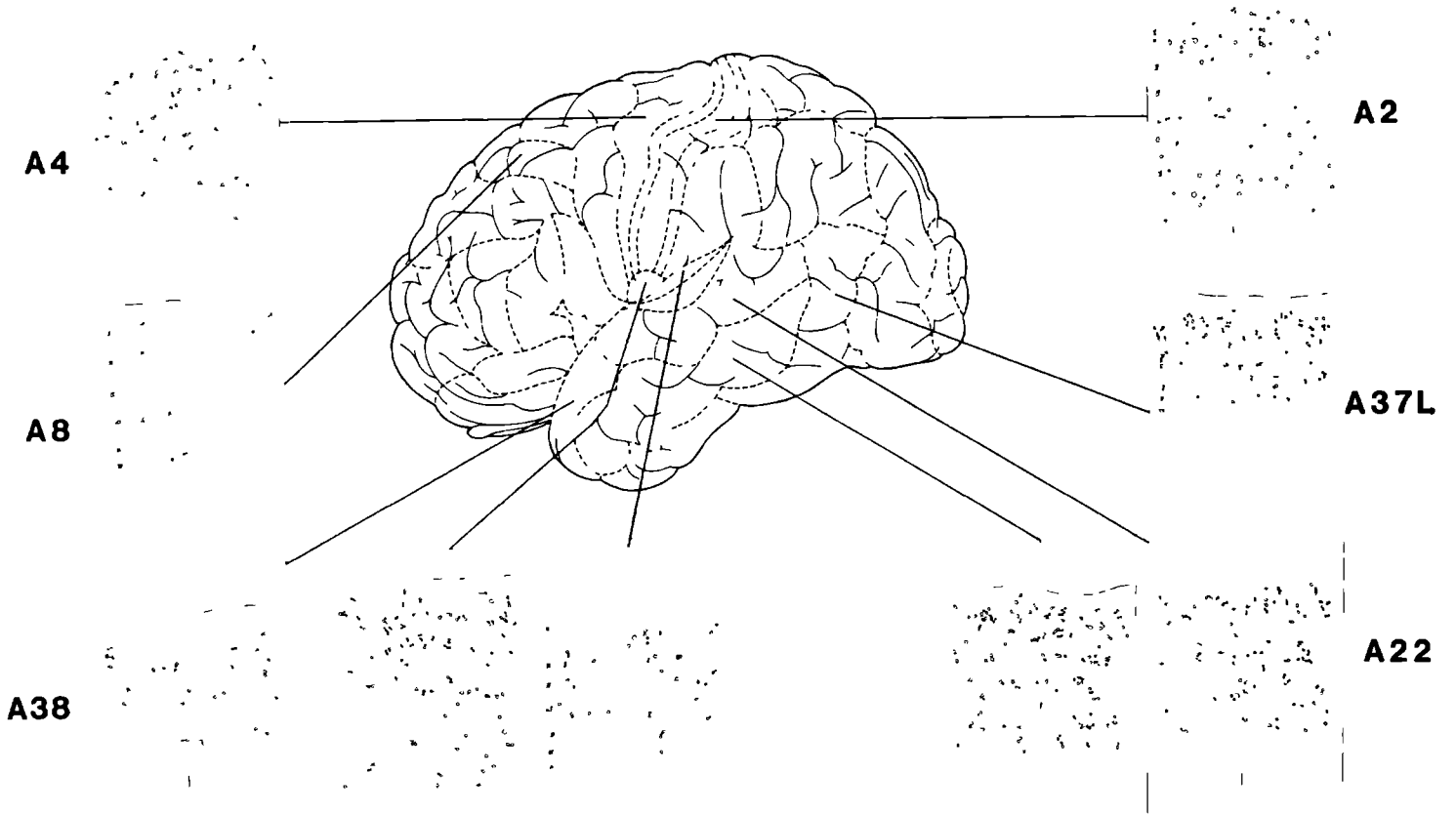

fig. III.3c

CASE 88177

LEFT HEMISPHERE

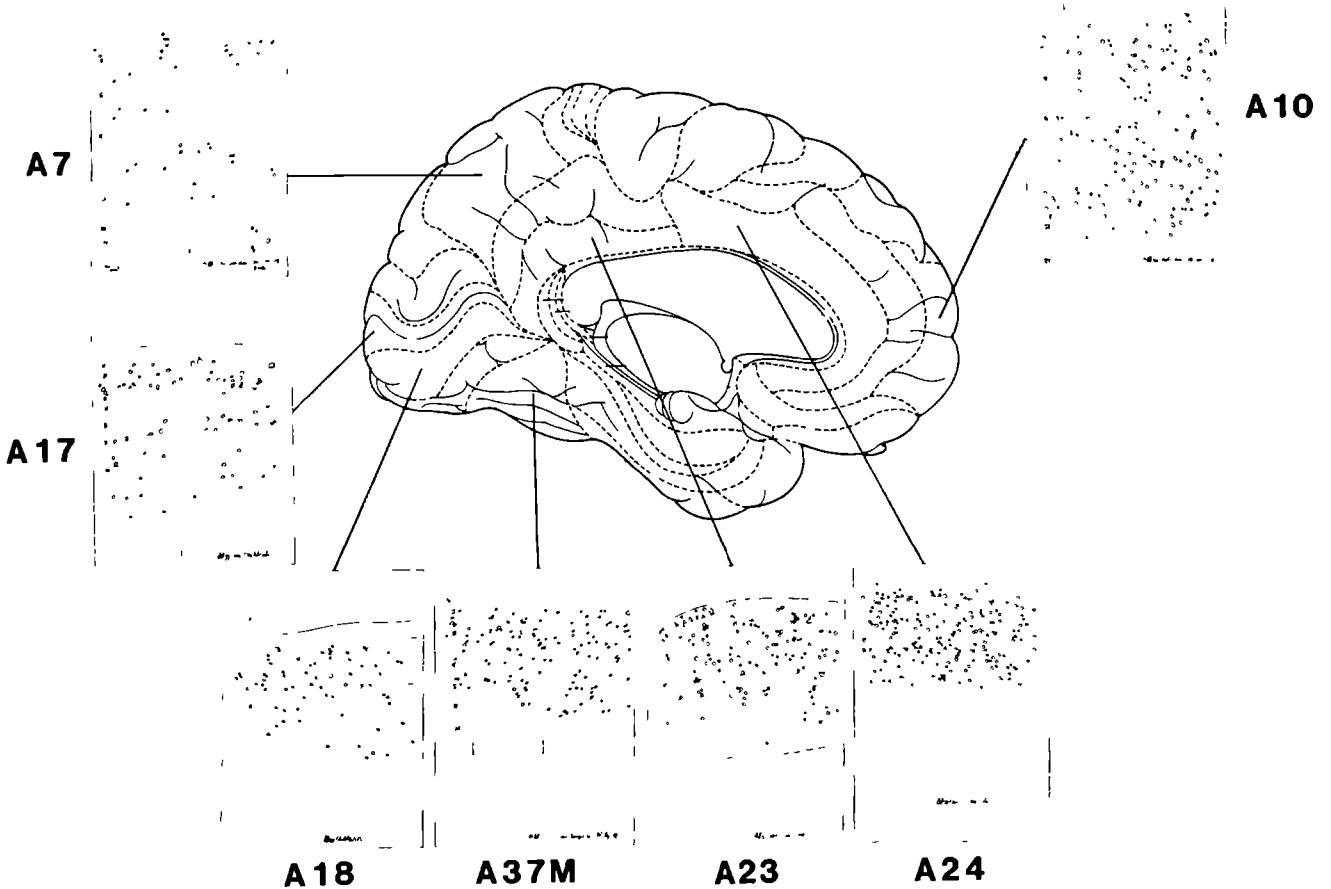

fig. III.3d

CASE 88177

LEFT HEMISPHERE

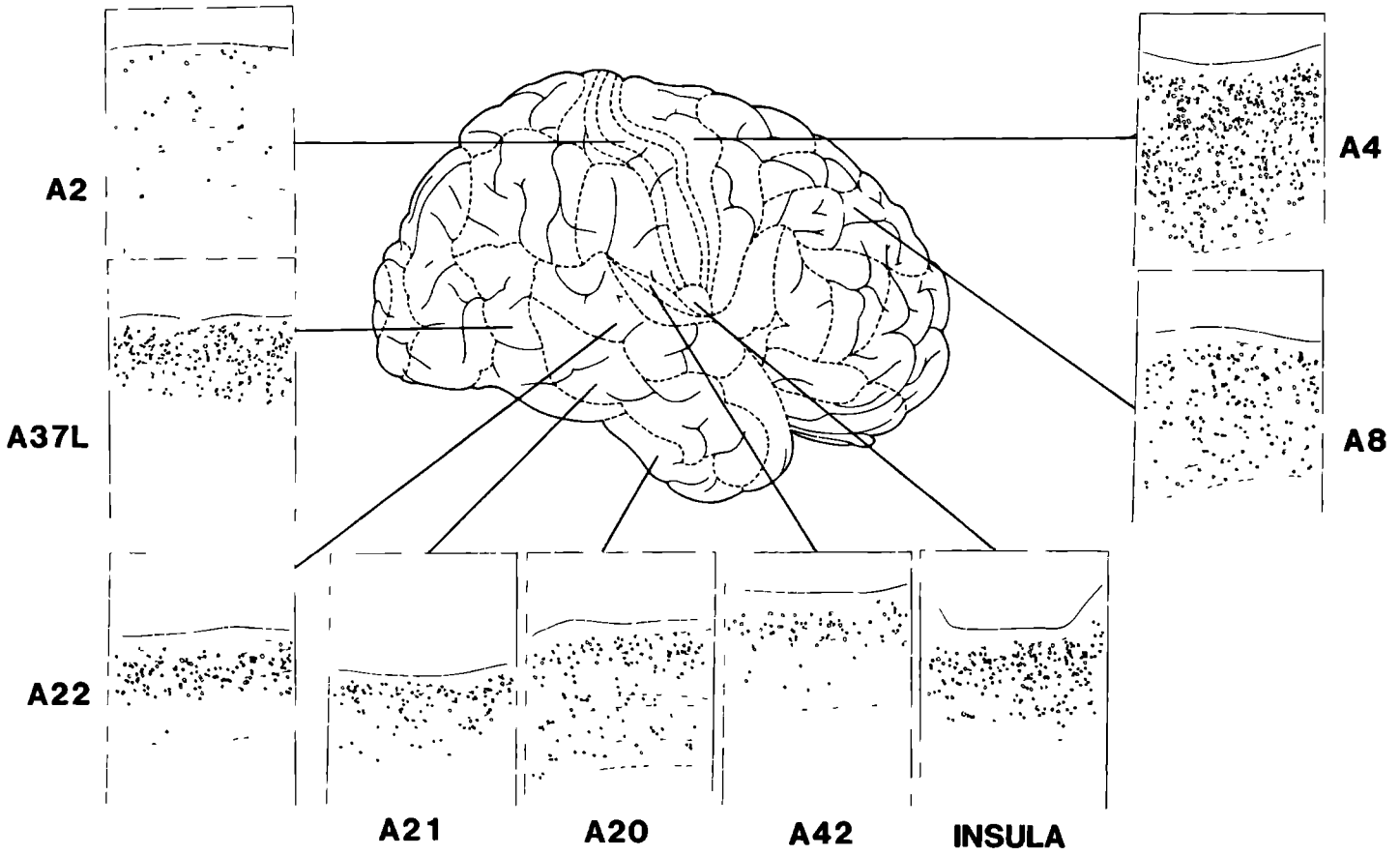

fig. III.4a

CASE 89033
RIGHT HEMISPHERE

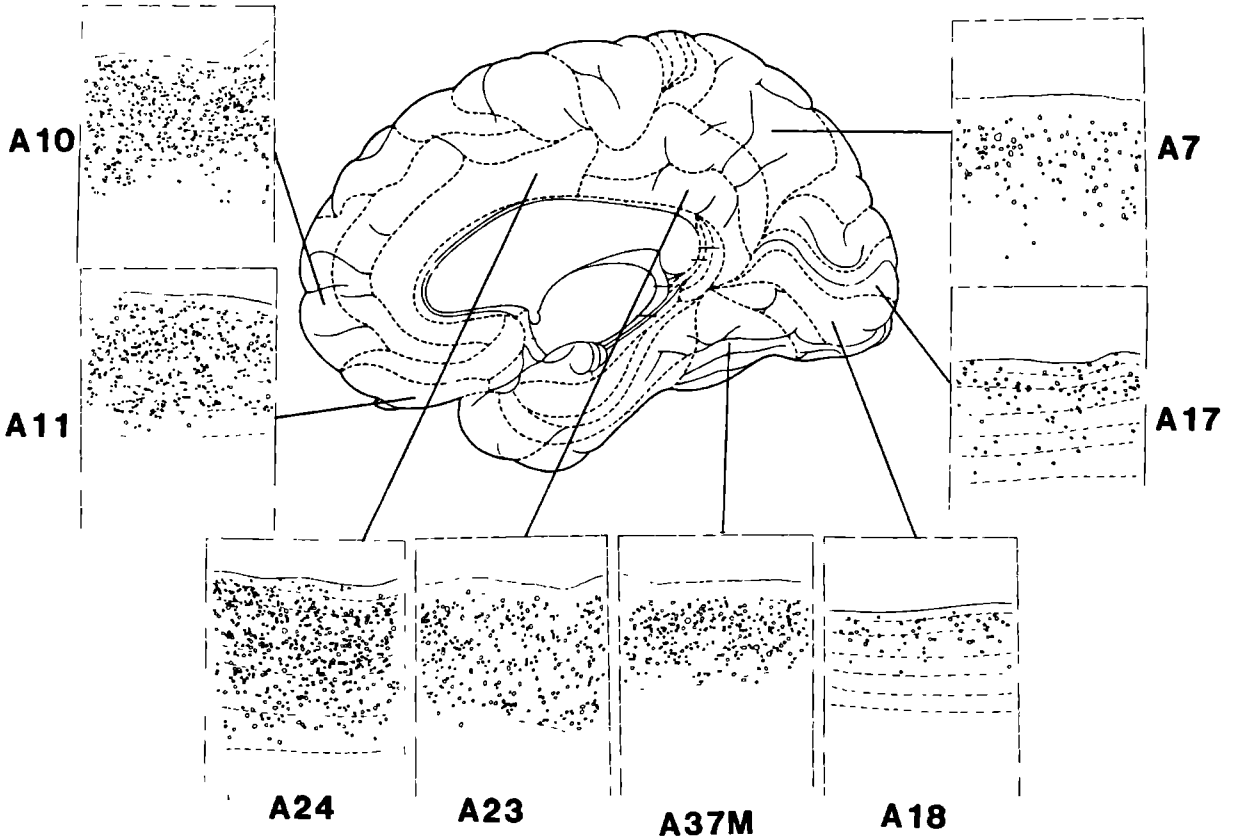

fig. III.4b

CASE 89033
RIGHT HEMISPHERE

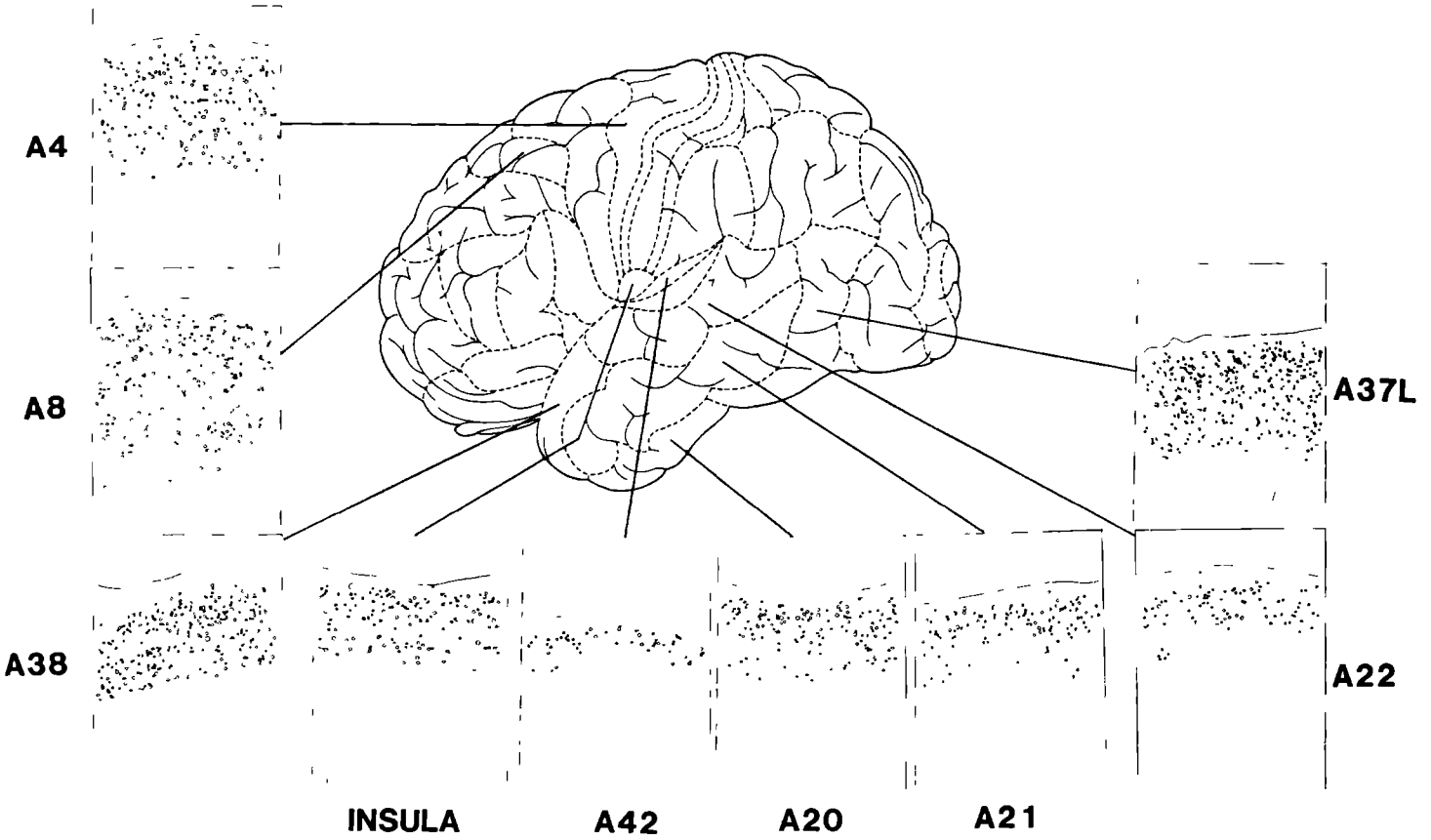

fig. III.4c

CASE 89033

LEFT HEMISPHERE

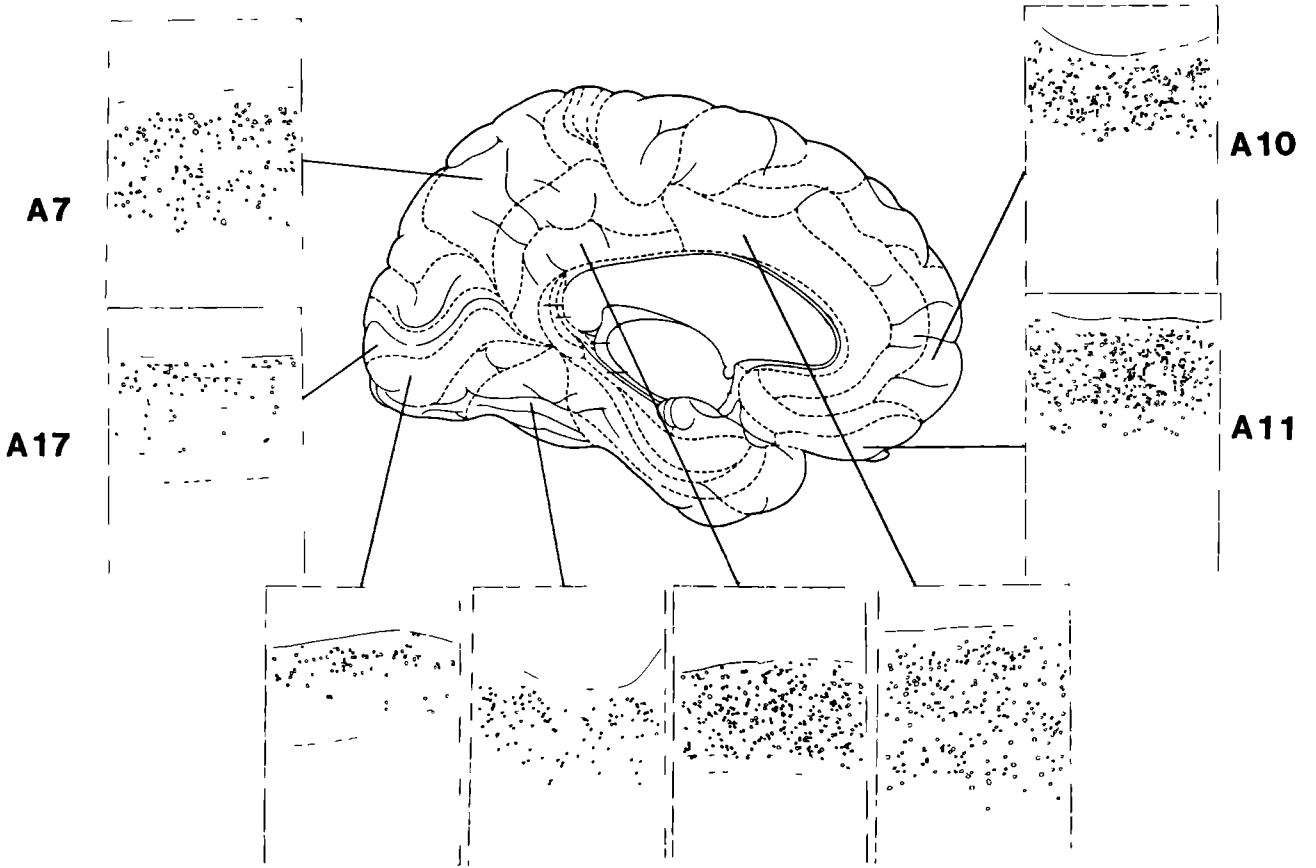

fig. III.4d

CASE 89033
LEFT HEMISPHERE

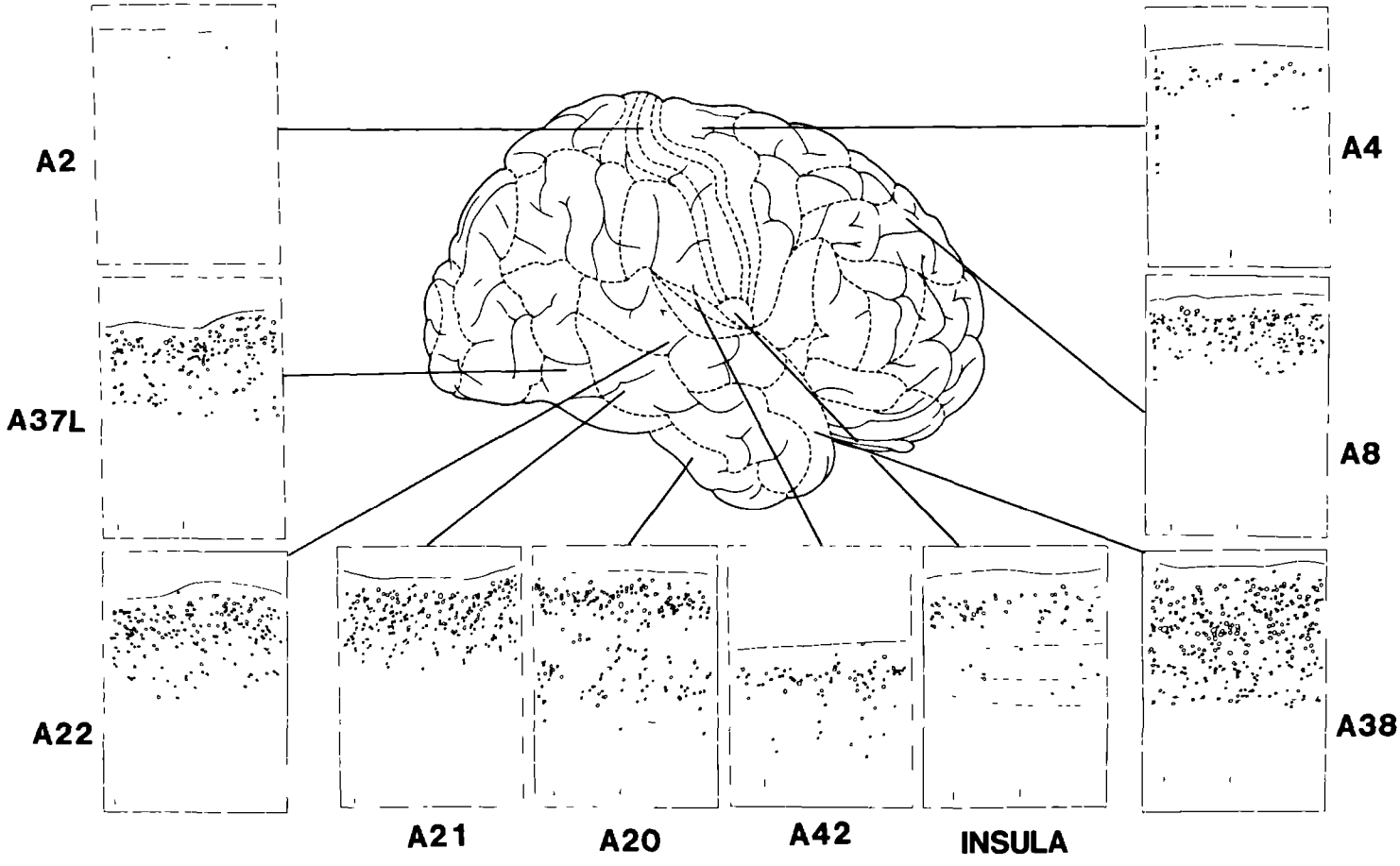

CASE 88243

RIGHT HEMISPHERE

fig. III.5a

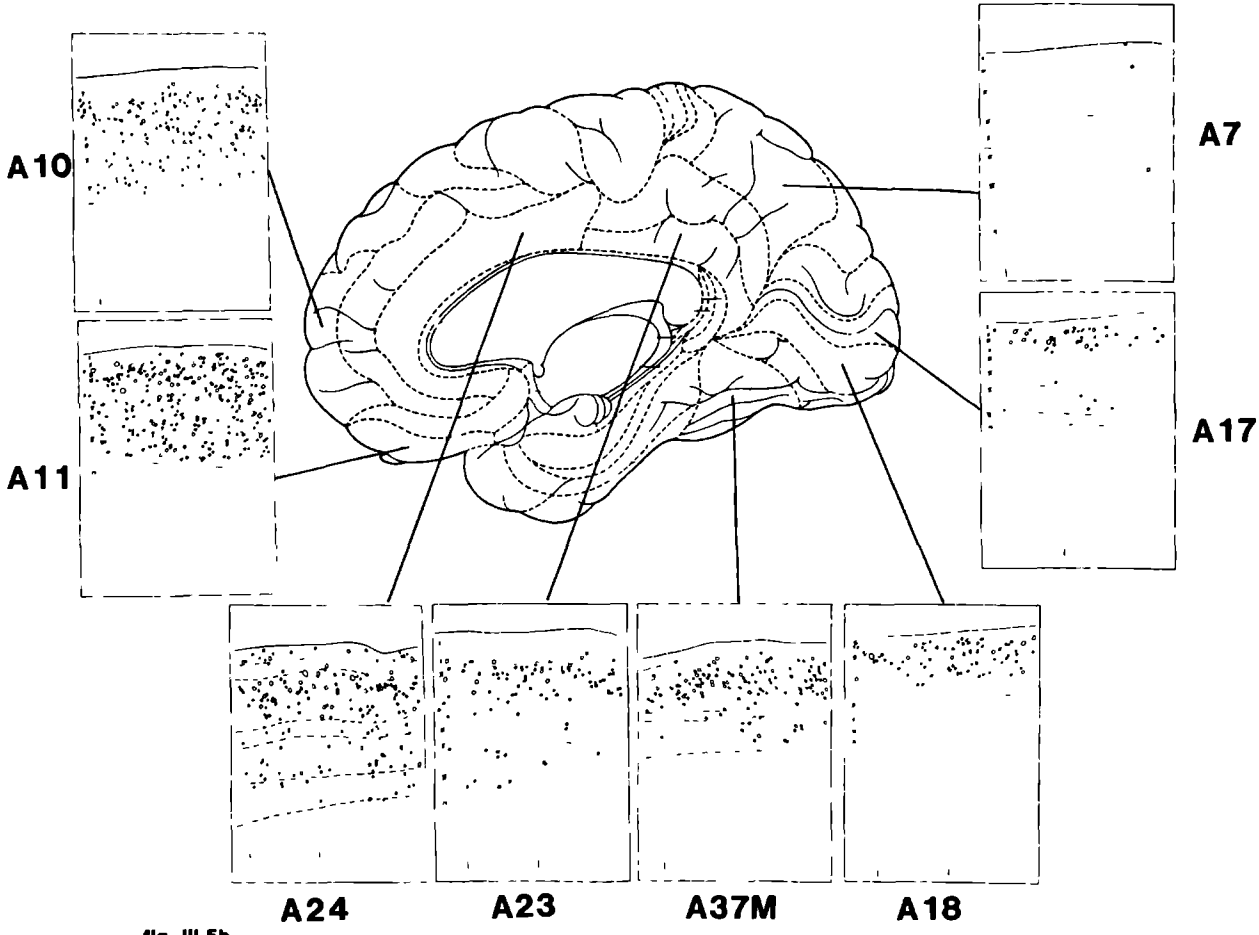

fig. III.5b

CASE 88243

RIGHT HEMISPHERE

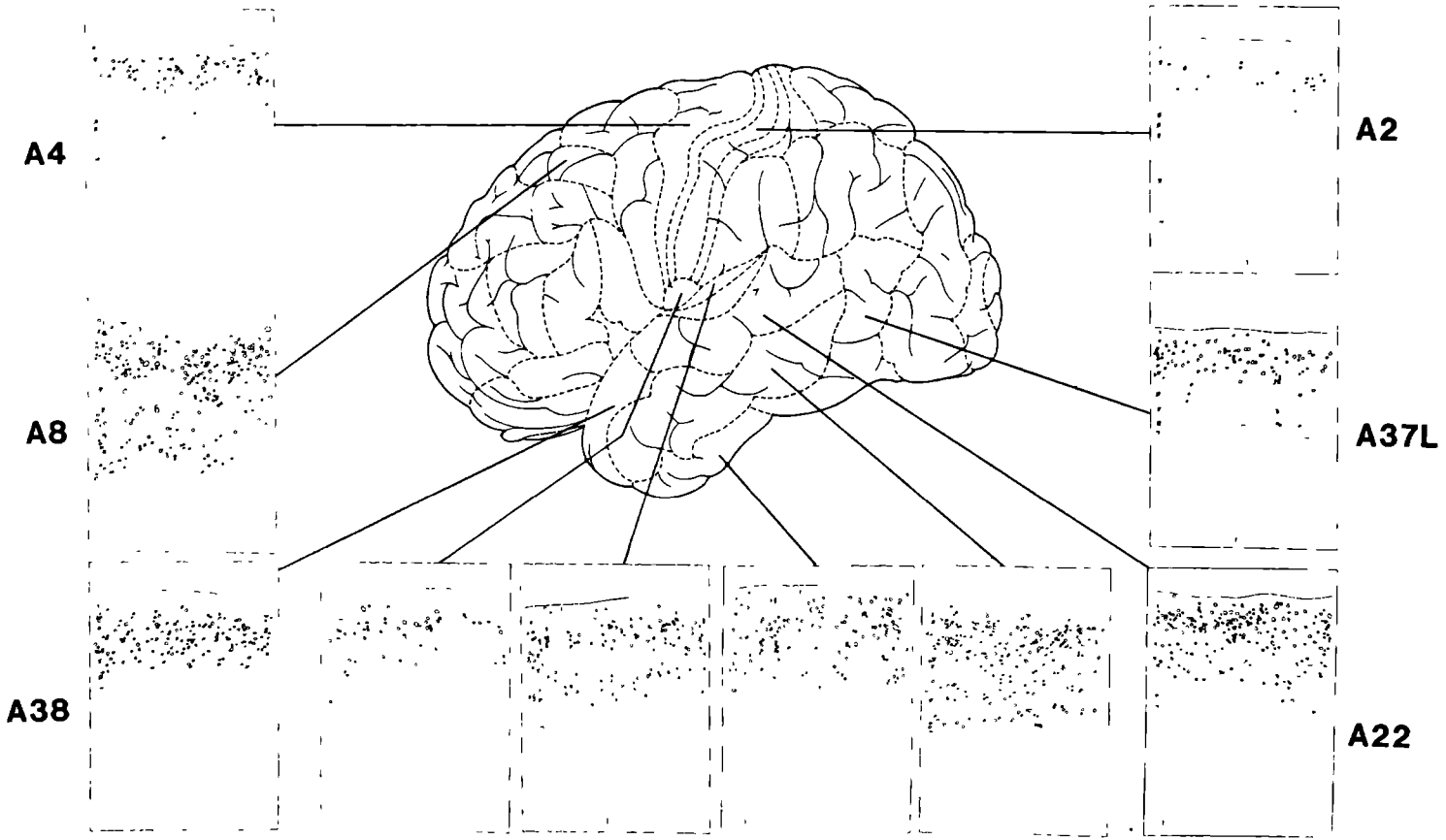

fig. III.5c

CASE 88243

LEFT HEMISPHERE

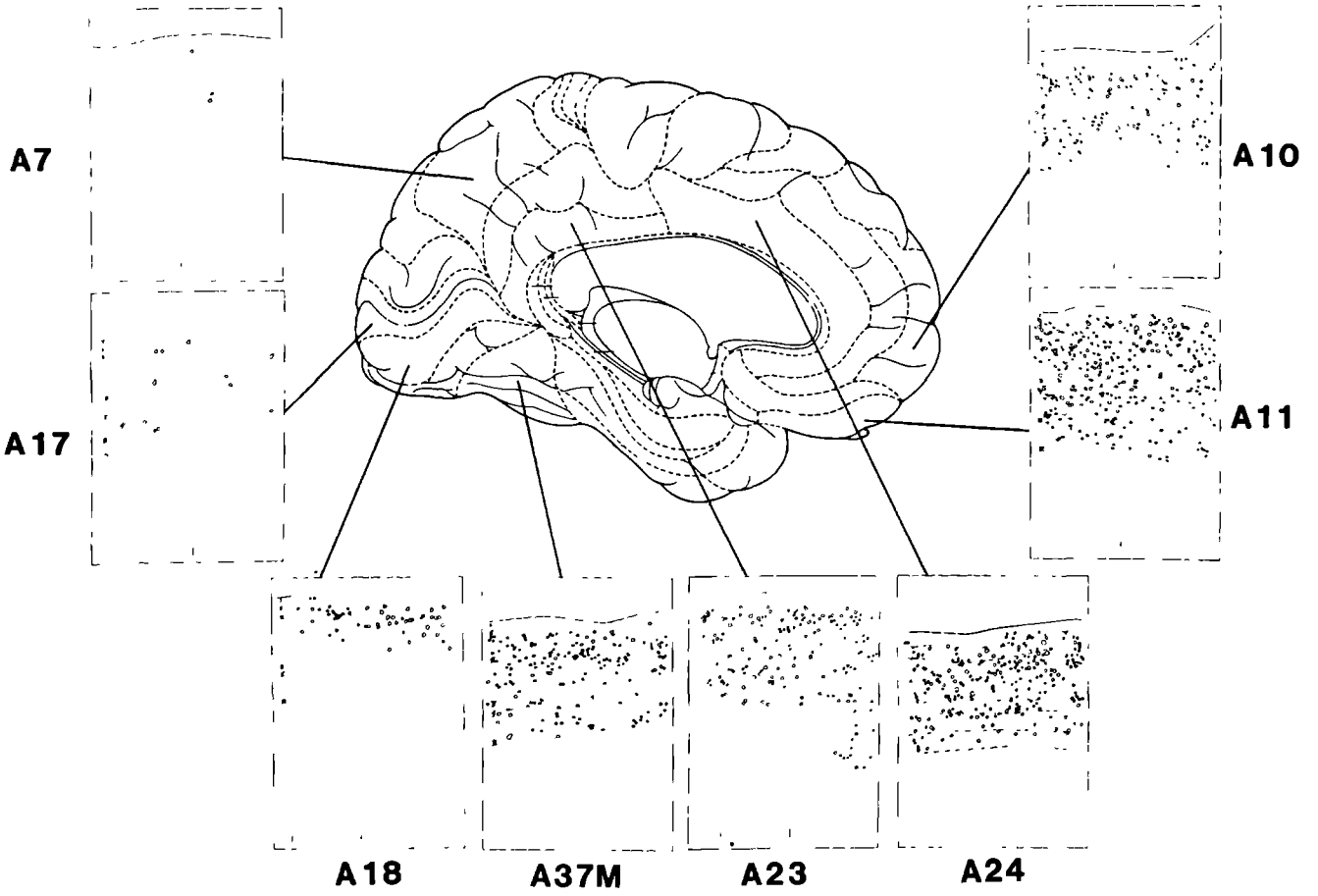

fig. III.5d

CASE 88243

LEFT HEMISPHERE

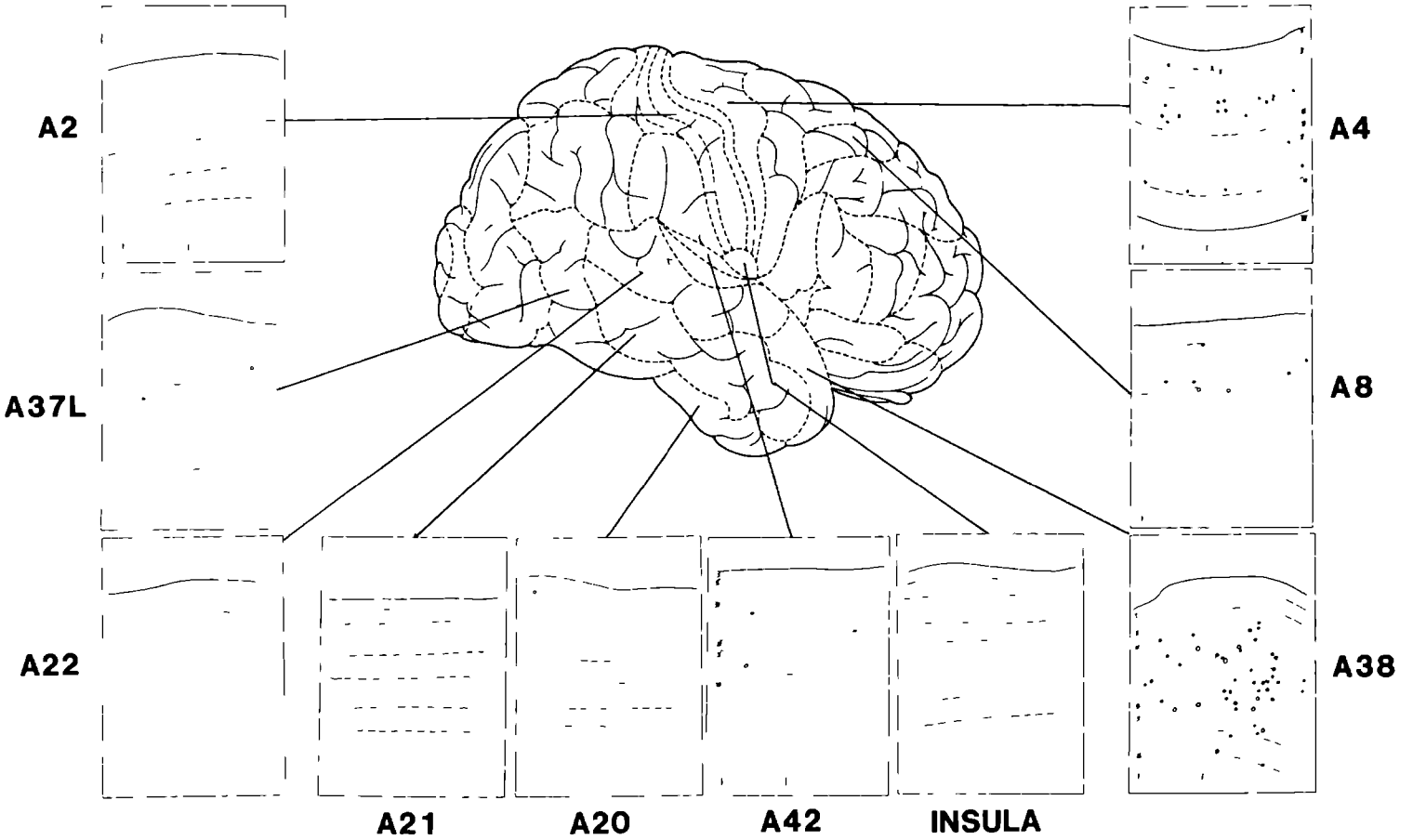

fig. III.6a

CASE 88271

RIGHT HEMISPHERE

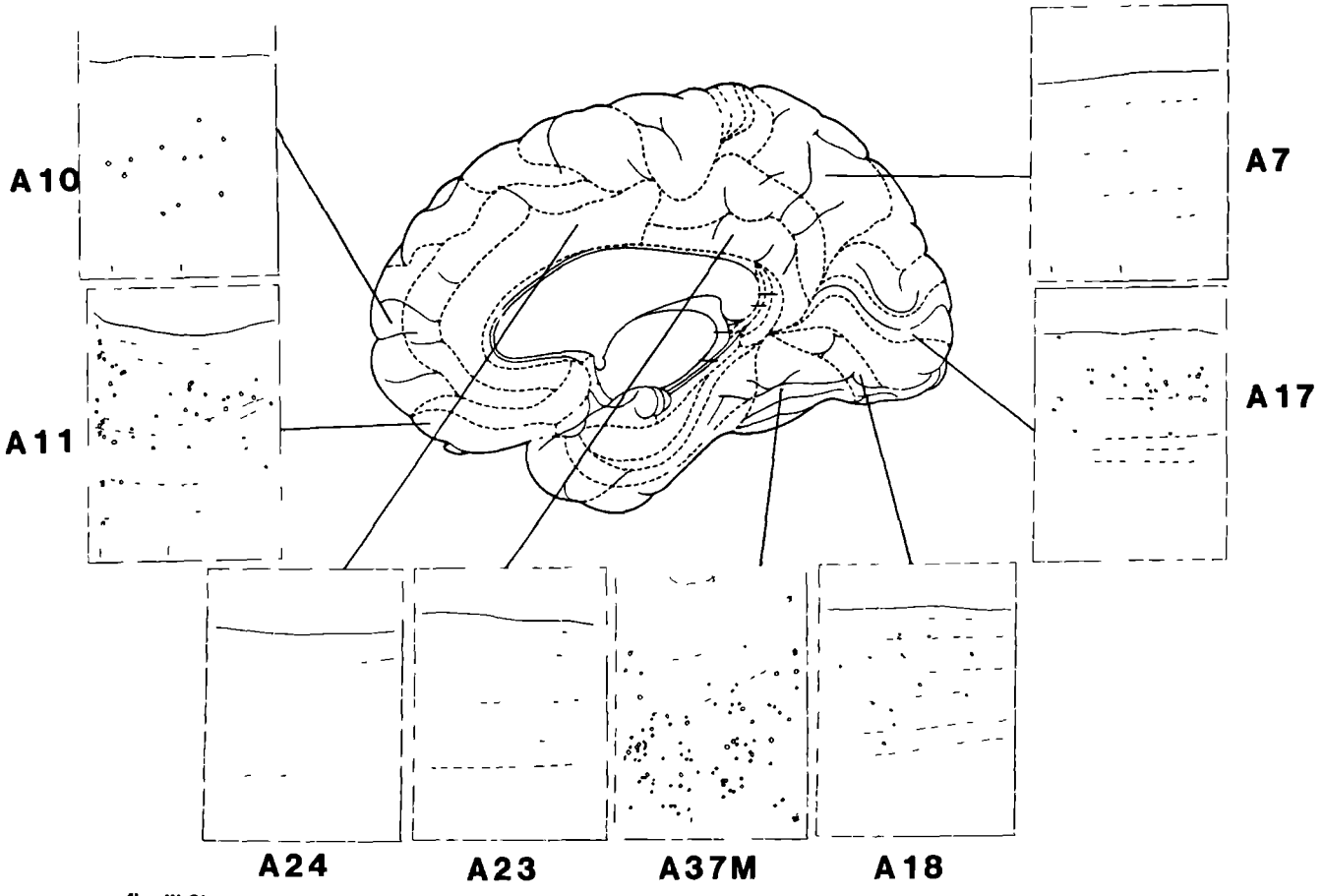

fig. III.6b

CASE 88271

RIGHT HEMISPHERE

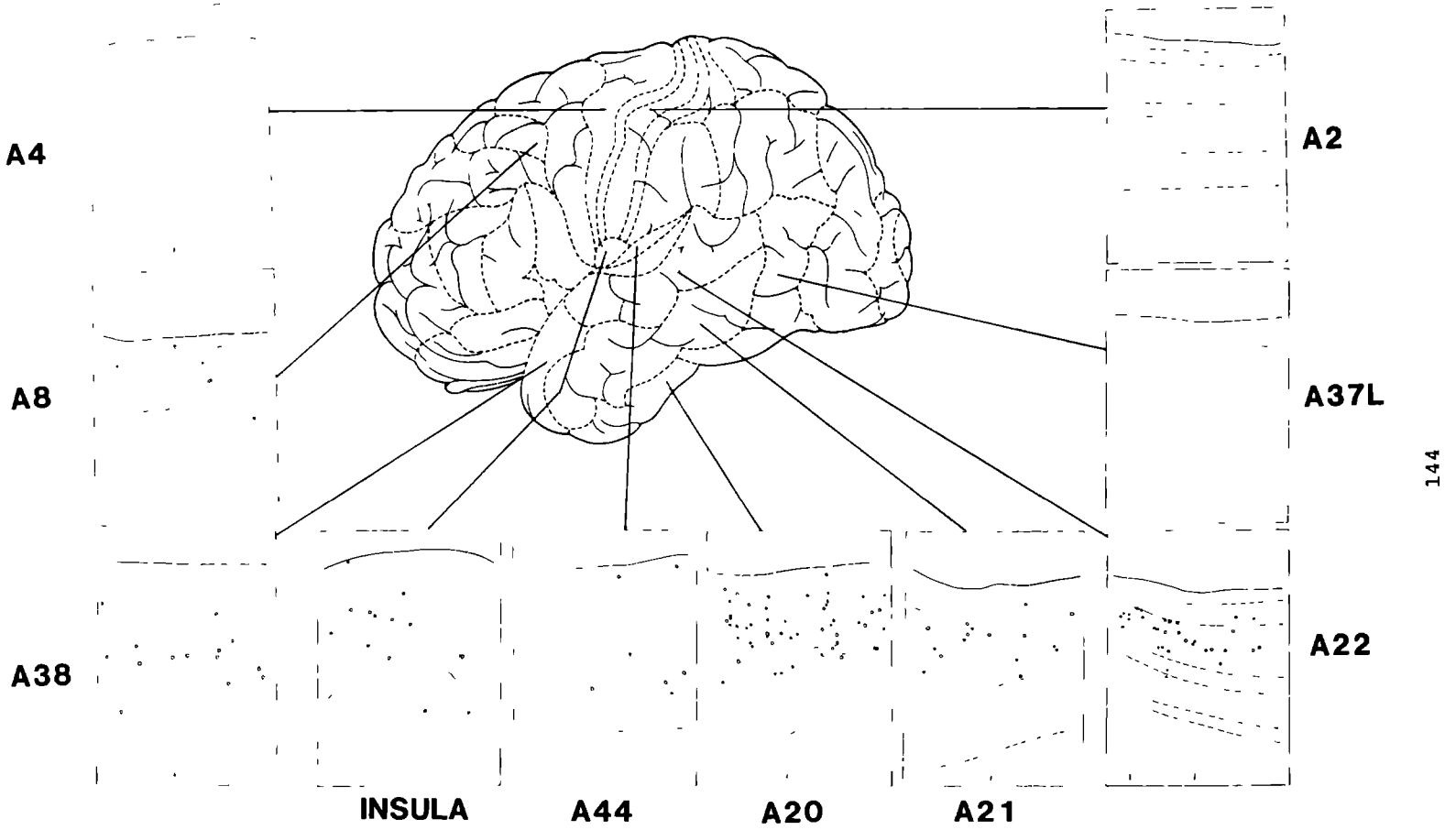

fig. III.6c

CASE 88271

LEFT HEMISPHERE

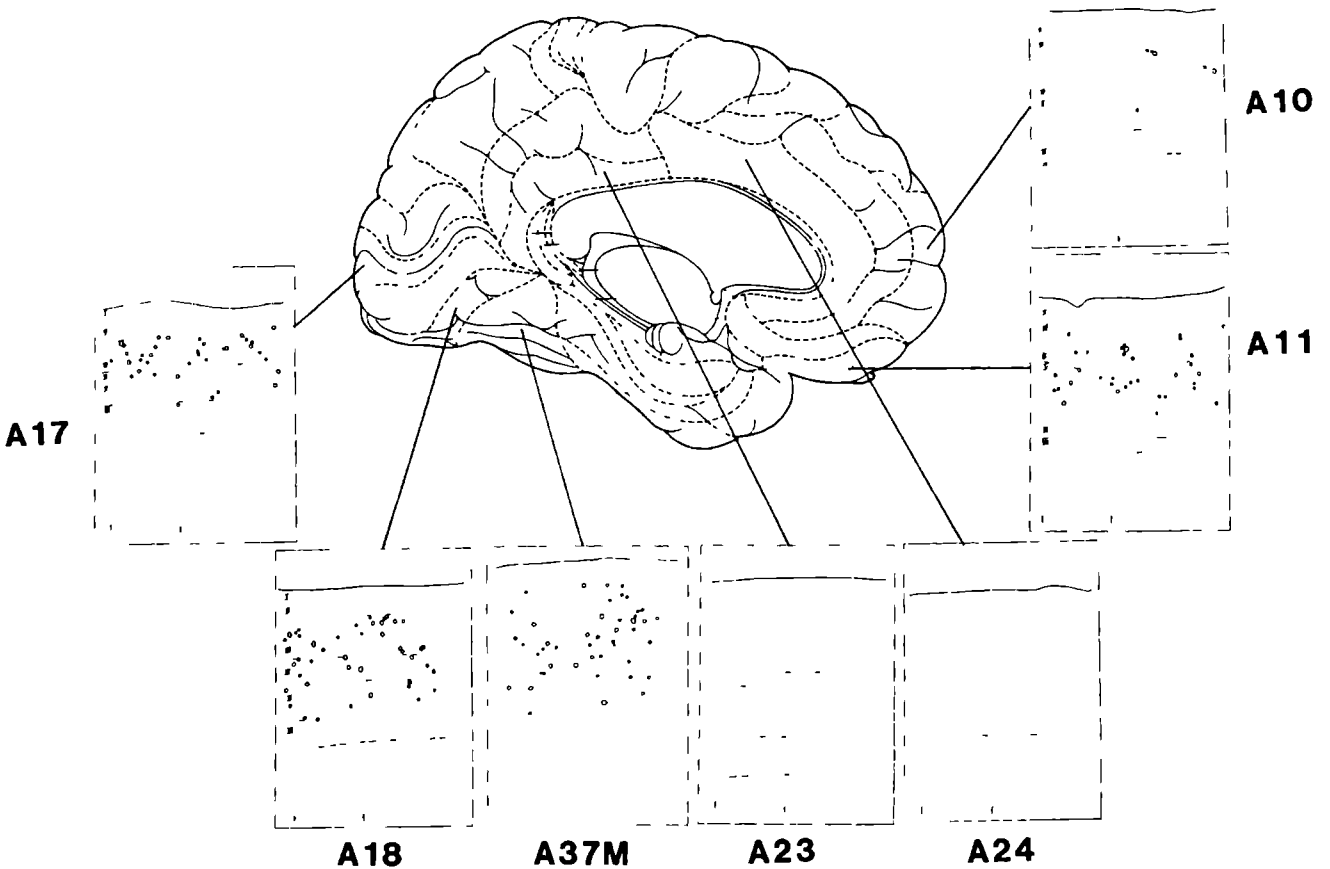

fig. III.6d

CASE 88271

LEFT HEMISPHERE

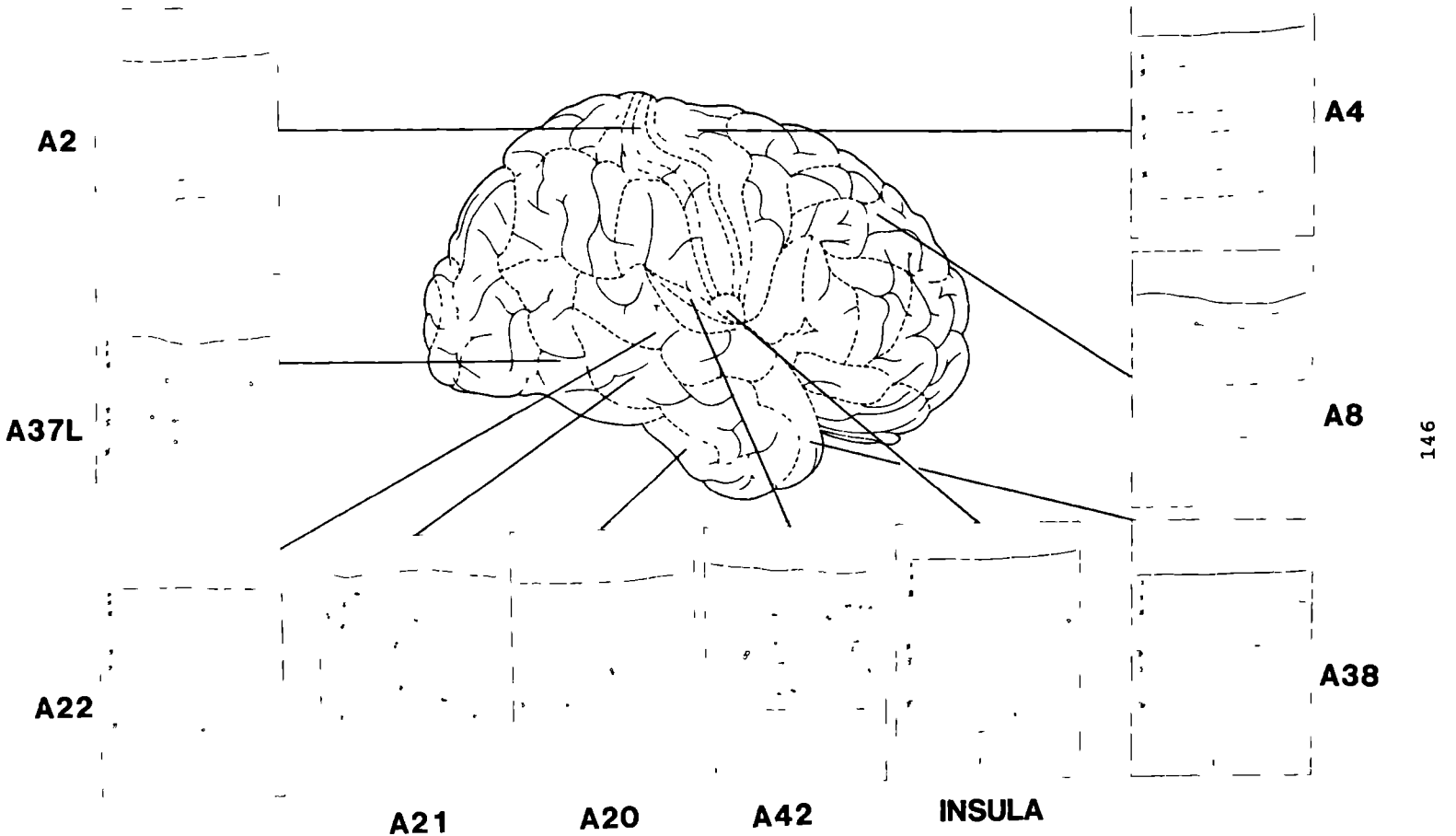

fig. III.7a

CASE 88269

RIGHT HEMISPHERE

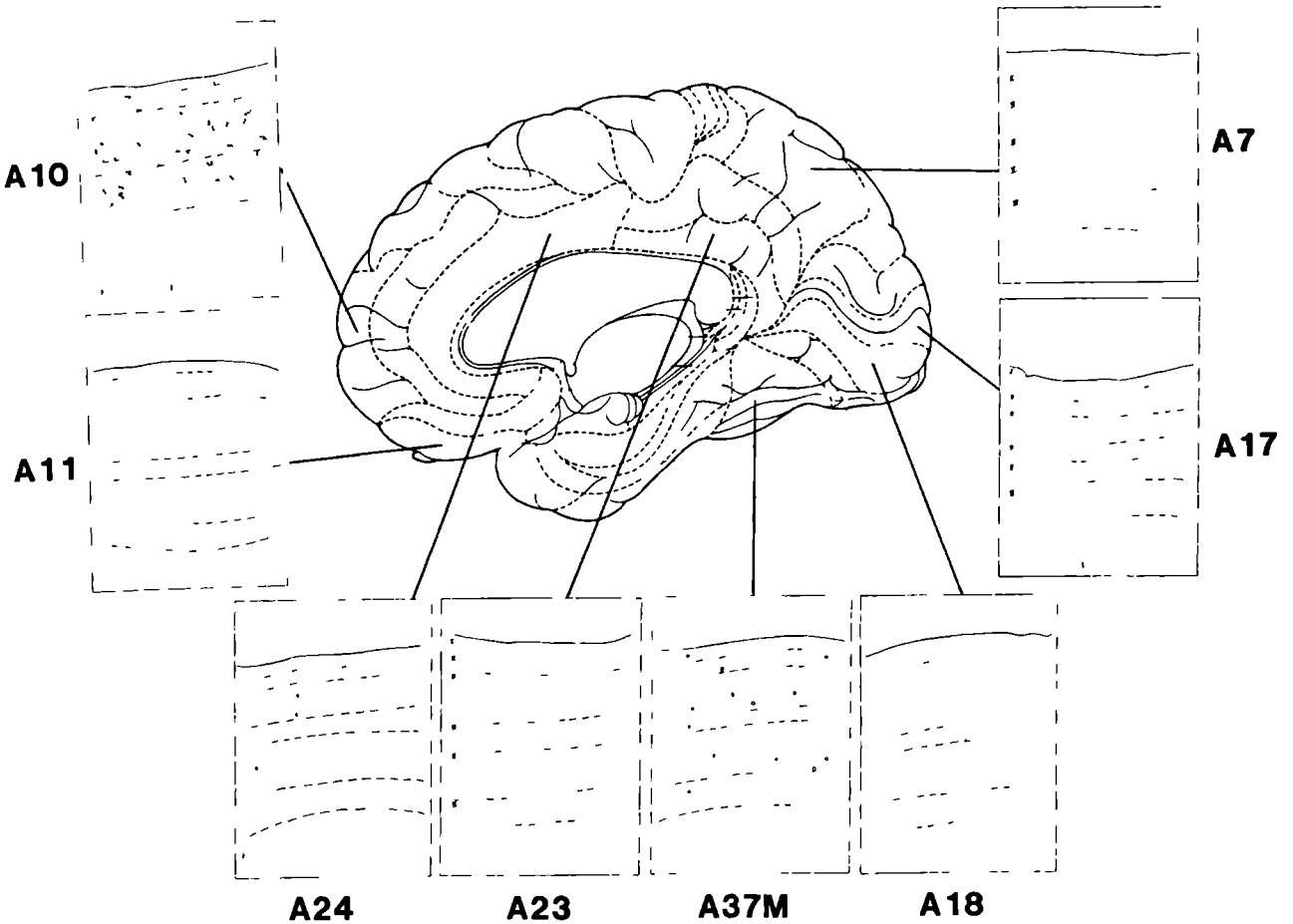

fig. III.7b

CASE 88269

RIGHT HEMISPHERE

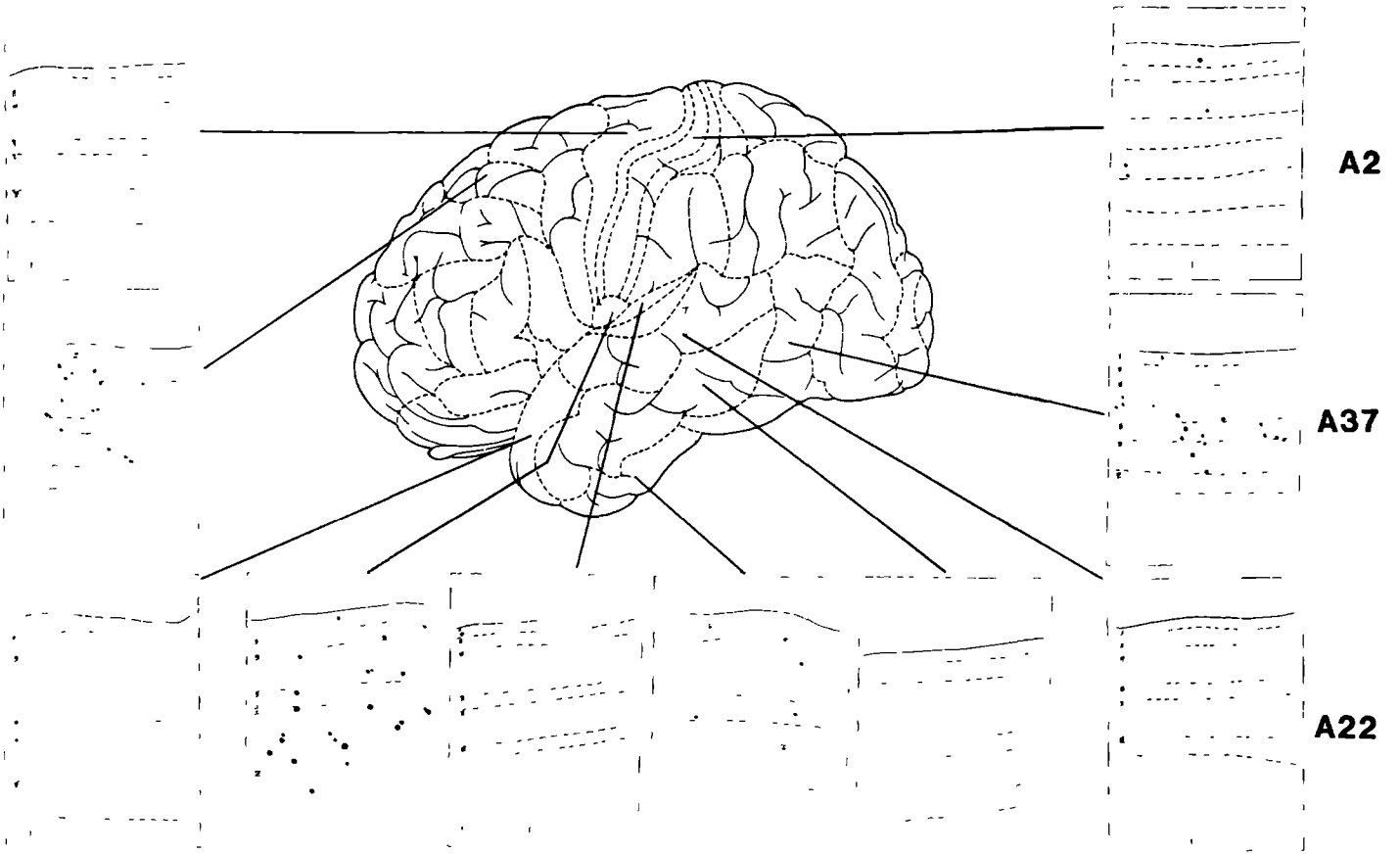

fig. III.7c

CASE 88269

LEFT HEMISPHERE

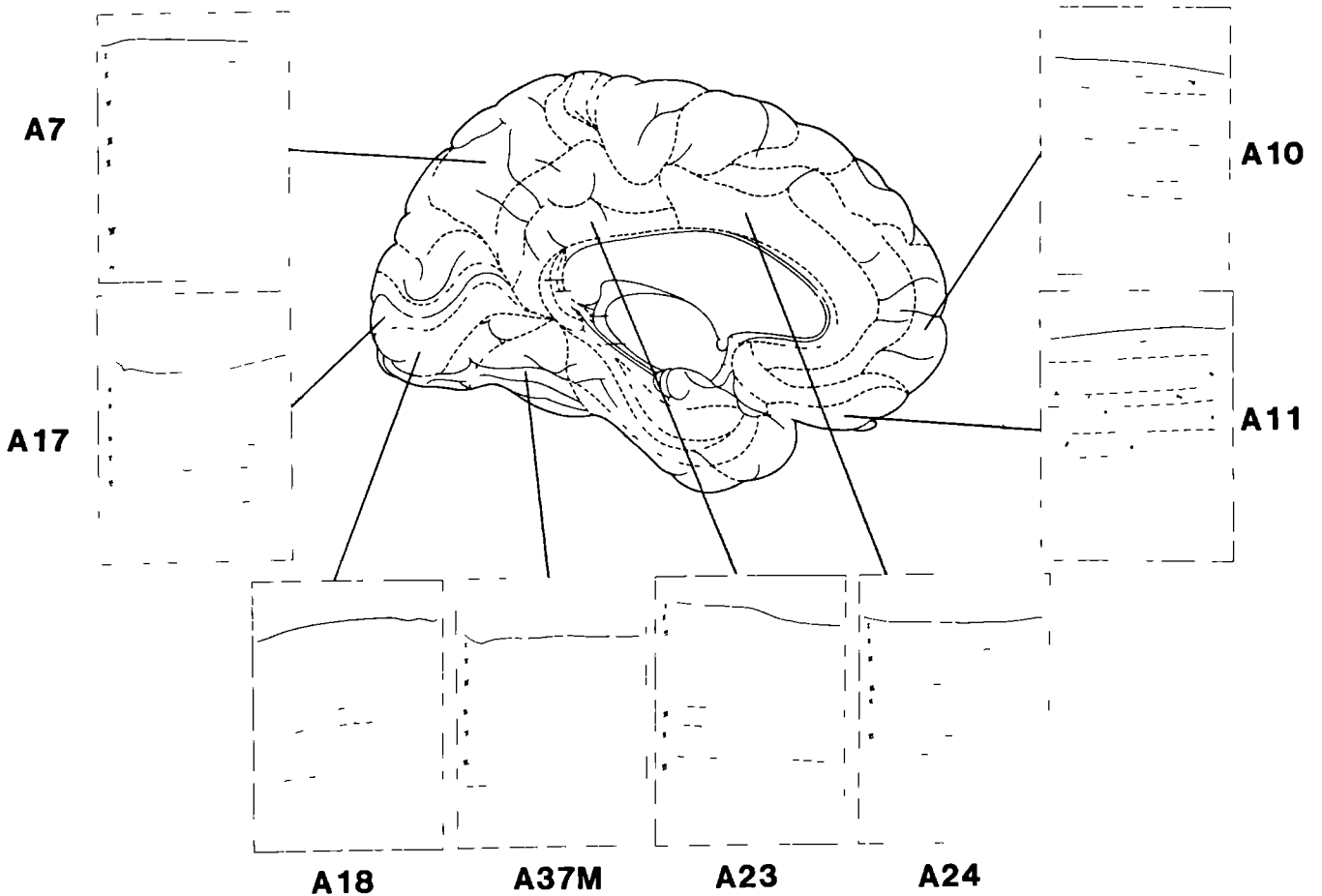

fig. III.7d

CASE 88269

LEFT HEMISPHERE

SENILE PLAQUES CORTICAL DISTRIBUTION
TOTAL DISTRIBUTION; YAMAMOTO STAINING

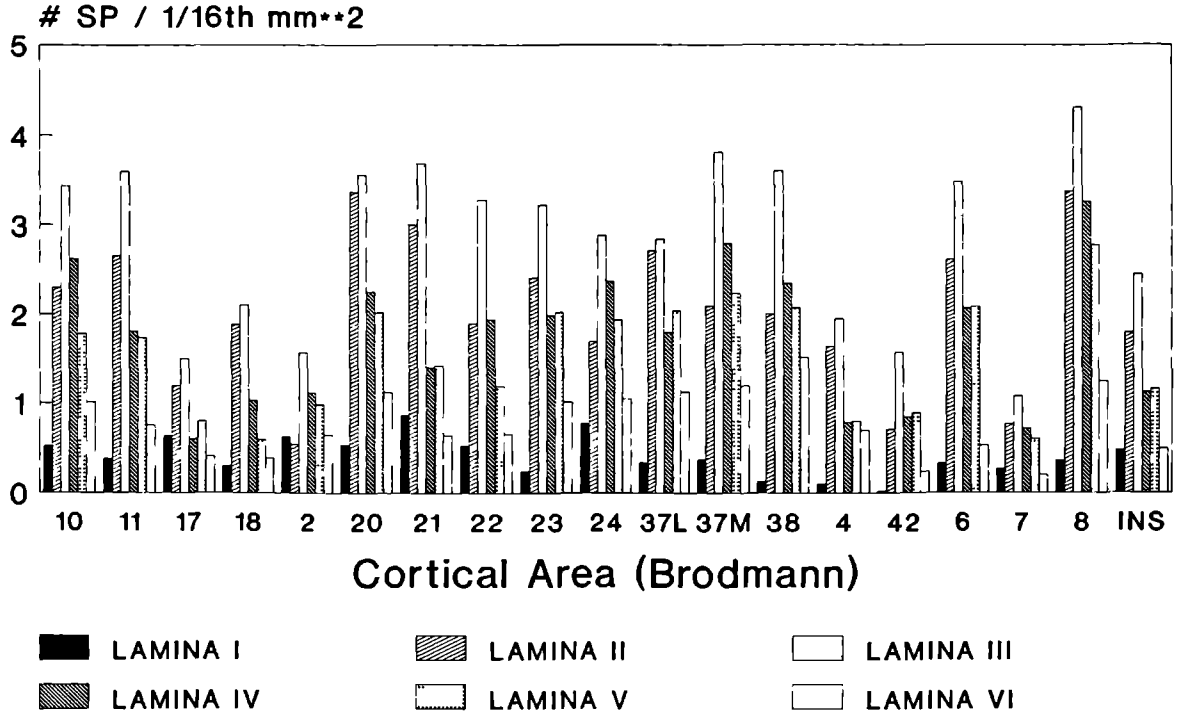

fig. III.8

TABLE 1: SENILE PLAQUE DISTRIBUTION IN VARIOUS CORTICAL AREAS
number of SP pro 1/16th square millimeter (standard error)
p-values of possible comparisons

AREA:10

		STUDENT'S T-TEST, p VALUES:	
L I	: 0.516 (0.13)	L I ~ L II	:<0.00009
L II	: 2.293 (0.57)	L I ~ L III	:<0.00009
L III	: 3.436 (0.43)	L I ~ L IV	:<0.00009
L IV	: 2.623 (0.82)	L I ~ L V	:=0.05
L V	: 1.778 (0.2)	L I ~ L VI	:=0.20
L VI	: 1.01 (0.16)	L II ~ L III	:=0.11
		L II ~ L IV	:=0.06
		L II ~ L V	:=0.004
		L II ~ L VI	:=0.0001
		L III ~ L IV	:=0.0053
		L III ~ L V	:=0.0014
		L III ~ L VI	:=0.0007
		L IV ~ L V	:<0.00009
		L IV ~ L VI	:<0.00009
		L V ~ L VI	:=0.19

AREA: 11

L I	: 0.3775 (0.14)	L I ~ L II	:<0.00009
L II	: 2.655 (0.52)	L I ~ L III	:<0.00009
L III	: 3.598 (0.608)	L I ~ L IV	:=0.025
L IV	: 1.806 (0.24)	L I ~ L V	:<0.00009
L V	: 1.735 (0.57)	L I ~ L VI	:=0.029
L VI	: 0.7543 (0.24)	L II ~ L III	:=0.28
		L II ~ L IV	:=0.0094
		L II ~ L V	:=0.35
		L II ~ L VI	:=0.0083
		L III ~ L IV	:=0.0038
		L III ~ L V	:=0.411
		L III ~ L VI	:=0.003
		L IV ~ L V	:=0.0024
		L IV ~ L VI	:=0.46
		L V ~ L VI	:=0.004

SENILE PLAQUE DISTRIBUTION IN VARIOUS CORTICAL AREAS (continued)

AREA: 17

		STUDENT'S T-TEST, p-VALUES:	
L I	:0.632 (0.24)	L I - L II	:=0.083
L II	:1.188 (0.34)	L I - L III	:=0.29
L III	:1.501 (0.27)	L I - L IV	:=0.0047
L IV	:0.602 (0.11)	L I - L V	:=0.16
L V	:0.798 (0.36)	L I - L VI	:=0.024
L VI	:0.406 (0.14)	L II - L III	:=0.18
		L II - L IV	:=0.0005
		L II - L V	:=0.32
		L II - L VI	:=0.002
		L III - L IV	:=0.002
		L III - L V	:=0.336
		L III - L VI	:=0.0096
		L IV - L V	:=0.0002
		L IV - L VI	:=0.177
		L V - L VI	:=0.0046

AREA:18

		STUDENT'S T-TEST, p-VALUES:	
L I	:0.30 (0.08)	L I ~ L II	:<0.00009
L II	:1.87 (0.51)	L I ~ L III	:<0.00009
L III	:2.10 (0.33)	L I ~ L IV	:<0.00009
L IV	:1.03 (0.38)	L I ~ L V	:=0.0002
L V	:0.596 (0.25)	L I ~ L VI	:=0.011
L VI	:0.39 (0.15)	L II ~ L III	:0.064
		L II ~ L IV	:0.15
		L II ~ L V	:0.011
		L II ~ L VI	:0.0008
		L III ~ L IV	:0.28
		L III ~ L V	:0.14
		L III ~ L VI	:0.0098
		L IV ~ L V	:0.06
		L IV ~ L VI	:0.0035
		L V ~ L VI	:0.0492

SENILE PLAQUE DISTRIBUTION IN VARIOUS CORTICAL AREAS (continued)

AREA:A 2

L I	:0.625	(0.31)
L II	:0.54	(0.25)
L III	:1.563	(0.52)
L IV	:1.112	(0.45)
L V	:0.98	(0.24)
L VI	:0.65	(0.19)

STUDENT'S T-TEST, p-VALUES:

L I - L II	:=0.29
L I - L III	:=0.11
L I - L IV	:=0.18
L I - L V	:=0.24
L I - L VI	:=0.20
L II - L III	:=0.05
L II - L IV	:=0.09
L II - L V	:=0.12
L II - L VI	:=0.35
L III - L IV	:=0.35
L III - L V	:=0.27
L III - L VI	:=0.04
L IV - L V	:=0.26
L IV - L VI	:=0.06
L V - L VI	:=0.08

AREA:A 20

L I	:0.5317	(0.18)
L II	:3.364	(0.78)
L III	:3.558	(0.45)
L IV	:2.249	(0.51)
L V	:2.016	(0.32)
L VI	:1.1167	(0.44)

STUDENT'S T-TEST, p-VALUES:

L I - L II	:<0.00009
L I - L III	:=0.0003
L I - L IV	:=0.0001
L I - L V	:=0.0125
L I - L VI	:=0.0004
L II - L III	:=0.0271
L II - L IV	:=0.064
L II - L V	:=0.0017
L II - L VI	:=0.0198
L III - L IV	:=0.31
L III - L V	:=0.067
L III - L VI	:=0.42
L IV - L V	:=0.028
L IV - L VI	:=0.247
L V - L VI	:=0.09

SENILE PLAQUE DISTRIBUTION IN VARIOUS CORTICAL AREAS (continued)

AREA:A 21

L I	:0.864	(0.42)
L II	:2.99	(0.66)
L III	:3.68	(0.48)
L IV	:1.405	(0.31)
L V	:1.42	(0.41)
L VI	:0.64	(0.29)

STUDENT'S T-TEST, p-VALUES:

L I - L II	:=0.069
L I - L III	:=0.33
L I - L IV	:=0.15
L I - L V	:=0.43
L I - L VI	:=0.13
L II - L III	:=0.13
L II - L IV	:=0.014
L II - L V	:=0.05
L II - L VI	:=0.01
L III - L IV	:=0.08
L III - L V	:=0.28
L III - L VI	:=0.05
L IV - L V	:=0.19
L IV - L VI	:=0.39
L V - L VI	:=0.13

AREA:A 22

L I	:0.528	(0.32)
L II	:1.89	(0.52)
L III	:3.276	(0.35)
L IV	:1.937	(0.51)
L V	:1.19	(0.30)
L VI	:0.66	(0.20)

STUDENT'S T-TEST, p-VALUES:

L I - L II	:=0.026
L I - L III	:=0.34
L I - L IV	:=0.033
L I - L V	:=0.36
L I - L VI	:=0.031
L II - L III	:=0.05
L II - L IV	:=0.45
L II - L V	:=0.016
L II - L VI	:=0.0008
L III - L IV	:=0.07
L III - L V	:=0.22
L III - L VI	:=0.015
L IV - L V	:=0.019
L IV - L VI	:=0.001
L V - L VI	:=0.05

SENILE PLAQUE DISTRIBUTION IN VARIOUS CORTICAL AREAS (continued)

AREA: A 23

		STUDENT'S T-TEST, p-VALUES:	
L I	:0.24 (0.19)	L I - L II	:=0.0032
L II	:2.41 (0.59)	L I - L III	:=0.0079
L III	:3.22 (0.51)	L I - L IV	:=0.0091
L IV	:1.98 (0.49)	L I - L V	:=0.10
L V	:2.01 (0.30)	L I - L VI	:=0.17
L VI	:1.01 (0.27)	L II - L III	:=0.32
		L II - L IV	:=0.29
		L II - L V	:=0.05
		L II - L VI	:=0.032
		L III - L IV	:=0.46
		L III - L V	:=0.09
		L III - L VI	:=0.05
		L IV - L V	:=0.09
		L IV - L VI	:=0.06
		L V - L VI	:=0.35

AREA: A 24

		STUDENT'S T-TEST, p-VALUES:	
L I	:0.77 (0.67)	L I - L II	:=0.48
L II	:1.64 (0.7)	L I - L III	:=0.23
L III	:2.88 (0.48)	L I - L IV	:=0.37
L IV	:2.37 (0.59)	L I - L V	:=0.47
L V	:1.93 (0.71)	L I - L VI	:=0.30
L VI	:1.05 (0.53)	L II - L III	:=0.21
		L II - L IV	:=0.34
		L II - L V	:=0.51
		L II - L VI	:=0.27
		L III - L IV	:=0.35
		L III - L V	:=0.23
		L III - L VI	:=0.44
		L IV - L V	:=0.34
		L IV - L VI	:=0.39
		L V - L VI	:=0.26

SENILE PLAQUE DISTRIBUTION IN VARIOUS CORTICAL AREAS (continued)

AREA: A 37l

		STUDENT'S T-TEST, p-VALUES:	
L I	:0.3355 (0.14)	L I - L II	:<0.00009
L II	:2.708 (0.67)	L I - L III	:<0.00009
L III	:2.8483 (0.83)	L I - L IV	:=0.0016
L IV	:1.79 (0.41)	L I - L V	:=0.0002
L V	:2.04 (0.53)	L I - L VI	:=0.0002
L VI	:1.125 (0.54)	L II - L III	:=0.26
		L II - L IV	:=0.07
		L II - L V	:=0.21
		L II - L VI	:=0.23
		L III - L IV	:=0.028
		L III - L V	:=0.08
		L III - L VI	:=0.09
		L IV - L V	:=0.22
		L IV - L VI	:=0.20
		L V - L VI	:=0.47

AREA: A 37m

		STUDENT'S T-TEST, p-VALUES:	
L I	:0.369 (0.17)	L I - L II	:=0.0001
L II	:2.088 (0.57)	L I - L III	:<0.00009
L III	:3.813 (0.74)	L I - L IV	:=0.0001
L IV	:2.788 (0.55)	L I - L V	:=0.0009
L V	:2.233 (0.44)	L I - L VI	:=0.0012
L VI	:1.188 (0.42)	L II - L III	:=0.017
		L II - L IV	:=0.43
		L II - L V	:=0.15
		L II - L VI	:=0.12
		L III - L IV	:=0.13
		L III - L V	:=0.03
		L III - L VI	:=0.02
		L IV - L V	:=0.19
		L IV - L VI	:=0.15
		L V - L VI	:=0.43

SENILE PLAQUE DISTRIBUTION IN VARIOUS CORTICAL AREAS (continued)

ARFA A 38

L I	:0.1315	(0.07)
L II	:1.999	(0.28)
L III	:3.605	(0.70)
L IV	:2.345	(0.47)
L V	:2.07	(0.43)
L VI	:1.518	(0.25)

STUDENT'S T-TEST, p-VALUES:

L I - L II	:<0.00009
L I - L III	:<0.00009
L I - L IV	:<0.00009
L I - L V	:<0.00009
L I - L VI	:=0.0001
L II - L III	:=0.0028
L II - L IV	:=0.05
L II - L V	:=0.0825
L II - L VI	:=0.32
L III - L IV	:=0.089
L III - L V	:=0.05
L III - L VI	:=0.0035
L IV - L V	:=0.38
L IV - L VI	:=0.0267
L V - L VI	:=0.0418

AREA:A 4

L I	:0.1	(0.062)
L II	:1.635	(0.35)
L III	:1.95	(0.31)
L IV	:0.7881	(0.21)
L V	:0.795	(0.22)
L VI	:0.698	(0.265)

STUDENT'S T-TEST, p-VALUES:

L I - L II	:<0.0009
L I - L III	:<0.0009
L I - L IV	:=0.0001
L I - L V	:=0.0001
L I - L VI	:<0.0009
L II - L III	:=0.31
L II - L IV	:=0.05
L II - L V	:=0 06
L II - L VI	:=0.14
L III - L IV	:=0.10
L III - L V	:=0.12
L III - L VI	:=0.26
L IV - L V	:=0.43
L IV - L VI	:=0.24
L V - L VI	:=0.28

SENILE PLAQUE DISTRIBUTION IN VARIOUS CORTICAL AREAS (continued)

AREA:A 42

L I	:0.02	(0.07)
L II	:0.71	(0.22)
L III	:1.57	(0.32)
L IV	:0.85	(0.29)
L V	:0.89	(0.40)
L VI	:0.24	(0.15)

STUDENT'S T-TEST, p-VALUES:

L I - L II	:<0.00009
L I - L III	:<0.00009
L I - L IV	:<0.00009
L I - L V	:<0.00009
L I - L VI	:<0.00009
L II - L III	:=0.12
L II - L IV	:=0.19
L II - L V	:=0.03
L II - L VI	:=0.09
L III - L IV	:=0.36
L III - L V	:=0.21
L III - L VI	:=0.01
L IV - L V	:=0.13
L IV - L VI	:=0.02
L V - L VI	:=0.0042

AREA: A 6

L I	:0.33	(0.19)
L II	:2 61	(1 7)
L III	:3.48	(1.16)
L IV	:2.07	(0.69)
L V	:2.09	(0.61)
L VI	:0.53	(0.27)

STUDENT'S T-TEST, p-VALUES:

L I - L II	:=0.0005
L I - L III	:=0.0026
L I - L IV	:=0.016
L I - L V	:=0.024
L I - L VI	:=0.26
L II - L III	:=0.19
L II - L IV	:=0.07
L II - L V	:=0.05
L II - L VI	:=0.017
L III - L IV	:=0.15
L III - L V	:=0.12
L III - L VI	:=0.03
L IV - L V	:=0.37
L IV - L VI	:=0.06
L V - L VI	:=0.08

SENILE PLAQUE DISTRIBUTION IN VARIOUS CORTICAL AREAS (continued)

AREA:A 7

L I	:0.2692	(0.19)
L II	:0.7723	(0.27)
L III	:1.074	(0.32)
L IV	:0.72	(0.25)
L V	:0.607	(0.18)
L VI	:0.202	(0.06)

STUDENT'S T-TEST, p-VALUES:

L I	- L II	:=0.08
L I	- L III	:=0.018
L I	- L IV	:=0.13
L I	- L V	:=0.33
L I	- L VI	:=0.0004
L II	- L III	:=0.20
L II	- L IV	:=0.39
L II	- L V	:=0.043
L II	- L VI	:<0.00009
L III	- L IV	:=0.14
L III	- L V	:0.0094
L III	- L VI	:<0.00009
L IV	- L V	:=0.066
L IV	- L VI	:=0.0001
L V	- L VI	:=0.0008

AREA: A 8

L I	:0.366	(0.17)
L II	:3.371	(0.53)
L III	:4.311	(0.43)
L IV	:3.258	(0.84)
L V	:2.775	(0.47)
L VI	:1.248	(0.22)

STUDENT'S T-TEST, p-VALUES:

L I	- L II	:=0.0001
L I	- L III	:=0.0011
L I	- L IV	:<0.00009
L I	- L V	:=0.0005
L I	- L VI	:=0.17
L II	- L III	:=0.21
L II	- L IV	:=0.05
L II	- L V	:=0.32
L II	- L VI	:=0.0042
L III	- L IV	:=0.0116
L III	- L V	:=0.37
L III	- L VI	:=0.0141
L IV	- L V	:=0.026
L IV	- L VI	:=0.0003
L V	- L VI	:=0.0084

SENILE PLAQUE DISTRIBUTION IN VARIOUS CORTICAL AREAS (continued)

AREA:INSULA

L I	:0.4805	(0.14)
L II	:1.7945	(0.33)
L III	:2.445	(0.46)
L IV	:1.123	(0.21)
L V	:1.163	(0.36)
L VI	:0.494	(0.20)

STUDENT'S T-TEST, p-VALUES:

L I	- L II	:=0.0005
L I	- L III	:<0.00009
L I	- L IV	:=0.05
L I	- L V	:=0.0002
L I	- L VI	:=0.07
L II	- L III	:=0.09
L II	- L IV	:=0.039
L II	- L V	:=0.38
L II	- L VI	:=0.02
L III	- L IV	:=0.0026
L III	- L V	:=0.14
L III	- L VI	:=0.0019
L IV	- L V	:=0.0148
L IV	- L VI	:=0.42
L V	- L VI	:=0.0128

From Table 1. concerning the laminar distribution of SP in the various cortical areas, some general observations can be made:

- In every area investigated, the concentration of SP is the highest in the third (and second) cortical layer.
- With the exception of Area 17 and Area 21, the numerical value of the concentration of SP is the lowest in Area 7.
- The significance of the differences in concentration, as reflected by the p-value in the Student's T-test, over the several cortical layers varies considerably.

The SP distribution, as observed in the cortex map suggests a preferential distribution over the upper cortical layers (L II and L III). To investigate the existence of a preferential laminar SP distribution, as a general scheme of the whole neocortex, all data were combined. These data are visualized in figure III.11. The same data are presented in a table (Table 2), in order to identify significant differences between the prevalence of SP in the various cortical layers:

GLOBAL LAMINAR SP DISTRIBUTION
STAINING: YAMAMOTO

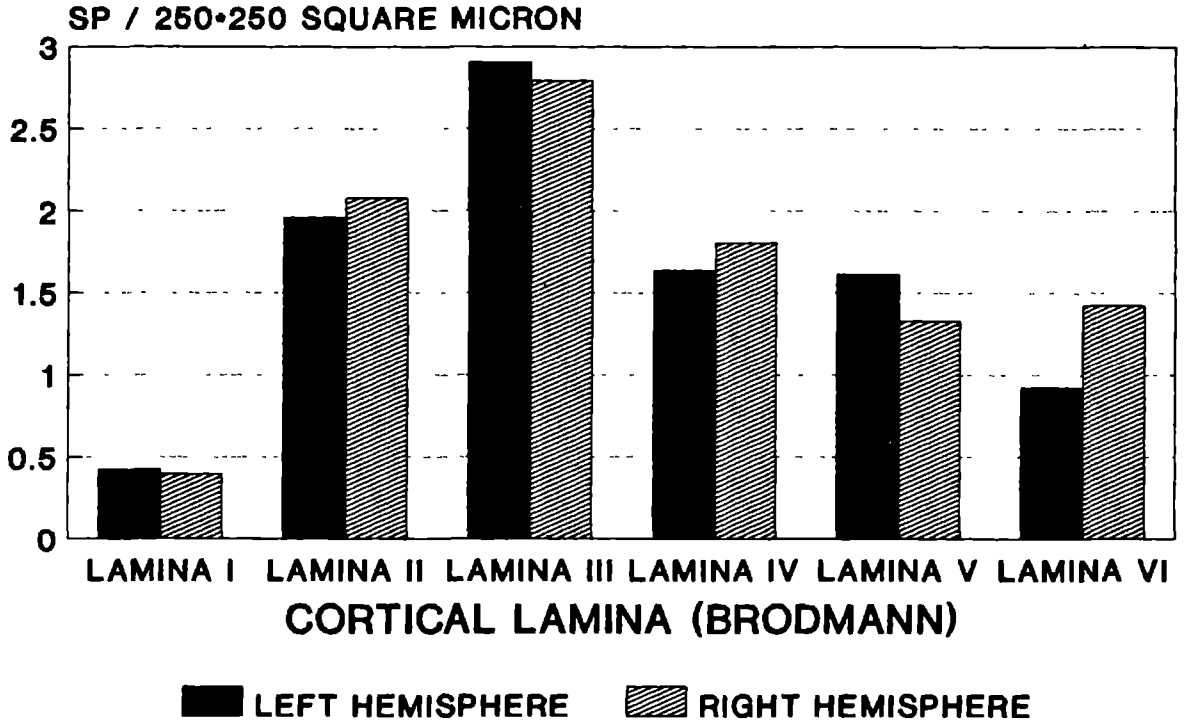

fig. III.9

MEAN AREAL SENILE PLAQUE DISTRIBUTION
YAMAMOTO-STAINING

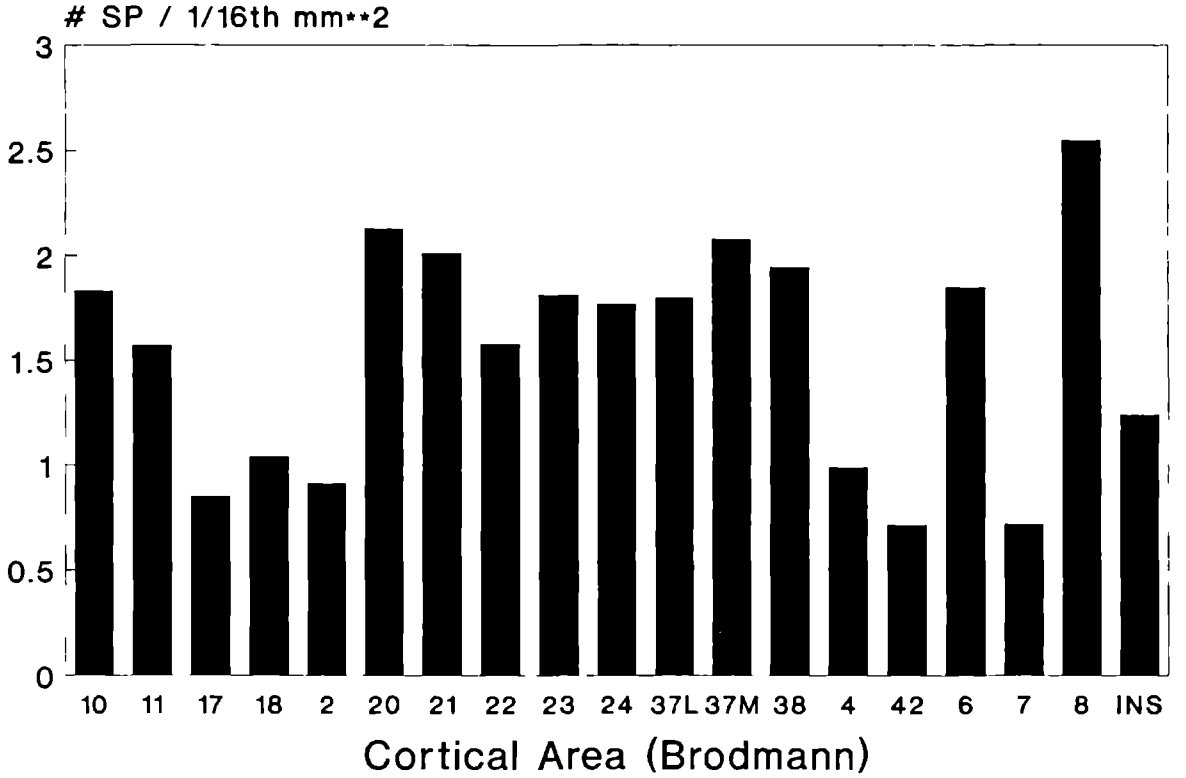

fig. III.10

AREAL SP DISTRIBUTION (rA)

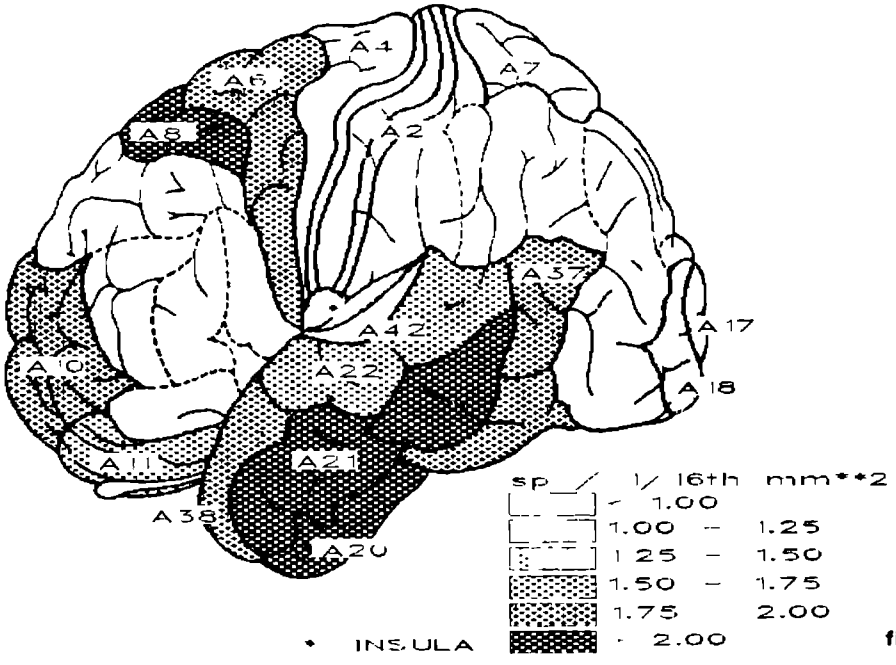

fig. III.11

AREAL SP DISTRIBUTION (rA)

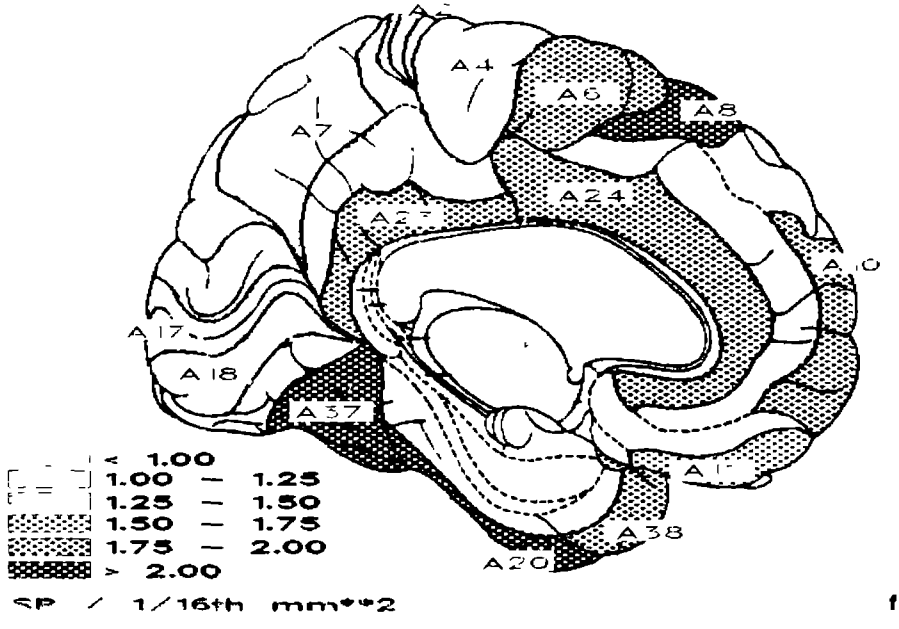

fig. III.12

TABLE 2.: GLOBAL LAMINAR SENILE PLAQUE DISTRIBUTION

STAINING: YAMAMOTO

	LEFT HEMISPHERE	RIGHT HEMISPHERE
L I :	0.425 (0.074)	0.3974 (0.074)
L II :	1.963 (0.192)	2.077 (0.207)
L III:	2.903 (0.192)	2.792 (0.194)
L IV :	1.64 (0.176)	1.806 (0.197)
L V :	1.611 (0.144)	1.3308 (0.136)
L VI :	0.924 (0.120)	1.4260 (0.792)

STUDENT'S T- TEST

L I - L II	<0.00009	<0.00009
L I - L III	<0.00009	<0.00009
L I - L IV	<0.00009	<0.00009
L I - L V	<0.00009	<0.00009
L I - L VI	<0.00009	<0.00009
L II- L III	0.48	0.22
L II- L IV	0.14	0.27
L II- L V	0.0004	<0.00009
L II- L VI	<0.00009	<0.00009
L III-L IV	0.139	0.43
L III-L V	0.0003	0.0001
L III-L VI	<0.00009	<0.00009
L IV- L V	0.0092	<0.00009
L IV- L VI	<0.00009	<0.00009
L V - L VI	0.0172	<0.00009

Table 2., concerning global laminar Senile Plaque distribution is obtained by pooling the results of the various cortical areas in order to detect a possible general pattern in Senile Plaque distribution. This way of data representation allows the following general observations:

- No difference between the left and the right hemispheres can be observed after pooling of the data (p=0.41, two tailed Student's T-test).
- Most of the SP are observed in the third cortical layer, but it should be noticed that the differences between the third layer and the two neighboring layers (L II and L IV) is not significant.
- The differences between the remaining layers e.g. L II and L IV, are highly significant.

III.4.2. The areal distribution of Senile Plaques as seen in Yamamoto-stained sections.

In the previous paragraph, the laminar distribution of the Senile Plaques, as seen in the Yamamoto-staining was studied. In this section the distribution of SP over the various cortical areas is examined, without paying attention to individual cortical laminae. In order to compare the concentration of SP of several areas, the mean concentration of SP for the overall thickness of the cortex is calculated by averaging the laminar concentrations.
The results obtained, are presented in the bar diagram 'Mean areal Senile Plaque distribution' (fig. III.10). From this figure, it can be concluded that the largest concentrations of SP are found in the cingular, temporal and insular regions. These data are also represented in figs. III.11 and III.12.
To make these comparisions more specific, the data are given in Table 3. In this table SP concentration is presented in 250*250*10 cubic micron, together with the standard error (SE).
In a separate table the corresponding p-values are given, using the two-tailed Student's T-test.
These t-values enable one to compare the various cortical areas. From this figure, it can be derived that the highest concentrations of the Yamamoto-plaques are found in the areas A 8 in the frontal lobe. This Area 8, the arcuate region, receives heavy projections from the first auditory association area (AA1), the first visual association area in the temporo-occipital region (VA1) and from the third somatosensory association area (SA3). These connections to the frontal Area 8 from the temporal and parietal lobe suggest an important center of integration of information in this Area.

As is shown in this study, the temporal regions (Areas 20,21, 37L and 38) are loaded with SP. The Area 38, the temporal pole receives information of various sensory modalities: via the third auditory

association area (AA3), the high order visual association areas (TE1, TH-TL-TF) have important connections with it. In terms of convergence of information from various modalities, Area 38 is important. Although Area 38 is comparably rich in connectivity with high order association areas, like Area 8, it is not so heavily affected by SP formation.

The somatosensory association areas are located in the parietal lobe, designated as Areas 5 and 7 by Brodmann. In our study, Area 7 was only slightly involved in SP formation.
For instance, the somatosensory association area A 7, is among the areas with the lowest SP concentration. Although the auditory association areas in the superior temporal gyrus have a similarly intense connectional network with other centers of information processing as the inferior part of the temporal lobe, containing the visual association areas, the area A 22 has a significantly lower number of SP.

The concentrations in the lower parts of the temporal lobe, A 20 and A 21 are lower than in Area 8. The difference between A 8 and A 20 proved to be significant (p=0.018).

The areas A 21 and A 22 are located in the middle and inferior part of the temporal lobe. The positions of these areas matches the location of the temporal visual association areas. These results are in accordance with the principle, formulated above that the larger number of SP is found in association areas.

According to the description of the auditory, visual and somatosensory information systems in the introduction, the information relayed through a large number of association areas reaches A 38, the temporal pole. The temporal pole in AD also belongs to the heavily affected cortical areas: 1.945(0.28) SP/250*250*10 micron**3. The concentration of SP in this area is significantly different from A 20 and A 22 (p-values 0.0085 and 0.03) but not so from A 21. Apparently, there exists a zone in the middle and lower temporal lobe, extending to the temporal pole, with a high concentration of SP. In this part of the temporal pole, the visual association areas are situated. The area A 22 covers more or less the region, in which the auditory association areas are located.
Of the somatosensory association areas, located in the superior and inferior parietal lobule, Area 7 is investigated in this study. According to our analysis the number of SP in this region is extremely low: 0.72(0.18) SP/250*250*10 micron**3. This number is even lower as in the primary motor area A 4 (p=0.0063) and the primary sensory area, A 2 (p=0.0078). This finding clearly contradicts the adagium, that the concentration of SP is

distributed following a gradient from primary to association areas.

The areas in the frontal lobe, which were investigated in this study are the Areas 8, 10, 11. The Areas 10 and 11 are moderately affected by SP formation. These frontal areas are connected with association areas [3]: Area 11 receives fibers from the VA3 area. Area A 10 receives information from AA2. Furthermore, also projections from these areas to the association areas exist: Area 10 projects for example to the secondary parasensory association areas [4].

III.5. THE DISTRIBUTION OF SENILE PLAQUES (SP), NEUROFIBRILLARY TANGLES (NFT) AND CONGOPHILIC ANGIOPATHY (CAA) USING THE CONGO-RED FLUORESCENCE TECHNIQUE.

In sections, stained with Congo-Red and viewed under UV-illumination, SP, NFT and CAA can be visualized and quantified as described in the previous chapter.
The data obtained for each hemisphere are represented in a bar diagram. NFT, SP and CAA are represented, in separate diagrams. In these diagrams, the number of the structures investigated is expressed as the number in a fixed volume of 250*750*10 cubic micron. In order to facilitate comparison between the diagrams, the sequence of the cortical areas on the abscissa is the same.
In our study of the distribution of NFT in control brains, one probably important feature could be noticed in Congo-Red stained sections and viewed under fluorescence microscopy: the structure, referred to in this study as "Congophilic Threads". These structures are investigated and scored according to the same methods as NFT or SP in the brains of the Alzheimer patients.

SP DISTRIBUTION IN CONGO-RED
Brain 87395; Left Hemisphere

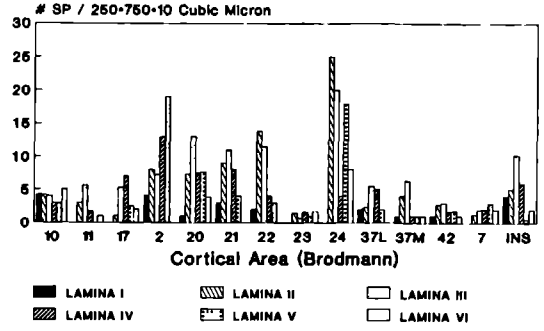

fig III.12b

NFT DISTRIBUTION IN CONGO-RED
Brain 87395; Left Hemisphere

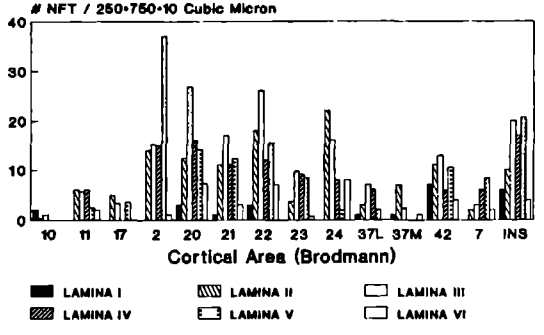

fig. III.13b

CAA DISTRIBUTION IN CONGO-RED
Brain 87395; Left Hemisphere

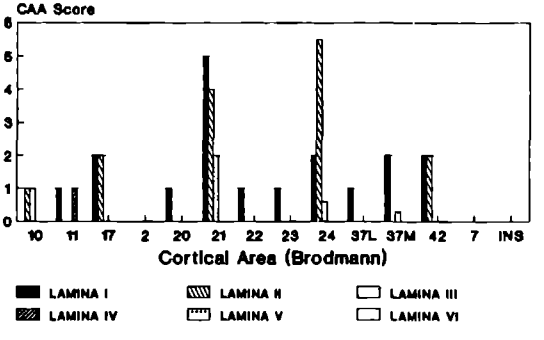

fig. III.28b

SP DISTRIBUTION IN CONGO-RED
Brain 87395; Right Hemisphere

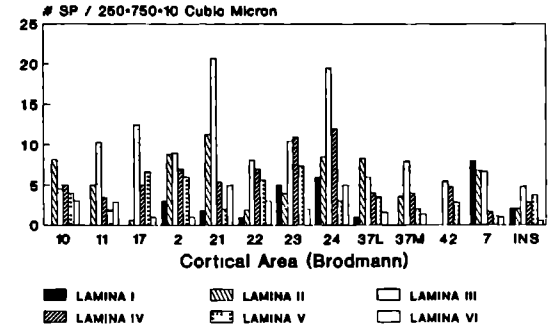

fig. III 21a

NFT DISTRIBUTION IN CONGO-RED
Brain 87395; Right Hemisphere

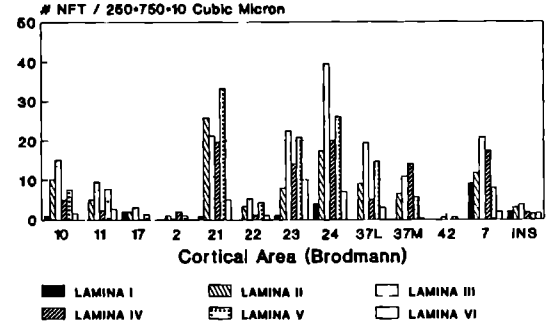

fig. III 13a

CAA DISTRIBUTION IN CONGO-RED
Brain 87395; Right Hemisphere

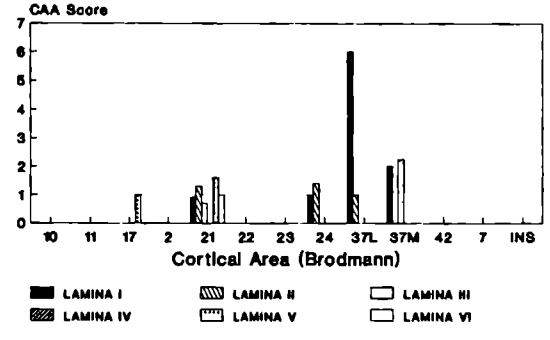

fig. 28a

SP DISTRIBUTION IN CONGO-RED
Brain 88177; Left Hemisphere

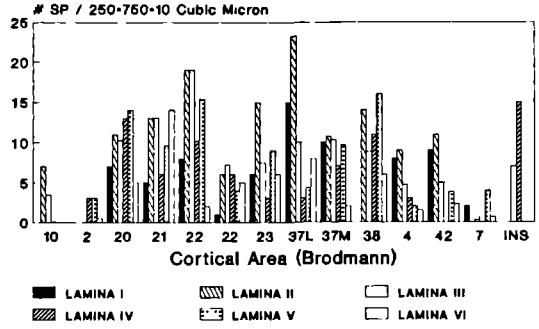

fig III 22b

NFT DISTRIBUTION IN CONGO-RED
Brain 88177; Left Hemisphere

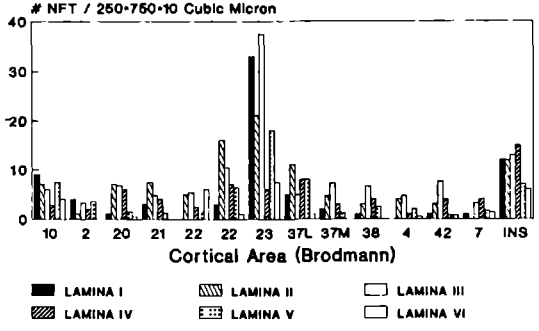

fig III 14b

CAA DISTRIBUTION IN CONGO-RED
Brain 88177; Left Hemisphere

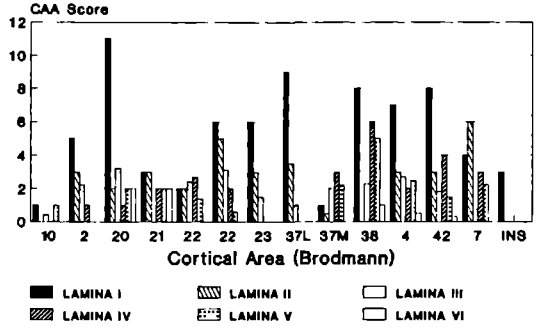

fig. III.29b

SP DISTRIBUTION IN CONGO-RED
Brain 88177; Right Hemisphere

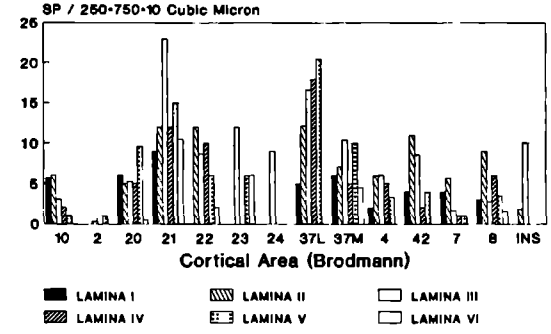

fig. III 22a

NFT DISTRIBUTION IN CONGO-RED
Brain 88177; Right Hemisphere

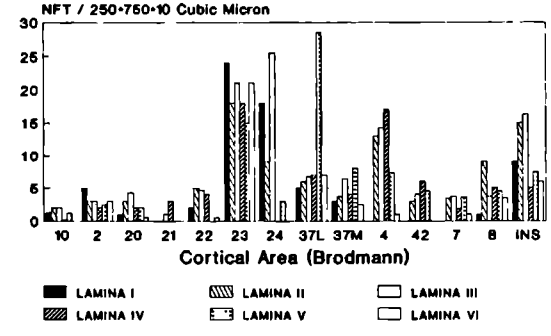

fig. III.14a

CAA DISTRIBUTION IN CONGO-RED
Brain 88177; Right Hemisphere

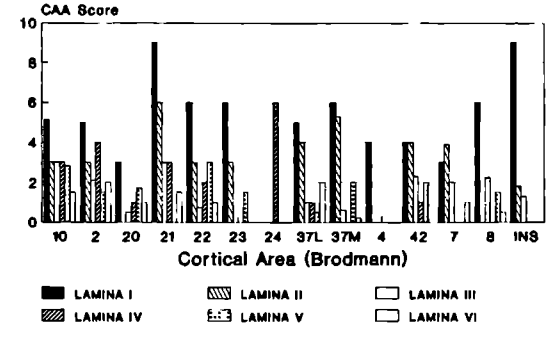

fig III.29a

SP DISTRIBUTION IN CONGO-RED
Brain 89033; Left Hemisphere

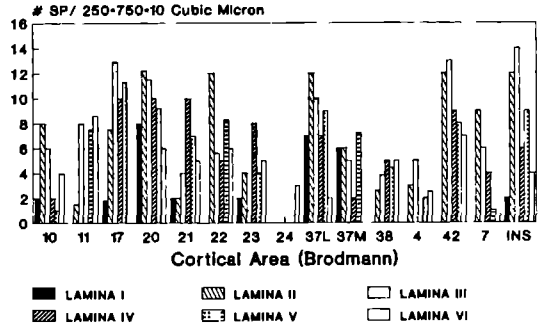

fig. III 23b

NFT DISTRIBUTION IN CONGO-RED
Brain 89033; Left Hemisphere

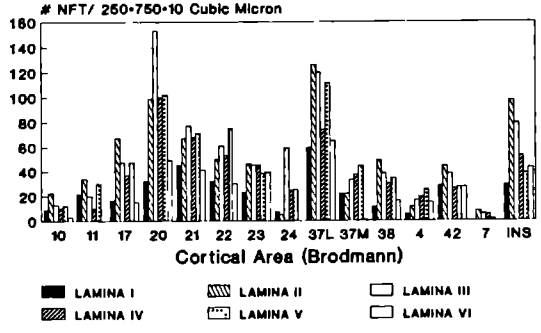

fig III 15b

CAA DISTRIBUTION IN CONGO-RED
Brain 89033; Left Hemisphere

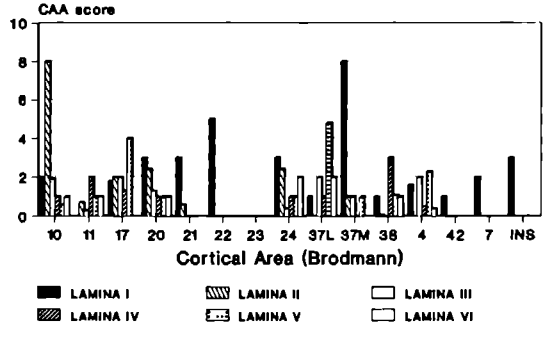

fig. III 30b

SP DISTRIBUTION IN CONGO-RED
Brain 89033; Right Hemisphere

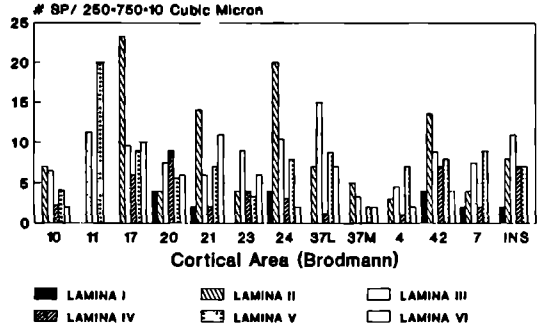

fig. III.23a

NFT DISTRUBUTION IN CONGORED
Brain 89033; Right Hemisphere

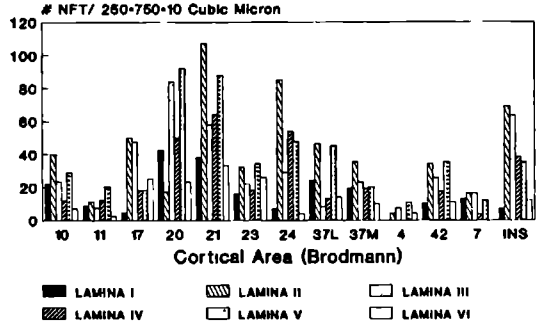

fig III.15a

CAA DISTRIBUTION IN CONGO-RED
Brain 89033; Right Hemisphere

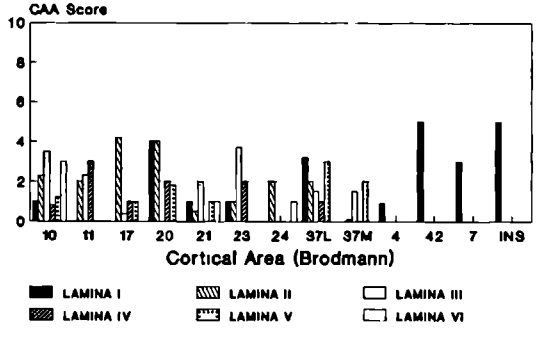

fig III.30a

SP DISTRIBUTION IN CONGO-RED
Brain 88243; Left hemisphere

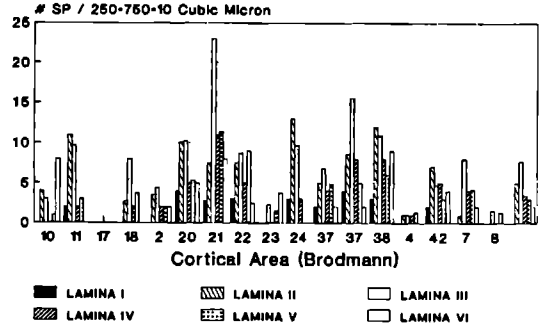

fig III 24b

NFT DISTRIBUTION IN CONGO-RED
Brain 88243; Left hemisphere

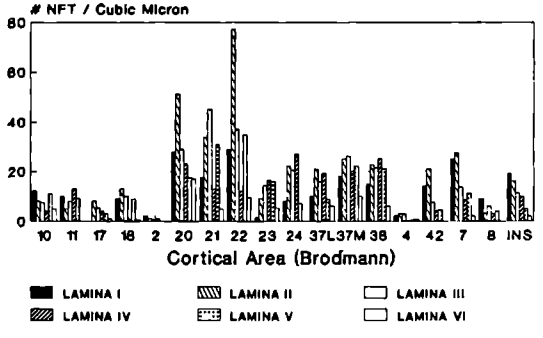

fig. III 16b

CAA DISTRIBUTION IN CONGO-RED
Brain 88243; Left Hemisphere

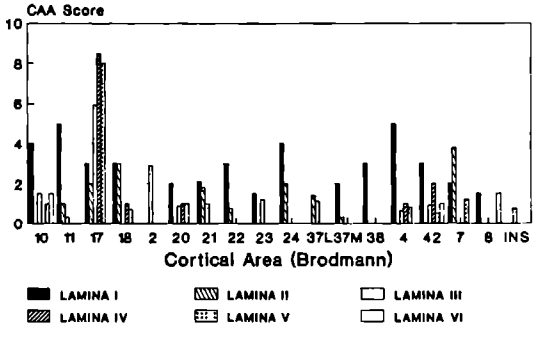

fig. 31a

SP DISTRIBUTION IN CONGO-RED
Brain 88243; Right Hemisphere

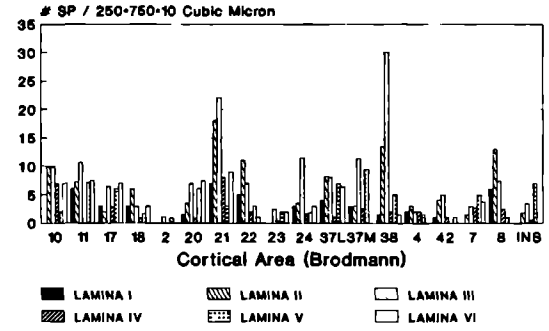

fig III.24a

NFT DISTRIBUTION IN CONGO-RED
Brain 88243; Right Hemisphere

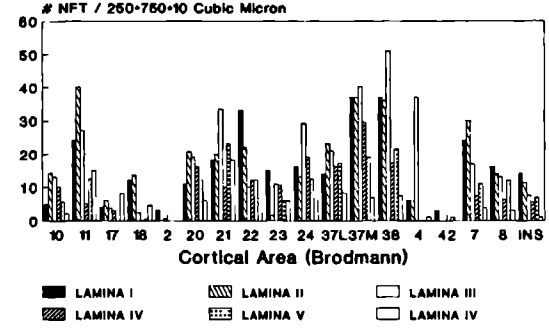

fig. III.16a

CAA DISTRIBUTION IN CONGO-RED
Brain 88243; Right Hemisphere

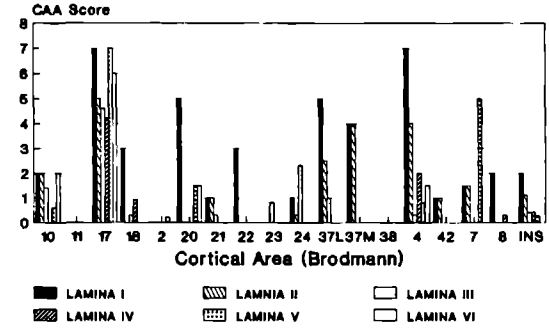

fig 31b

SP DISTRIBUTION IN CONGO-RED
Brain 88268; Left Hemisphere

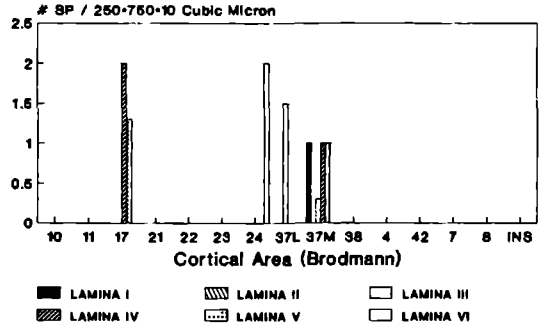

fig III 25b

CONGOPHILIC THREADS IN FLUORESCENCE
Brain 88268; Left Hemisphere

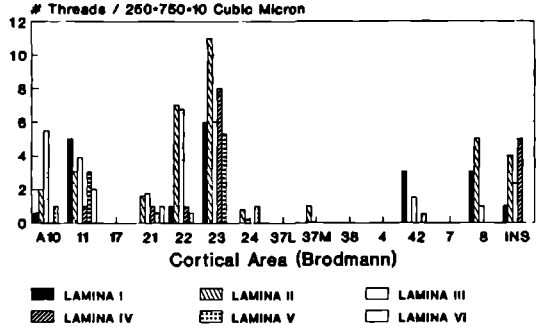

fig. III 17b

CAA DISTRIBUTION IN CONGO-RED
Brain 88268; Left Hemisphere

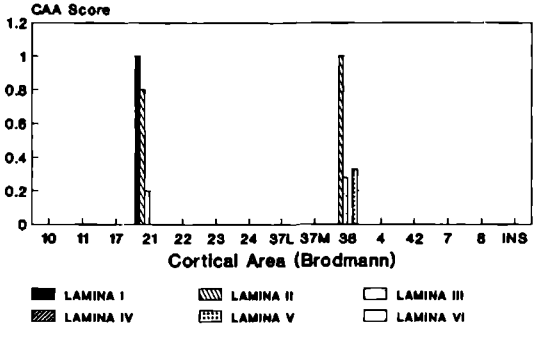

fig III.32b

SP DISTRIBUTION IN CONGO-RED
Brain 88268; Right Hemisphere

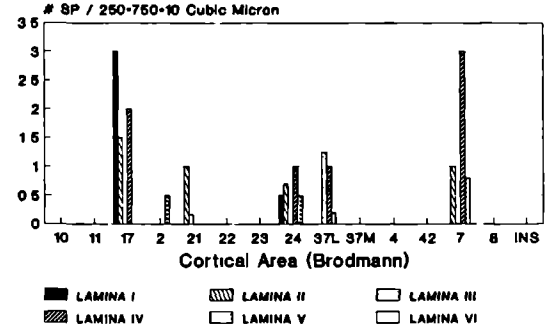

fig III.26a

CONGOPHILIC THREADS IN FLUORESCENCE
Brain 88268; Right Hemispere

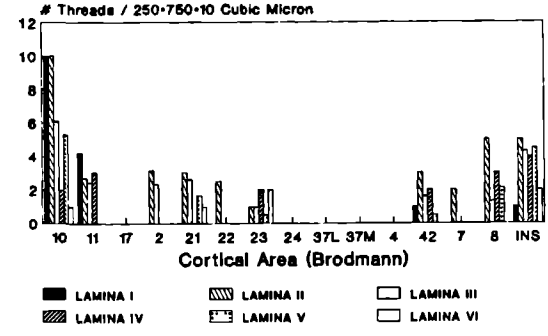

fig III.17a

CAA DISTRIBUTION IN CONGO-RED
Brain 88268; Right Hemisphere

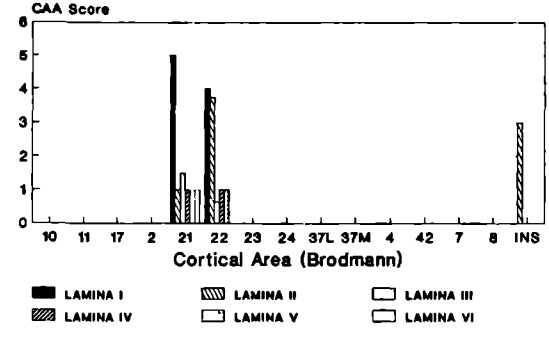

fig III.32a

CONGOPHILIC THREADS IN FLUORESCENCE
Brain 88271; Left hemisphere

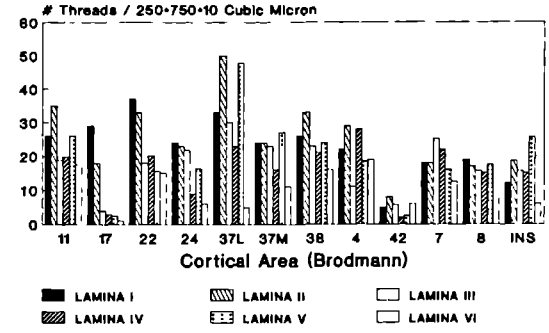

fig III 18b

CONGOPHILIC THREADS IN FLUORESCENCE
Brain 88271; Right Hemisphere

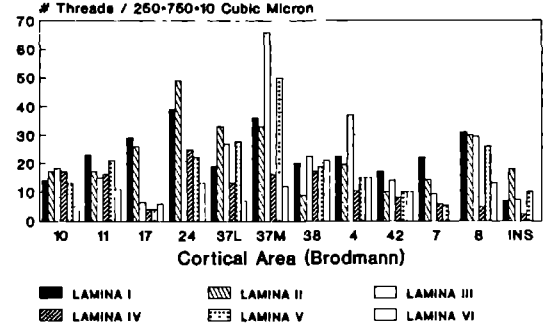

fig III.18a

CONGOPHILIC THREADS IN FLUORESCENCE
Brain 88269; Right Hemisphere

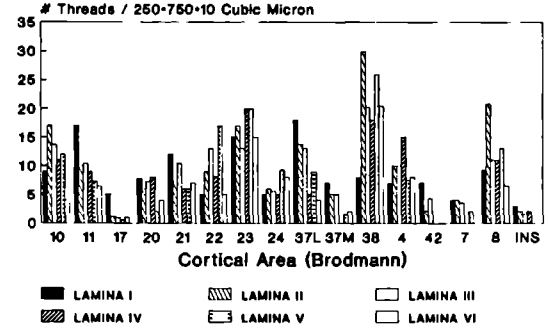

fig III 19a

CONGOPHILIC THREADS IN FLUORESCENCE
Brain 88269; Left Hemisphere

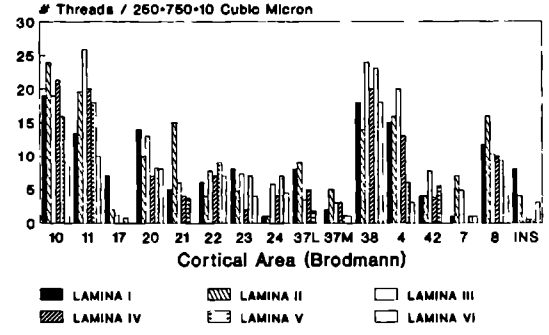

fig III.19b

SP DISTRIBUTION IN CONGO-RED
Brain 88269; Right Hemisphere

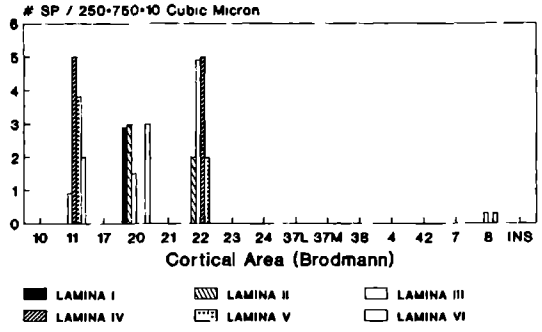

fig III 26a

SP DISTRIBUTION IN CONGO-RED
Brain 88269; Left Hemisphere

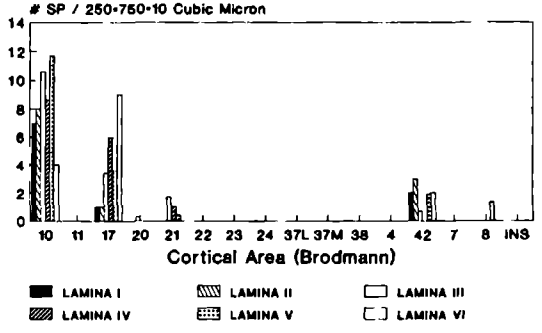

fig III 26b

SP DISTRIBUTION IN ALZHEIMER'S DISEASE
Right Hemisphere; Congo-Red

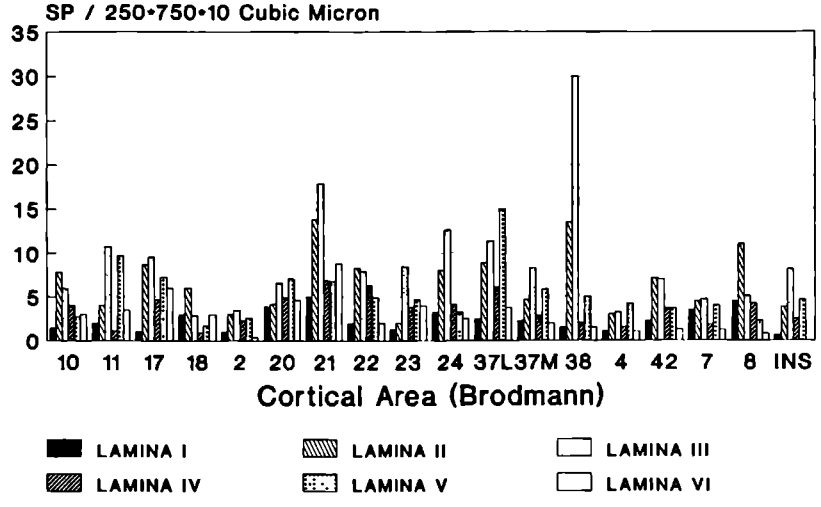

fig. III.27a

SP DISTRIBUTION IN ALZHEIMER'S DISEASE
Left Hemisphere; Congo-Red

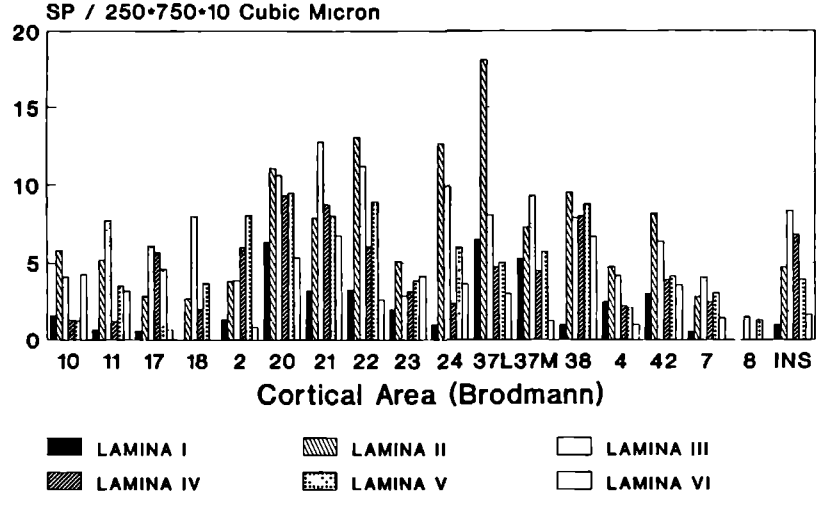

fig. III.27b

NFT DISTRIBUTION IN ALZHEIMER'S DISEASE
Right Hemisphere; Congo-Red

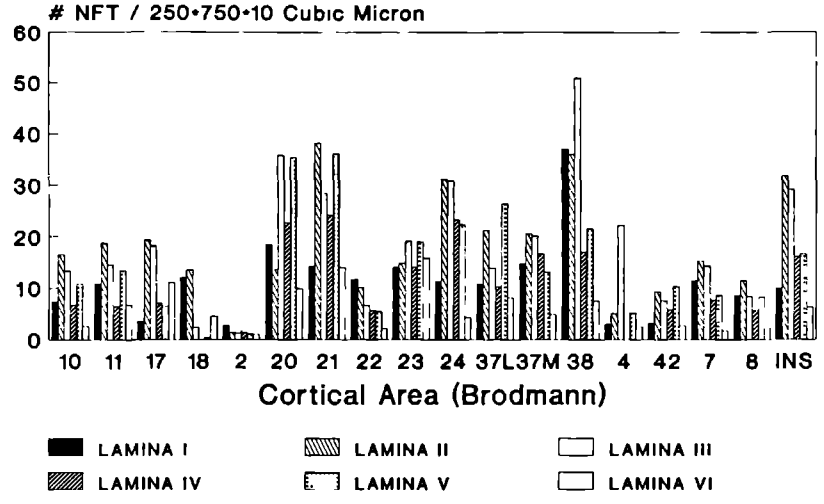

fig. III 20a

NFT DISTRIBUTION IN ALZHEIMER'S DISEASE
Left Hemisphere; Congo-Red

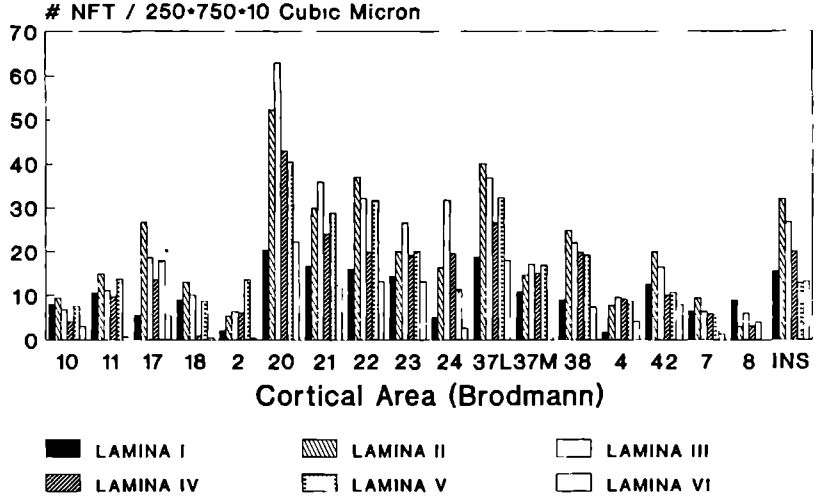

fig. III.20b

CAA DISTRIBUTION IN ALZHEIMER'S DISEASE
Right Hemisphere; Congo-Red

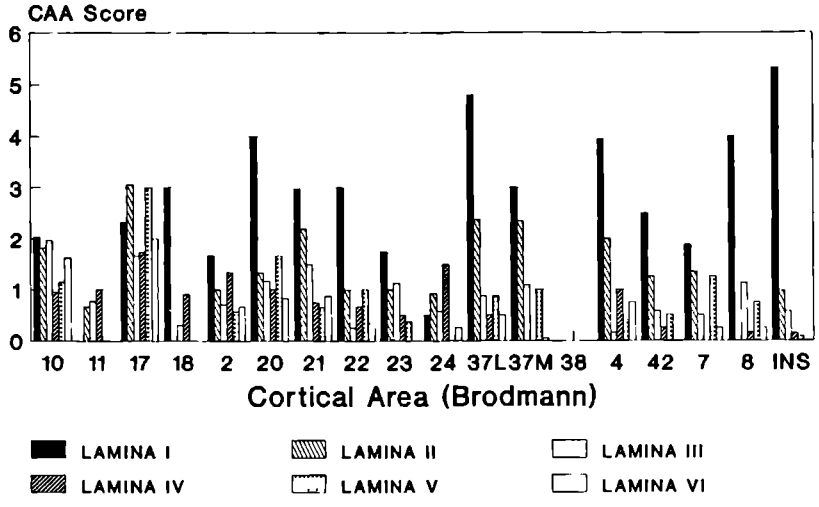

fig III 33a

CAA DISTRIBUTION IN ALZHEIMER'S DISEASE
Left Hemisphere; Congo-red

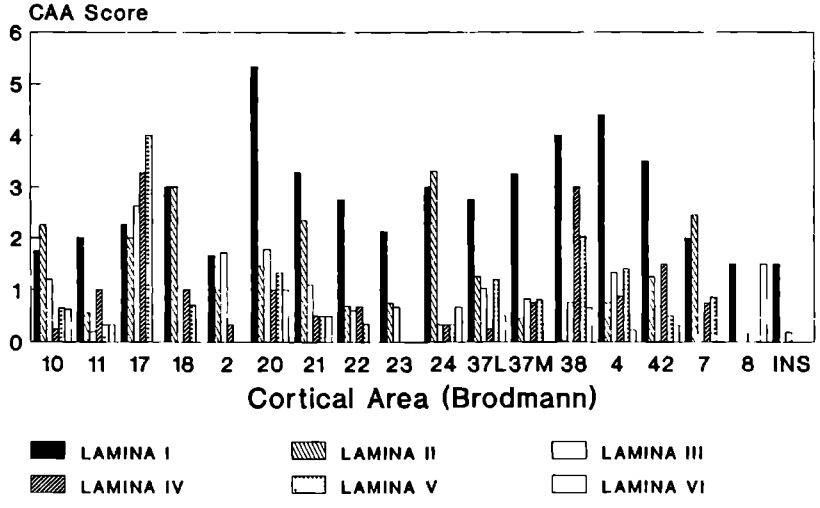

fig III 33b

III.5.1. The distribution of Neurofibrillary Tangles (NFT) using the Congo-Red fluorescence technique.

In this section, a general description is given, based on visual inspection of the distribution diagrams of neurofibrillary tangles in the individual cases.

THE ALZHEIMER CASES

III.5.1.1. Case 87395 (fig III.13a-b).
When reviewing the distribution of NFT in the two different hemispheres, a relatively large variation in the distribution is apparent. Also, an abundance of NFT in the Cingulate Gyrus and Lobus Temporalis is easily noticed. A considerable difference between the two hemispheres is observed: this is especially apparent when Area 2, Area 22, Area 42, Area 7 and Insula of the two hemispheres are compared.

III.5.1.2. Case 88177 (fig III.14a-b).
In case 88177, the presence of the NFT's is prominent in several cortical fields of the temporal lobe. The areas located in the Cingulate Gyrus, such as Areas 23 and 24 are not as heavily involved as in the former case. The presence of NFT in the Insular region is conspicuous.
In this case Area 7, a multimodal region of sensory integration, displays only few NFT's are observed, when compared to areas, located in the temporal brain regions.

III.5.1.3. Case 89033 (fig III.15a-b).
The distribution of NFT is more global: even primary sensory areas, such as Area 17 and Area 42 are more involved. Again, the temporal region remains heavily affected. Conspicuous is the abundance of NFT in the Insular regions in this brain. As a whole, the pattern is more symmetrical when compared with the previous cases.

III.5.1.4. Case 88243 (fig III.16a-b)
Comparing both hemispheres in this brain suggest an asymmetry in the affection by neurofibrillary tangles. The major concentrations of NFT are observed in the temporal lobe. The primary sensory areas are only slightly affected. The involvement of the Insular region is not as prominent as in the previous cases. In this case a relatively strong involvement of Area 7 is noticed.

CONTROL CASES
In the control cases no NFT are noticed. However, a congophilic structure was noticed in the fluorescent microscope: a thin thread-like structure, suggestive of early tangle formation. These congophilic threads (CT) are often localized within the neurons, but they also were observed without a direct relationship to a perikaryon, as seen in the same field of vision, using transmittant visual light. Whether these structures are to be interpreted as "precursors" of NFT will be discussed in the chapter concerning the general discussion.

III.5.1.5. Case 88268 (fig III.17a-b).
The overall number of Congophilic treads in this brain is low in comparison with the other three control cases. The CT are located in the cingulate and the frontal region. These CT are not observed in the primary sensory region Area 17 and in the primary motor region Area 4. Interestingly, also an involvement of the insular region is observed.

III.5.1.6. Case 88271 (fig III.18a-b).
In this case the largest number of CT is to be found. Practically every cortical area is affected. No preference for a particular cortical area could be detected.

III.5.1.7. Case 88269 (fig III.19a-b).
Case 88269 takes an intermediate position as far as the prevalence of the CT is concerned. Few CT's are observed in the primary visual Area 17 and nearly equal numbers in Area 7. The Areas 38 and 8 display the largest numbers CT in this brain.

When all the diagrams representing the NFT distribution in a hemisphere, are compared, it may be concluded, that the pattern in each brain is somewhat different. This difference can be due to a difference in the total concentration of NFT's, but also to a different distribution pattern of NFT's over the various cortical regions, although a basic pattern seems to be apparant. Congophilic threads are also observed in AD; in the present study, only the NFT are scored in these cases.

From these descriptions of the individual cases, a large interhemispheral and interindividual variation is noticed. In the individual cases, when compared, a common pattern of distribution is discernable, however individual variations are large.
Comparing the average involvement of SP and NFT formation shows all the cases of AD to be more or less involved in the formation of SP and NFT.
For example, in case 89033, Area 17 in both hemispheres is heavily affected by SP formation, in comparison to other areas of the same brain. A comparable pattern is seen in case of the NFT formation.

NEUROFIBRILLARY TANGLES IN CONGO-RED

Summary diagram

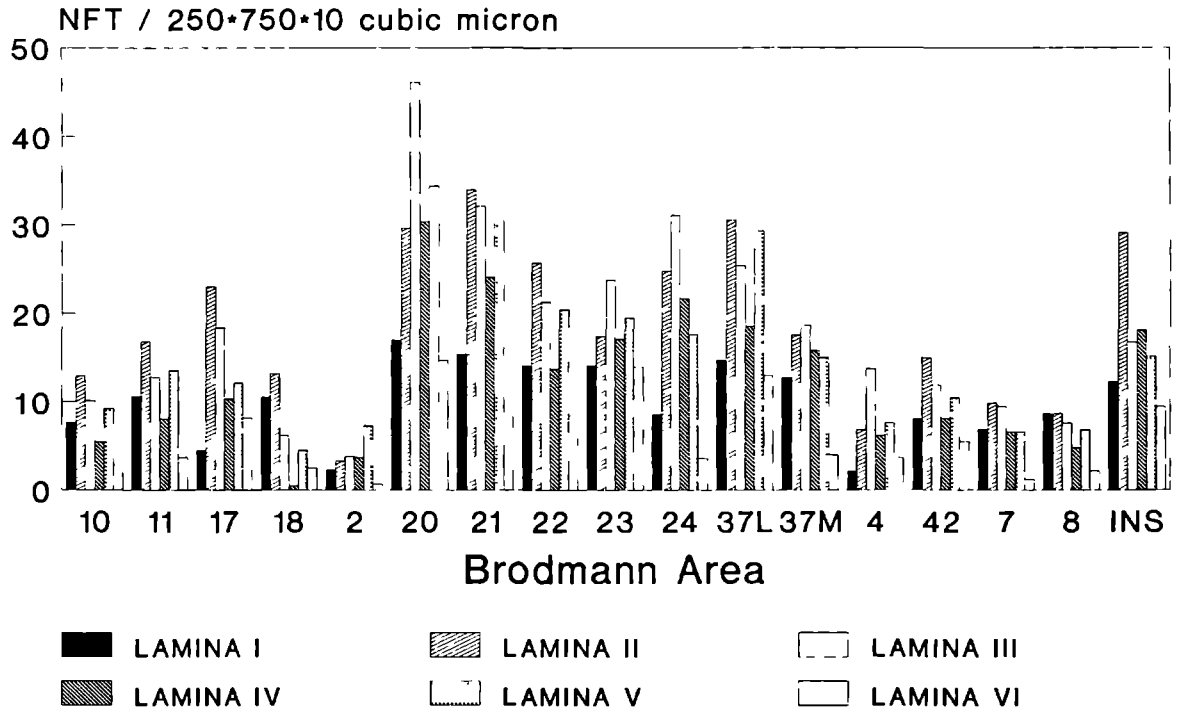

fig. III.20c

TABLE 4.
THE MEAN NEUROFIBRILLARY TANGLE CONCENTRATION PER LAMINA IN THE VARIOUS NEOCORTICAL AREAS

Brodmann Area:	Neocortical Layer					
	L I	L II	L III	L IV	L V	L VI
10	7.66	12.98	10.1	5.48	9.35	2.81
11	10.66	16.83	12.86	8.05	13.6	3.68
17	4.5	23	18.35	10.28	12.13	8.17
18	10.5	13.25	6.2	.5	4.55	2.5
2	2.3	3.33	3.825	3.67	7.33	0.67
20	16.99	29.96	46.12	30.43	34.46	14.74
21	15.43	34.01	32.16	24.08	32.5	13.16
22	14.14	25.73	21.32	13.77	20.48	8.43
23	14.18	17.38	23.84	17.14	19.5	14.43
24	8.57	24.77	31.17	21.71	17.61	3.57
37L	14.75	30.66	25.41	18.53	29.4	13.04
37M	12.75	17.58	18.62	15.81	14.99	3.98
38	16	27.5	29.15	19	19.625	7.375
4	2.13	6.83	13.75	6.16	7.56	3.63
42	8	15	11.89	8.14	10.47	5.53
7	6.86	9.83	9.48	6.61	6.60	1.19
8	8.67	8.67	7.58	4.77	6.83	2.17
INS	12.25	29.15	16.8	18.16	15.18	9.44

TABIE 5:
THE SIGNIFICANCE OF THE DIFFERENCE IN LAMINAR DISTRIBUTION OF NFT AS EXPRESSED BY THE p-VALUE OF THE STUDENT'S T-TEST

Comparision:	Brodmann Area: 10	11	17	2
I - II	0.018	0.09	0.0000	0.0041
I - III	0.44	0.29	0.0002	0.0027
I - IV	0.05	0.01	0.0069	0.0028
I - V	0.18	0.46	0.0012	0.0000
I - VI	0.0014	0.046	0.05	0.059
II - III	0.02	0.044	0.22	0.42
II - IV	0.0015	0.002	0.03	0.44
II - V	0.097	0.08	0.09	0.002
II - VI	0.0000	0.007	0.0072	0.0011
III- IV	0.04	0.027	0.089	0.48
III- V	0.22	0.33	0.25	0.0048
III- VI	0.0011	0.10	0.01	0.0009
IV - V	0.0078	0.008	0.22	0.0038
IV - VI	0.0218	0.18	0.14	0.0009
V - VI	0.0004	0.05	0.045	0.0000

Comparision:	Brodmann Area: 21	22	23	24	37L	37M
I - II	0.0074	0.0375	0.21	0.0000	0.0056	0.45
I - III	0.073	0.16	0.47	0.006	0.0089	0.44
I - IV	0.074	0.36	0.46	0.0014	0.27	0.46
I - V	0.02	0.047	0.36	0.0017	0.017	0.37
I - VI	0.33	0.06	0.42	0.033	0.36	0.001
II - III	0.12	0.18	0.22	0.021	0.41	0.49
II - IV	0.12	0.07	0.18	0.06	0.025	0.41
II - V	0.31	0.44	0.13	0.05	0.29	0.42
II - VI	0.0059	0.0036	0.26	0.0000	0.016	0.008
III- IV	0.48	0.26	0.43	0.25	0.035	0.40
III- V	0.24	0.22	0.33	0.28	0.37	0.43
III- VI	0.04	0.01	0.45	0.0006	0.023	0.008
IV - V	0.24	0.08	0.39	0.45	0.056	0.35
IV - VI	0.04	0.03	0.39	0.0002	0.39	0.011
V - VI	0.01	0.0043	0.30	0.0003	0.038	0.0006

TABLE 5(continued):
THE SIGNIFICANCE OF THE DIFFERENCE IN LAMINAR DISTRIBUTION OF NFT AS EXPRESSED BY THE p-VALUE OF THE STUDENT'S T-TEST (continued)

Comparision:	Brodmann Area: 38	4	42	7	8	INS
I - II	0.27	0.08	0.023	0.42	0.24	0.0000
I - III	0.28	0.0000	0.11	0.06	0.18	0.0001
I - IV	0.22	0.0005	0.40	0.0055	0.03	0.0053
I - V	0.33	0.0004	0.11	0.0034	0.15	0.034
I - VI	0.046	0.023	0.49	0.000	00.03	0.038
II - III	0.47	0.0013	0.18	0.043	0.37	0.22
II - IV	0.10	0.0117	0.019	0.004	0.047	0.017
II - V	0.15	0.0097	0.18	0.0025	0.31	0.0041
II - VI	0.02	0.23	0.02	0.0000	0.05	0.0038
III- IV	0.10	0.16	0.08	0.07	0.05	0.058
III- V	0.16	0.18	0.50	0.047	0.41	0.0136
III- VI	0.025	0.0134	0.11	0.0000	0.07	0.012
IV - V	0.10	0.47	0.08	0.37	0.04	0.18
IV - VI	0.33	0.0535	0.42	0.0003	0.41	0.17
V - VI	0.07	0.047	0.11	0.0005	0.079	0.469

An other primary sensory field, Area 42 is also fairly heavy affected, both by SP and NFT formation.
The formation of CAA in the four brain varies considerably:
From inspection of the figures, representing the CAA distribution in the individual cases, an order of increasing involvement in CAA formation can be given:

88268 (control with some CAA) - 87395 - 88243 - 89033 - 88177,

the last case being most heavily affected.
From the diagrams of the CAA distribution, the large differences in especially the areal distribution is apparent.

III.5.1.8. The mean distribution of NFT.
In figure III.20a-b the mean distribution of NFT is given per hemisphere. These two bar diagrams are obtained by pooling the data per hemisphere, per area and per lamina. In comparing these two bar diagrams, the cortical areas located in the cingulate and temporal gyri may be noticed as the regions most involved. Considered as a whole, both hemispheres are equally affected. Interestingly, the insular region is nearly as heavily involved in tangle formation as is the temporal region. The frontal cortical regions (e.g. the Areas 8, 10 and 11) are not affected to the same degree. The secondary visual area, Area 18, seems no more involved than the primary visual field, Area 17. The primary sensory fields, such as the somatosensory, the acoustic and the visual primary fields are affected too, be it to a lesser degree. The concentration of NFT's in the primary motor area is of the same magnitude as is the case in these primary sensory areas. Interestingly, also the tri-modal sensory field Area 7, and Area 8, another field of integration of information, are involved to the same degree as the primary sensory fields.

In order to compare between the various layers within the cerebral cortical areas, the mean NFT concentration per lamina and per cortical area is calculated. In this calculation, left and right hemispheres are taken together. These data are presented in the following bar diagram (fig III.20c) and the value of the variables are given in Table 4, 'The mean NFT concentration in the various neocortical areas'. This table is followed by another (Table 5), containing the p-values as calculated using the two-tailed Student's T-test, to identify significant differences between the number of NFT's in seperate neocortical laminae.
The differences between the individual layers are called significant when the value of p is smaller than 0.05. Using this coefficient, the Congo-Red fluorescence method demonstrated significant laminar differences in NFT distribution in some areas, (e.g. Area 10) but failed to do so in others (e.g. Area 23).

From this last figure (fig III.20c), the presence of NFT seem to be more pronounced in some areas, especially so in the gyrus cinguli (Area 23 and 24) and the temporal regions. The frontal Areas 10, 11 and 8, are less loaded with NFT. The primary sensory Areas 17, 2 and 42, are relatively spared. The insular region is heavily affected.

III.5.2. The distribution of Senile Plaques (SP) using the Congo-Red fluorescence technique.

The distribution of Senile Plaques using the Congo-Red fluorescence technique is determined for each of the brains investigated. First, a description of each case is given. This description is based on the bar diagrams, representing the SP distribution in the individual cases.

THE ALZHEIMER CASES

III.5.2.1. Case 87395 (fig. III. 21 a-b)
The distribution of SP demonstrates a slight preference of the SP for the cingular and the temporal regions. In this brain SP seem to be more or less evenly distributed among the various cortical areas.

III.5.2.2. Case 88177 (fig. III. 22 a-b)
The cortical areas investigated in this brain show a relative sparing of the primary sensory area, Area 2. The same goes for Area 7. Again, the most SP rich areas are to be found in the cingular and temporal regions.

III.5.2.3. Case 89033 (fig. III. 23 a-b)
In reviewing the bar diagrams of this case, one can notice every cortical area to be affected, with the result that in this case no preferential region for SP can be ascertained.

III.5.2.4. Case 88243 (fig. III. 24 a-b)
In case 88243, a slight preference for SP's to accumulate in the cingular and temporal regions is noticed.

THE CONTROL CASES

In case 88271 no SP were noticed in the cortical areas studied.

III.5.2.5. Case 88268 (fig. III. 25 a-b)
In this control case, only very few SP are found in some cortical areas. Their number is about 1/10th of the number often found in the various layers in Alzheimer-diseased brains. In this brain few

SP were found in Area 17 and in the temporo-occipital region (e.g.in Area 37 L). In the right hemisphere some SP were seen in Area 7.

III.5.2.6. Case 88269 (fig. III. 26 a-b)
Some SP are found in the frontal region (Areas 10 Left and 11), in the Temporal region (Area 42) and in the Cingulate region (Areas 21 and 22). Some single SP are present in Area 8.

In the control cases investigated, only very few SP were present. However, the presence of the SP in brains of persons, who functioned normally is important for the possible rol of this lesion in the disease process.

In general, when reviewing the cases one can notice a large variance in the distribution pattern over the hemispheres, of Senile Plaques, as seen in the Congo-Red staining. In order to evaluate a possible general trend, the data concerning the left and right hemispheres are averaged and presented in two separate bar diagrams (fig. III.27 a-b).
From these figures it can be deduced that the cortical laminae containing more than 15 SP's pro 250*750*10 cubic micron are to be found in the cingular (e.g. Area 21 Right) and the temporo-occipital regions (e.g. Areas 37L and 37M).
In order to evaluate laminar distribution patterns in SP distribution based on the Congo-Red Fluoescence method, all data concerning the laminae of one particular area were pooled, from all available hemispheres. In this way the number of areas investigated for the presence of NFT, SP and CAA per area and per lamina amounted to 8, making a statistical analysis of the differences observed feasable.
Mean SP concentration per cortical lamina is given in the summary diagram ' Senile Plaques in Congo-Red' (fig. III. 27c). The numbers of SP pro 250*750*10 Cubic micron are given in a table presenting the mean values of SP concentration (Table 6). Another table is added, providing the p-values of the possible comparisons between all cortical layers in one particular cortical area (Table 7). These p-values are obtained using the two-tailed Student's t-test. The p-values for the comparision of the various cortical layers between the various areas themselves show a large variation: some cortical areas (e.g. Area 20) show no clear significance in the laminar distribution pattern, while a laminar distribution pattern shows to be statistically significant in another area, e.g. Area 11.

The laminar distribution pattern of SP using the Congo-Red fluorescence method, will be discussed later.

SENILE PLAQUES IN CONGO-RED

Summary diagram

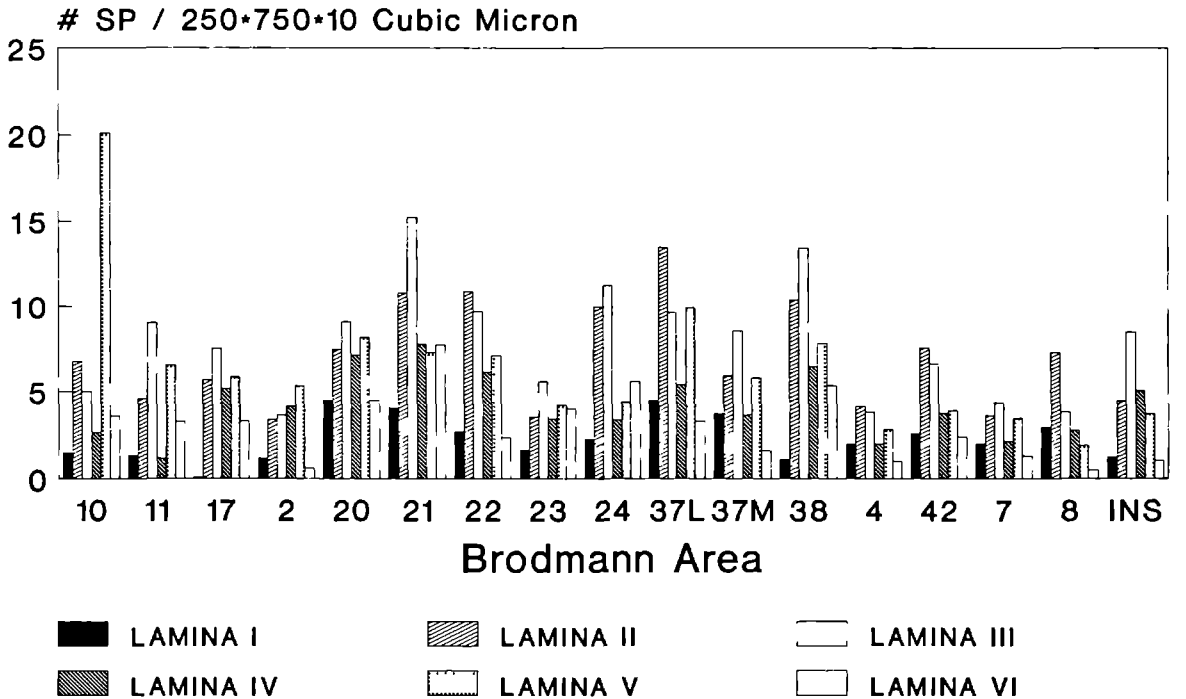

fig. III.27c

TABLE 6:
THE MEAN SENILE PLAQUE CONCENTRATION IN THE VARIOUS NEOCORTICAL AREAS, USING THE CONGO-RED FLUORESCENCE METHOD

Brodmann Area:	Neocortical layer					
	L I	L II	L III	L IV	L V	L VI
10	1.5	6.8	5.0	2.65	2.01	3.625
11	1.33	4.61	9.03	1.18	6.6	3.3
17	.08	5.68	7.55	5.15	5.86	3.33
2	1.16	3.4	3.66	4.16	5.33	0.58
20	4.5	7.5	9.1	7.18	8.18	4.48
21	4.075	10.81	15.25	7.8	7.325	7.75
22	2.71	10.91	9.71	6.14	7.14	2.35
23	1.625	3.55	5.61	3.48	4.26	4.062
24	2.28	10.01	11.24	3.39	4.41	5.61
37L	4.5	13.46	9.66	5.41	9.92	3.375
37M	3.75	5.91	8.57	3.68	5.8	1.61
38	1.125	10.4	13.425	6.5	7.85	5.375
4	2	4.16	3.86	2	2.85	1
42	2.625	7.58	6.68	3.8	3.925	2.41
7	2	3.65	4.375	2.16	3.5	1.3
8	3	7.33	3.86	2.8	1.93	0.5
INS	1.25	4.46	8.5	5.08	3.775	1.06

TABLE 7:
THE SIGNIFICANCE OF THE DIFFERENCE IN LAMINAR DISTRIBUTION OF SP AS EXPRESSED BY THE p-VALUE OF THE STUDENT'S T-TEST

Comparision:	Brodmann Area:				
	10	11	17	2	20
I - II	0.31	0.06	-	0.0099	0.17
I - III	0.46	0.23	0.003	0.017	0.50
I - IV	0.47	0.058	0.033	0.003	0.08
I - V	0.072	0.0014	0.001	0.0002	0.30
I - VI	0.17	0.08	0.0008	0.015	0.25
II - III	0.29	0.02	0.034	0.38	0.17
II - IV	0.30	0.0065	0.0094	0.27	0.32
II - V	0.14	0.042	0.019	0.06	0.32
II - VI	0.08	0.42	0.021	0.006	0.067
III - IV	0.48	0.15	0.17	0.19	0.08
III - V	0.06	0.0003	0.33	0.033	0.31
III - VI	0.19	0.024	0.36	0.0008	0.25
IV - V	0.06	-	0.03	0.16	0.18
IV - VI	0.18	0.003	0.27	0.003	0.032
V - VI	0.01	0.037	0.47	0.0001	0.13

Comparision:	Brodmann Area:				
	21	22	23	24	37L
I - II	0.02	0.029	0.0087	-	0.0005
I - III	0.0003	0.08	0.019	0.0008	0.23
I - IV	0.22	0.46	0.042	0.035	0.32
I - V	0.038	0.11	0.27	0.0009	0.0009
I - VI	0.042	0.073	0.16	0.26	0.076
II - III	0.041	0.27	0.34	0.10	0.0007
II - IV	0.08	0.04	0.21	0.0076	0.0042
II - V	0.37	0.20	0.03	0.09	0.41
II - VI	0.354	0.0036	0.0023	0.0012	0.0002
III - IV	0.0045	0.10	0.34	0.054	0.12
III - V	0.026	0.41	0.06	0.47	0.0001
III - VI	0.024	0.0083	0.0051	0.0076	0.21
IV - V	0.14	0.13	0.11	0.056	0.0028
IV - VI	0.15	0.061	0.0094	0.10	0.036
V - VI	0.47	0.011	0.06	0.0082	0.0003

TABLF 7(continued):
THE SIGNIFICANCE OF THE DIFFERENCE IN LAMINAR DISTRIBUTION OF SP AS EXPRESSED BY THE p-VALUE OF THE STUDENT'S T-TEST

Comparision:	Brodmann Area:				
	37M	38	4	42	7
I - II	0.10	0.0039	0.39	0.043	0.30
I - III	0.40	0.0001	0.07	0.40	0.41
I - IV	0.21	0.017	0.05	0.44	0.01
I - V	0.38	0.0032	0.12	0.38	0.43
I - VI	0.004	0.04	0.0078	0.21	0.006
II - III	0.07	0.042	0.11	0.0694	0.38
II - IV	0.31	0.21	0.079	0.049	0.0046
II - V	0.065	0.47	0.18	0.03	0.24
II - VI	0.029	0.10	0.01	0.012	0.0029
III - IV	0.15	0.025	0.39	0.45	0.0073
III - V	0.47	0.06	0.37	0.29	0.34
III - VI	0.0027	0.015	0.061	0.14	0.0045
IV - V	0.14	0.20	0.28	0.32	0.0033
IV - VI	0.01	0.27	0.086	0.16	0.37
V - VI	0.0024	0.097	0.037	0.29	0.0082

Comparision:	Brodmann Area:	
	8	INS
I - II	0.077	0.0006
I - III	0.49	0.0024
I - IV	0.51	0.0001
I - V	0.09	0.0018
I - VI	0.044	0.48
II - III	0.09	0.28
II - IV	0.089	0.25
II - V	0.027	0.33
II - VI	0.01	0.0022
III - IV	0.44	0.11
III - V	0.08	0.45
III - VI	0.04	0.005
IV - V	0.08	0.13
IV - VI	0.044	0.0008
V - VI	0.17	0.0042

III.5.3. The distribution of Congophilic Angiopathy (CAA) using the Congo-Red fluorescence technique.

The Congophilic Angiopathy was investigated in the AD cases and in controls.
In doing so, CAA is semi-quantitatively scored using the CAA-score defined in the previous chapter.

THE ALZHEIMER CASES

III.5.3.1. Case 87395 (fig. III. 28 a-b)
This first case shows no pronounced involvement of cortical microvessels, as seen in the Congo-Red fluorescence technique. The left hemisphere is the more affected one. Within this left hemisphere the Areas 21 and 24 are involved most. These same areas are also affected in the contralateral hemisphere. The Areas 2, 7 and the Insular region on both sides, are free from congophilic angiopathy.

III.5.3.2. Case 88177 (fig. III. 29 a-b)
This case is heavily affected by CAA. Virtually all areas are involved. The CAA is mainly found in the first cortical layer, but it is not excluded from others either. The distribution of CAA over the two hemispheres is not symmetrical. In the left Insular region, the CAA is limited to layer I.

III.5.3.3. Case 89033 (fig. III. 30 a-b)
One of the particularities here is the fact, that in brain 89033 in both hemispheres the CAA-process is limited to the first cortical layer in several areas (e.g. Area 42, Area 7 and the Insular region). Furthermore, in some areas CAA is found in all cortical layers (e.g. Areas 10 and 20). In comparison with our first two cases, this brain seems to be moderately affected.

III.5.3.4. Case 88243 (fig. III. 31 a-b)
The CAA is mainly limited to the upper cortical layer. Noteworthy is a rather heavy involvement of Area 17 and Area 4.

CONTROL CASES
Investigation of the control material did not reveal CAA except for the case number 88268.

III.5.3.5. Case 88268 (fig. III. 32 a-b)
The prevalence of CAA in this brain is limited to Area 21 and Area 38 on the left hemisphere. The right hemisphere demonstrates a considerable amount of CAA, but strictly limited to the three Areas 21, 22 and the Insular region.

III.5.3.6. The laminar distribution of CAA per area.
A separate diagram (fig. III.33 c) summarizes all data per lamina and per area of both sides. The number of observations (n=8) allows for statistical analysis of the interlaminar differences. The values of the mean congophilic angiopathy laminar distribution for the various neocortical areas is given in a table (Table 8). The p-values according to the two tailed Student's T-test of all interlaminar combinations per neocortical area are given in Table 9. According to this table the difference between L I and L II is significant in the majority of the areas. Sometimes, due to the absence of SP in a particular lamina in an area, no p-value could be calculated (e.g. in the Insular Region). In these cases the p-value should be considered zero. These instances are indicated by a hyphen.
The laminar distribution of the CAA, as seen in Congo-Red will be discussed later.

TABLE 8:
THE MEAN CONGOPHILIC ANGIOPATHY DISTRIBUTION IN THE DIFFERENT NEOCORTICAL AREAS

Brodmann Area:	Neocortical layer					
	L I	L II	L III	L IV	L V	L VI
10	1.88	2.03	1.59	0.16	0.90	0.125
11	1.0	0.616	0.48	1.0	0.16	0.16
17	2.3	2.53	2.15	2.5	2.5	1.0
2	1.66	1.0	1.2	0.83	0.28	0.33
20	4.14	1.2	0.82	0.85	1.28	0.78
21	3.125	2.275	1.3	0.625	0.575	0.687
22	2.85	0.81	0.44	0.67	0.62	0.14
23	1.93	0.875	0.9	0.25	0.1875	0.00
24	1.57	1.94	0.47	1.0	0.14	0.42
37L	3.775	1.8	0.95	0.375	1.04	0.50
37M	3.125	1.38	0.95	0.375	0.9	0.025
38	3.0	0.25	0.575	2.25	1.525	0.5
4	4.25	1.16	0.93	0.91	1.06	0.4
42	3	1.25	0.625	0.875	0.5	0.16
7	1.937	1.90	0.33	0.375	1.05	0.125
8	3.16	0.03	0.73	0.1	0.5	0.66
INS	2.75	0.362	0.3	0.05	0.025	0.000

TABLE 9:
THE SIGNIFICANCE OF THE DIFFERENCE IN LAMINAR DISTRIBUTION OF CAA AS EXPRESSED BY THE p-VALUE OF THE STUDENT'S T-TEST

Comparision:	Brodmann Area:				
	10	11	17	2	20
I - II	0.08	0.011	0.12	0.065	0.017
I - III	0.06	0.018	0.47	0.034	0.0032
I - IV	0.027	0.083	0.22	0.076	0.003
I - V	0.01	0.007	0.20	0.0012	0.002
I - VI	0.037	0.007	0.42	0.0043	0.0006
II - III	0.0065	0.35	0.14	0.31	0.12
II - IV	0.003	0.08	0.034	0.46	0.0083
II - V	0.001	0.031	0.03	0.0097	0.008
II - VI	0.003	0.03	0.16	0.036	0.018
III - IV	0.30	0.14	0.20	0.29	0.048
III - V	0.13	0.018	0.18	0.017	0.046
II - VI	0.35	0.018	0.44	0.07	0.11
IV - V	0.25	0.0026	0.47	0.0084	0.48
IV - VI	0.44	0.005	0.16	0.031	0.29
V - VI	0.23	0.49	0.15	0.17	0.28

Comparision:	Brodmann Area:				
	21	22	23	24	37L
I - II	0.097	0.039	0.017	0.27	0.01
I - III	0.0017	0.0082	0.012	0.033	0.0001
I - IV	0.0051	0.031	0.0004	0.094	-
I - V	0.0007	0.032	0.0001	0.0006	0.03
I - VI	0.0005	0.001	*	0.02	0.0007
II - III	0.015	0.15	0.41	0.012	0.0072
II - IV	0.044	0.43	0.016	0.23	0.0015
II - V	0.0053	0.44	0.0029	0.0003	0.21
II - VI	0.004	0.0018	*	0.0091	0.047
III - IV	0.26	0.19	0.022	0.0051	0.15
III - V	0.24	0.18	0.004	0.010	0.0005
III - VI	0.19	0.0076	*	0.40	0.12
IV - V	0.10	0.50	*	0.0001	-
IV - VI	0.07	0.0022	*	0.0032	0.002
V - VI	0.44	0.0021	*	0.01	0.013

TABLE 9 (continued):
THE SIGNIFICANCE OF THE DIFFERENCE IN LAMINAR DISTRIBUTION OF CAA AS EXPRESSED BY THE p-VALUE OF THE STUDENT'S T-TEST

Comparision:	Brodmann Area:				
	37M	38	4	42	7
I - II	0.16	-	0.13	0.0397	0.03
I - III	0.001	0.028	0.016	0.0018	0.012
I - IV	0.003	0.28	0.0065	0.024	0.13
I - V	0.0025	0.16	0.013	0.0007	0.19
I - VI	-	0.004	0.001	-	0.0002
II - III	0.0045	-	0.077	0.036	0.0007
II - IV	0.014	-	0.028	0.37	0.0065
II - V	0.011	-	0.064	0.013	0.15
II - VI	-	-	0.0043	0.0001	-
III - IV	0.23	0.023	0.23	0.058	0.076
III - V	0.27	0.052	0.43	0.26	0.0011
III - VI	-	0.068	0.031	0.0023	0.0116
IV - V	0.44	0.30	0.29	0.022	0.0315
IV - VI	-	0.0076	0.085	0.0002	0.0012
V - VI	-	0.018	0.038	0.0059	0.0001

Comparision:	Brodmann Area:	
	8	INS
I - II	-	0.0001
I - III	0.11	-
I - IV	0.0045	-
I - V	0.056	-
I - VI	0.049	-
II - III	-	0.089
II - IV	-	0.001
II - V	-	-
II - VI	-	-
III - IV	0.014	0.0006
III - V	0.21	-
III - VI	0.15	-
IV - V	0.0052	0.0125
IV - VI	0.0081	-
V - VI	0.37	-

CONGOPHILIC ANGIOPATHY IN CONGO-RED

Summary diagram

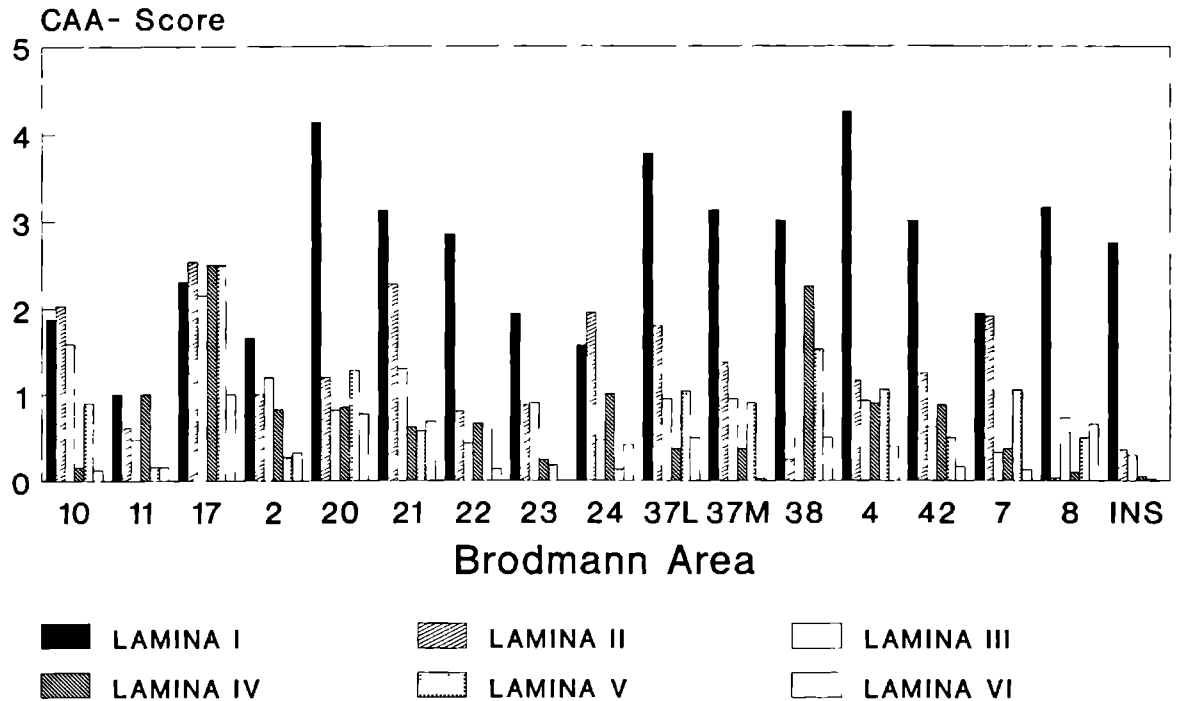

fig. III.33c

III.5.4. The correlation between the distributions of Senile Plaques (SP), Neurofibrillary Tangles (NFT) and Congophilic Angiopathy (CAA).

In the figure the 'Laminar mean distribution of NFT, SP and CAA' (fig. III.34), the results of all areas investigated of all the cases are pooled per lamina. In this way a general distribution pattern can be indicated. The results are given in Table 10. Using the results of all areas studied, the significance, expressed by the p-value in the two tailed Student's T-test is calculated for all combinations between the various cortical layers.

LAMINAR MEAN DISTRIBUTION OF NFT,SP AND CAA

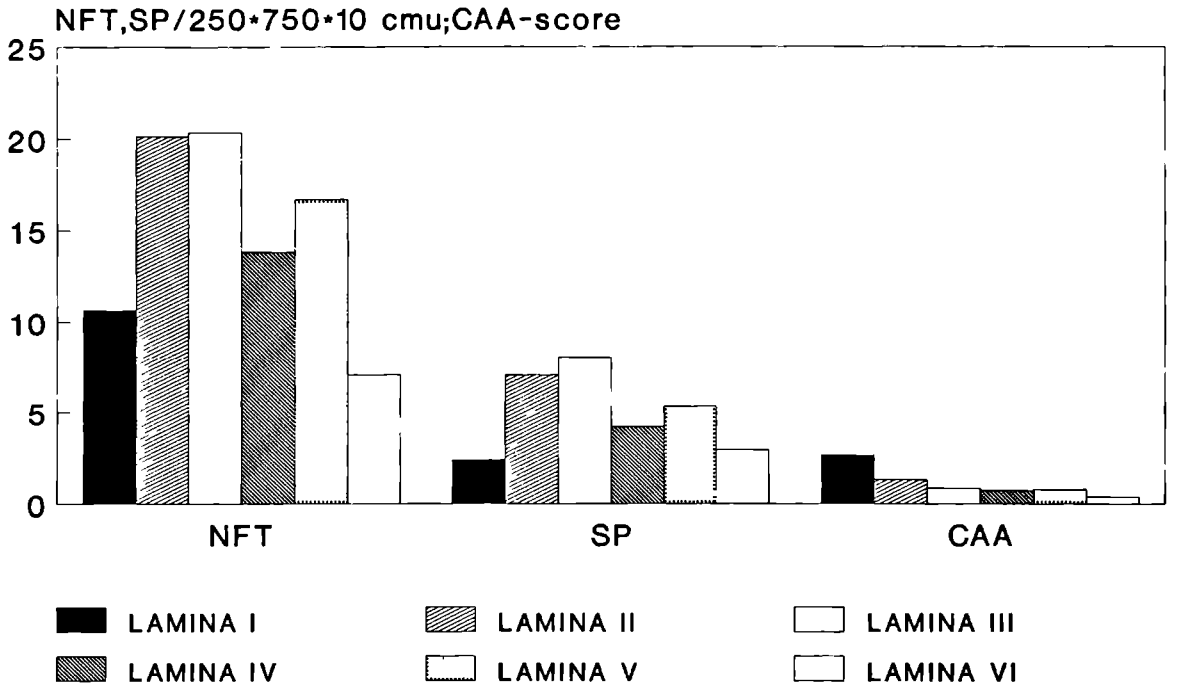

Staining: Congo-Red Fluorescence method

fig. III.34

TABLE 10:
THE MEAN CORTICAL DISTRIBUTION OF NEUROFIBRILLARY TANGLES, SENILE PLAQUES AND CONGOPHILIC ANGIOPATHY IN ALZHEIMER'S DISEASE

A. DISTRIBUTION OF NFT, SP AND CAA OVER THE VARIOUS CORTICAL LAYERS

	NFT	SP	CAA
LAMINA I	10.66	2.41	2.67
LAMINA II	20.13	7.06	1.33
LAMINA III	20.35	8.05	0.86
LAMINA IV	13.83	4.25	0.75
LAMINA V	16.68	5.35	0.79
LAMINA VI	7.07	2.96	0.39

NFT and SP are given in number per volume of 250*750*10 cubic micron.
CAA is given in the CAA-score.

B. SIGNIFICANCE ACCORDING TO THE PAIRED STUDENT'S T TEST :

LAMINAE TO COMPARE:	NFT	SP	CAA
L I - L II	0.0000	0.0000	0.0000
L I - L III	0.0000	0.0000	0.0000
L I - L IV	0.0000	0.0186	0.0000
L I - L V	0.0000	0.0000	0.0000
L I - L VI	0.1148	0.3399	0.0000
L II - L III	0.3694	0.0000	0.0000
L II - L IV	0.0000	0.0000	0.041
L II - L V	0.0248	0.0000	0.0078
L II - L VI	0.0000	0.0000	0.0000
L III- L IV	0.0000	0.0020	0.0000
L III- L V	0.0495	0.2357	0.0000
L III- L VI	0.0000	0.0000	0.0000
L IV - L V	0.0005	0.014	0.2297
L IV - L VI	0.0000	0.0067	0.0000
L V - L VI	0.0000	0.0000	0.0000

According to these data, NFT are preferentially located in Lamina II and III. No statistical difference between these two layers concerning the NFT concentration was found. Except for a non-significant difference in NFT concentration for the layers I and VI.
Summarizing: the largest numbers of NFT are found in the layers II-III and V. The layer IV, situated between these cortical layers has a significant lower number of NFT's. The lowest number of NFT is found in the layers I and VI.

Most SP are found in layer III. However, the difference between the SP number in the layers III and V does not show to be significant. The lowest number is found in the layers I and VI.

When reviewing the data representing the distribution of congophilic angiopathy, a gradient is noticed from the first cortical layer to the white matter. Except for the difference between layer IV and V, all subsequent layers, e.g. I - II, II - III etc. show a significant difference. From these data, it can be concluded, that congophilic angiopathy is a phenomenon principally related to the superficial cortical layers and becomes increasingly rare towards the white matter.
From the shape of the bar diagrams of the mean NFT, SP and CAA distributions, a correlation between NFT and SP is suggested, but not between SP and CAA.
In order to answer this question, the Pearson's corelation-coefficient is calculated [5]. These results are summarized in Table 11.

TABLE 11:
THE PEARSON'S CORRELATION COEFFICIENT AND ITS STATISTICAL SIGNIFICANCE OF THE CORRELATIONS NFT-SP AND CAA-SP.

CORTICAL LAMINA:	CORRELATION:	
	NFT - SP	CAA - SP
L I :	0.06 ns	0.342 **
L II :	0.46 **	0.13 ns
L III :	0.231 *	-0.04 ns
L IV :	0.254 **	-0.03 ns
L V :	0.246 *	0.08 ns
L VI :	0.347 **	0.24 *

Statistical Significance: * : $p < 0.05$; ** : $p < 0.01$; ns : not significant.

The results represented in this table indicate that the presence of Neurofibrillary Tangles is (statistically) related to the presence of Senile Plaques. This is true for all cortical layers, except for the first one. This correlation is the strongest in the third layer. These correlations are significant. A correlation between SP and Congophilic angiopathy proved to exist in the first cortical layer, but was practically absent from the layers with large numbers of neurons.
The possible significance of these findings will be discussed later.

III.5.5. The general areal distribution of Senile Plaques, Neurofibrillary Tangles and Congophilic Angiopathy using the Congo-Red Fluorescence method.

In the previous paragraphs, the main issue was the distribution of SP, NFT and CAA in the individual cases, per lamina and per cortical area. In this section, the data are analysed to identify the distribution pattern of SP, NFT and CAA per cortical area. To this end, the laminar distribution is disregarded and the mean concentration of SP and NFT is calculated, resulting in an average concentration throughout the whole thickness of the neocortex. The CAA-score is also averaged over the various layers, resulting in an index for areal involvement in the process of congophilic degeneration of the microvessels.
The results obtained are presented in the bar diagram 'Mean areal SP, NFT and CAA distribution' (fig. III.35). The numerical representation of these data is to be found in the matching table. In order to make comparisons between the various cortical areas, for each possible match of two areas, the p-value is given in the subsequent tables (Tables 12 - 15). These tables may be used, for instance, to find that the concentration of NFT in area A 20 amounts 24.66 per 250*750*10 cubic micron with a standard error of 10.1 and that the concentration of NFT in area A 21 amounts 21.6 with a standard error of 7.49 per 250*750*10 cubic micron. Using the table of p-values this difference shows to be not significant ($p>0.05$), i.e. $p = 0.19$. Comparing the concentration of SP in these same areas results in a significant difference in the SP concentration ($p=0.018$). However, the difference in mean CAA-score proves not to be significant ($p=0.417$). Applying these tables allows one to probe every combination of pairs of the areas under investigation for a significant difference in NFT and/or SP concentration and a different involvement of the CAA.

MEAN AREAL SP, NFT AND CAA DISTRIBUTION
CONGO-RED FLUORESCENCE METHOD

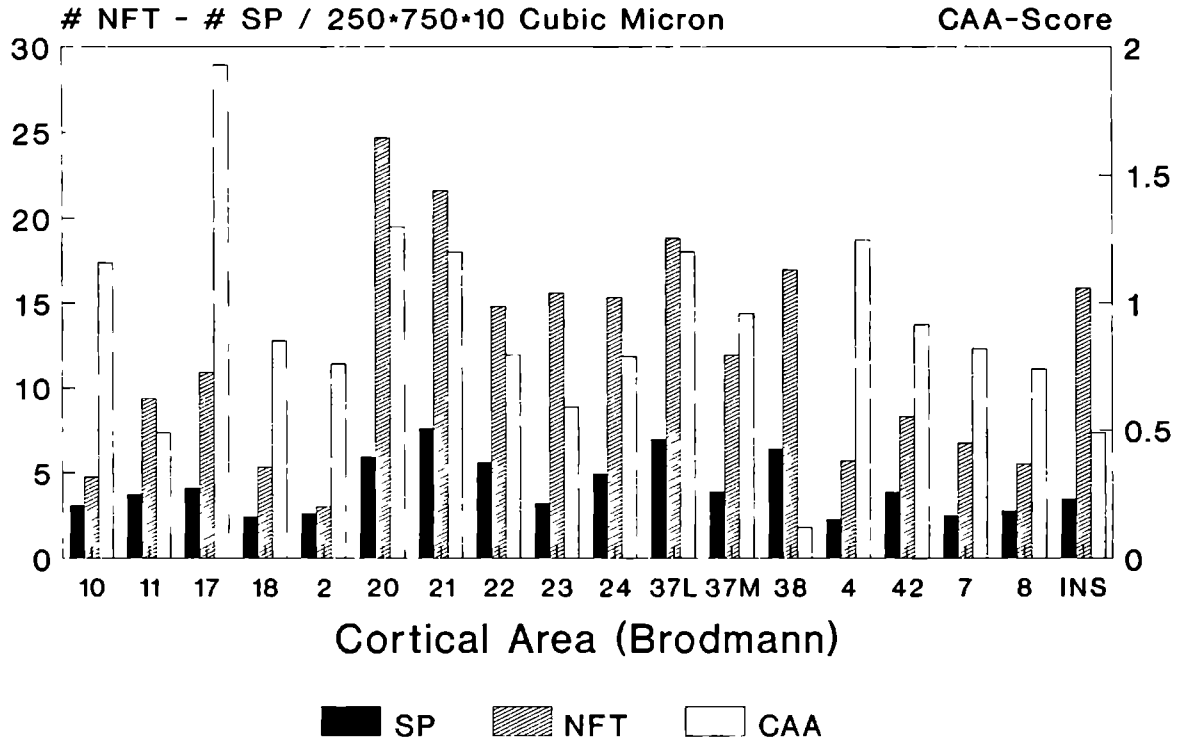

fig. III.35a

AREAL SP DISTRIBUTION (CR)

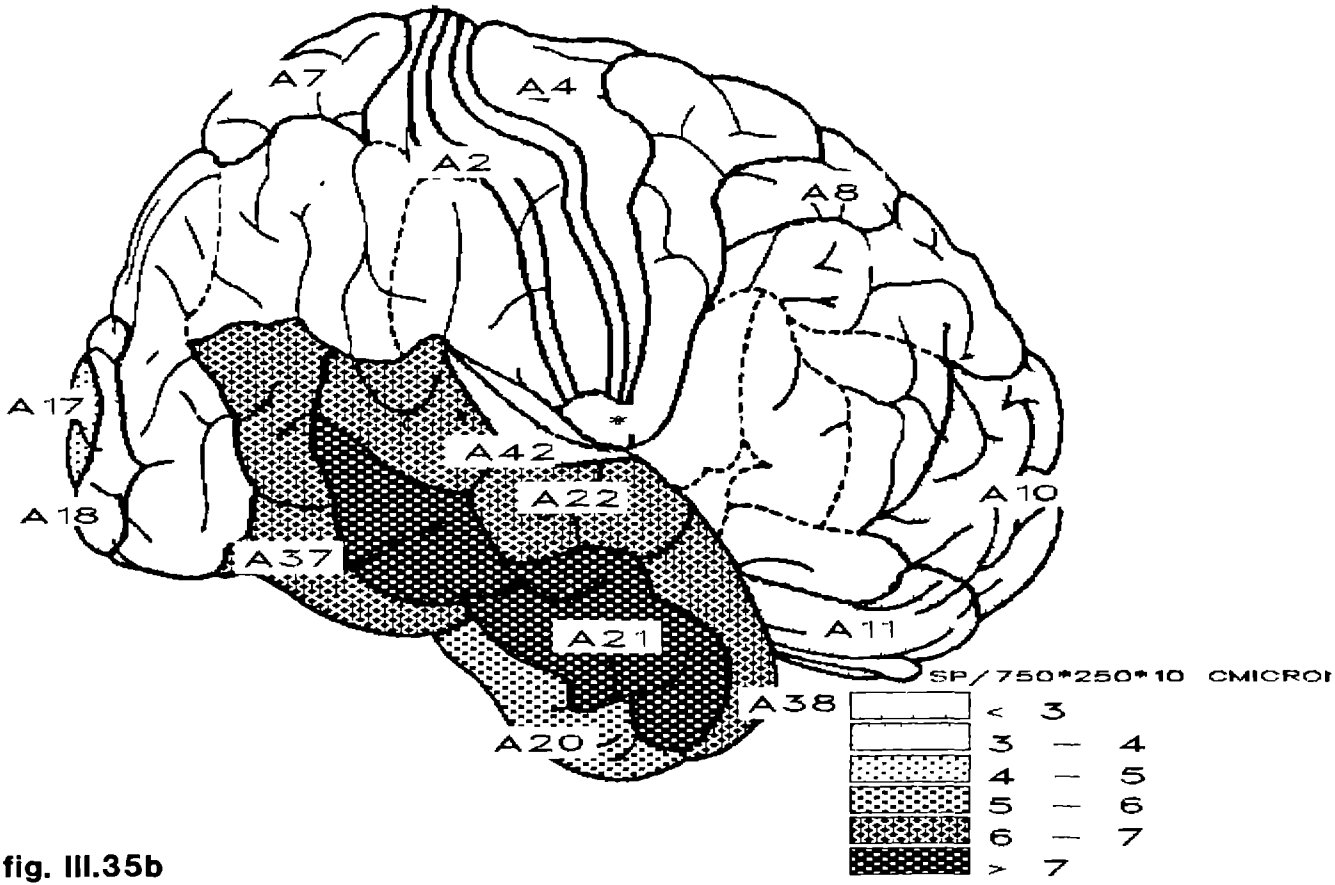

fig. III.35b

AREAL SP DISTRIBUTION (CR)

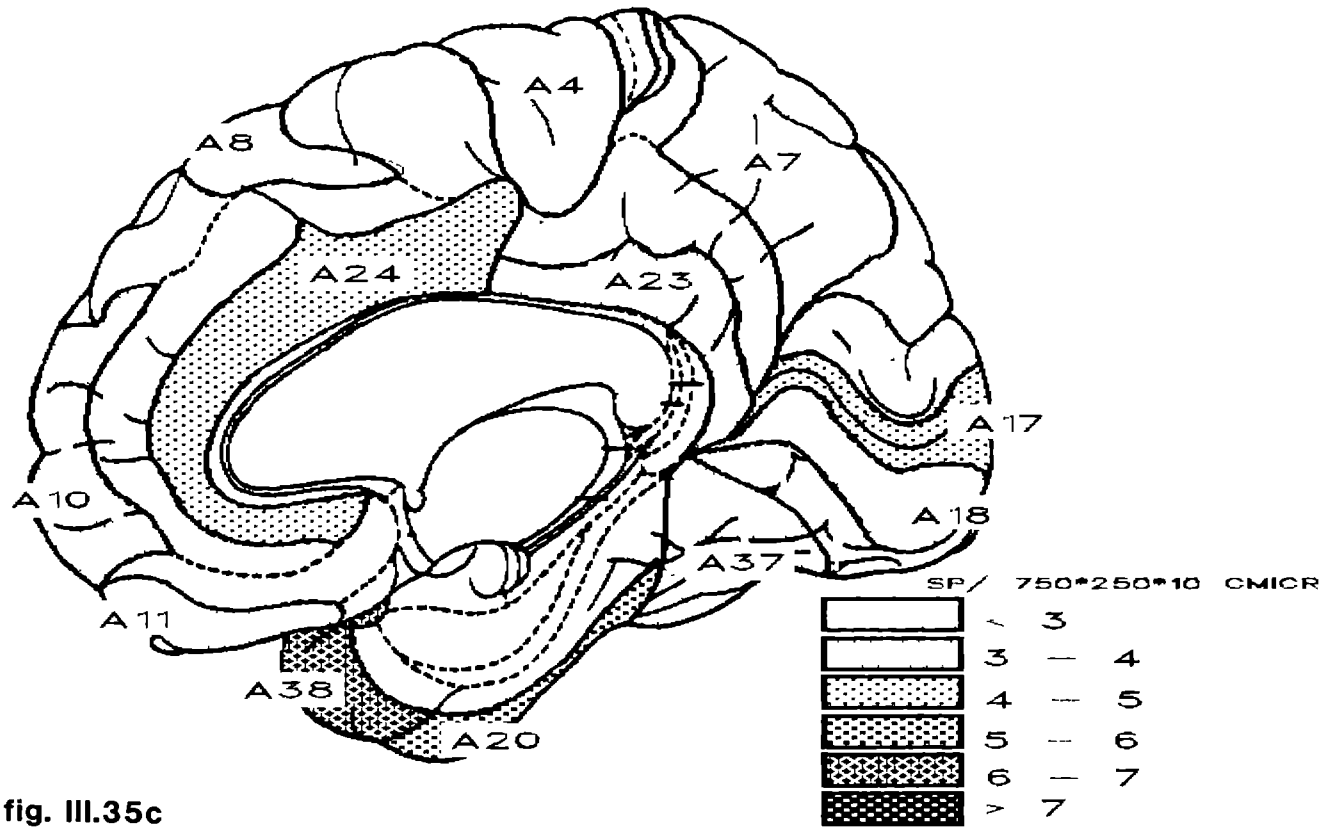

fig. III.35c

AREAL NFT DISTRIBUTION (CR)

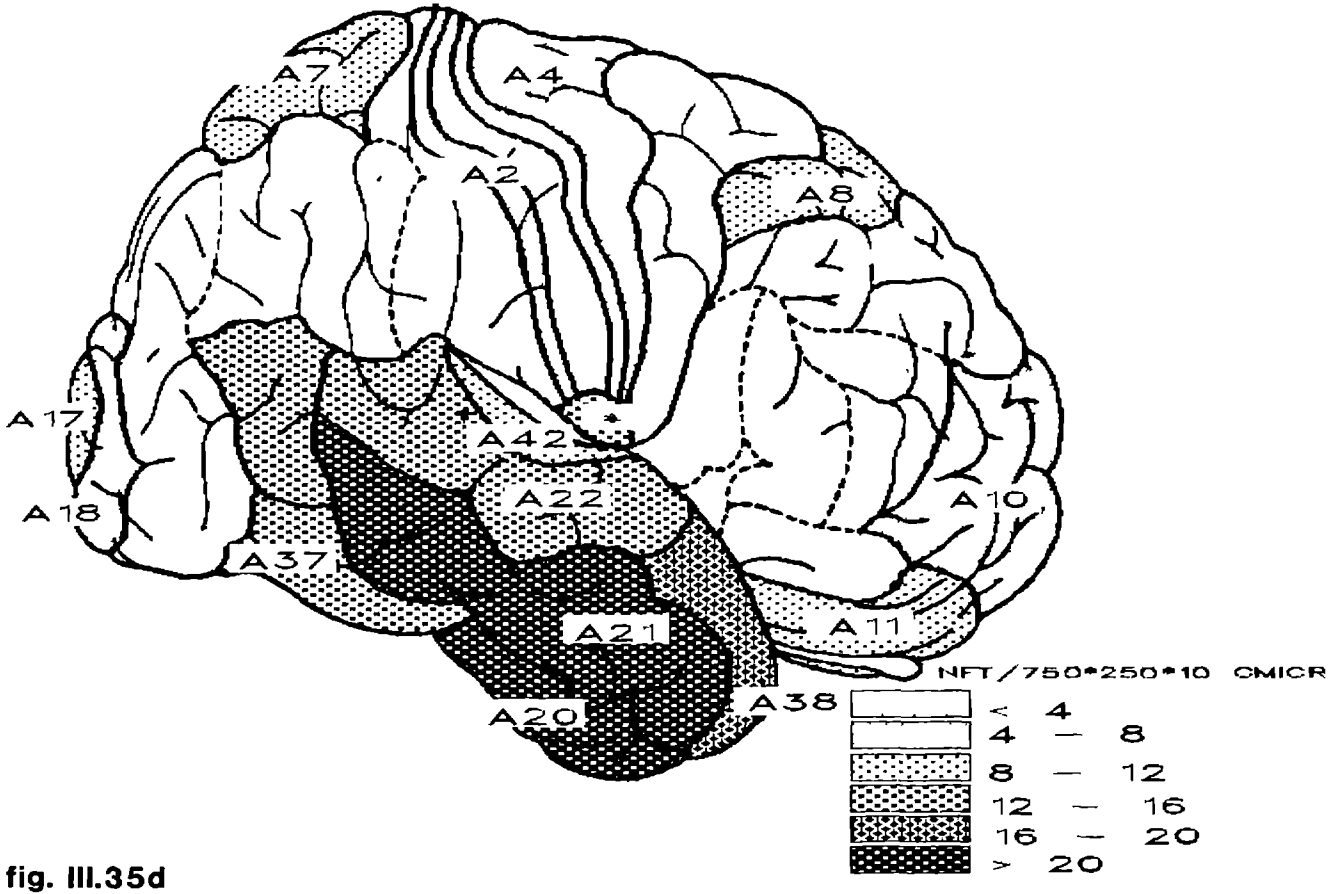

fig. III.35d

AREAL NFT DISTRIBUTION (CR)

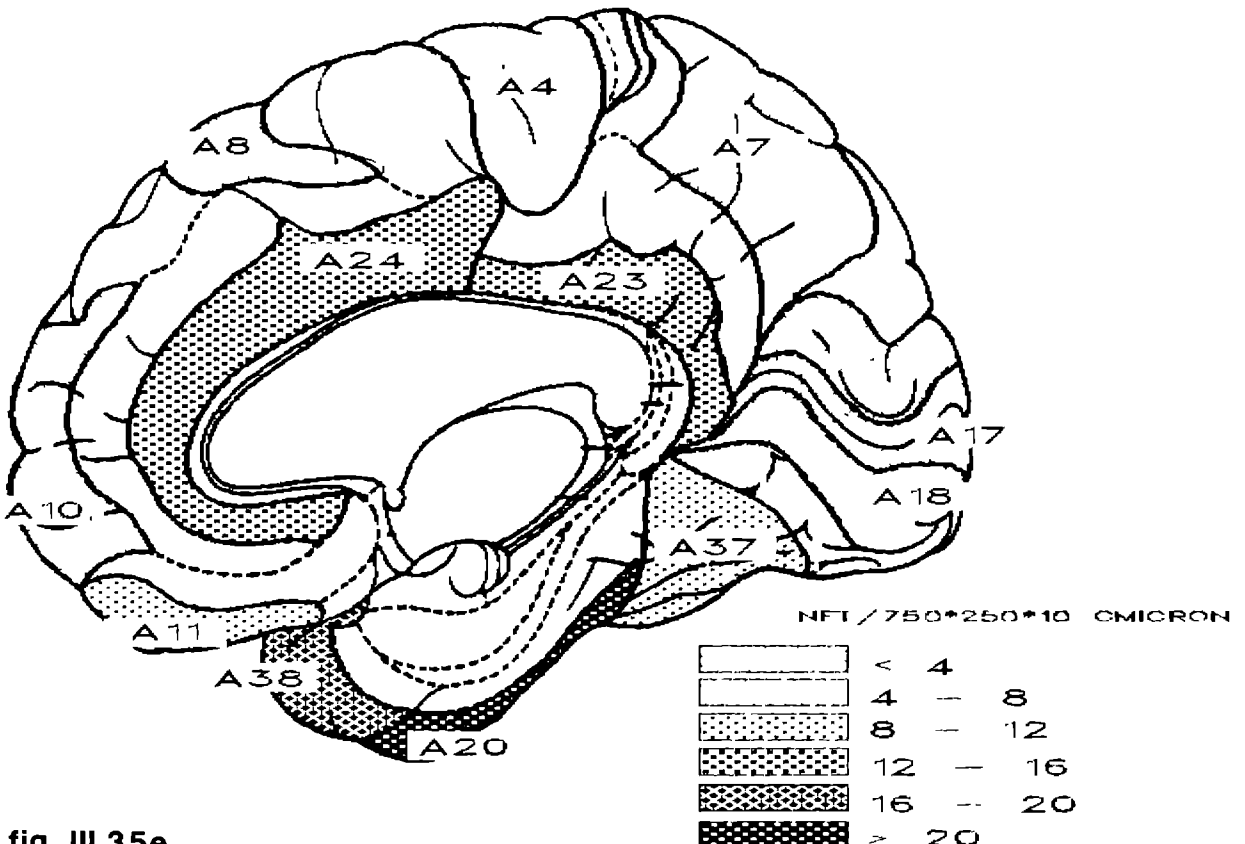

fig. III.35e

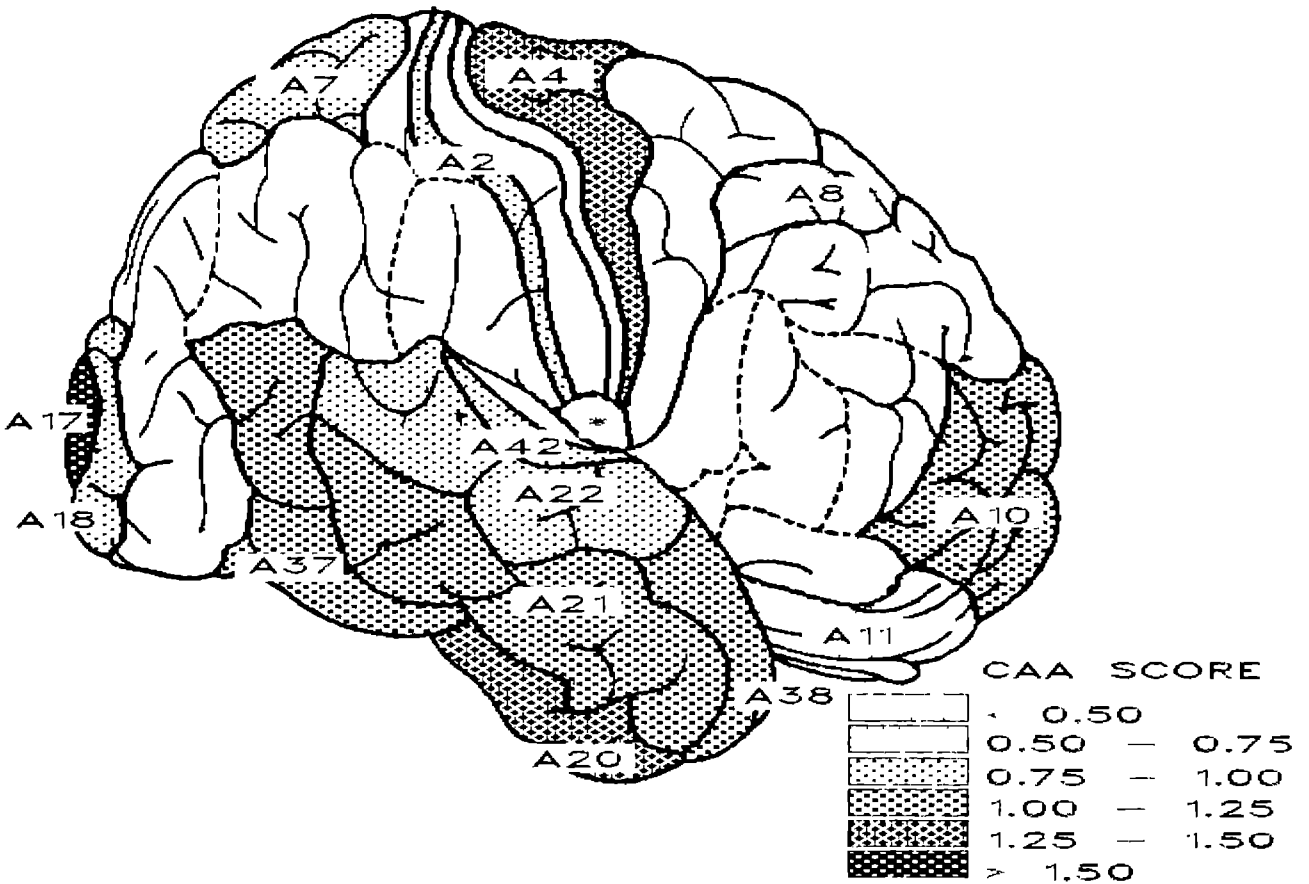
AREAL CAA SCORE DISTRIBUTION
A7
A4
A2
A8
A17
A42
A22
A10
A18
A37
A21
A11
A38
A20
CAA SCORE
< 0.50
0.50 — 0.75
0.75 — 1.00
1.00 — 1.25
1.25 — 1.50
> 1.50

fig. III.35f

CAA—SCORE DISTRIBUTION

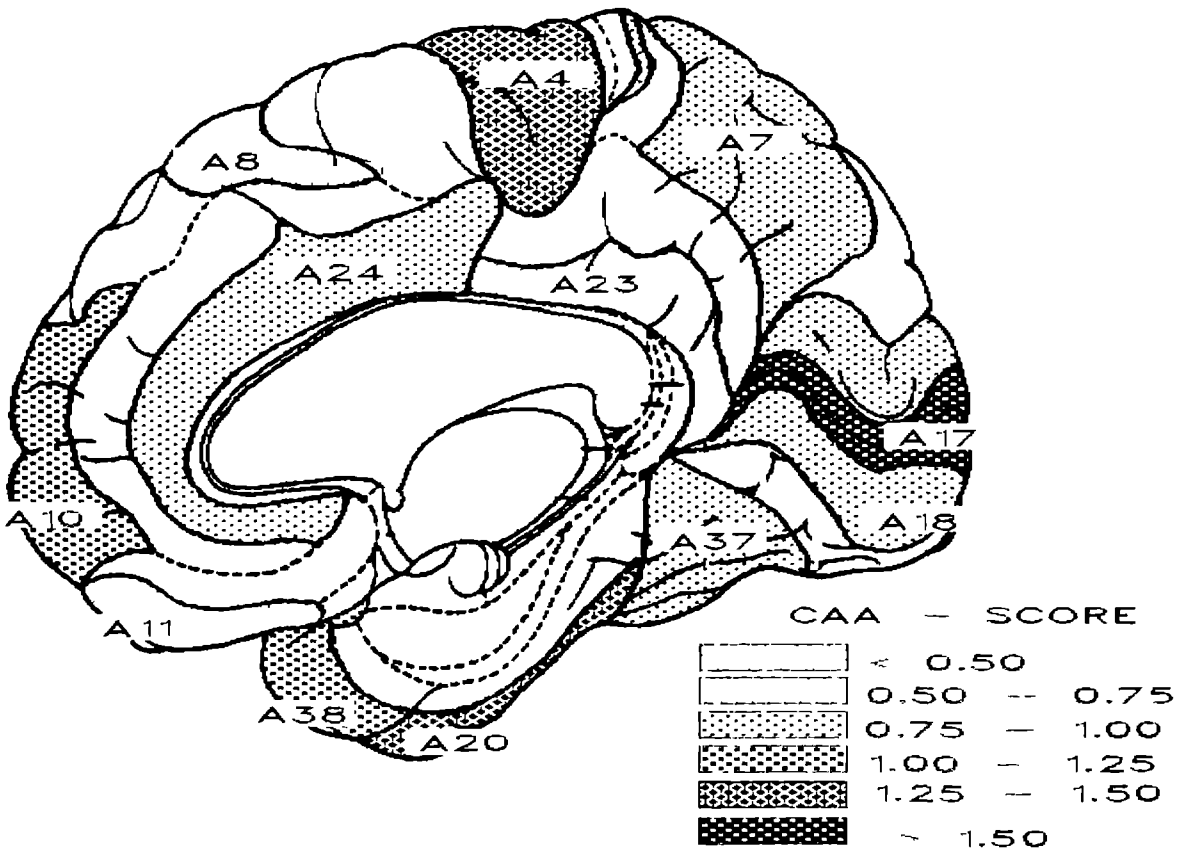

fig. III.35g

TABLE 12: MEAN AREAL SP, NFT AND CAA DISTRIBUTION USING THE CONGO-RED FLUORESCENCE METHOD

Cortical Area: (Brodmann)	SP (# / 250*750*10 Cubic Micron)	NFT	CAA (CAA-Score)
10	3.08 (0.37)	4.75 (1.18)	1.16 (0.32)
11	3.75 (0.52)	9.38 (2.55)	0.49 (0.18)
17	4.10 (1.17)	10.91 (5.55)	1.93 (0.74)
18	2.42 (0.07)	5.35 (0.67)	0.85 (0.25)
2	2.61 (1.18)	3.02 (1.78)	0.76 (0.43)
20	5.93 (0.68)	24.66 (10.1)	1.30 (0.34)
21	7.60 (0.89)	21.6 (7.49)	1.22 (0.34)
22	5.6 (0.84)	14.8 (5.88)	0.80 (0.30)
23	3.23 (0.77)	15.6 (3.33)	0.59 (0.23)
24	4.92 (1.38)	15.34 (3.15)	0.79 (0.14)
37L	6.97 (1.32)	18.82 (8.87)	1.20 (0.23)
37M	3.89 (0.66)	11.95 (3.36)	0.96 (0.22)
38	6.39 (1.16)	16.95 (5.26)	1.12 (0.71)
4	2.26 (0.50)	5.72 (1.80)	1.25 (0.38)
42	3.87 (0.74)	8.29 (3.44)	0.92 (0.32)
7	2.43 (0.43)	6.72 (1.73)	0.82 (0.28)
8	2.78 (1.20)	5.53 (1.83)	0.74 (0.36)
INS	3.45 (0.60)	15.85 (5.62)	0.49 (0.19)

TABLE 13:
SIGIFICANCE OF THE MEAN AREAL DIFFERENCES IN SENILE PLAQUE DISTRIBUTION AS OBSERVED USING THE CONGO-RED FLUORESCENCE METHOD
Significance expressed in p-value of the Student's T-test

1 - 2:0.25	2 - 3:0.011	3 - 4:0.0000
1 - 3:0.0017	2 - 4:0.0000	3 - 5:0.49
1 - 4:0.0000	2 - 5:0.01	3 - 6:0.08
1 - 5:0.0015	2 - 6:0.13	3 - 7:0.33
1 - 6:0.037	2 - 7:0.0135	3 - 8:0.21
1 - 7:0.0018	2 - 8:0.039	3 - 9:0.189
1 - 8:0.0076	2 - 9:0.039	3 - 10:0.21
1 - 9:0.0067	2 - 10:0.001	3 - 11:0.17
1 - 10:0.0001	2 - 11:0.005	3 - 12:0.18
1 - 11:0.0000	2 - 12:0.097	3 - 13:0.26
1 - 12:0.02	2 - 13:0.068	3 - 14:0.014
1 - 13:0.02	2 - 14:0.42	3 - 15:0.16
1 - 14:0.30	2 - 15:0.049	3 - 16:0.0057
1 - 15:0.009	2 - 16:0.16	3 - 17:0.19
1 - 16:0.32	2 - 17:0.13	3 - 18:0.069
1 - 17:0.052	2 - 18:0.16	
1 - 18:0.04		

4 - 5:0.00	5 - 6:0.078	6 - 7:0.11
4 - 6:0.00	5 - 7:0.32	6 - 8:0.22
4 - 7:0.00	5 - 8:0.20	6 - 9:0.24
4 - 8:0.00	5 - 9:0.18	6 - 10:0.01
4 - 9:0.00	5 - 10:0.22	6 - 11:0.007
4 - 10;0.00	5 - 11:0.18	6 - 12:0.43
4 - 11:0.00	5 - 12:0.09	6 - 13:0.23
4 - 12:0.00	5 - 13:0.25	6 - 14:0.10
4 - 13:0.00	5 - 14:0.013	6 - 15:0.29
4 - 14:0.00	5 - 15:0.15	6 - 16:0.025
4 - 15:0.00	5 - 16:0.005	6 - 17:0.034
4 - 16:0.00	5 - 17:0.18	6 - 18:0.43
4 - 17:0.03	5 - 18:0.066	
4 - 18:0.00		

TABLE 13 (continued):
SIGNIFICANCE OF THE MEAN AREAL DIFFERENCES IN SENILE PLAQUE DISTRIBUTION AS OBSERVED USING THE CONGO-RED FLUORESCENCE METHOD
Significance expressed in p-value of the Student's T-test

7 - 8:0.32	8 - 9:0.45	9 - 10:0.039
7 - 9:0.28	8 - 10:0.05	9 - 11:0.027
7 - 10:0.09	8 - 11:0.037	9 - 12:0.29
7 - 11:0.07	8 - 12:0.26	9 - 13:0.41
7 - 12:0.13	8 - 13:0.45	9 - 14:0.028
7 - 13:0.40	8 - 14:0.029	9 - 15:0.44
7 - 14:0.0096	8 - 15:0.40	9 - 16:0.005
7 - 15:0.24	8 - 16:0.008	9 - 17:0.47
7 - 16:0.002	8 - 17:0.43	9 - 18:0.18
7 - 17:0.31	8 - 18:0.17	
7 - 18:0.081		

10 - 11:0.47	11 - 12:0.013	12 - 13:0.26
10 - 12:0.023	11 - 13:0.06	12 - 14:0.065
10 - 13:0.077	11 - 14:0.0009	12 - 15:0.34
10 - 14:0.0023	11 - 15:0.025	12 - 16:0.013
10 - 15:0.04	11 - 16:0.0002	12 - 17:0.37
10 - 16:0.0008	11 - 17:0.04	12 - 18:0.35
10 - 17:0.0512	11 - 18:0.007	
10 - 18:0.014		

13 - 14:0.091	14 - 15:0.035	15 - 16:0.0065
13 - 15:0.40	14 - 16:0.19	15 - 17:0.51
13 - 16:0.05	14 - 17:0.11	15 - 18:0.22
13 - 17:0.38	14 - 18:0.12	
13 - 18:0.24		

16 - 17:0.031	17 - 18:0.37
16 - 18:0.017	

Key to the table:

1:A10	2:A11	3:A17	4:A18	5:A2	6:A20	
7:A21	8:A22	9:A23	10:A24	11:A37L	12:A37M	13:A38
14:A4	15:A42	16:A7	17:A8	18:INS		

TABLE 14: SIGNIFICANCE OF THE MEAN AREAL DIFFERENCES IN NFT DISTRIBUTION AS OBSERVED USING THE CONGO-RED FLUORESCENCE METHOD
Significance expressed in p-value of the Student's T-test

1 - 2:0.025	2 - 3:0.0129	3 - 4:0.0000
1 - 3:0.0000	2 - 4:0.0001	3 - 5:0.0045
1 - 4:0.003	2 - 5:0.13	3 - 6:0.016
1 - 5:0.186	2 - 6:0.0000	3 - 7:0.066
1 - 6:0.0000	2 - 7:0.0001	3 - 8:0.33
1 - 7:0.0000	2 - 8:0.0003	3 - 9:0.13
1 - 8:0.0000	2 - 9:0.08	3 - 10:0.07
1 - 9:0.003	2 - 10:0.17	3 - 11:0.021
1 - 10:0.0019	2 - 11:0.0000	3 - 12:0.13
1 - 11:0.0000	2 - 12:0.077	3 - 13:0.22
1 - 12:0.0003	2 - 13:0.09	3 - 14:0.0046
1 - 13:0.0019	2 - 14:0.136	3 - 15:0.14
1 - 14:0.177	2 - 15:0.067	3 - 16:0.0083
1 - 15:0.0003	2 - 16:0.21	3 - 17:0.0008
1 - 16:0.08	2 - 17:0.031	3 - 18:0.30
1 - 17:0.47	2 - 18:0.0017	
1 - 18:0.0000		

4 - 5:0.0008	5 - 6:0.0000	6 - 7:0.19
4 - 6:0.0000	5 - 7:0.0000	6 - 8:0.04
4 - 7:0.0000	5 - 8:0.0002	6 - 9:0.0034
4 - 8:0.0000	5 - 9:0.0063	6 - 10:0.0017
4 - 9:0.0000	5 - 10:0.0213	6 - 11:0.39
4 - 10:0.0000	5 - 11:0.0000	6 - 12:0.0035
4 - 11:0.0000	5 - 12:0.0059	6 - 13:0.0014
4 - 12:0.0000	5 - 13:0.065	6 - 14:0.001
4 - 13:0.0002	5 - 14:0.49	6 - 15:0.0039
4 - 14:0.0008	5 - 15:0.0049	6 - 16:0.0001
4 - 15:0.0000	5 - 16:0.34	6 - 17:0.0000
4 - 16:0.0000	5 - 17:0.19	6 - 18:0.0464
4 - 17:0.039	5 - 18:0.0001	
4 - 18:0.0000		

TABLE 14 (continued) SIGNIFIANCE OF THE MEAN AREAL DIFFERENCES IN NFT DISTRIBTION AS OBSERVED USING CONGO-RED FLUORESCENCE METHOD
Significance expressed in p-value of the Student's T-test

7 - 8:0.12	8 - 9:0.05	9 - 10:0.32
7 - 9:0.0068	8 - 10:0.027	9 - 11:0.0006
7 - 10:0.0038	8 - 11:0.047	9 - 12:0.49
7 - 11:0.26	8 - 12:0.05	9 - 13:0.36
7 - 12:0.0065	8 - 13:0.11	9 - 14:0.0075
7 - 13:0.027	8 - 14:0.001	9 - 15:0.45
7 - 14:0.001	8 - 15:0.637	9 - 16:0.0157
7 - 15:0.0075	8 - 16:0.002	9 - 17:0.0008
7 - 16:0.0001	8 - 17:0.001	9 - 18:0.032
7 - 17:0.0000	8 - 18:0.47	
7 - 18:0.14		

10 - 11:0.0003	11 - 12:0.0024	12 - 13:0.37
10 - 12:0.32	11 - 13:0.0036	12 - 14:0.007
10 - 13:0.25	11 - 14:0.0000	12 - 15:0.46
10 - 14:0.024	11 - 15:0.0028	12 - 16:0.149
10 - 15:0.29	11 - 16:0.0001	12 - 17:0.0007
10 - 16:0.045	11 - 17:0.0000	12 - 18:0.034
10 - 17:0.0035	11 - 18:0.053	
10 - 18:0.014		

13 - 14:0.05	14 - 15:0.0054	15 - 16:0.013
13 - 15:0.42	14 - 16:0.36	15 - 17:0.0006
13 - 16:0.073	14 - 17:0.18	15 - 18:0.042
13 - 17:0.016	14 - 18:0.0001	
13 - 18:0.10		

16 - 17:0.10	17 - 18:0.0000
16 - 18:0.0001	

Key to the table:

1:A10	2:A11	3:A17	4:A18	5:A2	6:A20
7:A21	8:A22	9:A23	10:A24	11:A37L	12:A37M
13:A38	14:A4	15:A42	16:A7	17:A8	18:INS

TABLE 15:
SIGNIFICANCE OF THE MEAN AREAL DIFFERENCES IN CAA
DISTRIBUTION AS OBSERVED USING THE CONGO-RED FLUORESCENCE METHOD
Significance expressed in p-value of the Student's T-test

1 - 2:0.01	2 - 3:0.001	3 - 4:0.003
1 - 3:0.018	2 - 4:0.30	3 - 5:0.05
1 - 4:0.0042	2 - 5:0.0085	3 - 6:0.03
1 - 5:0.33	2 - 6:0.0165	3 - 7:0.04
1 - 6:0.46	2 - 7:0.0077	3 - 8:0.017
1 - 7:0.44	2 - 8:0.037	3 - 9:0.0068
1 - 8:0.29	2 - 9:0.10	3 - 10:0.010
1 - 9:0.10	2 - 10:0.30	3 - 11:0.009
1 - 10:0.042	2 - 11:	3 - 12:0.0068
1 - 11:0.11	2 - 12:0.14	3 - 13:0.227
1 - 12:0.07	2 - 13:0.004	3 - 14:0.033
1 - 13:0.117	2 - 14:0.018	3 - 15:0.034
1 - 14:0.48	2 - 15:0.010	3 - 16:0.018
1 - 15:0.49	2 - 16:0.032	3 - 17:0.004
1 - 16:0.10	2 - 17:0.21	3 - 18:0.005
1 - 17:0.0003	2 - 18:0.23	
1 - 18:0.04		

4 - 5:0.0077	5 - 6:0.30	6 - 7:0.417
4 - 6:0.016	5 - 7:0.37	6 - 8:0.32
4 - 7:0.0046	5 - 8:0.18	6 - 9:0.14
4 - 8:0.021	5 - 9:0.084	6 - 10:0.008
4 - 9:0.050	5 - 10:0.009	6 - 11:0.14
4 - 10:0.37	5 - 11:0.083	6 - 12:0.10
4 - 11:0.047	5 - 12:0.064	6 - 13:0.11
4 - 12:0.07	5 - 13:0.214	6 - 14:0.45
4 - 13:0.0097	5 - 14:0.34	6 - 15:0.47
4 - 14:0.014	5 - 15:0.32	6 - 16:0.31
4 - 15:0.0061	5 - 16:0.18	6 - 17:0.15
4 - 16:0.017	5 - 17:0.07	6 - 18:0.06
4 - 17:0.18	5 - 18:0.04	
4 - 18:0.11		

TABLE 15 (continued)
SIGNIFICANCE OF THE MEAN AREAL DIFFERENCES IN CAA
DISTRIBUTION AS OBSERVED USING THE CONGO-RED FLUORESCENCE METHOD
Significance expressed in p-value of the Student's T-test
(continued)

7 - 8:0.24	8 - 9:0.24	9 - 10:0.0034
7 - 9:0.08	8 - 10:0.016	9 - 11:0.48
7 - 10:0.0034	8 - 11:0.25	9 - 12:0.40
7 - 11:0.09	8 - 12:0.186	9 - 13:0.02
7 - 12:0.06	8 - 13:0.066	9 - 14:0.12
7 - 13:0.13	8 - 14:0.30	9 - 15:0.112
7 - 14:0.46	8 - 15:0.30	9 - 16:0.25
7 - 15:0.43	8 - 16:0.47	9 - 17:0.47
7 - 16:0.22	8 - 17:0.26	9 - 18:0.26
7 - 17:0.11	8 - 18:0.11	
7 - 18:0.33		

10 - 11:0.031	11 - 12:0.38	12 - 13:0.016
10 - 12:0.05	11 - 13:0.024	12 - 14:0.091
10 - 13:0.001	11 - 14:0.13	12 - 15:0.07
10 - 14:0.005	11 - 15:0.11	12 - 16:0.18
10 - 15:0.0024	11 - 16:0.26	12 - 17:0.46
10 - 16:0.0089	11 - 17:0.45	12 - 18:0.34
10 - 17:0.12	11 - 18:0.25	
10 - 18:0.099		

13 - 14:0.16	14 - 15:0.47	15 - 16:0.277
13 - 15:0.17	14 - 16:0.28	15 - 17:0.141
13 - 16:0.11	14 - 17:0.13	15 - 18:0.041
13 - 17:0.04	14 - 18:0.069	
13 - 18:0.05		

16 - 17:0.27	17 - 18:0.43
16 - 18:0.104	

Key to the table:

1:A10	2:A11	3:A17	4:A18	5:A2	6:A20
7:A21	8:A22	9:A23	10:A24	11:A37L	12:A37M
13:A38	14:A4	15:A42	16:A7	17:A8	18:INS

III.6. THE DEMONSTRATION OF GRANULOVACUOLAR DEGENERATION IN THE NEOCORTEX.

The granulovacuolar degeneration was described in the hippocampus by Simchowicz in 1911 (see section 1.3.2.5.), but never in the neocortical areas.
During investigation of the various neocortical areas in case 88177, this fenomenon was observed in other regions than the Hippocampal formation. This pathological formation was first found in the Gyrus cinguli (photograph 2). After analysis of the various cortical areas, GVD appeared also to be present in the Insular and the fronto-orbital regions. The GVD was not found in the other areas. The prevalence of the GVD was limited to large pyramidal neurons of L III and L V. In the anterior cingulate region, GVD was also demonstrated to be present within the same neuron with a NFT (photograph 2). This GVD was seen in two of the five AD cases. No GVD was observed in the control cases. The observation was made first in NISSL stained sections and later confirmed in HE stained sections.

photograph 2.

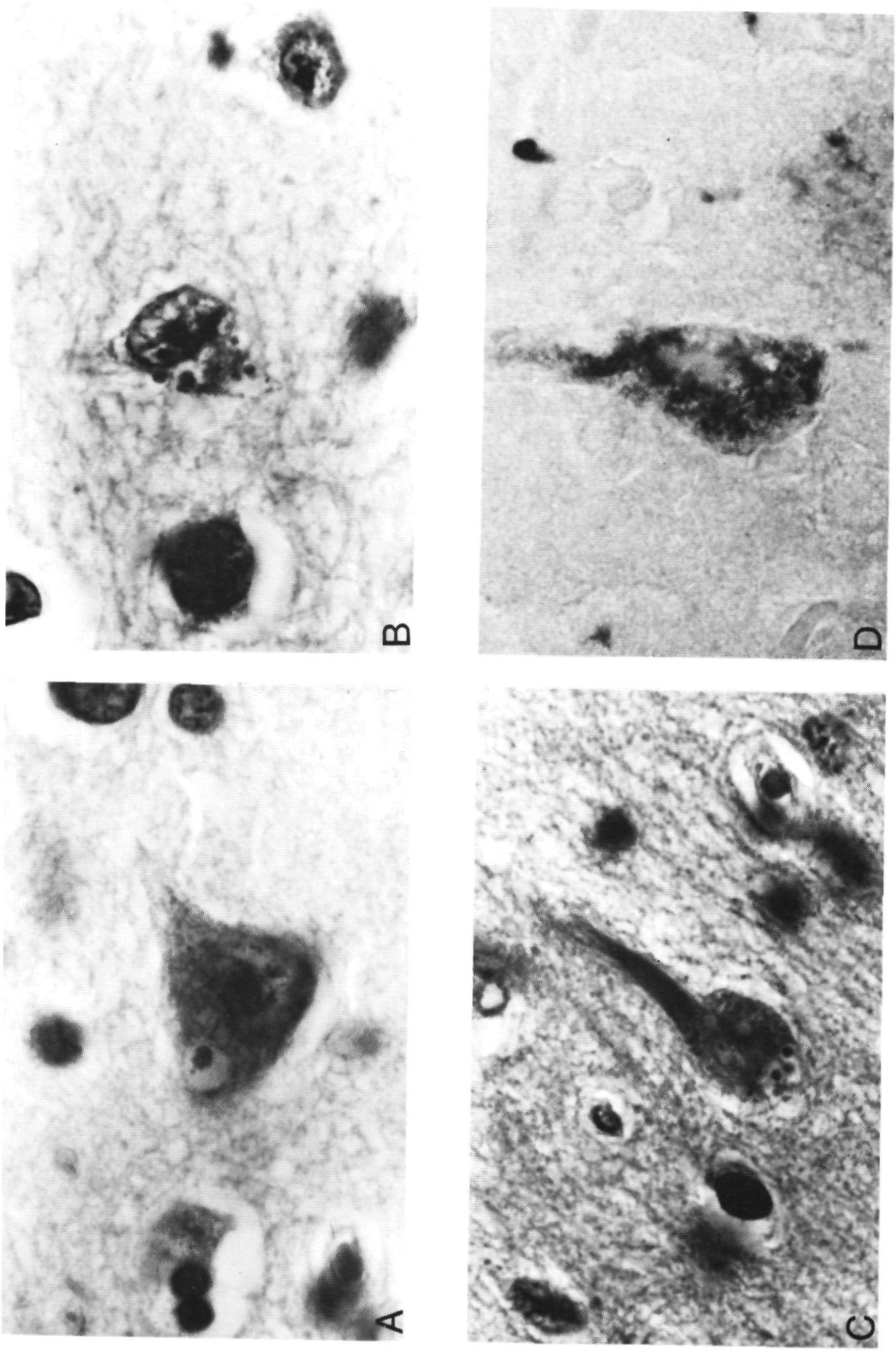

photograph 2.
Upper two photographs:
(left): Cortical pyramidal cell with granulovacuolar degeneration in the cingulate gyrus (case 88177), HE-stain magn. 400x;
(right): Neuron in insular region, (case 88177), HE-stain magn. 400x.
Lower two photographs:
(left): granulovacuolar degeneration with intracellular neurofibrillay tangle (case 89033) HE-stain magn. 400x.
(right): GVD in Acetylcholesterase stain. Case 67 year old woman suffering from AD, (fresh frozen tissue), insular cortex, magn. 400x.

III.7. CORRELATIONS OF NEOCORTICAL SENILE PLAQUE DISTRIBUTION AND NEURON COUNTS IN THE NUCLEUS BASALIS MEYNERT COMPLEX.

In a paralel study, the neuron number in the nucleus basalis of Meynert was investigated in the same cases as used in the present study. In this parallel study, the numbers of neurons larger than 37.5 micron were analyzed.
The various subdivisions as given by Mesulam [6] are known to have different projection areas. The areas reported by Mesulam having projections to the neocortex are:

- Ch 4al, projecting to Area 11,
- Ch 4am to the Areas 7 and 23,
- Ch 4i to Area 8, and
- Ch 4p to the Areas 20 and 22.

In the various cortical areas, the mean SP concentration within one cortical Area was calculated using the data presented in chapter. Correlations between these structures were only made when data both concerning the neuron number in the subdivision of the Nucleus basalis Meynert complex as well as the data concerning the SP concentration were available for the same hemisphere.
Statistical analysis was performed using Pearson's correlation test.
A significant negative correlation was invariably found between the cortical SP concentration in a cortical area and the number of neurons larger than 37.5 micron in the various subdivision of the NbM (range Pearson's r: -0.61 - -0.93). Nearly all these correlations proved to be significant (p range: 0.08-0.003).
Between the CAA-score per cortical Area and the number of neurons in the subdivisions of the NbM considerablely large correlation coefficients were found (range Pearson's r:0.06 - 0.42), however, the p-values of each of these coefficient was larger than 0.05 (p value range: 0.06 - 0.25). No correlation was found between the NFT concentration in the target area and the cell loss in the part of the NbM projection to this Area.

Table 16. CORRELATION BETWEEN SP CONCENTRATION AND CAA-SCORE IN A CORTICAL AREA AND THE NUMBER OF LARGE NEURONS IN THE SUBDIVISION OF THE NUCLEUS BASALIS (MEYNERT) PROJECTING TO THESE AREAS

		SP		NFT		CAA-score	
Area:	NbM:	r	p	r	p	r	p
11	Ch4al	-0.69	0.03	-0.34	0.33	-0.52	0.12
7	Ch4am	-0.77	0.003	-0.42	0.17	-0.51	0.09
23	Ch4am	-0.71	0.009	-0.06	0.84	-0.55	0.06
8	Ch4i	-0.61	0.08	-0.02	0.95	-0.58	0.09
20	Ch4p	-0.93	0.003	-0.29	0.53	-0.50	0.25
22	Ch4p	-0.70	0.02	-0.22	0.52	-0.41	0.21

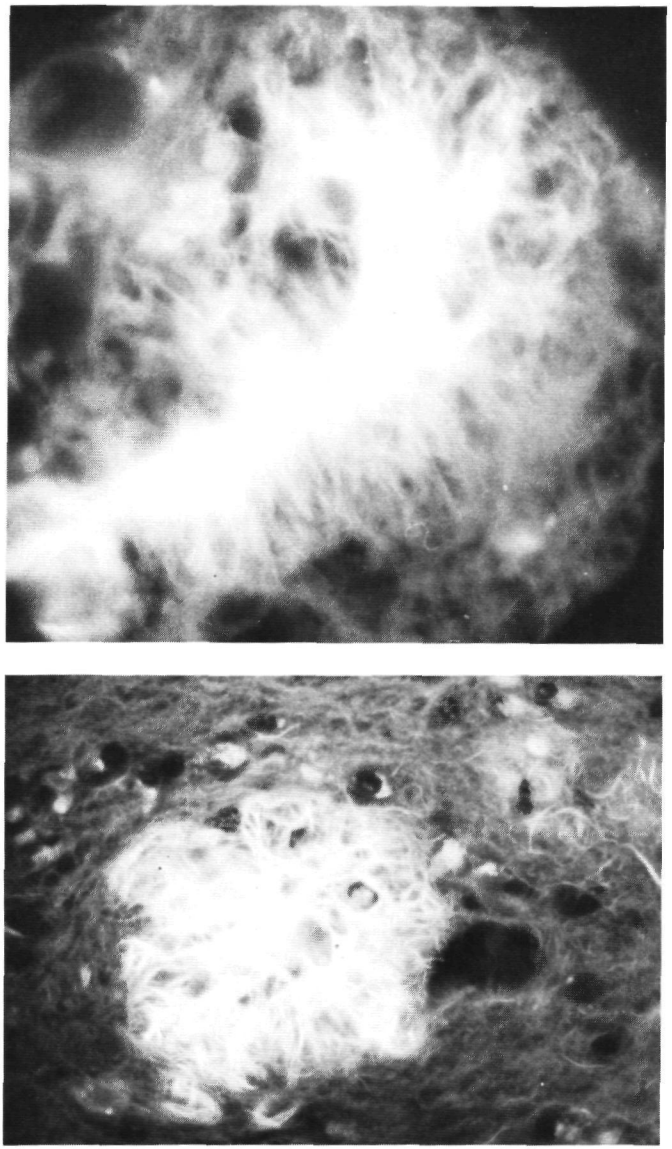

Photograph 3.

Photograph 3.
In the lower micrograph, a cortical bloodvessel is visable. From the wall of the vessel, filaments are 'invading' the neuropil.
(Congo-red fluorescence, 450x magn., Case 88177, Area 24)

In the upper micrograph, a Senile Plaque, as visable in the upper cortical layers I and II is demonstrated. In the micrograph, the lumina of cortical bloodvessels, containing erythrocytes are noticed. From the vessel wall, congophilic filaments are invading the neuropil.
(Congo-red fluorescence, 1000x magn., Case 89033, Area 24)

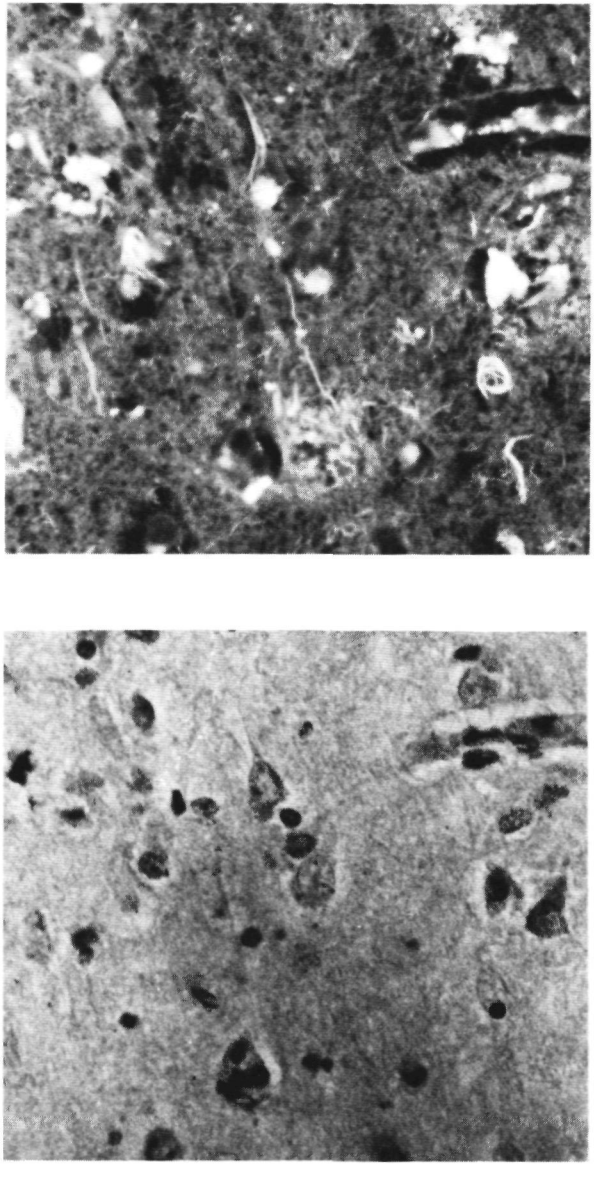

Photograph 4.

Photograph 4.
Two sister sections of a field of vision in L V, A 22, Case 89033. In the upper micrograph, the Congo-red image under fluorescence is given. Numerous changes are noticed, such as neurofibrillary tangles, and senile plaques.
Inthe lower micrograph, exactly the same field of vision is depicted. The micrograph is taken using transmitting visual light microscopy.
Notice the absence of NFT, as demonstrated in the upper micrograph from the same place in the lower micrograph.

1.Braak H, Braak E, Ohm T, Bohl J. Alzheimer's disease: mismatch between amyloid plaques and neuritic plaques, Neurosc Lett 103:24-28 (1989)

2.Brodmann K. Vergleichende Lokalisationslehre der Grosshirnrinde in ihren Prinzipien dargestellt auf Grund des Zellenbaues. Leipzig, 1909.

3.Petrides M, DN Pandya. Association fiber pathways to the frontal cortex from the superior temporal region in the rhesus monkey. J Comp Neurol (1988) 273:52-66.

4.Pandya DN, LA Vignolo. Intra- and interhemispheric projections of the precentral, premotor and arcuate areas in the rhesus monkey. Brain Res (1971) 26:217-233.

5.Bland M. An Introduction to Medical Statistics. Oxford Medical Publications. Oxford (UK), 1987.

6.Mesulam MM, EJ Mufson, AI Levey, BH Wainer. Cholinergic innnervation of cortex by the basal forebrain: cytochemistry and cortical connections of the septal area, diagonal band nuclei, nucleus basalis (substantia innominata) and hypothalamus in the rhesus monkey. J Comp Neurol (1983) 214:170-197.

IV. DISCUSSION.

IV.1. THE MACROSCOPIC ATROPHY OF THE NEOCORTEX IN ALZHEIMER'S DISEASE.

In Chapter III macroscopic neocortical changes are reported. Analysis of the neocortex in patients, using unbiased stereological methods demonstrated a volume loss of 41 % as compared to sex and age-matched controls ($p = 0.0008$, MW-test). This value suggests a preferential atrophy of the neocortex. Moreover, analysis showed a loss of 38 % in neocortical surface ($p = 0.017$ MW-test), and no significant loss of neocortical thickness. Thus, the general neocortical atrophy, defined as macroscopic loss of volume, can be explained in terms of surface loss and not as a decrease in cortical thickness.

In order to explain this finding, we must consider the anatomy of the neocortex, as discussed in Chapter I. In our description of the cytoarchitectonics, the laminar organization is described (I.2.2.2). The perikarya are arranged in a laminar fashion. Therefore, if the neocortical atrophy in AD is mainly due to loss of laminarly arranged structural elements (e.g. the perikarya of neurons) then a thinning of the cortical thickness is to be expected. However, our results do not demonstrate such a loss of cortical thickness.

In section I.2.2.2.2. a columnar arrangement, superimposed on the tangential layer pattern of the cortex, and extending from the surface of the cortex down through all layers is described. These columnar arrangements could be the principal functional and structural units of the neocortex.

The surface loss described in this study (section III.6), could be explained in two ways:

* as a loss of mean diameter of these columnar structures,

or,

* as a reduction in the total number of these columnar structures.

From our data, no distinction can be made by macroscopic analysis between these two explanations. However, together with a reported columnar distribution of SP reported in the literature [1], the surface loss esthablished in this study, stresses the importance of the columnar organisation for the neuropathologic processes in the neocortex in cases of AD.

IV.2. THE DETERMINATION OF NERVE CELL LOSS IN THE NEOCORTEX.

As stressed in the introduction, the determination of cortical volume is important: every other measurement is influenced by it. In almost every study on neuron numbers, a neuronal concentration is given. This concentration is defined as a number per unit of volume. When changes of this value are considered to be a reflection of the changes in absolute number, a severe mistake may be made because changes in concentration may be due to changes in volume or due to changes in absolute number or to a combination of the two. If accurate information about volume change of a structure is lacking, no useful interpretation of change of neuronal concentration can be made. This not only is true for the hemispheres as a whole, but especially so if their constituent parts are considered. In order to determine the volume of a structure, one should be able to identify all the borders of this structure in a confident manner.In the neocortex this cannot be done per area or per lamina, rendering the determination of neuron loss in AD, quite futile.

The importance of determination of volume in order to get reliable results concerning possible changes of neuron number in the neocortex in AD is also stressed a recent review [2]. A decrease of neuronal density in excess of the 10-60 % decline found in normal aging has been described in AD cortex. The percental decrease in neuronal density in AD compared to age-matched controls varies from 0 to 60 %. A decrease in volume suggests that findings of age-related decrease of neuronal density as found in cerebral cortex in normal aging underestimate neuronal loss.

In AD, a large loss of volume is reported in the present study. The degree of change in volume varies in different parts of the neocortex. Furthermore, as reported in this study, the distribution of SP and NFT is laminarly arranged, therefore specific laminar changes in volume might be expected. In order to get a reliable estimate of neuron number in a particular lamina, in a particular cortical Area the volume of this lamina must be estimated. No reliable method for doing this exists.

In conclusion, because volume changes of the neocortex are indispensable for the determination of absolute cell numbers, and because no method is available to estimate the volume of a cortical lamina of a particular cortical Area, no attempt was made to determine neuron loss per lamina and per Brodmann Area in the present study.

IV.3 THE DISTRIBUTION OF NFT.

IV.3.1. The mean laminar distribution of NFT

The distribution of NFT in the present study is determined in Congo-red stained sections and analyzed using fluorescence microscopy (section II.4.2.). As remarked in the introduction, only limited data concerning laminar distribution of NFT is available from the literature. In the study of Pearson et al. [7], a modification of the Palmgren method was used, a selective stain for NFT. In quantifying the NFT distribution, the cortex was not subdivided into the cortical layers according to Brodmann, but rather divided into supra- and infragranular portion. Furthermore, only data concerning the Areas 17, 18 and 21 were reported. Qualitatively however, the largest concentration of NFT was reproted in L III and L V, with L IV 'virtually clear between them'.

In a study by Lewis et al. [6], data on the laminar distribution are presented for the Areas 17, 18, 20, 22 and 42. The NFT are predominantly observed in L III and L V, "however, there were striking differences in the proportion of NFT in these 2 layers between different areas". Our data also indicate areal differences in the distribution pattern of NFT among the various cortical areas.
In the report by Lewis, no numerical data concerning laminar NFT distribution are given.
Our study confirms the data from these two reports [6,7]: the largest concentration of NFT is found in L III and L II. The concentration in L IV is significantly lower (table 10). The concentration of L V is significantly lower than in L III and L II, higher than in L IV. Inspecting the laminar distribution pattern, as represented by fig. III.34, the NFT distribution appears to be of the bimodal type.
No additional numerical data of NFT concentration per lamina and per area are available from the literature.

IV.3.2. The mean areal distribution pattern of NFT

The data available in the literature on the mean areal NFT distribution are described in the introduction (section I.4.2.1.). Only concerning a limited number of cortical areas, data on the regional distribution of NFT is available. According to this literature, the least dense NFT concentrations are found within the

primary sensory areas. Data, obtained in the present study, concerning the distribution of NFT per area are represented in section III.4.5. (Table 12 and fig. III.35a,d,e.). Table 12 shows the largest concentration of NFT to be present in the temporal lobe (Areas 20, 21 and 37L). A large concentration also exists in the gyrus cinguli (Areas 23 and 24). The lowest NFT concentration is found within the primary somatosensory Area 2 and the primary motor Area 4.

The cortical maps, representing the areal density of NFT are represented in the figs. III.35 e-d. From these figures, the involvement of the temporal lobe is apparent. Also the involvement of the cingulate gyrus is conspicious. Comparing the distribution of NFT and Senile Plaques as observed in the Congo-red fluorescence method a large degree of similarity is noticed (fig. III.35a-e).

Comparing the data available from the literature and the data presented in our study (fig. III.35a-e) a similarity is noticed. The studies available for comparison agree as to the low concentration found in the primary sensory areas resulting from the present study (cf. fig. III.35a, or table 12.). Also an increase in NFT concentration is noticed, when Area 42, the primary auditory area, is compared with Area 22, the auditory association area (Student's t-value: 0.029 (cf. table 13)). In our study, however, a higher mean areal NFT concentration was found for Area 17, the primary visual area, as compared to Area 18, the visual association area (Student's t value: <0.0009 (cf. table 13.)). This latter result is not in agreement with the study of Lewis, in which the contrary result was reported.

From comparison of the data available in the literature and those from our study, the idea, that NFT concentration increases from primary sensory areas to association areas must be taken with caution, because experimental data are conflicting on this subject. No proof was found in the present study to support this concept.

IV.4. THE DISTRIBUTION OF CONGOPHILIC AMYLOID ANGIOPATHY.

The distribution of the CAA over the cortical laminae was analyzed, using the CAA-score (section II.5), in order to get semi-quantitative results. Scoring the CAA for every microscopic field investigated in quantifying the concentration of NFT and SP resulted in an elaborate map of laminar distribution of CAA.
Averaging the CAA-score over all cortical areas investigated resulted in the mean laminar CAA-score. No comprehensive study, concerning the areal and the laminar distribution of CAA in AD is available from the literature.
Data concerning the mean laminar distribution over the six cortical layers are presented in table 10 and fig. III.34. From this figure, a distribution pattern differing considerably from that of the NFT and the SP is noticed. CAA is most frequently observed in L I, next frequently in L II, next in L III etc. (cf. table 10).
From this unique CAA distribution pattern, an obligatory involvement of cortical bloodvessels in SP formation cannot be concluded.

IV.5. THE DISTRIBUTION OF SENILE PLAQUES.

In this study, SP distribution was studied employing two different techniques, the Yamamoto-plot technique and the Congo-Red fluorescence technique. The results are given in fig. III.8 and III.27c, respectively.
When these figures are compared, important differences are noticed. For instance, Area 8 seems to present a higher SP density in fig. III.8 than in fig.III.27c. The same is true for Area 23.
This difference may be explained by a different affinity of the staining procedure for the different types of SP. In our analysis, no distinction was made between possible subtypes of SP, by subdividing the scored SP into different categories, such as discussed in section I.3.2.3..
Preparations silver-stained for neurofibrillary changes reveal the presence of 'primitive' and 'mature' forms of neuritic plaques [3,4]. Congo-red preparations exhibit especially amyloid rich SP, eg. the 'burned out' plaque. The question whether all or only a proportion of the patches recognizable in sections silver-stained for amyloid correspond to members of the SP family as seen in adjacent Congo-Red preparations and observed with polarized light, or as seen in sections silver-stained for neurofibrillary changes, was investigated by Braak et al. [5]. They demonstrated that silver-stained sections reveal cortical amyloid deposits, that are not stained by the Congo-red method. It should be realized, however, that in their study, the Congo- red sections were not investigated using fluorescent microscopy. From the same study, it may be concluded, that silver-stained sections demonstrate preferentially other SP types than do the Congo-red stained sections.
It can be speculated, that the difference found between figs. III.8 and III.27c, representing the SP distribution making use of our two different SP analyzing methods, can be partially explained by a somewhat different affinity for SP with a different amount of amyloid deposits of the two staining methods used .
Comparing however the global laminar distribution of SP in the Yamamoto-method (fig. III.9) and the Congo-Red fluorescence method (fig. III.34), some observations can be made:

* the concentrations of SP in the different layers, investigated according to the two methods, are comparable.
* the laminar distribution pattern is similar, but the concentration of SP in L I in CR-F is larger.

The difference in L I between the two methods may be due to SP-like structures, connected with CAA (cf. Photograph 3).

IV.5.1. The Yamamoto-maps of neocortical plaque distribution.

In plotting SP, no subdivision according to type has been made. A reliable subdivision of SP should have necessitated the use of higher magnification on projecting the transsections of the cortex. With the apparatus used, 80x magnification provided an optimal projection: the light intensity facilitated a distinction between neuropil and SP, also in the somewhat darker stained sections, without loosing the possibility to recognize the cellular and fiber components of the cortex. The easy recognisability of larger neurons facilitated a reliable subdivision of the various cortical areas into layers, according to cytoarchitectonic criteria described in the literature (as reviewed in the introduction (section I.2.2.2.). In subdividing the cortex into layers, no further subdivision of these layers was made. Consequently, L IV in the area striata (Area 17) was also not subdivided.
The Yamamoto-maps give a reliable picture of the actual SP distribution in the individual areas investigated. Existing studies on SP distribution never present the actual distribution of the SP in the individual case. Study of these maps is important, however, in order to assess inter-individual variations. In our material, strips of cortex of 2625 micron width are analyzed. Compared to other studies on SP distribution with a strip width of 500 micron [6] this results in a five fold increase of sampling surface of the cross section of cortex studied. The plottings of SP with the Yamamoto-projection method allow direct visual comparisons between the hemispheres analyzed here.

IV.5.2. The global laminar distribution of Senile Plaques.

The laminar distribution of SP in the different cortical areas investigated provide us also with an answer to the question, whether a generally valid pattern of SP distribution among the six different cortical layers exists. Such a general laminar distribution is important, because diffuse subcortical projection systems have generally speaking a preferential laminar pattern of distribution. A comparison of the laminar SP distribution with the laminar pattern of these systems can provide clues concerning a possible role of these systems in SP formation.
Also, a general laminar pattern of SP distribution can be based on the local columnar organization of the cerebral cortex. The columnar organization (cf. section I.2.2.2) may be considered as

a general concept of functional cortical organization. This is especially interesting in relation to the theory elaborated by Pearson [7], that SP could be formed in the regions of termination of the projecting fibers of neurons which degenerate with NFT formation [8].
The largest SP concentrations are found in L III and L II (figs. III.11 and III.34, Tables 2 and 10) according to both methods used. Our data derived from Congo-Red stained material agrees with the qualitative impression of Pearson et al. [9], that most SP are to be found in L III and L V.
The data from our study concerning the global distribution of NFT is similar in shape to that of SP, L III and L II displaying the largest concentrations, followed by L V and separated by L IV, which has significant lower values (cf. fig. III.34).

As was already noticed [10], non-pyramidal cells of layer IV have predominantly axonal ramifications ascending into layers II and III. Perhaps this may be considered as an argument in favor of the idea that in SP formation these non-pyramidal cortical neurons may be involved in SP formation, because SP seems at least to be predominantly present in their short projection trajectory.
Interruption of the projection of neurons from L IV to L III and L II may have consequences for local information processing, supposed to take place in a columnar cortical module.

IV.5.3. The areal distribution of Senile Plaques.

Data on the distribution of the SP from the literature were discussed in the introduction. Summarizing this literature [11,12,13], it may be stated that SP are demonstrated to be most numerous in the association areas of the frontal and temporal cortices. They are rather less numerous in areas of parietal and occipital cortex and are always less so in primary visual, auditory, somatosensory and motor cortices [14].
According to our results based on the Yamamoto stained material, Area 8 is most affected by SP formation (SP/250*250*10 cubic micron (SE): (2.55 (0.33)). The difference in SP concentration with Area 20, the next most seriously affected area according to this part of our study, is significant. Most areas of the temporal lobe studied (Areas 20, 21, 22, 37L and 37M) are also severely affected. The areas in the frontal lobe (Areas 8, 10 and 11) and of the gyrus cinguli (Areas 23 and 24) show a lower SP concentration. In contrast, the visual areas (Areas 17 and 18) and the auditory area (Area 42) are among the least affected. The distribution of the

SP is mapped in figure 'Mean areal SP Distribution (Ya) (fig. III.12). Comparing these data with the data based on the Congo-Red stained material (Table 12), no particularly high concentration of SP is found for Area 8 (2.78 (1.20), number of SP/250*750*10 cubic micron (Standard Error)) in the CR stained material, but high concentrations of SP are found in the areas of the temporal lobe (Areas 20, 21, 22, 38, 37L and 37M). The areas of the frontal lobe (Areas 8, 10, 11) and the cingulate gyrus (Areas 23 and 24) show a lower SP concentration. Although diffferences exist between these two methods, both methods emphazise the involvement of the temporal lobe in SP formation, especially of the middle temporal gyrus. In both methods, the primary sensory areas (Area 17 and 42) are not severely affected. Also, the concentration of SP in the somato-sensory association region (Area 7) is low in both methods. Low counts of SP are found in the motor cortex (Area 4) according to both methods.

Our results are largely consistent with the literature (cf section I.4.1.1.). The temporal and frontal areas display a high SP concentration, the primary sensory and motor cortices a far lower one. Especially interesting is the relatively low concentration in Area 7, a finding, also noticed in the study of Jamada [15].
The present study demonstrates that not every region of the cortex is affected by SP formation to the same degree. Although the data concerning the mean areal concentration conform well with the literature, considerable interindividual differences between the cases themselves are demonstrated in this study (cf. figs. III.1-32).

IV.5.4. The distribution of SP and the association areas.

In the introduction several theories concerning the non-randomness of distribution of SP are reviewed from the literature (section I.5.1). As a general idea, neural pathways -i.e. fibers connecting different parts of the nervous system- form a pattern of connections which may explain this non-randomness. The formation of SP for instance, involves neurites, as is demonstrated easily in every routine silver stained section. Axon transport is possible in different directions, from the endings of neural fibers to the perikaryon and vice versa. Factors, influencing the formation of SP and NFT may, in theory, be transported in both directions along the neural fibers. The pattern of connectivity of the various different cortical regions is reviewed briefly in the first chapter (section I.2.3). If factors inducing the formation of SP are formed

or taken up and transported initially by certain groups or types of neurons, these factors then, are thought to be transported along the patterns of connectivity of these neurons to other areas. In the latter areas, these factors may induce SP or NFT formation. The distribution of pathology of AD in the cortex according to this theory is thought to be the result of existing connections.
Several theories, reviewed earlier, such as those of Appel et al.[16], German et al. [17] and Pearson et al. [18] are based on these assumptions. In these theories, a lack of production of some growth factor resulting in retrograde degeneration of received projection fibers or a chemical damaging factor taken up from the environment or an infectious agent entering via a particular porte d'entree (e.g. the nasal mucosa) is proposed. Alternatively, a protein factor inducing SP and NFT formation may originate from the pathologically changed neurons themselves.
Because the association areas receive more projections from other cortical areas than e.g. the primary sensory areas, the larger density of SP and NFT in association areas according to the data from the literature (cf. section I.4.1.1.) is explained by the latter theory.
The idea, that the concentration of SP in a particular area depends from the place of the area in the hierarchy of integration of information, which would result in a higher concentration of SP in the higher order- and multi-modal association areas is only partly confirmed by our results.
In conclusion, the distribution of areal SP density, as presented in this study, confirms a strong involvement of areas located in the temporal lobe. Also, the involvement of the frontal lobe appears from the present data.
The concept, however, that the density of SP is directly related to the connectivity of the area in question is not valid for all association areas. The relatively low concentration of SP in Area 7, a higher order somatosensory association area, contradicts this theoretical principle. The eventual role of cortico-cortical connections in the distribution of SP and NFT will be discussed in the next section, in connection with the laminar organization of the cortico-cortical projections.

IV.6. A CORRELATION BETWEEN LAMINAR SP AND LAMINAR NFT DISTRIBUTION.

Because the mean distribution of NFT and SP in the neocortex are both bimodal and looking quite similar in shape in the bar diagrams, the correlation coefficient of Pearson and its statistical significance was determined for a laminar correlation between SP and NFT.
In this study, the laminar distribution of SP, the laminar distribution of NFT and the laminar distribution of CAA was studied. The question addressed in this section of the discussion concerns the possible relationship between SP, NFT and CAA. These structures were scored using Congo-Red stained sections. The data were obtained from all cortical fields analyzed of all AD cases investigated. The concentrations of SP and NFT and the CAA-score were determined in the same fields of vision under fluorescence microscopy. The data were converted to concentration per lamina. From all the areas used, the mean concentration was obtained. These data represent the global distribution as seen in the average AD brain.

In case of the NFT - SP comparison, Pearson's correlation coefficients for the various cortical layers were obtained, ranging from 0.46 ($p<0.01$) to 0.24 ($p<0.05$) (Table 11).
These results can be interpreted as a spatial i.e., laminar relationship between NFT and SP. This relationship is a statistical one, a causal relation between SP formation and local neuron degeneration being a possible explanation. Because congophilic amyloid degeneration of the cerebral vessels is often thought to be related to SP formation, the correlation between CAA and SP formation was investigated in the same material: only in L I and L VI a statistical correlation was found. In L I no correlation between NFT and SP was demonstrated.
In Congo-Red sections, often SP were found, but relatively seldom NFT, although, occasionally, small NFT were found in the sparsely distributed neurons of L I.
From our investigation concerning the laminar distribution of SP the conclusion is prompted, that in AD two different types of senile plaque formation may occur (1) SP formation connected or caused by Congophilic Amyloid Angiopathy, and (2) SP formation in close relation with degenerating local cortical (inter-)neurons.
In L I, congophilically degenerated vessels may be involved in SP formation. These SP may be formed by congophilic filaments

'invading' the neuropil as demonstrated in photograph 3. In other cortical laminae, neurofibrillary degenerating neurons may be involved. The different origing of the senile plaques of L I and of L II through L VI may explain the different values of the correlation coefficents between NFT - SP and CAA - SP for L I on the one hand and the layers L II through L VI on the other hand. Based on these observations, two main types of SP could be postulated:
type I: many occuring in L I and generally rich in amyloid,
type II:occuring in all cortical layers, and comparatively rich in (fibrillary) degenerated neurites.

IV.7. SP LAMINAR DISTRIBUTION IN RELATION TO CORTICO-CORTICAL CONNECTIONS.

The intrinsic connections between two adjacent areas in the occipital and temporal lobe are arranged according to a fixed scheme; for instance, from the primary visual area, Area 17, to the temporal cortex a stepwise connection of forward connections exists. These forward projections usually have their origin primary in L III, with terminations in and around L IV. Reciprocal connections originate from neurons in L V and L VI and terminate in L I of the caudally adjacent regions [19].

If the SP, made visible using the Yamamoto-method, were related to the terminal fields of these forward corticocortical projecting fibers, as suggested by Pearson (section I.5.1), the major SP concentration is to be expected in L IV. If the reciprocal fibers were of main interest for the SP distribution, the major SP concentration should be expected in L I.
If corticocortical projections were the far most important way of spreading the disease by inducing pathological changes at the endings of their fibers, the laminar distribution of SP is expected to be the result of the forward and backward cortico-cortical projection. The SP should be localized primarily in L I and L IV. The distribution of SP as demonstrated in this study, with its prominent presence of SP in L II, L III and L V (cf. figs III.9 and III.34) seem to contradict an important role for the cortico-cortical connectivity in the process of distributing the neuropathological determinants of AD over the neocortex.

In conclusion, the results concerning the global laminar SP distribution do not favor a cortico-cortical spread of the SP from primary sensory via unimodal towards multi-modal association areas. Alternatively, the supposition that SP are formed at the endings of degenerating projecting neurons made by Pearson et al. [7] may be erroneous. On the basis of our result, no definite choice can be made between these two suggestions.

IV.8. SP LAMINAR DISTRIBUTION IN RELATION TO D I F F U S E CORTICOPETAL PROJECTING SYSTEMS.

Because the diffuse projecting systems send the (collateral) corticopetal fibers to a large number of different cortical regions, the mean global laminar SP distribution is compared with the information on laminar ending patterns of these systems.

The cholinergic projection systems

According to the cholinergic hypothesis [20, 21] the neurons of the cholinergic basal forebrain nuclei, such as the nucleus basalis magnocellularis (Meynert) and the diagonal band of Broca are degenerated in AD. These cholinergic neurons are supposed to perform important functions in cognitive functions [22].
As noted in the introductory chapter, laminar variations of cortical cholinergic innervation exists among different regions within and across species, but no conclusive remarks can yet be made on this issue [23]. For instance, in the rat cerebral cortex 13 different laminar patterns of ChAT staining can be found [Lysakowski et al, 1989].
However, some information about the distribution of ChAT, a marker of cholinergic fibers is available for human controls. As stated in the introduction, the ChAT-activity in human controls,is highest at the level of layers II and IV of the temporal and frontal cortex, whereas in Alzheimer's disease the topographical laminar distribution of ChAT-activity seems lost completely [24, 25].
The laminar distribution of SP with its accent on the third and fifth cortical layer, seems not in agreement with this laminar distribution of the cholinergic fibers: This observation seems to rule out a primary function in cortical SP formation for the corticopetal projecting fibers, originating from the basal forebrain nuclei. However, no conclusive judgement can be passed, because more information about the cholinergic fiber distribution is needed in the non-diseased human brain.

The monoaminergic systems.

Comparing the fiber distribution of dopamine-beta-hydroxylase immuno-reactivity (DBH-IR) positive fibers as described in the two studies available and our general SP distribution map, no definite match in laminar patterns could be decided. In their study of the DBH immunoreactivity in normal human brain, Gaspar et al. [26]

noticed that DBH-IR vertical fibers were more frequent in L II and L III.
Also, the TH-IR positive fiber distributions did not match our SP distribution. However, the observation of occasionally occuring small, local accumulations of TH-IR in L II - III is interesting: could these accumulations be connected with early SP formation?
Unfortunately, no more data from the literature concerning the laminar distribution in the human brain concerning the distribution of DBH-IR and TH-IR positive fibers are available. As demonstrated by Gaspar et al. [26] the distribution in the human cerebral cortex of DA innervation as possibly indicated by the TH-IR, exhibits distinct differences when compared with monkey brain. This makes comparison of human data with studies on DBH-IR and TH-IR performed on animal brain not apropriate.

IV.9. CORRELATIONS OF NEOCORTICAL SENILE PLAQUE DISTRIBUTION AS SEEN IN CONGO-RED STAINED SECTIONS AND NEURON COUNT IN THE NUCLEUS BASALIS (MEYNERT).

If the cortical SP concentration per area on one hand and the loss of neurons larger than 37.5 micron in the nucleus basalis (Meynert) on the other hand are correlated, a significant negative relationship is found between SP formation in a certain cortical area and neuronal cell loss in that part of the basal nucleus, projecting to that area. This relationship was suggested earlier in the studies by Arendt et al. [27] and Mann et al. [28]. However, it is important to realize, that these correlations are statistical in nature and may not represent causal relationships. From our data, it is not possible to derive a sequence of events: SP formation in the cortex can precede nuclear cell loss in the cholinergic projection system, or vice versa.
A theory concerning the causal relationship between cholinergic cell loss and the mean areal SP distribution can be constructed as follows. Central cholinergic neurons are known to need nerve growth factor (NGF) for growth and maintenance. Apparently, when no NGF is available in the targets of cholinergic innervation for the cholinergic fibers, degeneration (such as shrinkage or even cell death) may occur [29]. SP formation in the cortex may impair NGF formation. Thus degeneration of the basal cholinergic neurons may be secondary to lack of growth factor. This lack of growth factor may be either caused by a diminished number of NGF producing cortical structures or by a diminished efficiency of NGF production by these structures or a combination of both.
According to this theory, degeneration of the cholinergic neurons is secondary to pathological changes in the neocortex.

IV.10. GRANULOVACUOLAR DEGENERATION.

Granulovacuolar degeneration (GVD) is an interesting feature. Immunohistochemistry showed the granules to possess a tubulin-like immunoreactivity suggesting that GVD, like the Senile Plaque (SP) and the NFT, may involve an abnormality of the cytoskeletal structure of the neurons [30]. A monoclonal antibody, raised against extracts from Alzheimer brain, that recognizes a phosphorylated epitope in high molecular weight neurofilament proteins and tau proteins, also immunostains GVD. This finding suggests that GVD contains phosphorylated proteins, possibly due to autophagy of phosphorylated perikaryal proteins that are increased in Alzheimer's disease [31]. In the present study, GVD is reported to occur in pyramidal neurons of the cingular and insular region, demonstrating that GVD is not limited to the hippocampal formation, as far as cortical structures as concerned. The importance of this finding depends on a theory of GVD formation and the role of the processes leading to GVD formation in the pathogenesis of AD. No such theory is available yet.

IV.11. CONGOPHILIC THREADS IN BRAINS OF CONTROL CASES.

Senile Plaques are known to occur during normal aging, in small numbers with increasing frequency from the fifth decade onwards in amygdala, hippocampus and neocortex [32]. In the senile human brain neuropilic threads have been reported [33]. Their presence was demonstrated in this last referred study by Braak et al. (1986) by application of the Gallyas silver staining technique, by immunostaining of paired helical filaments and by electronmicroscopy. In our Congo-Red fluorescent technique congophilic threads, similar in morphology to the argentophilic threads as demonstrated by Braak et al. were noticed. In all three control brains congophilic threads were present. The variation in distribution between the different hemispheres is comparatively large. No definite distribution pattern is noticed when the different figures (figs.III. 17-19). are compared. Because these structures may be thought of as being the Congo-Red 'counterpart' of the neuropil threads seen by Braak in the Gallyas staining, and these latter have been demonstrated to be associated with PHF, a major component of NFT [34], a relation with the NFT formation in AD is suggested. However, no evidence exists to the exact relation of these threads to the NFT. In our material, no NFT were noticed in those cortical areas investigated in the brains of controls, containing congophilic threads. This leaves open the question of the relationship between congophilic threads and NFT. Congophilic Threads may be precursors of NFT formation. No clinical or neuropathological meaning for the congophilic threads has been found yet.

IV.12. A THEORY ON ALZHEIMER'S DISEASE AND ITS PATHOGENESIS.

From our data, some concepts concerning the relationship between the distribution of pathologic changes (as represented by the SP, NFT and CAA distribution) and clinical manifestation of Alzheimer's disease may be formulated.
One of the clinical features in the description of AD patients is the apparent disturbance of higher cognitive functions [35], which need not to be directly related with memory disturbances, such as apraxia, disturbances in language and visuospatial skills.
The idea of higher cortical functions to be localized within circumscribed cortical areas (association areas) has been repeatedly challenged by advances in cognitive psychology [36, 37]in the form of the theory of parallel distributed processing (PDP) of information [38].
The classical idea of cortical information processing is a sequential processing of (sensory) information through " successive stages of intramodular elaboration allowing progressively more complex discriminations of the features of a particular stimulus. Then, by a series of further connections, this sensory information, now in a highly complex form, is conveyed to polymodal zones for cross-modal interchange of information, to the paralimbic and limbic areas for investment with emotional tone and placement in memory, and to the frontal association areas where both sensory and limbic data are integrated in preparation for the organism to respond to sensory stimuli by an appropriate response" (Pandya PN, B Seltzer (1982) [39]. According to these hierarchical models of cortical function,sensory signals are progressively elaborated in sensory association areas, and the information flow is mainly unidirectional, i.e. from sensory through associational to motor. Examples of this idea of cortical flow of information are given in the first chapter.

In a different view, the flow of information is not directed along such hierarchical paths of increasingly elaborated information processing areas, but along parallel systems of information processing with perhaps equal functions. Studies on cerebral blood flow in normal subjects performing psychological tasks support a parallel distributed processing model of cortical functions [40].The act of thinking increases blood flow in multiple cortical fields in cortical zones outside the immediate sensory association areas, and, predictably, the constellation of cortical areas activated differs with different "types" of thinking. This

constellation of cortical areas may sometimes coincide with the classical hierarchical pathways. One cannot escape the conclusion that the constellation of areas activated by spatial thought processes, for instance, represents the same type of circuitry that is interconnected by corticocortical connections described in the nonhuman primate. From the work of Hubel et al. [41] and Shipp et al.[42] it is known that different features from the visual world are processed in parallel in visual cortical areas. According to the modern view of information processing, large amounts of data can be processed with comparatively simple units of processing, like individual neurons or cortical columns, when a large number of these units are working parallel on this bulk of information. Important for information processing becomes the connectivity between the various cortical units.

In AD, macroscopic atrophy, defined as a volume loss, is explained by a loss of cortical surface. Such a surface loss could be explained by the 'dropping out' or, alternatively, by a decrease in mean diameter of radial units, like the cortical columns. Cortico-cortical connectivity is organized in a columnar fashion [43]. The loss of columnar units may result in a disturbance of these cortico-cortical connections and may give rise to the disturbance of especially the higher cerebral functions. It is this disturbance of higher cerebral functions, which is characteristic for the clinic of Alzheimer's disease.
In the present study, all cortical areas are demonstrated to be involved in the disease process. If SP formation results in a degeneration of cortico-cortical connections, then AD should be interpreted as a global disconnection syndrome. Thus the disturbance of especially higher cognitive functions may be related more to the number of cortical areas affected that to the concentration of SP in a particular cortical area. All our AD material was derived from patients suffering from severe forms of AD, and all these cases demonstrated an involvement of every cortical area investigated, as demonstrated by SP formation.

The recent research on the genetic background in AD is of interest [44]. A genetic background for the disease makes the suggestion of an infectious agent which spreads along neural pathways in the brain less probable. If a genetic backgroud exists, then all nerve cells, or a particular population of nerve cells could be 'programmed' to degenerate. Secondarily to this degeneration of cortical neurons, corticopetal projecting fiber systems such as the cholinergic system may degenerate. The degeneration of the corticopetal projecting nuclei may be explained by a shortage of

trophic factor, normally produced by the neurons with which these projecting neurons synapse. For example, the target cells of cortical cholinergic innervation in the cerebral cortex degenerate. Thus, these cells are not able to produce NGF any more in sufficient quantity, and therefore cause the cholinergic system to degenerate.

The degeneration of other systems, such as the noradrenergic locus coeruleus could be explained likewise, if a still unknown growth factor for these neurons is postulated. Then lack of this growth factor due to cortical nerve cell degeneration, could cause cell loss in the locus coeruleus.

In conclusion, the degeneration of subcortical corticopetal projecting nuclei may be secondary to neocortical degenerative processes.

IV.13. CONCLUSIONS.

Our results indicate a non-random distribution of SP, NFT and CAA. The SP -, NFT- and CAA concentrations differ between different cortical areas and between different cortical laminae within these cortical areas.
The estimates of cortical volume and surface indicate a preferential loss of cortical surface in order to explain the neocortical atrophy, observed in our cases. The change in cortical volume suggests all data reported in the literature concerning neocortical neuron loss to be severely biased.
The quantification of the distribution of NFT, SP and CAA demonstrated the global laminar distribution pattern of SP and NFT to be similar but different from the global distribution pattern of CAA.
Comparison of the SP distribution with the data available from the anatomical literature on hodology of the primate brain did not favor a theory of distribution of the disease along (specific) connectional pathways in the brain.
In this study GVD is reported to occur in the neocortex.

1.Armstrong RA, D Myers, CUM Smith. Further studies on the patterns of senile plaques in senile dementia of the Alzheimer type (SDAT) with a hypothesis on the colonization of the cortex. Neuro Res Comm (1989) 4:17-24.

2.Coleman PD, DG Flood. Neuron numbers and dendritic extent in normal aging and Alzheimer's disease (review). Neurobiol Aging (1987) 8:521-545.

3.Campbell S, RC Switser, TL Martin. Alzheimer's plaques and tangles: A controlled and enhanced silver staining method. Soc Neurosci Abstr (1987) 13:678.

4.Gallyas F. Silver staining of Alzheimer's neurofibrillary changes by means of physical development. Acta Morphol Acad Sci Hung (1971) 19:1-8.

5.Braak H, E Braak, T Ohm, J Bohl. Alzheimer's disease: mismatch between amyloid plaques and neuritic plaques. Neurosc Lett (1989) 103:24-28.

6.Lewis DA, MJ Campbell, RD Terry JH Morrison. Laminar and regional distributions of Neurofibrillary Tangles and Neuritic plaques in Alzheimer's Disease: A quantitative study of visual and auditory cortices. J Neurosci (1987) 7:1799-1808.

7.Pearson RCA. The evolution of Alzheimer neuropathological changes. At the conference: Aging of the brain and Dementia:Ten Years Later. Florence May 31-June 3, 1989.

8.German DC, CL White, DR Sparkman. Alzheimer's disease: Neurofibrillary tangles in nuclei that project to the cerebral cortex. Neurosc (1987) 21:305-312.

9.Pearson, RCA, MM Esiri, RW Hiorns, GK Wilcock, TPS Powell. Anatomical correlates of the distribution of the pathological changes in the neocortex in Alzheimer's disease. Proc Natl Acad Sci (USA) (1985) 82:4531-4534.

10.Martin, K.A.C. Neuronal circuits in the cat visual cortex, In: Cerebral Cortex, vol 2, E.G. Jones and A. Peters (eds), pp 241-284. NY, Plenum, (1984).

11.Esiri MM, RCA Pearson, TPS Powell. The cortex of the primary auditory area in Alzheimer's disease. Brain Res (1986) 366:385-387.

12.Rogers J, JH Morrison. Quantitative morphology and regional and laminar distributions of Senile Plaques in Alzheimer's Disease. J Neurosci (1985)10:2801-2808.

13.Duyckaerts C, J-J Hauw, F Bastenaire, F Piette, C Poulain, V Rainsard,F Javoy-Agid, P Berthaux. Laminar distribution of neocortical plaques in senile dementia of the Alzheimer type. Acta Neuropath. (1986) 70:249-256.

14.Mann DMA. Neuropathological and neurochemical aspects of Alzheimer's disease. In:Handbook of Psychofarmacology, Vol.20 LL Iversen, SD Iversen, SH Snyder (eds.) (1988) New York, p9.

15.Jamada M, P Mehraein. Verteilungsmuster der Senilen Veranderungen im Gehirn. Die Beteiligung des limbischen Systems bei Morbus Alzheimer. Arch Psychiat Neurol (1968) 211:308-324.

16.Appel SH. A unifying hypothesis for the cause of amyotrophic lateral sclerosis, Parkinsonism, and Alzheimer disease. Ann Neurol (1981) 10:499-505.

17.German DC, CL White, DR Sparkman. Alzheimer's disease: Neurofibrillary tangles in nuclei that project to the cerebral cortex. Neurosc (1987) 21:305-312.

18.Pearson RCA, MM Esiri, RW Hiorns, GK Wilcox and TPS Powell. Anatomical distribution of the pathological changes in the neocortex in Alzheimer's Disease. Proc Natl Acad Sci (USA) (1985) 82:4531-4534.

19.Barbas H. Pattern in the laminar origin of corticocortical connections. J Comp neurol (1986) 252:415-422.

20.Hedren JC, RG Struble, PJ Whitehouse, DL Price. Topography of the magnocellular basal forebrain system in human brain. J Neuropathol Exp Neurol (1984) 43:1-21.

21.Mesulam MM. Central cholinergic pathways- neuroanatomy and some behavioral implications. In: Neurotransmitters and cortical function. M Avoli (ed.) New York (1988):237-260.

22.Sillito AM, PC Murphy. The cholinergic modulation of cortical function. In: Cerebral Cortex. Vol 6.EG Jones, A Peters (eds) New York (1987):161-185.

23.Lysakowski A, Wainer BH, Bruce G, Hersh LB. An atlas of the regional and laminar distribution of choline acetyltransferase immunoreactivity in rat cerebral cortex. Neuroscience (1989) 28:291-336.

24.Perry EK, Atack JR, Perry RH, Hardy JH, Dodd PR, Edwardson JA, Blessed G, Tomlinson BE, Fairbairn AF. Intralaminar neurochemical distributions in human midtemporal cortex: comparison between Alzheimer's disease and the normal. J Neurochem (1984) 42:1402-1410.

25.Sorbi S, Piacentini S and Amaducci L. Intralaminar distribution of neurotransmitter-related enzymes in cerebral cortex of Alzheimer's disease. Gerontology (1987) 33:197-202.

26.Gaspar P, B Berger, A Febvret, A Vigny, JP Henry. Catecholamine innervation of the human cerebral cortex as revealed by comparative immunohistochemistry of tyrosine hydroxylase and dopamine -beta hydroxylase. J Comp Neurol (1989) 279:249-271.

27.Arendt T, V Bigl, A Tennstedt and A Arendt. Correlation between cortical plaque count and neuronal loss in the nucleus basalis in Alzheimer's disease. Neurosci Lett (1984) 48:81-85.

28.Mann DMA, PO Yates, B Marcyniuk. Correlation between senile plaque and neurofibrillary tangle counts in cerebral cortex and neuronal counts in the cortex and subcortical structures in Alzheimer's disease. Neurosci Lett (1985) 56:51-55.

29.Hefti F, WJ Weiner. Nerve growth factor and Alzheimer's disease. Ann Neurol (1986) 20:275-281.

30.Price DL, RJ Altschuler, RG Struble, MF Casanova, LC Cork, DB Murphy. Sequestration of tubulin in neurons in Alzheimer's Disease. Brain Res (1986) 385:305-310.

31.Dickson DW, H Ksiezak-Reding, P. Davies, SH Yen. A monoclonal antibody that recognizes phosphorylated epitope in Alzheimer neurofibrillary tangles, neurofilaments and tau proteins immunostains granulovacuolar degeneration. Acta Neuropathol (Berl) (1987) 73:254-258.

32.Mann D, CM Tucker, PE Yates. The topographic distribution of senile plaques and neurofibrillary tangles in the brains of non-demented persons of different ages. Neuropath Appl Neurobiol (1987) 13:123-139.

33.Braak H, E Braak, I Grundke-Iqbal, K Iqbal. Occurrence of neuropil threads in the senile human brain and in Alzheimer's Disease: A third localization of paired helical filaments outside of neurofibrillary tangles and neuritic plaques. Neurosc Lett (1986) 65:351-355.

34.Kidd M. Paired helical filaments in electron microscopy of Alzheimer's disease. Nature (1963) 197:192-193.

35.Berg L, JC Morris. Clinical aspects of Alzheimer's disease. Curr Op Neurol Neurosurg (1989) 2:445-450.

36.Bugbee NM, PS Goldman-Racik. Functional 2-deoxyglucose mapping in association cortex: Prefrontal activation in monkeys performing a cognitive task. Soc Neurosc Abstr (1981) 7:416.

37.Rumpelhart DE, JL McClelland. Parallel Distributed Processing. Vol. I + II. London (1987).

38.Nadel L, LA Cooper, P Culicover, RM Harnish (eds). Neuronal connections, mental computation. Cambridge (MA), (1989).

39.Pandya PN, B Seltzer. Intrinsic connections and architectonics of the posterior parietal cortex in the rhesus monkey. J Comp Neurol (1982) 204:196-210.

40.Roland PE, L Friberg. Localization of cortical areas activated by thinking. J Neurophysiol (1985) 53:1219-1243.

41.Hubel DH, MS Livingstone. Complex-unorientated cells in a subregion of primate area 18. Nature (1985) 315:325-327.

42.Shipp S, S Zeki. Segregation of pathways leading from area V2 to areas V4 and V5 of macaque monkey visual cortex. Nature (1985) 315:322-325.

43.Eccles JC. The cerebral neocortex: A theory of its operation. In: Cerebral Cortex Vol.2, EG Jones, A Peters (Eds.) New York (1984).

44.Genetics and Alzheimer's disease. Sinet PM, Y Lamour, Y Christen (eds). Berlin, 1988.

V. SUMMARY AND CONCLUSIONS

The neuropathological changes in Alzheimer's disease were first described in the neocortex, by Alois Alzheimer in 1907. Eversince the neocortex remained in the focus of interest in subsequent studies on this disease.
The study of the neocortex in Alzheimer's disease involves not only microscopic examination of the material but also macroscopic analysis: one of the main features on macroscopic inspection of a brain of a patient having suffered from this disease is a widening of the sulci and a thinning of the gyri as signs of an important cortical atrophy. In this study, atrophy is defined as a loss of cortical volume. A change in cortical volume can result from either a decrease of cortical thickness, leaving the surface of cortex unchanged or from a decrease in cortical surface, leaving the cortical thickness unchanged, or a combination of both. Quantitative analysis of this neocortical atrophy is difficult, because most techniques available are influenced by the complex geometrical structure of the neocortex. In this study (Chapter III.1), a specific technique is employed in order to obtain data, independent of the cortical geometrical structure. This technique made an unbiased estimation of cortical volume and cortical surface possible. Using this technique, it was possible to demonstrate in AD a neocortical volume loss of 41 % and a surface loss of 38 %. These results explained the macroscopic atrophy of the neocortex as a result of loss of cortical surface, with practically no loss of cortical thickness. This result points to a certain pattern of neocortical atrophy in Alzheimer's disease, which as is speculated here, may be related to the (functional) organization of the neocortex in vertically orientated modules of cortical function, the cortical columns.
The important microscopical changes noticed in the cerebral cortex are senile plaques (SP), neurofibrillary tangles (NFT) and congophilic amyloid angiopathy (CAA). In the literature, changes in neocortical content of a large number of neurotransmitters within the neocortex were reported. In the literature it was suggested, that the distribution pattern of senile plaques and neurofibrillary tangles were not at random. This fact prompted the idea, that Alzheimer's disease could be caused by an agent, which might spread along specific pathways (chapter I.5). In order to evaluate the distribution patterns of the senile plaques and the neurofibrillary tangles, the hodology of the neocortex is reviewed briefly (Chapter I).
In order to evaluate a possible distribution pattern a procedure was developed to map the senile plaques of each brain investigated. These maps are presented in figs. III.1-7. The sections used in

this procedure were stained according to a modified Bielschovsky silver staining, the Yamamoto staining.
The distribution of senile plaques, neurofibrillay tangles and congophilic angiopathy was studied in Congo-red stained sections, which were analyzed using fluorescence microscopy (Chapter II).

The plottings of the Yamamoto - stained plaques were quantified, per hemisphere, per cortical area, and per cortical layer. The numerical data allowed statistical analysis in order to demonstrate a laminar distribution pattern of senile plaques in all cortical areas investigated. By pooling the data per cortical area in all cases investigated, differences in areal concentrations between the different cortical areas could be demonstrated. Pooling all areas in a laminar fashion made it possible to identify the most affected cortical layers on a global scale. This laminar pattern of senile plaque distribution is compared with data concerning the laminar distribution pattern of fiber endings of corticopetal and corticocortical connecting systems.

In the Congo-red stained material, the distribution of senile plaques, neurofibrillary tangles and congophilic angiopathy is investigated per cortical area and per lamina. The data are represented in bar diagrams (figs. III.13-32). The data were analyzed in a fashion analogous to the Yamamoto data. Furthermore, the number of senile plaques, of neurofibrillary tangles and a scoring scale of congophilic amyloid angiopathy were correlated, using Pearson's correlation test. In this analysis, every field of vision is used.

Our data demonstrate the existence of a laminar distribution of senile plaques using the plotting method, based on Yamamoto-stained material. No difference in distribution pattern between both hemispheres was found. Most senile plaques were demonstrated in the supra granular layers II and III (table 2, fig. III.9).
The areal distribution of senile plaques demonstrated the larger concentrations to be localized in the areas of the temporal lobe. In the frontal lobe and the gyrus cinguli a large number of senile plaques was noticed. Interestingly, the concentration in an important association region of somatosensory information, Area 7 was low (fig. III. 10-12).
These data concerning senile plaque distribution as seen in the Yamamoto-plotting method are in agreement with the distribution of senile plaques, as seen in the Congo-Red fluorescence method.
The areal distribution pattern of senile plaques appeared to be correlated with the number of large neurons in the nucleus basalis

(Meynert) projecting to particular Brodmann Areas (Section III.3.). No distinct correlation with the pattern of laminar endings of ChAT positive fibers reported in the not-diseased brain and the laminar senile plaque distribution was found, while an association between noradrenergic fiber ending distribution in non-diseased brain and laminar senile plaque distribution was suggested.
In studying the different cortical areas, a location, unreported in the literature, of granulovacuolar degeneration (GVD) was demonstrated. GVD was found in the cingular and insular regions. GVD is reported to be connected with cytoskelettal components, such as the paired helical filaments, a major constituent of the NFT. This may emphasize that the neural degeneration in the hippocampus is similar in nature to the degeneration in the neocortex.

In general, no conclusive evidence of the association of any particular fiber system with the senile plaque and the neurofibrillary tangle distribution was found in our study. Nor was an association between SP formation and CAA demonstrated as a general feature. The disturbances of higher cortical function may be explained as a result of the global distribution of the neocortical pathology. As a consequence, based on the model of distributed processing of information (PDP) in the brain the disturbances of higher cortical function are hypothezised to result from the universal presence of SP and NFT, and not from pathology in one single cortical field or projection system.

In summary, the most important findings in this study are the lack of correlation of the distribution pattern of senile plaques and neurofibrillary tangles with one particular fiber system, the demonstration that macroscopic atrophy of the neocortex results mainly from a reduction of cortical surface and the demonstration of granulovacuolar degeneration in a neocortical localization.

V. SAMENVATTING EN CONCLUSIES.

In 1907 werden door Alois Alzheimer de neuropathologische veranderingen in de neocortex bij de ziekte van Alzheimer voor het eerst beschreven. Sindsdien is de neocortex in het brandpunt van de belangstelling bijven staan.
Deze studie van de neocortex bij de ziekte van Alzheimer betreft niet alleen het microscopisch onderzoek van het material, maar ook macroscopische analyse: een van de meest opvallende verschijnselen bij macroscopische inspectie van het brein van een patient, die aan deze ziekte geleden heeft, is een verwijding van de sulci en een dunner worden van de gyri, dit alles als teken van een belangrijke corticale atrofie. In deze studie wordt corticale atrofie gedefinieerd als een verlies van cortex volume. Een verandering van dit cortex volume kan het gevolg zijn ofwel van een afname van de gemiddelde cortex dikte, waarbij de totale corticale oppervlakte onvenanderd blijft, ofwel van een afname van het corticale oppervlakte, ofwel van een afname van zowel coticale dikte als van cortex oppervlakte. Quantitative analyse van deze neocorticale atrofie is moeilijk, omdat de meeste technieken die hiervoor beschikbaar zijn worden beinvloed door de complexe geometrische corticale structuur. In deze studie (hoofdstuk III.1) wordt een techniek gebruikt, welke resultaten geeft, die in hoge mate niet door die geometrische structuur worden beinvloed. Deze techniek maakt een zgn. 'onbeinvloedde' afschatting van cortex volume en oppervlak mogelijk. Met deze techniek kon een neocortex-volume verlies van 41 %, en een oppervlakte verlies van 38 % worden aangetoond. Deze resultaten doen de macroscopische corticale atrofie verklaren als het resultaat van een cortex oppervlakte verlies, zonder een verlies van cortex dikte.
Dit resultaat wijst op een bepaald patroon van neocorticale atrofie bij de ziekte van Alzheimer, dat, zoals in deze studie wordt geponeerd, te maken kan hebben met de (functionale) organisatie van de neocortex gekenmerkt door verticaal georienteerde modules van corticale functie, the cortex kolommen.
De meest belangrijke microscopische veranderingen, die in de ziekte van Alzheimer in de neocortex kunnen worden opgemerkt, zijn de senile plaques (SP), neurofibrillaire tangles (NFT) en de congofiele amyloid angiopathie (CAA). In de literatuur wordt gesuggereerd, dat seniele plaques en neurofibrillaire tangles niet ad random verdeeld waren. Dit gegeven deed het idee opkomen, dat de ziekte veroorzaakt zou worden door een agens, dat zich via specifieke verbindingen binnen het centraal zenuwstelsel verspreiden zou (Hoofdstuk I.5). Ter evaluatie van de verdelingspatronen van de seniele plaques en de neurofibrillaire tangles, de hodologie van de neocortex is kort samengevat (Hoofdstuk I).
Om een mogelijk distributie patroon van seniele plaques te detecteren en te evalueren, werd een methode ontwikkeld om deze in kaart te brengen in elk onderzocht brein. Deze kaarten worden weergegeven in figs. III.1-7. De histologische coupes worden voor deze methode gekleurd volgens een gemodificeerde Bielschovski zilver kleuring, de zgn. Yamamoto-kleuring.
De verdeling van de seniele plaques, neurofibrillaire tangles en congofiele angiopathie is ook bestudeerd in met Congo-rood gekleurde coupes, die dan weer met fluorescentie microscopie werden

geanalyseerd.

De kaarten, die de verdelingen van de seniele plaques, zoals deze te zien waren in de Yamamoto-kleuring werden ook gekwantificeerd. Dit gebeurde per hemisfeer, per cortex gebied, en per cortex laag. Deze data maakten een statistische analyse mogelijk, teneinde een laminaire verdeling van de seniele plaques te onderzoeken aan te tonen in alle in fig. II.2. aangegeven cortex velden. Door 'pooling' van de data van alle onderzochte gevallen konden verschillen in concentraties per veld worden aangetoond. Door laagsgewijze alle onderzochte gebieden bij elkaar te nemen, was het mogelijk de meest aangedane cortexlagen te identificeren. Dit laminar patroon van seniele plaque verdeling is vergeleken met de schaarse gegevens van de literatuur betreffende het laminaire verdelingspatroon van vezeleindigingen van corticopetale en cortiococorticale verbindingssystemen.

In het Congo rood gekleurde materiaal werd de distributie van seniele plaques, neurofibrillaire tangles en congofiele amyloid angiopathie onderzocht per gebied en per cortex laag. De data zijn weergegeven in staafdiagrammen (figs. III.13-32). De data zijn op een vergelijkbare manier geanalyseerd als die afkomstig van het Yamamoto materiaal. Daarenboven werden de correlaties tussen de aantallen van seniele plaques, neurofibrillaire tangles en een scooring op de congofiele amyloid angiopathie schaal berekend, gebruik makend van de correlatie test vlgs. Pearson. Hiervoor is elk gebied van de breinen afkomstig van de gevallen van de ziekte van Alzheimer, gebruikt.

De gegevens gelevered door deze studie laten het bestaan zien van een laminaire verdeling van de seniele plaques. Er werd geen verschil gevonden in verdelingspatroon tussen de linker en de rechter hemisfeer. Het grooste aantal seniele plaques werd gevonden in de supragranulaire lagen L II en L III (tabel 2, fig. III.9). De verdeling van seniele plaques over de verscheidene cortex gebieden liet een concentratie van plaques zien in de gebieden van de temporale lobus. Ook in de lobus frontalis en de gyrus cinguli zijn grote concentraties plaques gevonden. Het is interessant op te kunnen merken, dat in een belangrijk gebied van associatie van somatosensore informatie, Brodmann Area 7, de plaque concentratie juist laag is (fig. III. 10-12).
Deze data betreffende de seniele plaque distributie, zoals deze gezien wordt in de Yamamoto-kaarten, zijn in overeenstemming met de senile plaque distributie, zoals deze wordt waargenomen in de Congo-rood fluorescentie methode. De verdeling over cortex arealen van de senile plques bleek te correleren met het aantal grote neuronen in de nucleus basalis (Meynert), die naar bepaalde Brodmann gebieden projecteren (Section III.3). Er wordt geen duidelijke correlatie gevonden tussen ennerzijds het patroon van laminaire eindigingen van ChAT-IR positieve vezels, zoals deze beschreven zijn in humane controle breinen en anderzijds het patroon van verdeling van senile plaques. Echter, aanwijzingen, dat een dergelijke relatie mogelijk bestaat tussen de noradrenerge eindvezel verdelingen en de seniele plaque distributie wordt door

de schaarse data gesuggereerd. Bij bestudering van de verschillende corticale gebieden werd ook granulovacuolaire degeneratie (GVD) opgemert, op een locatie, waar vroegere literatuur geen melding van heeft gemaakt. GVD is gevonden in de cingulaire en insulaire gebieden. GVD is in verband gebracht met cytoskeletcomponenten, zoals de zgn. Paired Helical Filaments (PHF), die een belangrijk bestanddeel vormen van de NFT. Dit benadrukt wellicht dat de neurale degeneratie in de hippocampus dezelfde achtergrond heeft als die in de neocortex.

In het algemeen gesproken is hier geen beslissend bewijs gevonden van een associatie van een bepaald vezelsysteem met de verdeling van seniele plaques en van de neurofibrillaire tangles. Ook kon geen algemene associatie tussen de verdeling van seniele plaques en die van de congofiele amyloid angiopathie gevonden worden.

De verstoring van de hogere cognitieve functies kan mogelijk worden uitgelegd als het gevolg van het globaal verdeeld zijn van de corticale pathologie. Ten gevolge hiervan zouden, uitgaande van het model van parallel gedistribueerde informatie verwerking (PDP) binnen de cortex, verstoringen van de hogere cognitieve functies het resultaat kunnen zijn van het feit, dat overal in de cortex pathologische afwijkingen zich voordoen, zoals wordt gedemonstreerd in deze studie.

Kort samengevat kan gesteld worden, dat deze studie geen aanwijzingen geeft voor het bestaan van een correlatie van de verdelingen van SP en NFT met bepaalde vezel systemen. Voorts maakt het onderdeel betreffende de macroscopische veranderingen van de neocortex bij de ziekte van Alzheimer duidelijk, dat de atrofie van de neocortex voornamelijk het gevolg is van een reductie van cortex oppervlak en niet zozeer van een 'dunner worden' van die cortex. Ook wordt in dit werk het voorkomen van GVD binnen de neocortex beschreven.

Dankwoord.

De schrijver dankt hierbij de analytische medewerkers van het Research Laboratorium voor morfologische Neurologie, Instituut voor Neurologie, voor het vele technische werk, in het bijzonder voor het histotechnische werk. Tevens wordt Dr. K. Renkawek bedankt voor haar bijdrage in de diagnostiek, maar ook voor de vaak levendige discussies aangaande de aetiologie en pathogenese van de Ziekte van Alzheimer. Ook geldt een woord van dank Dr. H. Ten Donkelaar, voor zijn bijdrage bij de dissectie van het materiaal.
De klinische medewerkers van het Instituut voor Neurologie worden bedankt voor hun geduld tijdens de eerste maanden van mijn opleiding, omdat juist in die tijd nog veel voorbereiding voor de publicatie van dit proefschrift moest worden verricht.

De schrijver van dit proefschrift werd op 10 maart 1959 geboren te Sliedrecht. Na het behalen van het einddiploma B aan het Johan de Witt gymnasium in 1977, ging hij Wis- Natuur- en Sterrekunde studeren aan de Rijksuniversiteit Utrecht. In 1979 ging hij geneeskunde studeren aan dezelfde universiteit. In 1985 en 1986 werden respectivelijk het doctoraal en het artsexamen behaald.
Vanaf februari 1986 tot september van ditzelfde jaar was hij werkzaam als wetenschappelijk assistent in het laboratorium voor celbiologie en histologie van de rijksuniversiteit Utrecht (vakgroepleider Dr. D. de Rooy). In de periode van september 1986 tot september 1989 verrichtte hij onderzoek naar de neocorticale veranderingen bij de ziekte van Alzheimer, in het kader van het WVVZCZS project.
Sinds september 1989 is hij als arts-assistent in opleiding tot neuroloog (opleider Prof. Dr. B.P.M. Schulte).

STELLINGEN

behorende bij het proefschrift

THE NEOCORTEX IN ALZHEIMER'S DISEASE

Nijmegen, 23 februari 1990

C.A.J. Broere

I. De atrofie van de neocortex bij patienten met de ziekte van Alzheimer is voornamelijk te verklaren uit een verlies van corticaal oppervlak en niet als een gevolg van afname van de gemiddelde cortex dikte.
(dit proefschrift)

II. Vanwege de sterke reductie in cortexvolume bij patienten lijdende aan de ziekte van Alzheimer ten opzichte van controle gevallen, is bepaling van neuron concentratie weinig betrouwbaar als maat voor neuraal celverlies.
(dit proefschrift)

III. Seniele plaques zijn non-random over de cortex doorsnede verdeeld.
(dit proefschrift)

IV. Het laminaire verdeling verdelingspatroon van senile plaques en van de neurofibrillaire tangles suggereren een verband tussen tangle en plaque formatie.
(dit proefschrift)

V. Het verspreidingspatroon van senile plaques over de neocortex is niet met een cortico-petaal of met een cortico-corticaal projectiesysteem in overeenstemming te brengen.
(dit proefschrift)

VI. Het maken van een 'high resolution magnetic resonace image' is een onmisbaar hulpmiddel bij de vroege diagnostiek van de ziekte van ALzheimer.
(GA Press, DG Amaral, LR Squire. Nature (1989) 341:54-57)

VII. Het feit dat men vanaf 1 januari 1990 bij de opgave van het belastbaar inkomen de aanschaf van personal computers niet meer in mindering kan brengen, zal de ontwikkeling van het wetenschappelijk onderzoek schaden.

VIII. Het schrijven van een proefschrift in een andere dan de moedertaal, komt de leesbaarheid ervan meestal ten goede.

IX. Het LINGUA-programma beoogt een extra stimulans te zijn voor het onderwijs in de "minder onderwezen talen van de Europese Gemeenschap": met ingang van 1 maart 1990 kan men voor onderwijsprogramma's betreffende het Engels, Frans, Duits, Spaans, Italiaans, Portugees, Grieks, Deens, Iers, Luxemburgs en het Nederlands een speciale financiering aanvragen. Het feit dat het klassiek Grieks en het Latijn van deze regeling zijn uitgesloten, talen die als geen andere gestalte hebben gegeven aan het cultureel erfgoed van Europa, illustreert de verschraling van dit Europees cultureel erfgoed zelf.
(LINGUA programma-informatie blad, EEG, 1989).

X. Bij de uitgave van boeken wordt te weinig rekening gehouden met het feit dat de rug het meest gelezen gedeelte is.